THE ROLE OF ATF4 IN HYPOXIA-INDUCED CELL DEATH IN CANCER

Luke R. G. Pike

A thesis submitted for the degree of
Doctor of Philosophy at Oxford University

St. John's College

April 15, 2011

Abstract

Cancer cells survive the harsh oxygen and nutrient deprivation of the tumour microenvironment through the selection of apoptosis-resistant and glycolytic clones, and the activation of cellular adaptive mechanisms in those clones (Cairns et al., 2011; Graeber et al., 1996). In particular, the integrated stress response (ISR) has been shown to be pivotal in cancer cell survival *in vivo* and the resistance of cancer cells to therapy (Harding et al., 2003). In recent years, it has become apparent that increased autophagy is one mechanism by which the ISR can confer resistance to stress (Kroemer et al., 2010).

ATF4 is a major transcriptional effector of the integrated stress response in severe hypoxia (<0.01% O_2). ATF4 is a well-established regulator of genes involved in oxidative stress, amino acid synthesis and uptake, lipid metabolism, protein folding, metastasis, and angiogenesis. Recent work has demonstrated an important role of ATF4 in promoting resistance to severe hypoxia through the transcriptional upregulation of MAP1LC3B and ATG5, essential components of the autophagy machinery (Rouschop et al., 2009b; Rzymski et al., 2010).

In this work, the author describes several novel ATF4 target genes, and examines their role in the regulation of autophagy and the resistance of cancer cells to severe hypoxia. In the first part of this thesis, the author shows that three BH3-only members of the Bcl-2 family of proteins—HRK, PUMA, and NOXA—are upregulated in response to severe hypoxia in an ATF4-dependent manner. In particular, the author shows that the poorly described BH3-only protein HRK is a direct target of transcriptional activation by ATF4, and that HRK induces autophagy in severe hypoxia, thereby providing the first evidence that the integrated stress response can transcriptionally trigger the autophagy process. In contrast to the previously described role of HRK in apoptosis, this thesis

demonstrates that HRK can play a pro-survival role in the context of breast cancer cells.

In the latter part of this thesis, the author identifies the essential autophagy gene ULK1 as an ISR target gene. The author shows that ULK1 expression in severe hypoxia is transcriptionally uregulated through direct activation by ATF4. The author identifies ULK1 as a crucial regulator of autophagy and mitophagy in both normoxia and severe hypoxia and shows that ULK1 plays a pivotal role in cancer cell survival. Furthermore, it is shown that human breast cancer patients with high levels of ULK1 relapse earlier than those with low levels of ULK1, thereby identifying ULK1 as a potential target for cancer therapy.

Acknowledgements

This thesis would never have been written without the help of many people. The author would like to thank them here. First of all, the author would like to acknowledge Cancer Research UK, the Rhodes Trust, NSERC, and St. John's College for their generous financial backing throughout this project. Thank you to David Ferguson for his TEM work, Francesca Buffa for her clinical analyses, James Murray for his analysis of ULK1 activity, and Kanchan Phadwal for her Imagestream® analysis.

There are many personal thanks that must also be given. Thank you to Dean Singleton for his tremendous patience and thoughtful scientific input, as well as with the revision of this work. Thank you to Alan McIntyre for his help with the spheroid work, his positive outlook, and revision of this work. Thank you to Jun Yang and Karim Bensaad for their inspiring work ethic and technical ability. Thank you to Manuela Milani, the "Italian bella", for her love and patience. Thank you to Tomasz Rzymski for getting this work started and seeing the author through his first, very trying year. Thank you to Anassuya Ramachandran and Harriet Gee for keeping the author's feet on the ground and tolerating his rants. Thank you to Alan Storey and to Katja Simon for their critical assessments during the transfer of status, and for their continued technical expertise and advice. Thank you to Julia Tejblum, for tolerating all of the author's imperfections and vices, and for her careful revision of this work. Thank you to Adrian Harris, for his inspiring energy, insight, and intelligence, and for his kind supervision and support over the last four years.

Finally, the author would like to thank **John (Sean) Brosnan** and **Daniel MacPhee**, without whom this rural Newfoundlander would never have found his way across "the pond" to embark on this tremendous learning experience. Most

importantly, thank you to **Roy** and **Ruth Pike**. Without their love and support, none of this would have been possible.

Abbreviations

4E-BP1, eukaryotic translation initiation factor 4E binding protein 1

A1, BCL2-related protein A1

ABT, Abbott pharmaceutical corporation

AKT, protein kinase B

AMBRA1, autophagy/beclin-1 regulator 1

AMPK, AMP-activated protein kinase

ANOVA, analysis of variance

APAF-1, apoptotic peptidase activating factor 1

ARNT, aryl hydrocarbon receptor nuclear translocator

ATF4, activating transcription factor 4

ATF6, activating transcription factor-6

ATG, autophagy related gene

ATP, adenosine triphosphate

BAD, BCL2-associated agonist of cell death

BAK, Bcl-2 homologous antagonist/killer

BAX, Bcl-2–associated X protein

BCL-w, BCL2-like 2

Bcl-XL, BCL2-like 1

BCL2, B-cell lymphoma 2

BCN1, beclin 1

Bcr-Abl, breakpoint cluster region- c-abl oncogene 1

BH1-4, BCL2 homology domains

BH3, BCL2 homology domain 3

BID, BH3 interacting domain death agonist

BIK/NBK, BCL2-interacting killer (apoptosis-inducing)

BIM, BCL2-like 11

BiP, Binding immunoglobulin protein or glucose-regulated protein 78

BMF, Bcl2 modifying factor

BNIP3, BCL2/adenovirus E1B 19kDa interacting protein 3

BNIP3L/NIX, BNIP3-like or NIP3-like protein X

BOK, BCL2-related ovarian killer

CAIX, carbonic anhydrase IX

Caspase, cysteine-aspartyl protease

ChIP, chromatin immunoprecipitation

CHOP, CCAAT/enhancer-binding protein homologous protein

COXIV, cytochrome c oxidase subunit IV

CQ, chloroquine

CREB, cAMP responsive element binding protein

CXCR4, chemokine (C-X-C motif) receptor 4

DFO, deferoxamine mesylate

DLC1, dynein light chain 1

DP5, death protein 5

DREAM, Drosophila RBF-, dE2F2-, and dMyb-interacting proteins

EEF2, elongation factor 2 kinase

EEF2K, eukaryotic elongation factor-2 kinase

eIF2α, eukaryotic translation initiation factor 2 alpha

EIF4E, eukaryotic translation initiation factor 4E

EIF4G, eukaryotic translation initiation factor 4G

ELISA, enzyme-linked immunosorbent assay

ER, endoplasmic reticulum

ERAD, ER associated degradation

ERBB2, v-erb-b2 erythroblastic leukemia viral oncogene homolog 2,
neuro/glioblastoma derived oncogene homolog

ERO1, endoplasmic oxidoreductin-1

ESCRT, endosomal complexes required for transport

FAD, flavin adenine dinucleotide

FIP200, focal adhesion kinase family interacting protein of 200kDA

GADD34, growth arrest and DNA damage-inducible protein 34

GADD45A, growth arrest and DNA-damage-inducible 45A

GCN2, general control non-repressed 2

GTP, guanosine triphosphate

H-Ras, v-Ha-ras Harvey rat sarcoma viral oncogene homolog

HDAC, histone deacetylase

HER2, human epidermal growth factor receptor 2

HIF, hypoxia inducible factor

HMGB1, high mobility group box protein 1

HRI, heme-regulated eukaryotic initiation factor eIF-2-alpha kinase

HRK, harakiri

HRP, horseradish peroxidase

IGFBP-2, insulin-like growth factor binding protein 2

IRE1, inositol-requiring enzyme-1

ISR, integrated stress response

JNK, c-Jun N-terminal kinase

Ki67, antigen identified by monoclonal antibody Ki-67

LDHA, lactate dehydrogenase A

LKB1, serine/threonine kinase 11

MAP1LC3B, microtubule-associated protein 1 light chain 3 beta; LC3-I and LC3-II refer to the unlipidated and lipidated cleaved forms, respectively

MCL-1, myeloid cell leukemia sequence 1

MDa, megadalton

MEF, murine embryonic fibroblast

Met-tRNA$_i^{Met}$, methionine-loaded initiator transfer RNA

MIR210, microRNA 210

mLST8, MTOR associated protein, LST8 homolog

mmHg, millimeters of mercury

MRI, magnetic resonance imaging

mTOR, mammalian target of rapamycin

mTORC1, mammalian target of rapamycin complex 1

mTORC2, mammalian target of rapamycin complex 2

MYC, myelocytomatosis oncogene

NDRG2, N-myc downregulated gene 2

NGF, neuron growth factor

NMR, nuclear magnetic resonance

NSAID, non-steroidal anti-inflammatory drug

p62, Ubiquitin-binding protein p62 or sequestosome 1

p70S6K, p70 fragment of S6 kinase

PAS, preautophagosomal structure

PDGF, platelet-derived growth factor

PDI, protein disulfide isomerase

PDK1, pyruvate dehydrogenase kinase, isozyme 1

PDK1, pyruvate dehydrogenase kinase, isozyme 1

PE, phosphatidylethanolamine

PERK, protein kinase RNA(PKR)-like ER kinase

PHD, proline hydroxylases

PI3K, phosphatidylinositol 3-kinase

PI3P, phosphatidylinositol 3-phosphate

PINK1, PTEN induced putative kinase 1

PKA, protein kinase A

PKR, protein kinase RNA-activated

PMA, phorbol 12-myristate 13-acetate

PMAIP1, PMA-induced protein 1

PML, promyelocytic leukemia protein

PRAS40, proline-rich Akt substrate, 40 kDa

PUMA, p53-upregulated modulator of apoptosis

Rab7, RAS-related GTP-binding protein 7

RAPTOR, regulatory associated protein of MTOR, complex 1

REDD1, regulated in development and DNA damage responses 1

RHEB, Ras homolog enriched in brain

Rictor, RPTOR independent companion of MTOR, complex 2

RNAi, RNA interference

ROS, reactive oxygen species

RT-qPCR, quantitative real time polymerase chain reaction

SCID, severe combined immunodeficiency

SCR, scrambled siRNA control

SDF1, stromal cell-derived factor 1

siRNA, short interfering RNA

SNARE, soluble NSF attachment protein receptor

TEM, transmission electron microscopy

TG, thapsigargin

TGN, trans Golgi network

TN, tunicamycin

TRAF2, TNF receptor-associated factor 2

TSC1, tuberous sclerosis 1

ULK1, UNC51-like kinase 1

uORF, upstream open reading frames

UPR, unfolded protein response

UTR, untranslated region

UVRAG, UV radiation resistance associated gene

VEGF, vascular endothelial growth factor

Vps34, vacuolar protein sorting 34

Wisp1, WNT1 inducible signaling pathway protein 1

XBP1, X-box binding protein 1

ZIPK, zinc finger interacting protein kinase

Table of Contents

List of Figures

Chapter 1 Introduction

1.1 Hypoxia and cancer

The microenvironment of an established solid tumour is both hostile and heterogeneous, characterized by extremes in pH, metabolite concentrations and, in particular, partial pressure of oxygen. Early lesions receive sufficient nutrients and oxygen through simple diffusion from nearby vessels in the surrounding normal tissue. However, as the nascent tumour outgrows the surrounding blood supply, the diffusion distance from these vessels increases. Eventually, tumour cells are exposed to an oxygen gradient: from efficient oxygenation of cells proximal to the stroma to near zero oxygenation of those in the peri-necrotic region (Bertout et al., 2008; Thomlinson and Gray, 1955).

1.1.1 Solid tumours contain regions of hypoxia

Before the advent of sophisticated polarographic sensors and MRI techniques for measuring oxygen levels, the existence of hypoxic regions within tumours was inferred by some very astute observations. In 1955, Thomlinson and Gray reported that some lung tumours grew as cords, which in cross-section appeared to be circular tissue surrounded by stroma (Thomlinson and Gray, 1955). They noted that tumour cells located more than 180μm from the blood vessels were observed to necrose and that a detectable band of viable cancer cells was always found between the necrotic area and these vessels. They thus suggested that a diffusion-limited oxygen gradient must exist in these tumours, with the level of oxygen decreasing to essentially zero at the necrotic center (Figure 1.1).

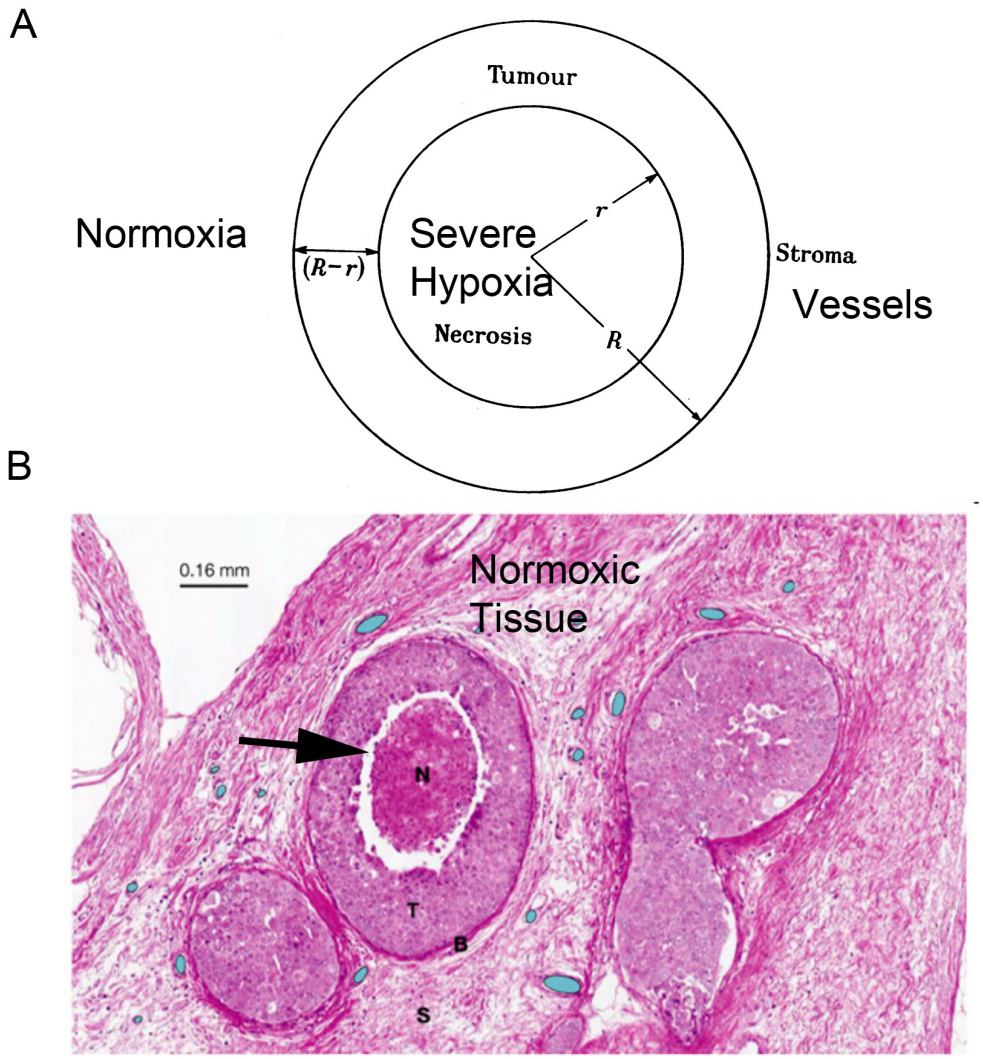

Figure 1.1 Solid tumours contain regions of hypoxia.

(A) Schematic diagram demonstrating diffusion-limited hypoxia. The width of the viable band of tumour (R-r) can be no more than 180μm due to a gradient of hypoxia from the vessels (outside) to the necrotic core (Thomlinson and Gray, 1955). (B) A haematoxylin and eosin stained biopsy sample of late state ductal carcinoma in situ. Blood vessels (blue), and stroma (S), basement membrane (B), viable tumour (T), and necrotic tumour (N) are indicated (adapted from (Gatenby and Gillies, 2004)). Arrow points to peri-necrotic region, which experiences severe hypoxia.

Polarographic electrodes confirmed the presence of hypoxia in solid tumours (Bertout et al., 2008; Lyng et al., 1997; Okunieff et al., 2005; Vaupel et al., 1992). Such studies have recorded tumour oxygen levels ranging from 0% to approximately 0.6% (100% = 760mmHg), while such low pressures are rarely ever achieved in normal tissues (Brizel et al., 1995; Vaupel et al., 1989a). Through the use of pimonidazole staining, Olive and colleagues have found that up to 35% of tumour cells in xenografts have hypoxia below 0.1% O_2 (Olive et al., 2002). Similarly, the presence of hypoxia in tumours has been confirmed through the use of NMR spectroscopy of ^{31}P signals to monitor hypoxia specific markers such as pimonidazole (Azuma et al., 1997; Vaupel et al., 1989b) and the use of hyperpolarized MRI (Pacheco-Torres et al., 2010).

Classically, two forms of hypoxia were described: chronic, diffusion-limited hypoxia, and acute, perfusion-limited hypoxia. The former, described above in the seminal work by Thomlinson, can result from tumours outgrowing their blood supply, altered oxygen delivery in spite of angiogenesis, or reduced oxygen carrying capacity of blood (Knowles and Harris, 2001). Acute, perfusion-limited hypoxia occurs due to transient alterations of blood flow and perfusion of the tumour tissue. *De novo* angiogenesis is a hallmark of solid tumours (Hanahan and Weinberg, 2000). This new vasculature is often imperfect, however, and as a result the delivery of oxygen and nutrients to the tumour can heterogeneous and transient with periods of hypoxia ranging from minutes to days.

The partial pressure of oxygen at sea level is 159 mmHg or 21%. In arterial and venous blood it is 12.5% and 5.2%, respectively (Stainsby and Eitzman, 1988). Most mammalian tissues exist at 2 to 9% O_2. Thus, hypoxia is usually defined as less than 2% O_2 and severe hypoxia (or anoxia) is defined as less than 0.01% O_2 (Bertout et al., 2008; Wouters and Brown, 1997). In this thesis, severe hypoxia will refer to less than 0.01% O_2, while moderate hypoxia will refer to 0.1% O_2.

1.1.2 Tumour hypoxia is associated with poor patient outcome

Clinical follow-up of patients with hypoxic tumours has clearly revealed that there is a link between tumour hypoxia and outcome. Polarographic electrode studies demonstrated that uterine cancer patients with tumour oxygen levels of less than 10mmHg (or 1.3%) had significantly worse disease-free and overall survival compared to patients with tumour oxygen above 10mmHg (Hockel et al., 1996). Immunohistochemical studies using CAIX as a surrogate marker for hypoxia demonstrated a clear association between tumour hypoxia and decreased survival and metastasis-free survival after radiation therapy in cervical cancer patients (Loncaster et al., 2001). Likewise, a microarray hypoxia gene signature developed from known hypoxia-regulated genes was prognostic for recurrence-free survival in a publicly available head and neck cancer data set (Winter et al., 2007).

It is now well established that patients with hypoxic tumours have a poorer prognosis than those with well-oxygenated tumours, irrespective of the mode of therapy (Graeber et al., 1996; Harris, 2002; Hockel et al., 1993). The radioresistance of hypoxic tumours has been established for many years. In 1923, Petry first observed a relationship between oxygen pressure and radiosensitivity in vegetable seeds (Bernier et al., 2004; Bertout et al., 2008). Later, Powers and Tolmach demonstrated the importance of oxygen in cancer radiotherapy (Powers and Tolmach, 1964). They irradiated lymphosarcomas in mice breathing either ambient air or hyperbaric oxygen (at 3 atmospheres of pressure) before transplanting them into new host mice. The tumours from the hyperbaric treatment group showed greater levels of cell death compared to the control group, suggesting that oxygen sensitized the tumours to radiotherapy. Churchill-Davidson went on to show similar effects in cancer patients treated with radiation in combination with hyperbaric oxygen (Churchill-Davidson, 1964a, b).

More recent work has clarified the effects of tumour hypoxia on radioresistance. Tumour cells exposed to oxygen pressures below 0.5mmHg or 0.06% O_2 (termed the radiobiologically hypoxic fraction) show almost complete radioresistance. At higher oxygen concentrations (between 0.1% and 2% O_2), partial radioresistance is observed (Wouters and Brown, 1997). Until recently, these effects have been largely attributed to the "oxygen fixation hypothesis", which states that free radicals generated by radiotherapy require intracellular oxygen to generate the greatest damage to DNA and other biomolecules. However, reports of late have implicated a role for intracellular signaling pathways activated by hypoxia in the resistance to radiotherapy (discussed below) (Harada et al., 2007; Liu et al.; Rouschop et al., 2009a; Rouschop et al., 2009b; Wouters and Koritzinsky, 2008; Wouters et al., 2004).

In addition to radioresistance, there is some evidence that hypoxia decreases the sensitivity of cancer cells to certain chemotherapeutic agents. Mostly through the use of *in vitro* cell culture and animal models, it has been suggested that hypoxic cells are less susceptible to doxorubicin, 5-fluorouracil, and methotrexate (Grau and Overgaard, 1992; Matthews et al., 2001; Wilson et al., 1989). It is quite likely that some of these effects are due to the reduced number of cycling cells in the hypoxic fraction, decreased perfusion of the tissue for drug delivery, and lower pH in the tumour microenvironment (for example, doxorubicin uptake is reduced by an acidic cellular microenvironment) (Minchinton and Tannock, 2006). However, it has also been suggested that adaptive signaling pathways may play a role in resistance, such as by upregulating multidrug resistance proteins (Comerford et al., 2002; Liu et al., 2009).

1.2 Adaptive mechanisms of hypoxia tolerance

Throughout the 1980s and the 1990s, much of the work in oncology research focused on the identification of the genetic alterations that arise as a result of

somatic mutation in tumour cells. This era heralded the discovery of oncogenes, tumour suppressor genes, and DNA repair mutations. Crucially, the concept of clonal selection was proposed and its key role in the development of cancer and the acquisition of resistance began to be understood (Hanahan and Weinberg, 2000; Nowell, 1976). Indeed, the hypoxic microenvironment drives malignant progression and selects for hypoxia-resistant clones. For example, Graeber and coworkers elegantly demonstrated that hypoxia selects for cells with diminished apoptotic potential both *in vitro* and *in vivo*, in part by selection for mutations of the p53 tumour suppressor gene (Graeber et al., 1996).

In recent years, however, the importance of adaptive mechanisms of resistance has been realized. Several of the adaptive mechanisms by which selected cancer cells are able to survive the harsh microenvironmental pressures of the tumour have been greatly elucidated, and their potential as targets for therapy has been highlighted (Gillies and Gatenby, 2007; Ruan et al., 2009; Semenza, 2000). Several O_2-reponsive pathways have been identified that play a major role in the resistance of tumour cells to hypoxia and to cancer therapy. These include the responses mediated by the hypoxia-inducible factor family of transcription factors, the kinase mammalian target of rapamycin, and the unfolded protein response (Wouters and Koritzinsky, 2008).

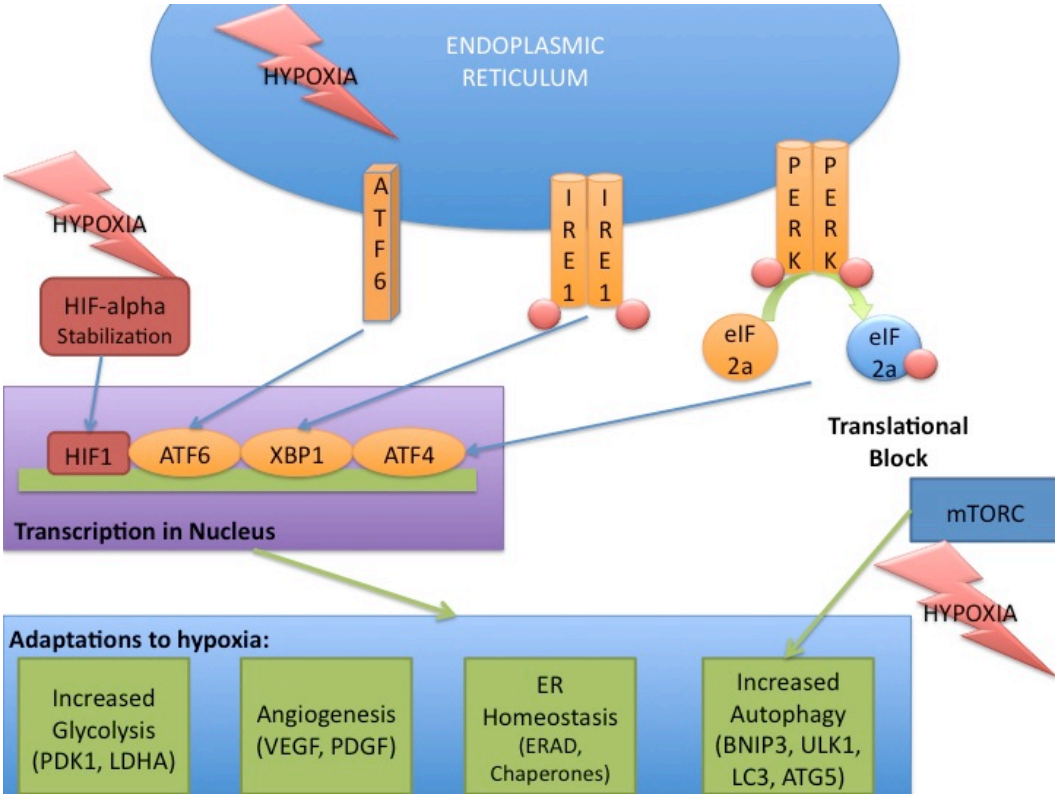

Figure 1.2 Adaptive mechanisms of hypoxia tolerance.

There are three major pathways of adaptation to hypoxia: the HIF pathway, the mTOR pathway, and the unfolded protein response.

1.2.1 The hypoxia-inducible factors

The hypoxia-inducible factors (HIFs) are a family of hypoxia-responsive transcription factors that have widespread effects on tumour cell metabolism, angiogenesis, metastasis, and survival. The HIFs are obligate heterodimers comprised of a labile alpha subunit and a stable beta subunit. There are three HIFα isoforms in mammals: HIF-1α, HIF-2α, and HIF-3α. HIF-1α is ubiquitously expressed in all cells, whereas HIF-2α and HIF-3α are selectively expressed in vascular endothelial cells, renal interstitial cells, liver parenchymal cells, and cells of myeloid lineage. HIF-1α and HIF-2α are structurally quite similar, though they can exert opposing effects on cellular biology (Harris, 2002; Majmundar et al., 2010; Semenza and Wang, 1992).

Regulation of the HIFs is achieved through the labile alpha subunit. In normoxic conditions, the HIFα subunit becomes hydroxylated by proline hydroxylases (PHDs). This post-translational modification targets the alpha subunit for ubiquitination by the E3 ubiquitin ligase, von Hippel-Lindau protein complex. The ubiquitinated unit is then quickly degraded by the proteasome. PHDs use O_2 as a substrate in the hydroxylation of HIFα. Thus, in the absence of oxygen, HIFα is stabilized and can form transcriptionally active heterodimers with HIFβ or ARNT. These bind to the *cis*-acting hypoxia response elements found in the promoter regions of target genes (Cockman et al., 2000; Ivan et al., 2001; Jaakkola et al., 2001; Kaelin and Ratcliffe, 2008; Kamura et al., 2000; Maxwell et al., 1999; Ohh et al., 2000; Tanimoto et al., 2000; Wang et al., 1995).

The HIFs regulate a wide variety of gene responses, playing a key role in various aspects of cancer development. The role of HIF-1 and HIF-2 has been well-studied: they regulate many of the same target genes, including those involved in proliferation (MYC, Cyclin D1), angiogeneisis (VEGF, PDGF), pH regulation (CAIX), apoptosis and autophagy (NDRG2, BNIP3), glucose metabolism (PDK1, LDHA), DNA damage response (GADD45A), microRNAs (MIR210), extraceullar matrix remodeling (LOX, MMP1), and cell migration and invasion. HIF-3 is thought to act as a dominant-negative regulator of HIF-1 and HIF-2 activity in certain contexts (CXCR4, SDF1) (Gordan and Simon, 2007; Harris, 2002; Majmundar et al., 2010).

Human cancer biopsy samples and mouse models have shown that the HIFs play an important role in cancer progression. Studies looking at total HIFα expression have correlated it with poor clinical prognosis in a variety of cancer types (Semenza, 2007). HIF-1 and HIF-2 are highly expressed in many cancers. The accumulation of HIF-1 has been associated with poor patient survival in early-stage cervical cancer, breast cancer, oligodendroglioma, ovarian cancer, endometrial cancer, and oropharyngeal squamous cell carcinoma (Bertout et al.,

2008). However, the impact of HIF-1 and HIF-2 on tumourigenesis seems to be highly context-dependent and is still quite controversial. In non-small-cell lung cancer and head an neck squamous cell carcinoma, for example, HIF-1α expression correlates with lower cancer stage or decreased patient mortality while HIF-2α expression is a negative prognostic factor (Majmundar et al., 2010).

1.2.2 Mammalian target of rapamycin

The mammalian target of rapamycin (mTOR) is an important intracellular integrator of signals pertaining to nutritional status, growth factors, and hypoxia. It transmits these signals to downstream effectors of proliferation, protein synthesis, and autophagy (Guertin and Sabatini, 2007). The mTOR kinase nucleates two signaling complexes: mTORC1 and mTORC2. mTORC1 is a rapamycin-sensitive signaling complex that responds to hypoxia, energy deprivation, and growth factors. It contains mTOR, RAPTOR, PRAS40, and mLST8 (Hara et al., 2002; Kim et al., 2002; Vander Haar et al., 2007). mTORC2, on the other hand, responds predominantly to growth factor signaling, contains Rictor, and is insensitive to rapamycin (Jacinto et al., 2004; Loewith et al., 2002). The biology and relevance of mTORC1 signaling are better described than that of its brother mTORC2, and are thought to be more pertinent to tumour hypoxia.

As part of mTORC1, the mTOR kinase is activated "in times of plenty"—that is, in the presence of ample nutrients, oxygen, and growth factors. Active mTOR stimulates the anabolic processes of protein synthesis and cell growth through the phosphorylation and activation of proteins such as S6 kinase (p70S6K) and eukaryotic elongation factor 2 kinase (EEF2), and the deactivation of eukaryotic translation initiation factor 4E binding protein 1 (4E-BP1). mTOR also blocks the catabolic process of autophagy by phosphorylation and inactivation of the key autophagy protein UNC51-like kinase 1 (ULK1) (autophagy and ULK1 will be

discussed more thoroughly in the sections that follow) (Browne and Proud, 2004; Ganley et al., 2009; Guertin and Sabatini, 2007; Wouters and Koritzinsky, 2008).

Hypoxia inhibits mTOR through multiple pathways (Figure 1.3). Hypoxia results in the stabilization of HIF-1α and transcription of the downstream genes REDD1 and BNIP3. REDD1 appears to interact with and reactivate the TSC1-TSC2 complex (DeYoung et al., 2008). In turn, this complex inhibits RHEB (GTP-loaded RHEB is essential for mTOR activity). Similarly, BNIP3 and PML can directly bind and to and block RHEB activity (Bernardi et al., 2006; Li et al., 2007). AMPK, on the other hand, seems to be activated by hypoxia-induced energy stress. Falling levels of ATP stimulate the activation of AMPK, which then phosphorylates and activates the TSC1-TSC2 complex, thereby blocking mTOR activity (Liu et al., 2006).

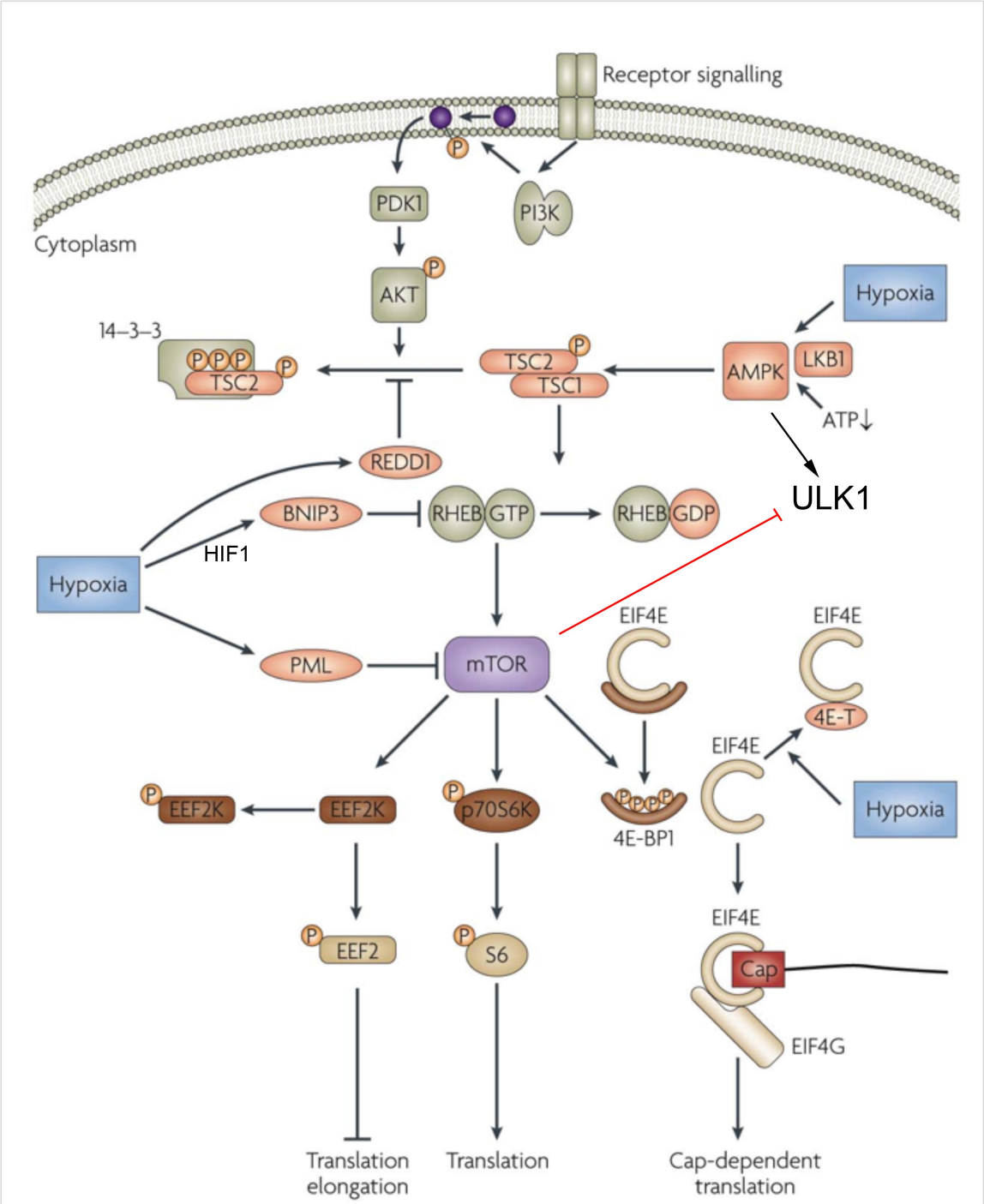

Figure 1.3 Hypoxic inhibition of mTOR.

Hypoxic inhibition of mTOR occurs by a variety of mechanisms. Adapted from (Wouters and Koritzinsky, 2008).

1.2.3 The unfolded protein response

1.2.3.1 Overview

A third oxygen-responsive pathway is the unfolded protein response (UPR). The UPR is a key regulator of endoplasmic reticulum homeostasis, and detects perturbations in protein folding and oxidative status. ER stress, as it is commonly termed, refers to a mismatch between the load of unfolded and misfolded proteins in the ER and the capacity of the cellular machinery to deal with that load. ER stress can be caused by changes in glycosylation, redox status, glucose availability, calcium homeostasis, and secretory protein load (Wouters and Koritzinsky, 2008). Severe hypoxia (<0.01% O_2) and prolonged moderate hypoxia are well-established inducers of ER stress (Koumenis et al., 2002; Romero-Ramirez et al., 2004). It is not certain how hypoxia causes this stress, but it has been suggested that O_2 plays a direct role in ER protein maturation, including oligosaccharide modifications, isomerization, quality control, protein export, and disulfide bond formation. In particular, several studies have shown that O_2 can act as a terminal acceptor of electrons in the process of disulfide bond formation, involving FAD, ERO1P, and PDI, which may explain the ER stress produced by hypoxia (Tu and Weissman, 2002, 2004).

ER stress is detected by three ER-resident transmembrane sensors: inositol-requiring enzyme-1 (IRE1), activating transcription factor-6 (ATF6), and protein kinase RNA(PKR)-like ER kinase (PERK). Each of these transmembrane proteins contain a luminal ER stress-sensing domain, which detects the accumulation of unfolded or misfolded proteins, and a cytoplasmic effector domain, which elicits an adaptive response to overcome this stress (Bernales et al., 2006; Schroder and Kaufman, 2005). In general, these adaptations can be classified into three groups:

- Reduction of misfolded protein load: inhibition of global mRNA translation, enhanced ER-associated protein degradation, and increased autophagy of organelles and protein aggregates
- Increased protein folding capacity: upregulation of chaperone proteins and oxidoreductases
- Activation of cell death: if ER stress is insurmountable and overwhelming, apoptosis pathways are activated to eliminate potentially pathogenic cells

1.2.3.2 Inositol-requiring enzyme-1

IRE1 is a type 1 ER-resident transmembrane protein with a novel luminal domain and a cytoplasmic portion that contains a protein kinase domain and an endonuclease domain (Cox et al., 1993; Credle et al., 2005). In unstressed conditions, the chaperone protein BiP maintains IRE1 in an inactive, monomeric form by binding to its luminal domain. Thus, when unfolded proteins accumulate in the ER lumen, BiP dissociates from IRE1 and binds to these proteins. Freed monomeric IRE1 then oligomerizes and undergoes trans-autophosphorylation at the cytoplasmic domain to form an active complex. To date, the only known target of the IRE1 kinase domain is itself (Papa et al., 2003; Shamu and Walter, 1996). Activated IRE1 can effect a downstream response in two ways: it can catalyze the splicing of an active transcription factor, or it can act as a site for protein-protein interaction to activate a downstream signaling cascade.

The endonuclease activity of IRE1 is well described. This enzymatic activity catalyzes the precise nucleolytic cleavage of an mRNA that encodes the transcription factor XBP1. IRE1 cuts the precursor mRNA of XBP1 at two locations, splicing out a short intron. This truncated form of the XBP1 mRNA encodes the active transcription factor (the unabridged version contains a frameshift, and the resulting protein is thought to act as an inhibitor of XBP1 signaling) (Calfon et al., 2002). This active transcription factor then translocates

to the nucleus, where it drives the expression of genes involved in adapting to ER stress (Ron and Hubbard, 2008).

The adaptor functions of IRE1 are less understood; however, it has been shown that the pro-apoptotic proteins BAX and BAK can directly interact with IRE1 to enhance UPR signaling (Hetz et al., 2006). Alternatively, IRE1 can form a complex with TRAF2 and AIP1 to signal downstream activation of c-Jun N-terminal kinase (JNK) (Luo et al., 2008; Urano et al., 2000), which can activate apoptosis and autophagy (Ogata et al., 2006).

1.2.3.3 Activating transcription factor-6

The ATF6 arm of the UPR is the most poorly described. Much like IRE1, ATF6 contains a luminal domain that is bound by BiP under unstressed conditions, and released with the accumulation of unfolded proteins in the ER (Ron and Walter, 2007). However, the mechanism of activation is quite different: ATF6 is synthesized as an inactive precursor, tethered to the ER membrane by a transmembrane segment. Once released from BiP, ATF6 is transported from the ER to the Golgi apparatus, where it is cleaved by two Golgi-resident enzymes—site 1 protease and site 2 protease (Haze et al., 1999). This action results in the release of the cytosolic, DNA-binding, portion of ATF6, which can then translocate to the nucleus and induce gene expression.

The downstream effects of ATF6 are poorly understood. However, it is thought that ATF6 activates a subset of UPR target genes (Ron and Walter, 2007). Specifically, it has been shown that a number of ATF6 target genes encode ER quality control proteins and ER-resident proteins (Adachi et al., 2008). Furthermore, ATF6 has been shown to be induced by hypoxia in a model of ischemia-reperfusion in rat myocardial cells, and to play a role in the survival of this stress both *in vitro* and *in vivo* (Doroudgar et al., 2009; Martindale et al.,

2006).

1.2.4 PKR-like ER kinase

PKR-like ER kinase (PERK) is structurally and functionally similar to IRE1. In unstressed cells, the ER luminal domain is bound by BiP in a monomeric state, rendering the sensor inactive. Under stressed conditions, the accumulation of unfolded proteins and sequestration of BiP results in the oligomerization of PERK and activating trans-autophosphorylation. Unlike IRE1, however, the kinase domain of PERK has a cytoplasmic target: eukaryotic translation initiation factor 2 alpha (eIF2α) (Bertolotti et al., 2000; Harding et al., 1999).

The phosphorylation of eIF2α at serine residue 51 is a crucial regulatory event in cellular control of translation. In unstressed cells, dephosphorylated eIF2α associates with the initiator Met-tRNA$_i^{Met}$ and GTP to form a tertiary complex. This complex associates with the 40S ribosome, loading it with the Met-tRNA$_i^{Met}$ to form the 43S preinititation complex. This complex can then bind an mRNA near the 5' cap, and scan along the molecule until it reaches and recognizes the start codon. Recognition of the translation start site results in the hydrolysis of GTP to GDP by eIF2 and dissociation of eIF2-GDP, allowing the large (60S) ribosomal subunit to bind and form the 80S initiation complex. However, with the onset of ER stress and activation of PERK, the phosphorylation of eIF2α inhibits the guanine nucleotide exchange factor eIF2B, which recycles eIF2 to its active GTP-bound form. This event prevents the formation of the GTP-Met-tRNA$_i^{Met}$-eIF2α complex, and thus globally represses mRNA translation (Harding et al., 2000; Koritzinsky et al., 2006; Ramaiah et al., 1992; Sudhakar et al., 2000; van den Beucken et al., 2006; Wek et al., 2006).

This UPR-mediated reduction in mRNA translation is crucial in reducing the load of newly synthesized proteins entering the ER lumen. This mechanism reduces

the burden on the protein-folding machinery of the ER, thereby reducing ER stress, with the added benefit of decreasing ATP consumption by costly and ineffectual protein synthesis. This tightly regulated mechanism, one would infer, is important for surviving ER stress (Lu et al., 2004b; Scheuner et al., 2001).

Like the other two arms of the UPR, PERK is activated by hypoxia. Autophosphorylation of PERK and downstream phosphorylation of eIF2α is observed within minutes in cells exposed to severe hypoxia, or somewhat more slowly in cells exposed to moderate levels of hypoxia. PERK activation is important for survival in hypoxic conditions. PERK knockout MEFs show increased sensitivity to hypoxia *in vitro*, and tumours derived from these cells grow slower and the hypoxic cells in these tumours display greater levels of apoptosis. Similarly, MEFs expressing an unphosphorylatable serine-51-alanine knock-in form of eIF2α are hypersensitive to ER stress and display retarded tumour growth (Bi et al., 2005; Dubois et al., 2009; Koritzinsky et al., 2007; Koumenis et al., 2002).

In addition to the important role of PERK in reducing global mRNA translation, it also plays a role in the selective translation of specific mRNA transcripts under hypoxia (Lu et al., 2004a). One such transcript is that of the protein activating transcription factor 4 (ATF4), a key transcriptional effector of the UPR (Ameri et al., 2004; Blais et al., 2004). The transcript of ATF4 contains two conserved upstream open reading frames (uORF) in the 5' untranslated region (UTR). The 5' proximal uORF is a positive, *cis*-acting element encoding a tripeptide. It facilitates ribosomal scanning and translation reinitiation at the next uORF. This second uORF encodes a peptide whose coding sequence overlaps the main ATF4 ORF further downstream, and thus serves to inhibit translation of the ATF4 transcription factor under unstressed conditions. However, with the onset of ER stress and phosphorylation of the bulk of cellular eIF2α, the time required for reinitiation substantially increases. As a result, reinitiation at the second uORF

fails to occur and the ribosome scans further along the transcript, reinitating at the *bona fide* ATF4 ORF (Vattem and Wek, 2004).
It is worthy to note that ATF4 is not the only transcript whose translation is regulated in this fashion. Similarly, CHOP and CAIX are regulated in this manner (Koritzinsky et al., 2006). Relevant to breast cancer, it has been shown that BRCA2 and other DNA repair proteins are inefficiently translated in severe hypoxia (Chan et al., 2008).

In addition to PERK, a number of other kinases are known to phosphorylate eIF2α and attenuate global mRNA translation. These include PKR, GCN2, and HRI. PKR is a ubiquitously expressed protein kinase that is activated by double stranded RNA and is thought to participate in the antiviral pathway mediated by interferon (Prostko et al., 1995; Srivastava et al., 1995; Srivastava et al., 1998). GCN2 is activated by uncharged tRNA molecules, and thus also by amino acid starvation (Zhang et al., 2002; Zhu et al., 1996). HRI is activated by heme depletion, and is predominantly expressed in erythroid cells (Uma et al., 1999). Thus, these four pathways converge on eIF2α, activating a common set of downstream effects. Due to the integrative nature of this network, signaling downstream of eIF2α has thus been termed the integrated stress response (ISR) (Harding et al., 2003). ATF4 is the main transcriptional regulator of the ISR and activates various UPR-target genes to reduce ER stress and return the ER to homeostasis (Figure 1.4).

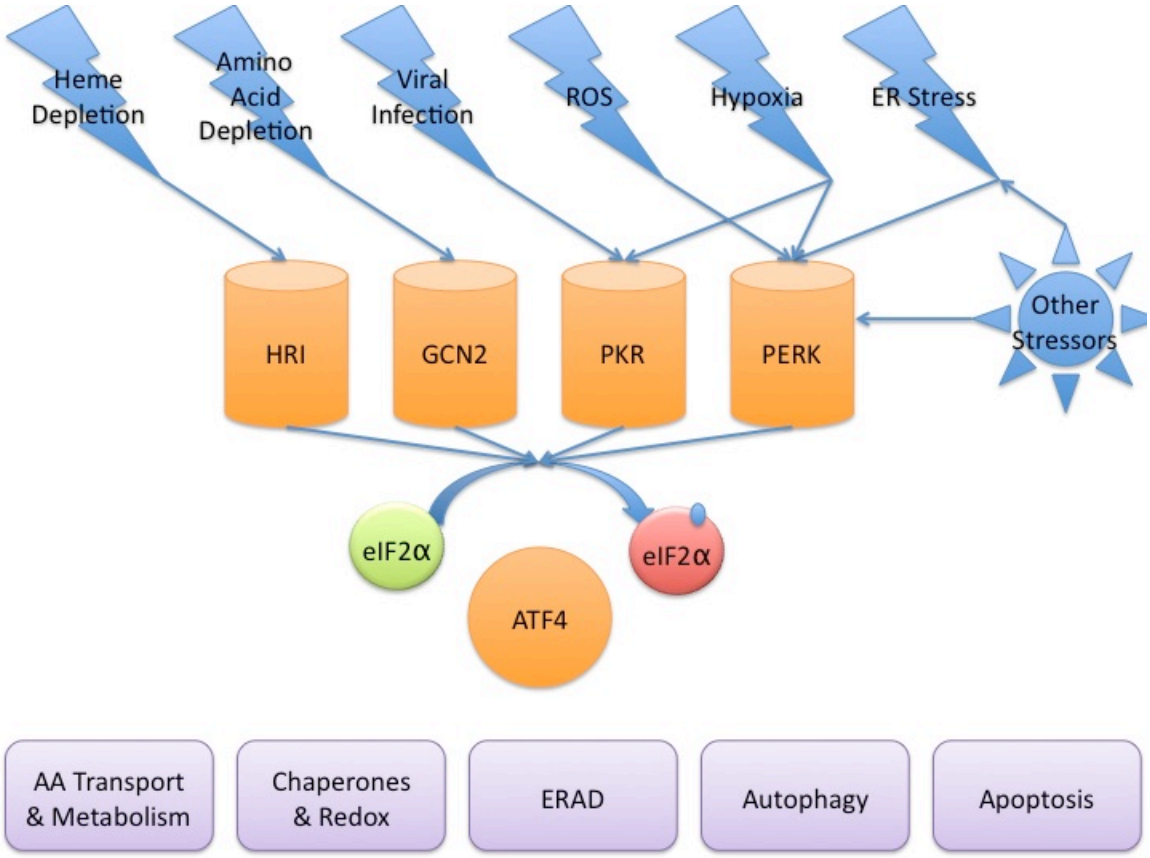

Figure 1.4 The integrated stress response.

The integrated stress response includes upstream activation of any of four kinase sensors that converge on the phosphorlyation of eIF2α and accumulation of ATF4.

1.2.5 ATF4 and the integrated stress response

ATF4 is induced in response to ER stress and by severe hypoxia in a PERK- and eIF2α-dependent fashion. Work from this lab and other groups demonstrated that ATF4 is upregulated in malignant breast cancer and cervical cancer in hypoxic areas of tumours (Ameri et al., 2004; Bi et al., 2005). ATF4 expression colocalizes with hypoxic areas in tumour xenografts derived from transformed MEFs, though not in those derived from MEFs with the eIF2α S51A knock-in mutation. ATF4 is strongly induced in a variety of cell lines in response to a variety of stressors, including severe hypoxia, thapsigargin, tunicamycin, proteasome inhibition,

glucose deprivation, amino acid deprivation, and oxidative stress (Rzymski et al., 2009).

The role of ATF4 in surviving ER stress has been a topic of controversy for some years. ATF4 can activate both pro- and anti-apoptotic pathways, depending on the cellular context, and the intensity and duration of the stress. The emerging model suggests, however, that in response to ER stress ATF4 initially activates pro-survival pathways and attempts to return the cell to homeostasis. Although, if these adaptations prove to be insufficient or untimely, there are latent mechanisms in place to activate cell death through apoptosis. For example, elegant work by Harding and coworkers showed that in response to ER stress, ATF4 regulates the expression of genes involved in translation, amino acid import, and metabolism (such as asparagine synthetase and glycine transporter 1), in redox or detoxification (such as ERO1 like oxidoreductase and heme oxygenase), transcription, protein secretion (such as pentaxin related gene), and signaling (such as IGFBP-2 and Wisp1) (Harding et al., 2003). The authors went on to show that ATF4 and the ISR plays a pivotal role in the resistance to oxidative stress both *in vitro* and in worms. More recent studies have implicated ATF4 in the regulation of glucose metabolism (Yoshizawa et al., 2009), lipogenesis (Bobrovnikova-Marjon et al., 2008), DNA damage(Bobrovnikova-Marjon et al.), angiogenesis (Bi et al., 2005; Ghosh et al.), and pH (van den Beucken et al., 2009). Furthermore, it has been shown that ATF4 plays a pivotal role in surviving amino acid deprivation and glucose deprivation through the upregulation of amino acid transporters (Ye et al., 2010). ATF4 can also protect cells through the activation of autophagy (Rzymski et al., 2009). Recent work by this group and others has shown that ATF4 can activate the transcription of the autophagic machinery, including MAP1LC3B, and ATG5 (Milani et al., 2009; Rouschop et al., 2010; Rzymski et al., 2010). A more in-depth discussion of the role of ATF4 in autophagy appears in the sections that follow.

There have been several studies that implicate ATF4 in a pro-death response to ER stress. Recent work has shown that ATF4 can activate ER stress-induced apoptosis in neuroectodermal tumour cells through transcriptional induction of the BH3-only protein NOXA (Armstrong et al., 2010). Treatment of tumour cells with the ERAD inhibitor Eer1 and bortezomib also induces ATF4-dependent cell death though NOXA (Wang et al., 2009). Similarly, ATF4 has been shown to drive apoptosis in response to ER stress and NSAIDs in neuronal cells and tumour cells, respectively, through the BH3-only protein PUMA (Galehdar et al., 2010; Ishihara et al., 2007).

As mentioned above, the duration of ER stress is important in determining cell fate. ATF4 plays a role in this timing mechanism through the induction of the transcription factor CHOP. CHOP has been suspected to cause apoptosis via repression of BCL2. Additionally, however CHOP transcriptionally induces the expression of GADD34 (Wang et al., 1998; Zinszner et al., 1998). GADD34 encodes the protein phosphatase targeting subunit involved in dephosphorylation of eIF2α. Thus, induction of GADD34 results in dephosphorylation of eIF2α, and derepression of protein translation. This negative feedback loop is known to play a role in the normal deactivation the ISR following the resolution of ER stress (Lee et al., 2009; Ma and Hendershot, 2003; Novoa et al., 2001). Additionally, however, if the ER stress has not been fully resolved, the derepression of translation is thought to overwhelm the cell, forcing ER stress induced apoptosis and cell death (Marciniak et al., 2004).

Despite the dual role of ATF4 in promoting both survival and death, ATF4 appears to be an important factor in the maintenance of solid tumours. There is a plethora of *in vitro* data to support the role of ATF4 and the ISR in the adaptation to hypoxia, nutrient deprivation, and oxidative stress, all of which are likely to be present in the microenvironment of a growing tumour (Rzymski and Harris, 2007; Rzymski et al., 2009). There are three major *in vivo* studies that have highlighted

the importance of ATF4 and the ISR in the maintenance of solid tumours. In 2005, Bi and coworkers showed that tumours derived from immortalized PERK$^{-/-}$ MEFs or S51A-eIF2α knock-in MEFs grow much more slowly than their wildtype counterparts, and contained a greater number of apoptotic cells in the hypoxic regions. They also showed that human tumour cells expressing a dominant negative PERK construct grew tumours much more slowly than the matched control cells (Bi et al., 2005). In 2010, work from the Wouters group demonstrated the therapeutic potential in targeting the ISR by producing a doxycycline-inducible S51A-eIF2α construct and stably expressing it in HCT116 colon cancer cells. They allowed tumours to reach about 150mm^3 before feeding the mice doxycycline. The growth of the S51A tumours slowed dramatically from this point, while the isogenic controls grew through the antibiotic treatment (Rouschop et al., 2010). Finally, Ye and coworkers considered the effects of the GCN2 arm of the ISR in nutrient deprivation. In this striking work, they showed that tumours derived from immortalized GCN2$^{-/-}$ MEFs or from HT1080 human tumour cells stably expressing an shRNA against GCN2 were unable to form tumours of substantial size, while their matched controls grew normally. They went on to show similar results in HT1080 cells stably expressing an shRNA against ATF4 (Ye et al., 2010). To date, this is the only study that has shown the effects of directly targeting ATF4 in human tumour cells in a xenograft model. In summary, these studies have demonstrated the importance of the ISR in tumour formation and maintenance, and in the tolerance of intratumoural hypoxia, nutrient deprivation, and ER stress.

1.3 Autophagy

Autophagy is an evolutionarily conserved catabolic process. Through the formation of double-membraned vesicles called autophagosomes, bulk cytoplasmic components (macroautophagy) are encapsulated and delivered to lysosomes, where they are degraded, recycling amino acids and nutrients.

Autophagy is an important survival mechanism for cells subjected to metabolic stress or starvation (Mizushima, 2005). In addition to generating valuable nutrients, damaged organelles such as mitochondria (mitophagy) or ubiquitinated protein aggregates (chaperone-mediated autophagy) can be selectively eliminated (Goldman et al.; Kanki and Klionsky, 2009; Kraft et al.). The work of this thesis is primarily concerned with macroautophagy, which will be simply called autophagy.

To date, genetic studies in yeast have identified more than 30 autophagy-related genes (ATGs) and many of their mammalian orthologs (Suzuki and Ohsumi, 2007; Xie and Klionsky, 2007). The process of autophagy is often described as triphasic (Figure 1.5):

1. The initation of phagophore formation.
2. The elongation of the nascent autophagosome and capture of cargo.
3. The maturation and fusion of the autophagosome with acidic lysosomes to form an autophagolysosome.

Following digestion by lysosomal acid hydrolases, the contents of the autophagolysosome are released to the cytosol for further use in the cell's metabolism.

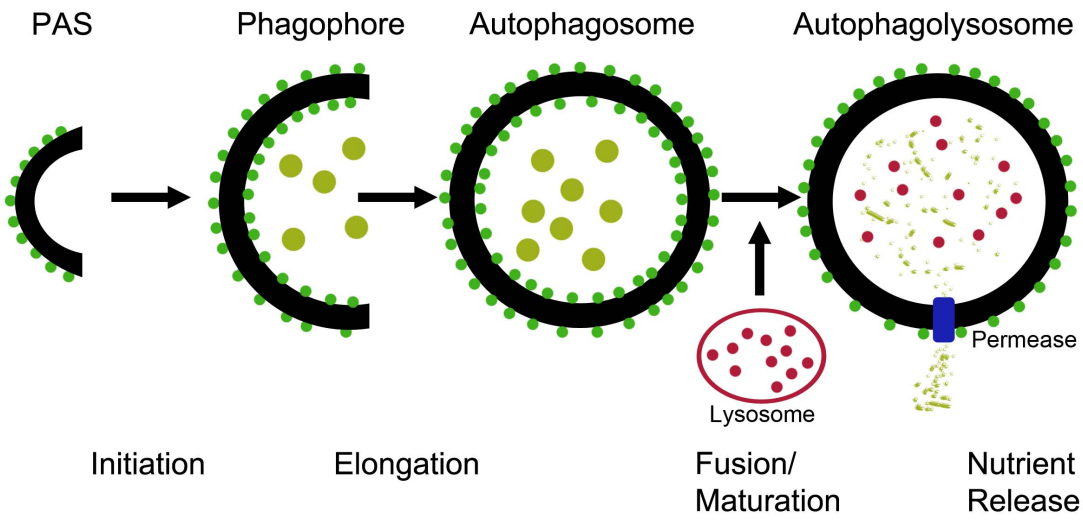

Figure 1.5 The process of autophagy.

Autophagy can be described as three steps: initiation, elongation, and fusion/maturation. Green dots represent LC3-II, yellow dots represent cytosolic cargo, and red dots represent lysosomal acid hydrolases. Following digestion of intravesicular contents, lysosomal permeases release materials back into the cytosol for future use.

Autophagy initiation requires the activity of the Vps34 class III phosphatidylinositol 3-kinase (PI3K) complex. Vps34 is part of a protein complex consisting of ATG6/beclin 1 (BCN1), AMBRA1, ATG14/barkor, UVRAG, and p150/Vps15(Itakura et al., 2008; Sun et al., 2008). Interaction of BCN1 and AMBRA1 with Vps34 enhances its PI3K activity, promoting the production of phosphatidylinositol-3-phosphate (PI3P). PI3P-enriched structures are formed upon starvation and are necessary for autophagy induction, though their exact role in the process of phagophore initiation is unclear(Axe et al., 2008). In the fed state, BCN1 is sequestered by the anti-apoptotic proteins BCL2 and Bcl-X_L, which thus repress PI3K activity. However, starvation or other stressors result in the liberation of BCN1 from this complex through the direct protein-protein interaction of BH3-only proteins with BCL2 or through the phosphorylation of BCL2 by JNK1 (Levine et al., 2008; Wei et al., 2008a; Wei et al., 2008b).

Recent work has also demonstrated the essential role of the mammalian ortholog of yeast ATG1, UNC51-like kinase 1 (ULK1) in the initiation and elongation phases of autophagy. ULK1 forms a complex with focal adhesion kinase family interacting protein of 200kDA (FIP200) and ATG13(Hara and Mizushima, 2009; Hara et al., 2008; Kamada et al., 2000) at the preautophagosomal stucture (PAS), where it can act to increase the activity of Vps34 and ATG9 (Di Bartolomeo et al., 2010; Reggiori et al., 2004; Young et al., 2006). In nutrient-rich conditions, mammalian target of rapamycin (mTOR) inhibits the activity of this complex by phosphorylating ULK1 and ATG13. However, under stress conditions, such as starvation, mTOR activity is attenuated and the ULK1 kinase complex becomes active, driving autophagosome formation (Kamada et al., 2000; Mizushima; Noda

and Ohsumi, 1998; Ravikumar et al., 2004; Wullschleger et al., 2006). Additionally, the ULK1 complex has been shown to interact directly with the nutrient-sensing AMPK. AMPK directly phosphorylates and activates ULK1 to promote the induction of autophagy in starvation (Kim et al.; Lee et al.; Zhao and Klionsky). As they are the major focus of this work, the regulation of BCN1 by the BH3-only proteins and of ULK1 will be discussed in greater detail in chapters three and four of this thesis, respectively.

Autophagosome elongation involves several key autophagy genes. ATG9 is a transmembrane protein that cycles between the trans-Golgi network and late endosomes or ER membranes, and is thought to play a role in the expansion of the nascent phagophore as it encloses its cargo. Additionally, there are two ubiquitin-like conjugation reactions that are necessary for elongation. The first of these involves the conjugation of ATG5, ATG12, an ATG16 to form an 800kDA complex. This complex is necessary for the expansion of the preautophagosomal membrane, though it is dispensable following closure of the autophagosome (Mizushima et al., 1998a; Mizushima et al., 1998b). The second reaction involves the conjugation of a phosphatidylethanolamine (PE) to the cleaved fragment of ATG8 or MAP1LC3 in mammals to form LC3-II. This lipidated form of LC3 is specifically targeted to the elongating autophagosome membrane, and unlike the ATG5-12-16 complex, remains bound to both the inner and outer membranes throughout the autophagic process. Thus, LC3-II is an excellent biomarker for following measuring autophagy (Kabeya et al., 2000; Tanida et al., 2004a, b). Immunocytochemistry for punctate LC3-positive structures or Western blotting for LC3-II protein levels are therefore well utilized tools in the study of autophagy (Klionsky et al., 2008).

Following closure of the phagophore about its cargo to form the autophagosome, autophagsomes will fuse with lysosomes to facilitate the digestion of autophagic cargo by acid hydrolases. This process involves many proteins, including ESCRT, the SNAREs, Rab7, and UVRAG (Gutierrez et al., 2004; Lee et al., 2007a; Lee and Gao, 2008; Ravikumar et al., 2008). Perturbation of the lysosomes themselves can

result in a blockade of fusion and digestion. Treatment with chemicals such as chloroquine or bafilomycin A1 inhibits the fusion of lysosomes with completed autophagosomes by inhibiting the lysosomal H^+-ATPase (Gonzalez-Polo et al., 2005; Marceau et al., 2009; Poole and Ohkuma, 1981). This prevents the digestion of not only the autophagic cargo, but also of the LC3-II bound to the inner membrane. Thus, flux through the autophagic pathway can be assessed by blocking fusion and measuring the accumulation of LC3-II by western blot or immunocytochemistry (Klionsky et al., 2008).

1.3.1 Autophagy as a survival pathway

As mentioned above, autophagy is a catabolic process. Through the formation of double-membraned vesicles, autophagy sequesters bulk cytoplasm, organelles, protein aggregates, and bacteria and routes them for destruction and recycling by the lysosome. Autophagy is activated in response to glucose deprivation, amino acid deprivation, growth factor withdrawal, treatment with cytotoxic drugs, radiation, reactive oxygen species, ER stress, and hypoxia. All mammalian cell types thus far examined have the autophagy pathway.

Autophagy has been termed "Type II Programmed Cell Death", while apoptosis is commonly referred to as "Type I Programmed Cell Death". This nomenclature arose from early studies in developmental biology, which implicated autophagy in the elimination of unnecessary cells from developing tissues. Additionally, there have been a few studies that have identified autophagy as a mode of cell death in response to radiation (Tsuboi et al., 2009), or hypoxia in cancer cells (Azad et al., 2008; Lenardo et al., 2009; Yu et al., 2004; Yu et al., 2006b). The hypotheses put forth by this work imagine that very high levels of autophagy result in the destruction of more and more cytoplasm and critical organelles, ultimately fatally crippling the cell.

Despite this potential role as a cell death mechanism, in recent years it has become increasingly clear that in most circumstances autophagy plays an important role in cell survival (Kroemer and Levine, 2008). In response to glucose or amino acid starvation, it is now well accepted that most cells activate autophagy to maintain nutrient and energy homeostasis (Kroemer and Levine; Rabinowitz and White). Genetic knockout MEFs for essential autophagy genes are sensitized to starvation-induced cell death (Egan et al.; Komatsu et al., 2005; Kuma et al., 2004; Yue et al., 2003). Similarly, autophagy is known to play an important role in removing damaged mitochondria. Reactive oxygen species and hypoxia, for example, can promote mitochondrial dysfuction. It has been shown that in some circumstances, mitophagy can be activated to remove these damaged and toxic organelles and reduce cellular free radicals, promoting survival (Scherz-Shouval et al., 2007; Semenza, 2009; Tracy et al., 2007; Tracy and Macleod, 2007; Zhang et al., 2008).

1.3.2 The role of autophagy in adaptation to hypoxia

Hypoxia induces autophagy by HIF-dependent and HIF-independent mechanisms. Under mild and moderate hypoxia, HIF-1 drives the expression of the BH3-only proteins BNIP3 and BNIP3L (NIX), which can disrupt interaction of BCN1 with BCL2, promoting autophagy. Alternatively, both BNIP3 and REDD1, have also been shown to activate autophagy through the inhibition of mTORC1 (Brugarolas et al., 2004; DeYoung et al., 2008). Interestingly, both BNIP3 and NIX have been shown to act as mitochondrial autophagy receptors, and to be essential for hypoxia-induced mitophagy (Youle and Narendra, 2011; Zhang and Ney, 2008).

Under conditions of severe hypoxia, the UPR plays a role in the induction and maintenance of autophagy. Work by this lab and others has shown that ER stress and severe hypoxia induce the transcription of the essential autophagy genes MAP1LC3B and ATG5 through the activity of ATF4 and CHOP, respectively (Rouschop et al., 2009a; Rouschop et al., 2010; Rzymski et al., 2010). Upregulation

of MAP1LC3B is important for maintaining high levels of autophagic flux in persistent hypoxia, and thus promotes cell survival. However, it is important to note that though MAP1LC3B and ATG5 are requisite components of the autophagy machinery, neither of them is involved in the initiation of autophagy.
In this regard, AMP kinase has been shown to play a potential role (Kroemer et al., 2010). AMPK is activated by metabolic stress and hypoxia, and has recently been shown to drive autophagy through direct phosphorylation and activation of the essential autophagy gene ULK1 (Egan et al., 2011; Kim et al., 2011). The work presented in this thesis uncovers an important link between the unfolded protein response and this pathway, demonstrating that ATF4 drives the transcriptional upregulation of ULK1 as well as the BH3-only protein HRK to initiate autophagy in severe hypoxia.

1.3.3 Autophagy and cancer

The role of autophagy in cancer is complex. Accumulating evidence squarely places autophagy as an important survival pathway in many cell types in response to nutrient starvation, hypoxia, chemotherapy, and so forth. However, in apparent contradiction to the prominent role of autophagy in cell survival, several studies have demonstrated that autophagy may in fact act to suppress tumourigenesis. In particular, work from Beth Levine's lab has found that BCN1 is a haploinsufficient tumour suppressor. Monoallelic deletion of *beclin 1* on chromosome locus 17q21 occurs in 40 to 75% of human ovarian, breast, and prostate cancers. Mice with heterozygous loss of *beclin 1* show an accelerated rate of spontaneous tumour development (Aita et al., 1999; Furuya et al., 2005; Liang et al., 1999; Pattingre et al., 2005). Similar results were obtained for other ATG4 (Marino et al., 2007).

Eileen White has provided two explanations for this phenomenon. First, in a series of elegant xenograft experiments, Kurt Degenhardt and Robin Mathew demonstrated that in apoptosis-deficient cells, inhibition of autophagy can result

in necrotic cell death (Degenhardt et al., 2006). *In vivo*, the elevated levels of necrosis can produce high levels of inflammation and promote tumour growth. Mathew went on to show that autophagy could suppress tumourigenesis by limiting the accumulation of p62, damaged mitochondria, ROS, and protein aggregates, which might lead to DNA damage and oncogene activation (Mathew et al., 2009; Mathew et al., 2007).

On the other hand, despite the evidence supporting a role for BCN1 as a haploinsufficient tumour suppressor gene, it is interesting to note that unlike many other tumour suppressor genes, it has never been found to be biallelically mutated in malignant cells (Qu et al., 2003). In contradiction to the work by White and colleagues in clean genetic models such as primary mouse mammary epithelial cells and immortalized baby mouse kidney epithelial cells, pharmacological targeting of autophagy in xenografts studies using aggressive human cancer cell lines demonstrate the potential efficacy of this strategy (Boya et al., 2005; Degenhardt et al., 2006; Karantza-Wadsworth et al., 2007; Rouschop et al., 2009b). However, the potential therapeutic efficacy of targeting the autophagy pathway in established tumours has yet to be demonstrated.

1.4 Specific Aims

It is clear that hypoxia activates a set of adaptive pathways that result in a more aggressive cancer phenotype. The integrated stress response is a major player in mediating resistance to metabolic stress and hypoxia. Recent work has implicated ATF4 as a regulator of the autophagy pathway through the transcriptional induction of the autophagic machinery. It is suspected that ATF4 may also play a part in the initiation of autophagy, but this has yet to be shown. Furthermore, a large body of evidence now exists to support the role of autophagy in tumour cell survival *in vitro* and *in vivo*, and clinical trials are underway using the choloroquine derivative hydroxychloroquine. However, a specific inhibitor of

autophagy has not yet been developed. Thus, this thesis seeks accomplish the following aims:

1. To identify ATF4 target genes that play a role in the hypoxic induction of autophagy in human cancer cells.
2. To characterize the expression and regulation of these genes in human cancer cell lines and spheroid models.
3. To determine the effects of targeting these genes on autophagy and cell survival, in the hopes of validating potential drug targets for cancer therapy.

Chapter 2 Materials and methods

2.1 Antibodies and Reagents

2.1.1 Antibodies

Table 2.1 List of antibodies used in this thesis.

Antibody	*Origin*	*Company*	*WB/IP*	*IF/IHC*
Acetyl-CoA Carboxylase	Rabbit	Cell Signaling Technology	1:500	
ATF4/CREB2	Rabbit	Santa Cruz Biotechnology	1:500	
CAIX (M75)	Mouse	In House	1:2000	1:50 (IHC)
CHOP/GADD153 (B3)	Mouse	Santa Cruz Biotechnology	1:500	1:50 (IHC)
Cleaved Caspase-3 (AF83)	Rabbit	RnD Systems		1:2000 (IHC)
COXIV	Rabbit	Abcam	1:5000	
HIF-1α	Mouse	BD Transduction Laboratories	1:1000	
HIF-2α	Mouse	AbD Serotec	1:500	
HMGB1	Rabbit	Cell Signaling Technology	1:500	
Ki67 (M7240)	Mouse	Dako		1:50 (IHC)
MAP1LC3 (5F10)	Mouse	Nanotools	1:2000	1:250 (IF)
mTOR	Rabbit	Cell Signaling Technology	1:500	
Myc Tag (9E10)	Mouse	In House	1:1000	
NOXA	Mouse	Abcam	1:500	
p70 S6 Kinase	Rabbit	Cell Signaling Technology	1:500	
PARP	Rabbit	Cell Signaling Technology	1:500	
Phospho-Acetyl-CoA Carboxylase (Ser79)	Rabbit	Cell Signaling Technology	1:500	
Phospho-AMPKα (Thr172)	Rabbit	Cell Signaling Technology	1:500	
Phospho-p70 S6 Kinase (Ser371)	Rabbit	Cell Signaling Technology	1:500	
Phospho-PERK	Rabbit	Biolegend	1:500	

(Thr980)				
Phospho-Raptor (Ser792)	Rabbit	Cell Signaling Technology	1:500	
Pimonidazole	Mouse	Chemicon International		1:50 (IHC)
PUMA	Rabbit	Cell Signaling Technology	1:500	
Raptor	Rabbit	Cell Signaling Technology	1:500	
ULK1	Rabbit	Cell Signaling Technology	1:500	
β-Actin (A5316)	Mouse	Sigma	1:2000	

2.1.2 Reagents

Table 2.2 List of chemical reagents used in this thesis.

Reagent	*Company*	*Working Concentration*
Thapsigargin	Calbiochem	300nM
Tunicamycin	Calbiochem	5μg/mL
Bortezomib	Millennium Pharmaceuticals	100nM
MG115	Calbiochem	10μM
MG132	Calbiochem	5μM
Arsenite	Sigma	5μM
DFO	Calbiochem	40μM
Caspase Inhibitor II (ZVAD-FMK)	Calbiochem	50μM
Chloroquine	Sigma	25μM
Bafilomycin A1	Calbiochem	100nM
Pepstatin A	Calbiochem	10μg/mL
E64D	Calbiochem	10μg/mL

2.2 Cell culture

MCF7, MDA-MB-231, HT29, A431, HCT116, HEK293, HeLa and U87 cell lines were provided by Cancer Research UK (Clare Hall), and were cultured in Dulbecco's Modified Eagle's Medium (DMEM) with 10% (v/v) FCS, supplemented with 100units/mL penicillin/streptomycin and 4mM L-glutamine (Gibco). Lines were incubated at 37°C in a non-humidified incubator with 95% air supplemented with 5% carbon dioxide.

2.3 Hypoxic incubations

For incubations in severe hypoxia (<0.01% O_2), the InVivo$_2$ 400 humidified gas-sorted incubator with a glove box (Ruskin) was used. A gas mix of 5% H_2, 5% CO_2, and 90% N_2 was fed into the system. A palladium catalyst maintained near-zero oxygen concentrations by reducing trace oxygen. For incubations in moderate hypoxia (0.1% O_2), a Heto-Holten CellHouse 170 incubator (RS Biotech) was utilized.

2.4 siRNA and DNA transfections

2.4.1 siRNA transfections

RNA interference was carried out using HiPerfect lipid-based transfection reagent as per the manufacturer's recommendations (Qiagen). In brief, cells were seeded at about 50% confluency (5x10^5 cells/100mm plate) either the day before transfection (MCF7 or MDA-MB-231 cells) or at the time of transfection (ie. reverse transfection; A431, HT29, HCT116) in 10mL of growth medium. RNA-lipid complexes were prepared by diluting the specific short interfering RNA molecules in Opti-Mem Glutamax (Invitrogen) and then adding HiPerfect to the mixture and incubating at room temperature for at least 10 minutes. Aliquots of this mixture were then added dropwise to cells in full medium. After 16 to 24 hours, cells were either exposed to hypoxia/drugs or reseeded to a different format for further experiments (for example, to coverslips for staining).

siRNA duplexes were obtained from Eurogentec. Three to four sequences were selected for each target, using Dharmacon's siDesign® Center. Generally, a pool of two to four duplexes was used at a final concentration of 20nM.

Table 2.3 List of siRNA sequences used in this thesis.

Gene	*Sense Sequence*	*Working Concentration*
ATF4	CCA CGU UGG AUG ACA CUU G	20nM
HRK	#1)GATCGTAGAAACACAGAAT #2)GGGAAGCCCTTTGGAAATC	20nM (10nM each)
NOXA	#1)CTACTCAACTCAGGAGATT #2)GCTACTCAACTCAGGAGAT #3)GAAACTTCTGAATCTGATA	20nM (6.6nM each)
PUMA	#1)GGAGACAAGAGGAGCAGCA #2)CCTGGAGGGTCCTGTACAA #3)CGGACGACCTCAACGCACA	20nM (6.6nM each)
Scrambled Control (BNIP3 SCR)	ACGCGACACGCAGGUCGUCAU	20nM
ULK1	#1)GCACAGAGACCGTGGGCAA #2)CCACGCAGGTGCAGAACTA #3)CGGAGAGCCTGCAGGAGAA #4)GAGCAAGAGCACACGGAGA	20nM (5nM each)

2.4.2 DNA transfections

DNA transfections were done using the Fugene 6 transfection reagent (Roche) according to the manufacturer's instructions. Cells were seeded to 80% confluency in full growth medium the day before transfection. Between 100ng and 5μg of DNA was diluted in Opti-Mem Glutamax (Invitrogen). In a separate tube, five times this amount of transfection reagent (reagent volume to DNA mass ratio of 5 to 1) was similarly diluted in Optimem and incubated for 5 minutes at room temperature. At this point, the contents of the tubes were combined and DNA-lipid complexes were allowed to form for 20 to 30 minutes at room temperature. Following this incubation, complexes were added to cells in full growth medium for 16 to 24 hours. At this point, culture medium was changed to

remove unused complexes and cells were treated with drugs/hypoxia or reseeded for additional experiments. Plasmids for DNA transfection included the open reading frames of ATF4 and HRK in either the pCG and pCMV3 backbones, respectively. pCG-ATF4 was cloned and described previously (Liang and Hai, 1997) , and pCMV3-HRK was obtained from OriGene.

2.5 Western Blotting

Following treatment with severe hypoxia, drugs, RNAi, and so forth, cells were washed with ice cold PBS, and lysed in ice-cold RIPA lysis buffer (Sigma), with Complete® Protease Inhibitors (Roche) and PhosphoStop Phosphatase Inhibitors (Roche) already added. A 25-gauge syringe was used to shear DNA and homogenize the samples.

40μg of protein was mixed with 4X LDS NuPage Sample Buffer (Invitrogen) and 10X Sample Reducing Agent (Invitrogen), and then heated for 10 minutes at 95°C to denature samples. Proteins were then resolved using SDS polyacrylamide gel electrophoresis (SDS-PAGE) using either pre-cast gels from Invitrogen (4-12% Tris-Acrylamide gradient gels or 16% Tris-Glycine gels) or handmade gels (6% gels, using Protogel reagents from National Diagnostics). A molecular weight marker, Rainbow Ladder Plus (GE Healthcare), was used. Following separation, proteins were transferred to PVDF membrane (Millipore) using a semi-dry system for most proteins or a wet transfer system for the transfer of larger proteins (>120kDa).

After transfer, membranes were blocked for 1 hour with 5% non-fat milk diluted in tris-buffered saline containing 0.1% tween-20 (Sigma) (TBS-T). Following block, primary antibodies were added (diluted in 5% milk/TBS-T) for an overnight incubation at 4°C. Washes were done with 3-4 times (at least 5 minutes each) in TBS-T. HRP-conjugated secondary antibodies raised against the primary

host (Dako) were then added (diluted 1:10,000 in 5% milk/TBS-T) and incubated for 1 hour at room temperature. Again, washes were done 3-4 times. Immunoreactivity was detected by chemiluminescence (ECL reagent and film, GE Healthcare).

2.6 Immunofluorescence

Cells were plated onto square coverslips in 6-well format. 16 to 24 hours later, adherent cells were exposed to hypoxia/drugs for the desired period of time. Following treatment, cells were washed twice in ice-cold PBS on ice and then fixed with methanol at -20°C for 20 minutes. Cells were washed twice more in ice-cold PBS following fixation, and then either stored at 4°C in PBS or processed immediately for staining.

Fixation with methanol makes additional permeabilization steps unnecessary. Thus, 5% FCS/PBS was added directly to coverslips in 6-well format for 2 hours at room temperature to block nonspecific interactions. This was followed by incubation with the primary antibody (diluted in 1% FCS/PBS) overnight at 4°C. Washes were done with PBS (4 x 5 minutes each). Secondary antibodies raised against the primary host and conjugated to a fluorescent probe (AlexaFluor series 488, 594, Invitrogen) were diluted 1:1000 in 1% FCS/PBS and added to the coverslips, and allowed to incubate for 2 hours at room temperature. Washes in PBS were repeated, and the coverslips were mounted onto slides using Vectashield mounting media with DAPI (Vector laboratories). These were sealed using nail polish. Confocal microscopy was done to analyze images.

2.7 RT-qPCR

Total RNA was extracted from cells using Tri Reagent (Sigma), as per the manufacturer's specifications. Reverse transcription of mRNA to produce cDNA was carried out using High Capacity Reverse Transcription Kits (Applied Biosystems), using 2μg of extracted RNA as per the manufacturer's recommendations. RT-qPCR was performed by the SYBR Green method using master mix from Bioline, and cycling was done with a Rotogene RG3000 (Corbett Research). Primers are listed in Table 2.4.

Table 2.4 List of RT-qPCR primers used in this thesis.

Gene	*Forward Primer*	*Reverse Primer*
BAK	CCTGCCCTCTGCTTCTGA	CTGCTGATGGCGGTAAAAA
BAX	ATGTTTTCTGACGGCAACTTC	ATCAGTTCCGGCACCTTG
BCL2	TTGACAGAGGATCATGCTGTACTT	ATCTTTATTTCATGAGGCACGTT
BIK	CCCTATGGAGGACTTCGATTC	GGCTCACGTCCATCTCGT
BIM	CATCGCGGTATTCGGTTC	TGCTTTGCCATTTGGTCTT
CHOP	AAGGCACTGAGCGTATCATGT	TGAAGATACACTTCCTTCTTGAACA
HRK	TACTGGCCTTGGCTGTGC	CACAGGGTTTTCACCAACCT
MCL1	AAGCCAATGGGCAGGTCT	GAACTCCACAAACCCATCCTT
NOXA	GGAGATGCCTGGGAAGAAG	CCTGAGTTGAGTAGCACACTCG
PUMA	GACCTCAACGCACAGTACGA	GAGATTGTACAGGACCCTCCA
Tubulin-α-6	CCCCTTCAAGTTCTAGTCATGC	ATTGCCAATCTGGACACCA
ULK1	TCATCTTCAGCCACGCTGT	CACGGTGCTGGAACATCTC

2.8 Chromatin immunoprecipitation assay (ChIP)

ChIP assays were carried out using the EZ-ChIP Kit (Millipore) as per the manufacturer's instructions. In brief, MCF7 cells were seeded to 80% in 100mm

format (three dishes per treatment) the day before treatment. The following day, cells were exposed to severe hypoxia for 24 or 48 hours or kept in normoxic conditions. At the time of harvest, DNA was cross-linked with 1% paraformaldehyde for 10 minutes at room temperature. Cross-linking was quenched for 5 minutes with 125 mmol/L of glycine. After sonification to 200-1000bp fragments, cell lysates were spun down and 100 µL of supernatant was diluted to 1 mL for immunopreciptation. Samples were pre-cleared with 60 µL of protein G beads. 4µg of anti-ATF4 antibody or IgG control was used for immunopreciptation of the cross-linked DNA-protein complexes. After serial washings, DNA-protein cross-links were reversed and DNA was extracted for PCR. Primers are listed in the table below:

Table 2.5 List of ChIP primers used in this thesis.

Primer Set	*Forward Primer*	*Reverse Primer*
CHOP	AGCCAAAATCAGAGCTGGAA	ACAAGTTGGCAAGCTGGTCT
CHR12	GGGGCCATTTAAAAGAGTAGTCGT	CCTTGTAAAAACCATCAGTCGTCA
HRK #1	TCATTCTTGGAACGCTACACC	GGTTTTATACTGCCCCCTGTAATC
HRK #2	CACAGGTGCCAGACATAGAAGA	CCACCGCAGAGTATAACCAAG
HRK #3	GTTCACAAAGAAAGCAGACAAGAAG	TGGCTAGAAACCTGACCCTAAA
HRK #4	GGGTTAAAAGTTACCTCTCGGTTT	CTCCTTGTGTTGTGCGTTTGT
ULK1 #1	GTGCGCTGCTTGGCCTAAGTGATG	ATCCGCTGGGGAGGAAAGGTTAGC
ULK1 #2	CCAGCGGATTTATGGGCTATGTCG	CCGCCCCCACTGCCTGTTCTCCTC
ULK1 #3	AAGGGGAAAAGGAGGGAGGAGGAC	GAGCCGGGCGTGACGAACA
ULK1 #4	CTGCGCGGGCGTCTCAG	GGCGAGGGCGCATCTCC
ULK1 #5	GCGCCTCCGCCTGAGTCC	ATCTCGGGGCGGGGATGC
ULK1 #6	CCAGCCCGACTTTCCTGTCCA	CTCCCCCAGACCCCAGTCCA

2.9 Transmission electron microscopy

Transmission electron microscopy (TEM) was done by Professor David Ferguson (Oxford University). In brief, A431 cells were reverse transfected with siRNA against ULK1, ATF4, or the SCR control. Following hypoxic exposure for 24 hours, cells were fixed in 2.5% gluteraldehyde in 0.1M cacodylate buffer and scraped into falcon tubes for further processing. From this point, Professor Ferguson

processed samples. Post-fixation was done in 2% osmium tetroxide in cacodylate buffer. Prior to dehyaration the samples were treated *en bloc* with 2% uranyl acetate in distiled water. Samples were then dehydrated in ethanol and treated with propylene oxide prior to embedding in Spurr's epoxy resin. 1µm sections stained with Azure A were examined by light microscopy to identify areas of interest. Thin sections of suitable areas were cut and stain with uranyl acetate and lead citrate prior to examination in a Jeol 1200EX electron microscope.

A semi-quatitative technique was applied to each sample where a random sample of cells was examined. To prevent observer bias, the first 100 cells in the sections from each sample were counted. Features quantified included; cell shape (round v flattened), presence or absence membranes accumulations within the cytoplasm of rounded cells and number of mitotic cells. In addition, the relative number of mitochondria unassociated with and the number with intimate associations with ER were counted and presented as a percentage of each. This was based on the counting of approximately 300 mitochondria per sample.

2.10 Colony formation assay

The day following transfection with siRNA molecules, A431 and MCF7 cells were trypsinized, accurately counted, and resuspended to 10,000 cells/mL. Serial dilutions were done to produce suspensions of 1000 cells/mL and 100 cells/mL. 60mm plates were seeded with 100, 1000, or 10,000 cells for each oxygen/RNAi combination. Seeded plates were immediately exposed to severe hypoxia for the designated period (cells were allowed to attach in the chamber) or not. Following this incubation, plates were returned to the normoxic incubator and colonies were allowed to form over a period of one to two weeks. Colonies were deemed large enough if they contained at least 50 cells. At this point, plates were washed with PBS and colonies were fixed with 50% ethanol/water containing 0.2% methylene blue (Sigma) for two hours at room temperature. Following fixation, excess dye

was washed away with tap water and plates were allowed to dry for one to two days. For the counting of colonies, the ColCount Colony Counter (Oxford Optronix) was used. Plates with 20-300 colonies were used in calculations. Untreated clonogenicity was calculated using the normoxic controls, and treatment groups were normalized to this value to calculate fraction survival.

2.11 Flow cytometry analysis of cell death

Cell death was quantified by flow cytometry, as previously described (Otsuki et al., 2003). In brief, cells were plated in 6-well format (50,000 cells/well) and transfected with siRNA as described above. 16 to 24 hours later, cells were exposed to severe hypoxia or drugs as desired. Following treatment, both floating and adherent cells were collected in 4mL FACS tubes. Following pelleting, and serial washes with PBS, cells were stained with annexin-V-AlexaFluor647 (Invitrogen) and propidium iodide (Invitrogen) in annexin-V binding buffer (BD Pharmagen). Tubes were incubated on ice for 10-15 minutes, and then processed by flow cytometry using a Cyan ADP Flow Cytometer (Dako). Data collection and analysis was done using Summit version 4.1 (Dako). Debris was gated out and the annexin-V positive population (both PI positive and PI negative) was used to calculate "cell death".

2.12 Flow cytometry for mitochondria

Cells were treated with RNAi and hypoxia as described for cell death analysis above. In this case, prior to collection, cells were first stained *in situ* with Mitotracker Red FM® (Invitrogen), as per the manufacturer's instructions. Following staining, cells were collected in FACS tubes, serially washed with PBS, and positive cells were counted with a Cyan ADP Flow Cytometer (Dako). An

unstained, negative control was included. Mean fluorescence was used to assess changes in mitochondrial number, as previously described (Kundu et al., 2008a).

2.13 Luminescent Assays

Caspase 3/7 protease activity was analysed using the CaspaseGlow® 3/7 Assay (Promega) as per the manufacturer's specifications. The CaspaseGlow® 3/7 consists of a luciferase substrate covalently bound to a DEVD caspase motif, as well as luciferase, buffer, and detergent. Addition of the reagent lyses cells and releases activated caspases that then cleave the DEVD motif from the molecule, yielding a luminescent signal, which is detected with a luminometer. Similarly, ATP levels were measured using the Cell-Titer Glo® Luminescent Cell Viability Assay (Promega) as per the manufacturer's specifications. ATP is used in a luciferase reaction, generating a luminescent signal directly proportional to ATP level.

In brief, cells were transfected with siRNA in 100mm format as described previously, and then reseeded to white-walled 96-well dishes at a density of 5000 cells/well. Cells were permitted to adhere overnight prior to exposure to severe hypoxia or drug. The diluted luminescent reagent was then dissolved in buffer as per the manufacturer's recommendations, and 100μL of this substrate was added to each well with a multi-channel pipettor. Following an incubation of 1 hour at 37°C, the luminescent signal was detected and quantified.

2.14 Three-dimensional spheroid growth assay

Rapid generation of single-tumour spheroids was achieved using the method developed by Ivascu and Kubbies (Ivascu and Kubbies, 2006). Following transfection with siRNA, cells were trypsinized and diluted to 25,000 cells/mL in

chilled culture medium. To this mixture, 25μL of Matrigel® (BD Biosciences) was added per mL of cells. 200μL of this mixture was added to each well of a 96-well conical plate (Corning), giving a final count of 5000 cells per well. These plates were immediately centrifuged for 10 minutes at 1000*g* to pellet cells at the bottom of the dish. The plates were then incubated overnight at 37°C, allowing spheroids to form. This time point, for the purposes of this study, was considered to be "Day 1".

Images of each spheroid were captured using an Axiovert 135 Microscope (Zeiss) and a 5x objective with an attached camera. ImageJ® version 1.43 (National Institutes of Health) was used to calculate spheroid volume.

To assess cell death in this model, spheroids were collected at day 3 and dissociated using Accutase® (PAA Laboratories GmbH). Three groups of three to four spheroids were analyzed for annexin-V staining by flow cytometry, as described above.

2.15 Immunohistochemistry

Immunohistochemistry was done on spheroids to assess clinically relevant markers of hypoxia, cell death, and proliferation. Slides were prepared from formalin-fixed paraffin-embedded (FFPE) blocks containing ten to twenty spheroids in each.

At the time of staining, slides were first dried at 60°C for 10 minutes, and then deparaffinized by two washes with histoclear (Fisher), and then rehydrated with serial dilutions of ethanol (from 100% to pure water), all for 5 minutes each. Antigen retrieval was done in Tris-EDTA buffer (pH 9) in a decloaking chamber (Biocare Medical). Block (Dako) was done for 10 minutes at room temperature, and primary diluted in spent RPMI media, and applied for 1 hour at room

temperature followed by a wash in PBS. Sections were incubated for 16 hours at 4°C with the primary antibody. Bound antibody was labeled with Novolink polymer (Leica), visualized by using 2,3- diaminobenzidine chromogen, and counterstained with hematoxylin.

2.16 Imagestream® analysis of autophagy

Imagestream® (IS100) is a multispectral flow cytometer combining standard microscopy with flow cytometry distributed (Cronus Technology) . It can acquire up to 100 cells/sec, simultaneously acquiring six images of each cell, including brightfield, scatter, and multiple fluorescent images.

In this thesis, Imagestream® was used to analyze autophagic flux. In brief, MCF7 cells transfected with siRNA for ULK1, HRK, or SCR were exposed to severe hypoxia for 24 hours. At this point, cells were trypsinized and collected in 15mL Falcon® tubes. Following washes with assay buffer (1% FCS/PBS), cells were stained with a violet live/dead marker (L34955 Component A, Invitrogen) and a red lysosome-specific dye (LysoID, Enzo Life Sciences). Cells were then fixed and permeabilized (eBioscience Fixation and Permeabilization kit) and stained with mouse-anti-LC3 (Nanotools) and goat-anti-mouse IgG-AlexaFluor546 (Invitrogen). Cells were imaged with the Imagestream® apparatus, and images were acquired for each respective channel. Single-stained controls were included for compensation. Following image acquisition, live cells were analyzed for colocalization of LC3 and lysosomes using the software package IDEAS 4.0.735. Autophagy levels were calculated by measuring percent colocalization of LC3 and LysoID double positive cells by plotting these LC3+Lyso+ (double positives) for bright detailed similarity (BDS) between LC3 and lysosomal markers against normalized frequency of cells. This analysis therefore gave an estimation of the number of autophagolysosomes per cell, in a sample of more than 5000 cells,

yielding a powerful assessment of autophagic flux. *Please note, data analysis was done by Dr. Kanchan Phadwal (Oxford University).*

2.17 HMGB1 ELISA

An HMGB1 ELISA kit from IBL International (GMBH) was used to quantitatively determine the levels of HMGB1 in the cell culture medium of cells undergoing necrosis. Elevated levels of HMGB1 in human serum or the cell culture medium are indicative of necrosis—the intracellular components of the cell spill out into the environment. One such component is HMGB1.

In brief, A431 cells were transfected with RNAi against ULK1 and ATF4, as previously described, and exposed to severe hypoxia for 36 hours. Cell culture medium was then collected and frozen at -80°C until processing. The kit was used as per the manufacturer's instructions.

The HMGB1 ELISA is a sandwich-enzyme immunoassay. The wells of a 96-well plate are coated with purified anti-HMGB1 antibody. HMGB1 in the sample binds specifically to the immobilized antibody, and is then recognized by a second peroxidase-conjugated antibody. Serial dilutions of a provided standard are prepared and used to prepare a standard curve. Thus, the exact concentration of HMGB1 in a given sample can be measured.

2.18 Polysomal Fractionation

2.18.1 Preparation of Sucrose Gradients

Fractionation buffer was made with DEPC water, containing of 0.3 M NaCl, 15 mM $MgCl_2$, 15 mM Tris-HCl (pH7.4), 0.1 mg/ml Cyclohexamide, and 0.1 mg/ml Heparin. Solutions of 50%, 40%, 30%, 25% and 20% sucrose in fractionation buffer were made up and kept on ice at 4°C. Note, the cyclokexamide and heparin must be added to the buffer when cold, prior to adding the sucrose. Beckman 15 ml ultracentrifuge tubes were used for the gradients. First, 3 mL of 50% sucrose was placed in the tube, and frozen at -80°C. Once frozen, 2 mL of 40% sucrose buffer was added, and frozen at -80°C, ensuring that the 50% sucrose layer did not thaw. This process was repeated with 1 mL of 30% sucrose, 2mL of 25% sucrose and finally, 2 mL of 20% sucrose. The gradients were kept at -80°C until the night before use, when they are left in a cold room at 4°C to thaw slowly overnight.

2.18.2 Preparation of cell extract

0.1mg/ml cyclohexamide was added to cells in the incubator (hypoxic or normoxic) for 3 mins at 37°C, then washed twice with acclimatized PBS containing cyclohexamide at 0.1mg/ml, prior to lysis in buffer (1%Triton X-100, 0.3M NaCl, 15mM MgCl2, 15mM Tris (pH 7.4), 0.1mg/ml cyclohexamide, 100 unitse RNAse-In (Ambion)). 200µg/ml heparin was added to the lysate. The sample was centrifuged to remove debris.

2.18.3 Size Fractionation of RNA

500 µl cell extract was placed on top of each sucrose gradient. The gradients were then placed in a SW-41Ti rotor, and centrifuged for 90 min at 39,000 rpm at 4°C. Meanwhile, the fractionator was prepared by cleaning all equipment and tubing in

ethanol and then DEPC-treated water containing RNAse Zap. The pump speed was set to 0.25 ml/min, and the time per aliquot 45 sec. The UV readings were set to record absorbance at 254 nm. Once the apparatus was ready, the gradients were mounted on the machine, and the inferior part of the tubes perforated with a hollow needle attached to the pump. Ensuring no bubbles are introduced, the gradients were forced out (with 80% sucrose buffer solution) through the UV spectrometer and in to approximately 30 aliquots. As the sucrose gradient passed through the spectrometer, it produced an absorbance plot that could be used to identify ribosomal structures. Polysomal fractions were pooled and RNA was extracted using Trizol LS.

2.19 Statistics

Statistical analyses were performed using Prism 4 for Mac (GraphPad Software). Error bars represent standard error in the mean, and P values were calculated by Student's T-test or one-way ANOVA, unless otherwise indicated.

Chapter 3 ATF4 regulates a program of BH3-only protein expression in response to severe hypoxia

In this chapter, the hypoxic regulation of several BCL2 family proteins by ATF4 is studied. The BH3-only proteins HRK, PUMA, and NOXA are induced at the mRNA level in severe hypoxia in an ATF4-dependent fashion. ATF4 acts directly at the promoter region of HRK to drive its transcription. HRK is required for the induction of autophagy in severe hypoxia, and loss of HRK sensitizes MCF7 cells to severe hypoxia. Ectopic expression of HRK fails to increase autophagy in normoxia, but may direct mitochondria for autophagic degradation. Loss or HRK fails to block spheroid growth in MCF7 cells.

3.1 Introduction

Intratumoural hypoxia is associated with poor prognosis, regardless of the mode of therapy (Harris, 2002). Hypoxia confers chemoresistance and radioresistance by selecting for cancer cells that have defects in apoptosis and by activating adaptive signaling pathways (Graeber et al., 1996). The integrated stress response is one such pathway that can protect cells from hypoxia. Specifically, recent work has shown that the ISR can protect cells from hypoxia by transcriptionally upregulating MAP1LC3B and ATG5, two components of the autophagy machinery machinery (Rzymski and Harris, 2007; Rzymski et al., 2009; Wouters and Koritzinsky, 2008). However, when such stress proves to be insurmountable, the ISR can also activate apoptosis to destroy potentially pathogenic cells (Hetz, 2007). The BCL2 family of proteins actively regulates both autophagy and apoptosis. In this chapter, the regulation of several members of this protein family by the integrated stress response transcription factor ATF4 is investigated, with a

focus on the role of the BH3-only protein HRK in autophagy and cell survival in severe hypoxia.

3.1.1 Apoptosis and the BCL2 family of proteins

In normal tissue, apoptosis is the physiological mechanism by which damaged cells are destroyed. In response to a cytotoxic insult, a signaling cascade is initiated which culminates in the activation of a series of cysteine-aspartyl proteases (caspases) that effect a program of organized cellular demolition (Taylor et al., 2008). The BCL2 family of proteins constitutes the molecular machinery responsible for controlling this process, translating a damaging insult into caspase activation and cell death. BCL2 serves as the prototype for the family, the members of which have at least one of the four conserved α-helical motifs termed BCL2 homology domains (BH1-4) (Oltvai et al., 1993). The family is divided according to function: the anti-apoptotic family members and the pro-apoptotic family members. The antiapoptotic family members contain four BH domains (BH1-4), and include BCL2, BCL-X_L, BCL-w, MCL-1, and A1. The pro-apoptotic family members are further classified into two groups: the multidomain family members and the BH3-only proteins. The multidomain family members contain three BH domains (BH1-3), and include BAX, BAK, and BOK. The BH3-only proteins are a group of diverse proteins that contain only the BH3 domain in common. Members of this family include BAD, BID, BIK/NBK, BIM, BMF, BNIP3/NIX, HRK, PUMA, and NOXA (Figure 3.1A) (Lomonosova and Chinnadurai, 2008). As their name suggests, the BH3-only proteins share only the homologous BH3 domain with the other family members (Figure 3.1B). The sequence alignment of the BH3 domain of harakiri, the BH3-only protein that will be the focus of this chapter, with the BH3-only protein BIK and the multidomain family members BAX and BCL2 is shown below.

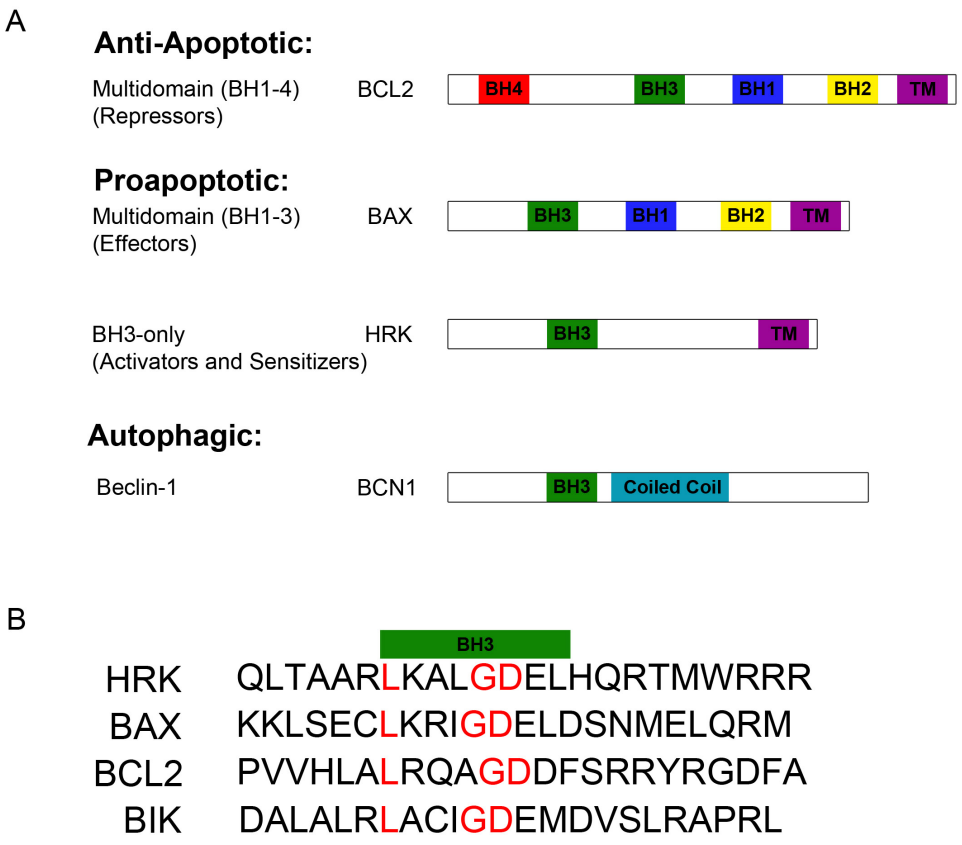

Figure 3.1 Structure of the BCL2 Family Proteins

The structure of the BH3-domain is the key to the function of the BCL2 family members. The BH1-3 domains of the anti-apoptotic family members, such as BCL2, form a hydrophobic grove into which the amphipathic BH3 domain of the pro-apoptotic family members can insert. The anti-apoptotic activity of BCL2 and its kin is wrought via this protein-protein interaction. In healthy cells, the death effector activity of the multidomain pro-apoptotic family members is neutralized through binding to the anti-apoptotic family members (Muchmore et al., 1996; Sattler et al., 1997). However, in response to a cytotoxic stress, such as DNA damage, hypoxia, or ER stress, the BH3-only members become activated in a stimuli and cell context specific manner. This activation can occur through transcriptional upregulation (PUMA, NOXA), or post-translational modifications such as phosphorylation (BAD) or cleavage (BID). The BH3-only proteins can then

bind to specific anti-apoptotic family members to release BAX and BAK, from their neutralizing hold, thereby sensitizing cells to apoptosis (Figure 3.2). Additionally, a subset of the BH3-only family members binds to and activates the pro-apoptotic family members directly (Ren et al., 2010). As a point of interest, in cancer cells, high levels of the BH3-only proteins are often present even in "unstressed" conditions. These BH3s are sequestered by equally high expression of anti-apoptotic family members. However, due to this tenuous balance, these cells are said to be "primed for death" (Certo et al., 2006).

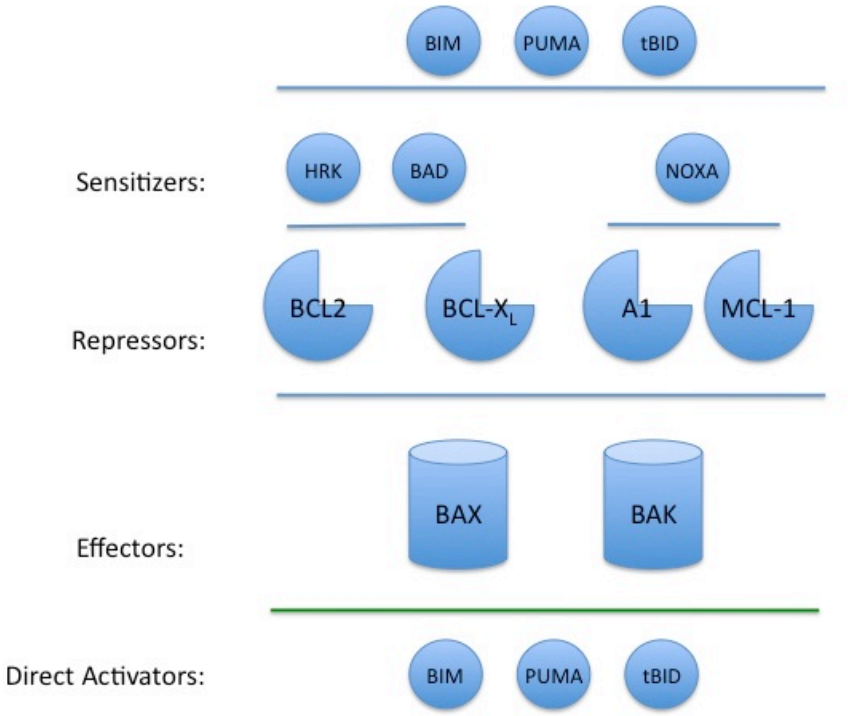

Figure 3.2 Interactions between BCL2-family proteins

Once activated, BAX and BAK oligomerize to form pores in the mitochondrial outer membrane. Mitochondrial outer membrane permeabiliziation permits intermembrane components such as cytochrome c to translocate into the cytosol where it forms a multimeric holoenzyme complex with APAF-1 and the initiator

caspase 9. This catalytically active "apoptosome" can then activate the effector caspases 3 and 7, which in turn cleave hundreds of intracellular substrates, effecting the organized cellular demolition that is apoptosis (Lomonosova and Chinnadurai, 2008; Taylor et al., 2008).

3.1.2 BH3-only proteins and autophagy

As noted above, the BH3-only proteins are most often described as effectors of apoptotic cell death. However, recent work has identified the essential autophagy protein beclin-1 (BCN1) as an atypical BH3-only protein (Oberstein et al., 2007). BCN1 is the mammalian homolog of yeast ATG6, and acts as an allosteric activator of the class III PI3K Vps34, and forms large protein complexes with Vps15, UVRAG, Ambra1, and Bif-1 (Levine et al., 2008). These interactions are required for the production of PI3P and autophagy initiation.

In mice and humans, BCN1 constitutively interacts with antiapoptotic proteins of the BCL2 family (BCL2, BCL-X_L, BCL-w, and MCL-1) via its BH3 domain (Elgendy et al., 2011; Erlich et al., 2007; Liang et al., 1999; Maiuri et al., 2007; Pattingre et al., 2005). This interaction occurs in the fed state, where it reduces the activity of the BCN1/Vps34 complex and therefore inhibits autophagy. When cells were exposed to starvation conditions, the amount of BCN1 coimmunoprecipitating with BCL2 or BCL-XL declined as autophagy increased**.**

This functional interaction therefore predicted a mechanism by which BH3-only proteins could activate autophagy. Indeed, subsequent studies have shown that in many cases this role is possible. In worms, expression of the BH3-only protein EGL-1 resulted in increased baseline autophagy (Maiuri et al., 2007). In human cells, treatment with the BAD-mimetic ABT737 decreased BCL2-BCN1 interaction and increased autophagy (Oltersdorf et al., 2005). In starvation conditions, knockdown of the BH3-only protein BAD reduced autophagy and this effect could

be reversed by treatment with ABT737 (Maiuri et al., 2007). Ectopic expression of BIK appeared to induce a form of caspase-independent cell death with autophagic features (Rashmi et al., 2008). Likewise, BNIP3/NIX was shown to increase mitochondrial autophagy in hypoxia in a HIF1-dependent manner (Zhang et al., 2008; Zhang and Ney, 2008). Interestingly, ectopic expression of either the BH3-only protein PUMA or the multidomain family member BAX was found to increase macroautophagy and mitophagy human cancer cells (Yee et al., 2009), indicating that the BH3-domain of either protein was sufficient to stimulate autophagy. Deregulated H-Ras activity was similarly shown to promote caspase-independent cell death with autophagic features though the NOXA-mediated displacement of BCN1 from MCL-1 (Elgendy et al., 2011). Alternatively, phosphorylation of BCL2 by JNK was shown to cause the dissociation of the BCN1-BCL2 complex and the induction of autophagy (Park et al., 2009; Shimizu et al., 2010). Thus, it is clear that the BH3 domain can be a potent inducer of autophagy in a variety of cellular contexts.

3.1.3 HRK, PUMA, and NOXA

3.1.3.1 HRK

Harakiri was discovered in 1997 in a yeast two-hybrid assay using BCL2 as bait (Inohara et al., 1997). Coimmunoprecipitation studies confirmed that HRK can bind to either BCL2 or BCL-X_L. Sequence analysis identified HRK as a BH3-only protein with a transmembrane domain, and the authors showed that ectopic expression of a FLAG-tagged HRK construct in 293T cells could induce apoptosis that could be rescued by coexpression of BCL2 or BCL-X_L. Truncation of the BH3 domain prevented the induction of cell death by HRK.

Later that year, the mouse ortholog of DP5 was discovered in a differential display for genes induced in sympathetic neurons following neuron growth factor (NGF)

withdrawal (Imaizumi et al., 1997). In this study, Imaizumi showed that DP5 expression could induce cell death and that this induction could be blocked by coexpression of BCL2, but he failed to identify DP5 as a BH3-only protein or as the mouse homolog of HRK. A year later, this connection was made by Kanazawa (Kanazawa et al., 1998).

Over the following years, HRK was shown to play an important role in apoptotic cell death in neurons both *in vitro* and *in vivo*. Several studies have shown that HRK is important in the cell death of neuronal cells following NGF withdrawal (Coultas et al., 2007; Imaizumi et al., 1997), amyloid beta protein treatment (Chen et al., 2006; Imaizumi et al., 1999), potassium deprivation (Coultas et al., 2007; Ma et al., 2007), axotomy (Imaizumi et al., 2004; Wakabayashi et al., 2002), polyglutamine protein aggregation (Young et al., 2009), spinal cord injury (Yin et al., 2005), and antibiotic treatment (Kalinec et al., 2005). Two studies have implicated HRK in the cell death process in hematopoietic progenitor cells (Sanz et al., 2000; Sanz et al., 2001), but this work was later refuted by an elegant study from Andreas Strasser's laboratory (Coultas et al., 2007). Importantly, $DP5^{-/-}$ mice are viable and develop normally, failing to express any obvious pathology or organ abnormalities (Coultas et al., 2007; Imaizumi et al., 2004).

Only one study has considered the *in vitro* role of HRK in cancer. Sanz showed that HRK expression was induced in human leukemia cells by Fas signaling and blockade of Bcr-Abl by inhibition of the DREAM transcriptional silencer (Sanz et al., 2002). On the other hand, there have been a number of reports indicating that HRK is downregulated in human cancer *in vivo*. In what appears to be an epigenetic mechanism involving hypermethylation of the HRK promoter region and the first exon (Obata et al., 2003), HRK mRNA and protein levels were found to be significantly reduced in secondary glioblastomas (Nakamura et al., 2005), primary central nervous system lymphomas (Nakamura et al., 2006), prostate cancer (Higuchi et al., 2008), and colorectal and gastric cancer cell lines (Obata et

al., 2003). The loss of HRK was associated with a reduced apoptotic index and decreased relapse-free survival.

The expression of HRK appears to be regulated at the transcriptional level. The original study identifying HRK noted a RNA destabilization motif in the 3' untranslated region of the HRK transcript (Inohara et al., 1997). It was later shown that HRK transcription was blocked in an interleukin-3-dependent manner in growing hematopoietic cells by the transcriptional repressor DREAM (Sanz et al., 2002; Sanz et al., 2001). In neuronal cells, HRK expression appears to be regulated through c-Jun N-terminal kinase (JNK). *In vivo* delivery of the JNK inhibitor SP600125 or antisense oligodeoxynucleotides to JNK attenuated DP5 induction and cell death in the neurons of mice following traumatic spinal cord injury(Yin et al., 2005). Similar results were obtained in an *in vivo* model of brain ishchemia-reperfusion(Guan et al., 2006). It was later shown that c-Jun and ATF2 (as well as other AP-1 transcription factors) bind to a conserved ATF sequence in the HRK promoter to induce its transcription in response to amyloid beta peptide (Chen et al., 2006), potassium deprivation (Ma et al., 2007), and NGF withdrawal (Towers et al., 2009) and in pancreatic β-cells in response to interferon gamma and interleukin-1β treatment (Gurzov et al., 2009).

The role of HRK in autophagy has not been studied. However, as described above, the BCL2 family binding profile of HRK resembles that of BAD (Chen et al., 2005; Inohara et al., 1997). Thus, it is possible that HRK could bind to BCL2 or BCL-X_L via its BH3 domain to release BCN1 and initiate autophagy. Alternatively, HRK has been shown to preferentially localize to the mitochondrion through its transmembrane domain (Sunayama et al., 2004). As such, it is possible that HRK might select mitochondria for autophagic degradation in a way similar to NIX (Zhang and Ney, 2008). The work of this chapter examines the regulation of HRK in hypoxia and the role of HRK in hypoxia-induced autophagy in breast cancer cells.

3.1.3.2 PUMA

P53 upregulated modulator of apoptosis (PUMA), as the name implies, is a p53-dependent BH3-only protein. PUMA was independently cloned by three groups in 2001. Two identified PUMA as a transcriptional target of p53 (Nakano and Vousden, 2001; Yu et al., 2001), while the other identified it as a BCL2-interacting protein in a yeast two-hybrid screen. PUMA is expressed as four splice variants, two of which, PUMA-α and PUMA-β, contain a BH3-domain. The particular role of each in the cell death process is not clear.

As with HRK, PUMA is a potent inducer of apoptotic cell death by direct interaction with the antiapoptotic proteins. Unlike HRK or NOXA, which selectively bind BCL2/BCL-X_L or MCL-1/A1, PUMA can bind to and inhibit all of the antiapoptotic family members (BCL2, BCL-X_L, MCL-1, BCL-w, and A1) (Chen et al., 2005), making it a much more potent inducer of cell death. There is also evidence derived from cell-free systems to support a role of PUMA in the direct activation of BAX and cytoplasmic p53, though the *in vivo* relevance of this interaction is less clear (Cartron et al., 2004; Chipuk et al., 2005; Kim et al., 2006; Kim et al., 2009; Letai et al., 2002).

PUMA is transcriptionally upregulated by the transcriptional activity of p53 (Kaeser and Iggo, 2002; Wang et al., 2007). Within two hours of DNA damage, p53 is recruited to the two p53 reponse elements in the PUMA promoter. A plethora of work has clearly placed PUMA as the major death effector in the p53 pathway (Vogelstein and Kinzler, 2004; Yu et al., 2003; Yu et al., 2006a).

Alternatively, PUMA can be activated by a number of p53-independent pathways in response to a diverse range of stimuli. ER stress, oxidative stress, and hypoxia can drive the transcription of PUMA through p53-dependent and p53-independent pathways. In particular, ER stress was shown to activate the transcription of and

cell death through PUMA (Li et al., 2006). While the work in this thesis was in progress, another group published that PUMA is an ATF4 target gene (Ishihara et al., 2007; Li et al., 2006).

There is one study that has demonstrated a potential role for PUMA in the activation of autophagy. Yee et al. showed that ectopic expression of PUMA or BAX in the presence of the pan-caspase inhibitor ZVAD-FMK increased autophagy, and particularly, mitophagy (Yee et al., 2009). However, it appeared that this process was BCN1-independent and could only be observed with inhibition of classical apoptosis. Thus, the relevance of this system to normal cell death processes is questionable.

3.1.3.3 NOXA

NOXA was initially isolated from an adult T-cell leukemia library in search for products involved in leukemogenesis (Hijikata et al., 1990). The transcript was induced by phorbol 12-myristate 13-acetate (PMA), and was therefore named PMA-induced protein 1 (PMAIP1). It wasn't until a decade later that the function of this protein was realized, when it was rediscovered using a differential display analysis of mRNA molecules induced by gamma radiation in wild type or IRF-1/p53 double-deficient MEFs. The discovered gene was termed NOXA (Latin for "damage"), and the search for the human counterpart indicated that it was the mouse homolog of PMAIP1. The strucutural analysis of NOXA also revealed a putative BH3-domain, placing it among the growing list of BH3-only proteins (Oda et al., 2000).

NOXA is a far less potent activator of apoptosis than other BH3-only proteins like BIM, BID, or PUMA. The reason for this difference was soon found in the binding profile of NOXA. Unlike BIM, BID, and PUMA, which bind to all known antiapoptotic BCL2 family members and to activate BAX and BAK oligomerization

by direct interaction, NOXA selectively binds to MCL1 and A1. This difference in binding affinity is due to subtle differences in the amino acids of the BH3 domain (Chen et al., 2005; Liu et al., 2003). Intriguingly, in addition to neutralizing the antiapoptotic activity of MCL1 by blocking its association with BAX or BAK, in some circumstances NOXA has been shown to target MCL1 for proteasomal degradation. This event has been shown to be required for cell death in response to UV irradiation, cytokine deprivation, and treatment with anticancer agents such as arsenic trioxide or histone deacetylase inhibitors (Inoue et al., 2007; Morales et al., 2008; Nijhawan et al., 2003; Opferman et al., 2003).

NOXA is transcriptionally upregulated through p53-dependent and p53-independent pathways. In response to DNA damaging agents, gamma irradiation, or adenovirus-mediated introduction of p53, NOXA mRNA is upregulated by direct binding of the p53 transcription factor to a p53 response element in the promoter region of the NOXA gene in a variety of cellular contexts (Fei et al., 2002; Hallaert et al., 2007; Oda et al., 2000). NOXA can also be activated by other p53 family members, such as p73 (Flinterman et al., 2005), or in a PKC-dependent fashion (Alves et al., 2006).

Interestingly, it has been shown that NOXA can be upregulated by HIF1 in hypoxia (Kim et al., 2004). ER stress has also been shown to be a potent inducer of NOXA expression (Li et al., 2006). Pharmacological inhibition of ER-associated degradation (ERAD) was shown to activate apoptosis through NOXA expression in an ATF4/ATF3 dependent manner (Wang et al., 2009).

Given that NOXA acts to induce apoptosis through inhibition of MCL1, and that MCL1 can bind to and repress the autophagic activity of BCN1, it is perhaps not surprising that NOXA has a role in inducing autophagy in some cellular contexts. Indeed, recent work has shown that deregulated H-Ras activity can lead to increased levels of both NOXA and BCN1. NOXA was shown to free BCN1 from an

inhibitory complex with MCL1, promoting BCN1-dependent autophagy and cell death (Elgendy et al., 2011).

3.2 Results

3.2.1 Hypoxia activates autophagy in breast cancer cell lines

The tumour microenvironment is harsh, and contains regions of glucose-deprivation, amino acid-deprivation, and hypoxia. One way in which cancer cells are known to survive intratumoural hypoxia is through the activation of autophagy (Degenhardt et al., 2006). Thus, at the outset of this work, the author sought to confirm the activation of autophagy by hypoxia. As such, MCF7 and MDA-MB-231 breast cancer cells were exposed to either moderate (0.1% O_2) or severe hypoxia (<0.01% O_2) for 24 or 48 hours. As expected, both moderate and severe hypoxia increased the expression of the autophagy marker LC3-II (lower band) in a time- and oxygen-dependent manner (Figure 3.3). Additionally, the cleavage of PARP, a well-known substrate of caspase 3 and of lysosomal calpains, was observed after 48 hours in the MCF7 cells, indicating that extended hypoxic exposure results in apoptotic or necrotic cell death (Shah et al., 1996). This death was reflected in the growth curve for MCF7 and MDA-MB-231 cells exposed to severe hypoxia (Figure 3.4). By 48 hours exposure to severe hypoxia, the number of adherent cells had decreased substantially, likely indicative of increased cell death and decreased proliferation (though propidium iodide or trypan blue exclusion staining would be necessary to confirm this phenotype). In the MCF7 cell line, the timing of LC3-II expression and PARP cleavage fit with the accepted model of autophagy as a hypoxia survival mechanism (Wouters and Koritzinsky, 2008), as PARP cleavage followed strong induction of LC3-II. However, PARP cleavage in MDA-MB-231 cells was far less prominent. Thus, it is possible that in this cellular context death is occurring through a non-apoptotic or calapin-independent mechanism (Figure 3.3).

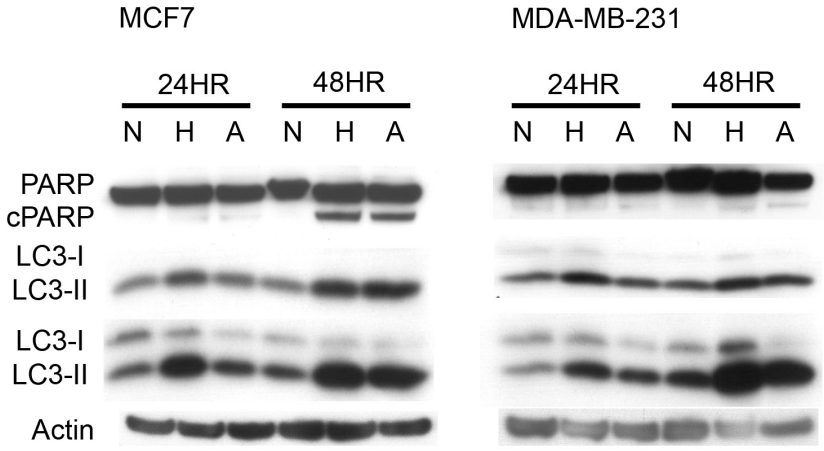

Figure 3.3 Both moderate and severe hypoxia result in the accumulation of LC3-II protein and the cleavage of PARP.

MCF7 and MDA-MB-231 breast cancer cells were exposed to normoxia (N, 21% O_2), moderate hypoxia (H, 0.1% O_2) and severe hypoxia (A, <0.01% O2) for 24 or 48 hours, after which cells were harvested and analyzed by western blotting using the indicated antibodies. LC3-II, the lower band, is a marker for autophagy. Cleaved PARP, lower band, is a marker for cell death. Representative images from at least N=2 independent experiments are shown.

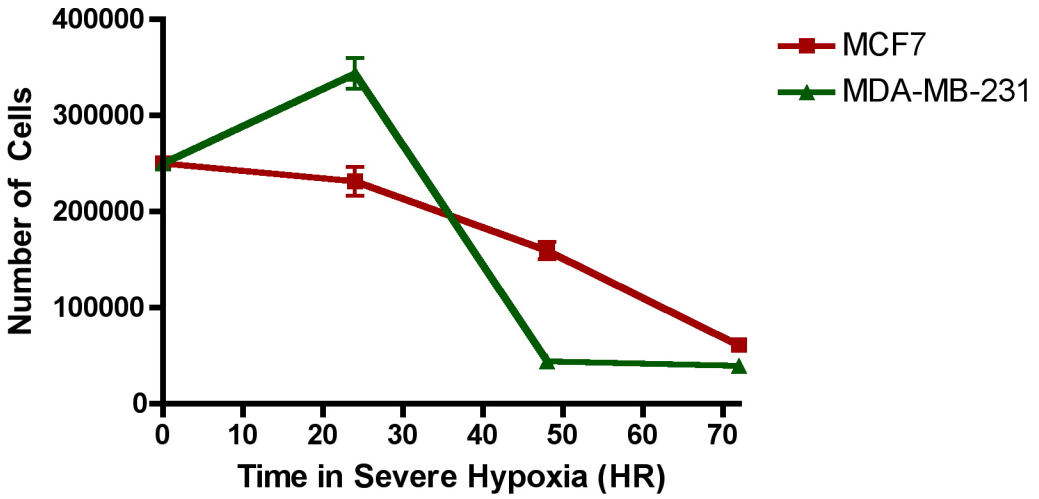

Figure 3.4 Extended exposure to severe hypoxia kills breast cancer cells.
MCF7 and MDA-MB-231 breast cancer cells were seeded at 250,000 cells per dish, and immediately exposed to severe hypoxia. At the indicated time points, dishes were removed from hypoxia and adherent cells were counted. N=3 independent experiments, error bars show standard error.

3.2.2 Severe hypoxia increases flux through the autophagy pathway

In most cell types, autophagy is a constitutively active process. Mammalian cells have a low level of basal autophagy happening all the time. If the autophagy process is considered to be comprised to two simple steps (a gross oversimplification), induction and degradation, then the rates of these reactions can be denoted v_1 and v_2, respectively. In this simplified description, the flux through the autophagy pathway is the sum of reactions (1) and (2). The rate of this reaction will be the lesser of v_1 or v_2.

(1)	Phagophore + Cargo	→	Autophagosome	v_1
(2)	Autophagosome + Lysosome	→	Digested nutrients	v_2

The nascent phagophore and autophagosome are studded with LC3-II protein. If the rate of autophagy induction increases without a change in the rate of degradation, then LC3-II protein will accumulate dramatically. If the total flux through the pathway increases with v_1 and v_2 being equal, then the level of LC3-II protein should appear nearly the same, despite much more cytoplasm being degraded into nutrients. However, if the degradation of autophagosomes in (2) is reduced by blocking lysosmal fusion or the activity of lysosomal hydrolases, then LC3-II protein will accumulate even though the rate of induction may be unchanged(Klionsky et al., 2008).

Thus, to confirm that the observed accumulation of LC3-II in severe hypoxia was in fact due to increased autophagy induction as opposed to decreased degradation, MCF7 and MDA-MBA-231 cells were treated with lysosomal inhibitors to prevent autophagosome degradation (Figure 3.5). The resultant increase in LC3-II under normoxia indicates that these cells have constituitively high levels of autophagy. The combination of lysosomal inhibitors and hypoxic exposure resulted in LC3-II levels greater than that stimulated by the inhibitors alone, indicating flux through the autophagy pathway increases with hypoxic stress.

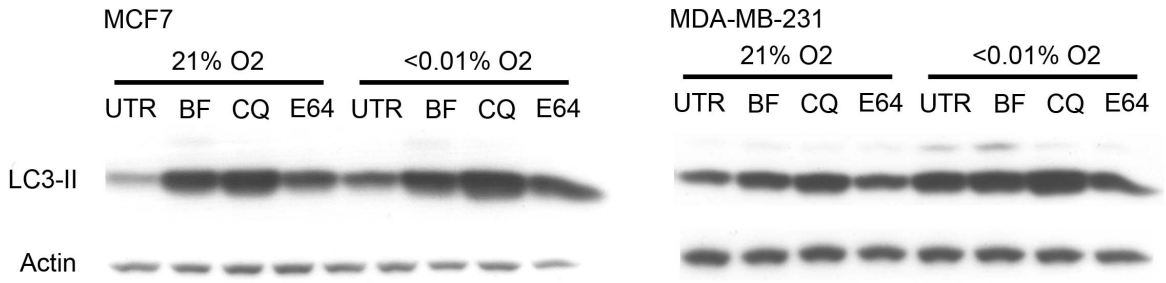

Figure 3.5 Severe hypoxia enhances LC3-II protein accumulation in MCF7 and MDA-MBA-231 breast cancer cells treated with lysosomal inhibitors. *MCF7 and MDA-MB-231 cells were treated with 0.1μM bafilomycin A1 (BF), 25μM chloroquine (CQ), or 10μg/mL of each E64D and pepstatin A (E64) and then immediately exposed to severe hypoxia. After 24 hours, cells were harvested and*

analyzed by western blotting using the indicated antibodies. Representative images from at least N=2 independent experiments are shown.

To further confirm these results, staining for LC3-positive puncta was done. In this assay, the accumulation of autophagosomes can be directly assessed by immunocytochemistry. As described in Chapter 1, LC3-II is incorporated into the nascent autophagosomes, which can be detected as LC3-positive puncta by immunocytochemistry (Klionsky et al., 2008). When MCF7 cells were exposed to severe hypoxia, the number of these puncta increased relative to the control (Figure 3.6). Furthermore, combined treatment with lysosomal inhibitors and hypoxia greatly enhanced the accumulation of these structures relative to treatment with inhibitors alone, indicating that hypoxia increases autophagic flux.

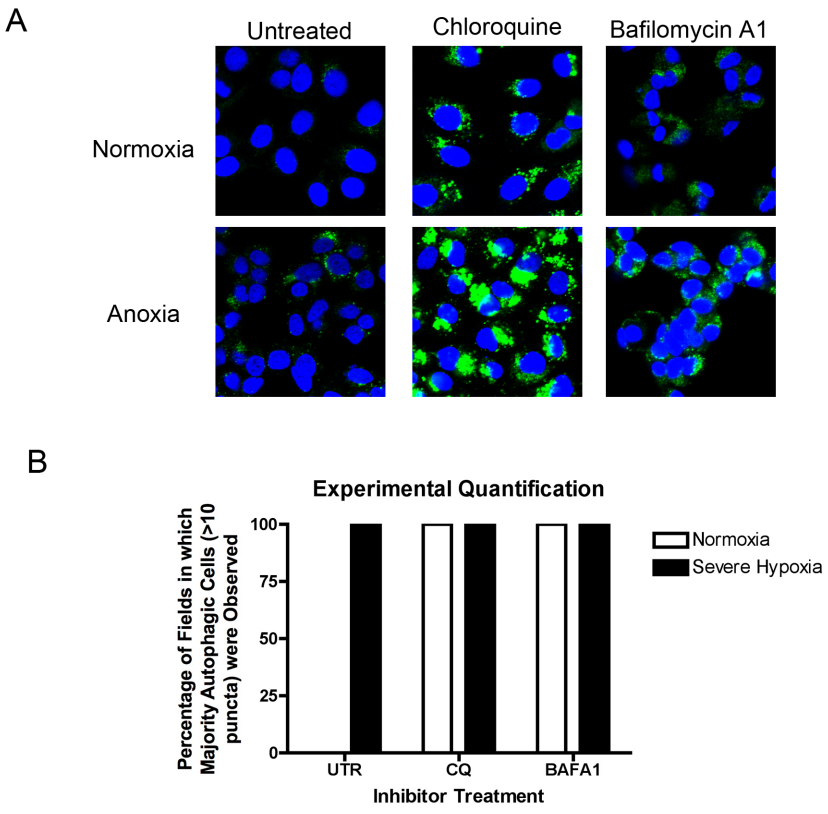

Figure 3.6 Severe hypoxia increases the accumulation of LC3-positive puncta in MCF7 cells treated with lysosmal inhibitors.

MCF7 cells were plated on coverslips and treated with 0.1μM bafilomycin A1 or 25μM chloroquine, and then immediately exposed to severe hypoxia. After 24 hours, cells were fixed and stained for endogenous LC3 (green) or DNA (blue), and visualized by confocal microscopy. (A) Representative images from at least N=3 independent experiments are shown. (B) The percentage of fields containing a majority autophagic cells was assessed and quantified for one such experiment.

3.2.3 Polysomal fractionation identifies mRNA transcripts that are preferentially translated in severe hypoxia

The identification and understanding of pathways that mediate adaptation to severe hypoxia in cancer cells may be therapeutically important. To this end, several studies from this group and others have focused on the identification of autophagy genes that are upregulated in severe hypoxia (Milani et al., 2009; Rouschop et al., 2009b; Rzymski et al., 2010). As described in Chapter 1, one of the primary functions of the ISR is the attenuation of protein synthesis. In severe hypoxia, phosphorylation of eIF2α by PERK inhibits global mRNA translation, reducing the energetic burden on the cell and preventing further accumulation of unfolded proteins in the ER (Koumenis et al., 2002; Rzymski and Harris, 2007).

This change in translation can be assessed by examining the association of ribosomes with mRNA. Through the use of sucrose gradients, ribosomes can be separated on the basis of size, and the amount of actively translated mRNA (associated with multiple ribosomes/polysomes) can be measured (Wouters et al., 2005). Indeed, when MCF7 cells were exposed to severe hypoxia, there was a rapid reduction in the association of mRNA with the polysomes (Figure 3.7).

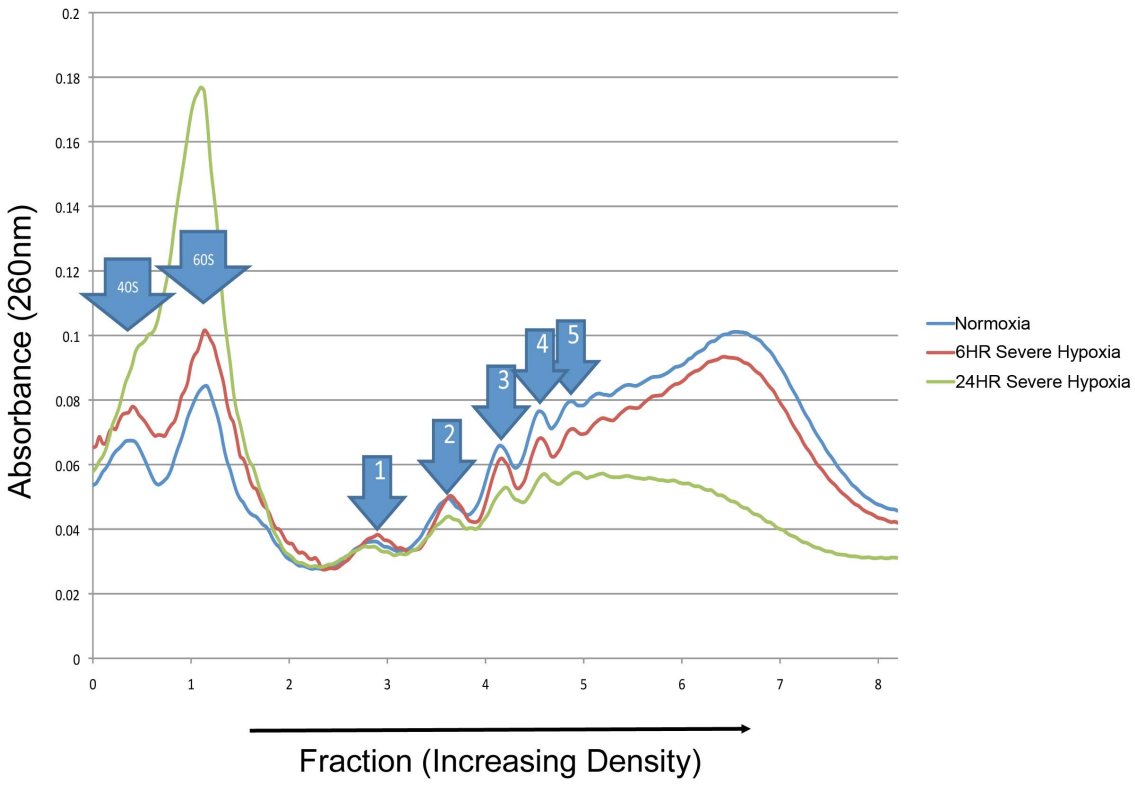

Figure 3.7 Ribosomal fractionation of MCF7 cells exposed to severe hypoxia. *MCF7 cells were exposed to normoxia or severe hypoxia for six or 24 hours. Cells were harvested and the ribosomal compartment was resolved through a sucrose gradient by ultracentrifugation. Fractions were collected and mRNA levels were assessed by absorbance at 260nm. The first and second peaks represent the free 40S and 60S ribosomal subunits, respectively. Each subsequent peak represents mRNA with additional ribosomes attached. N=3 individual dishes for each treatment were pooled in N=1 independent experiments.*

Polysomal mRNA was isolated from MCF7 cells after 24 hours in severe hypoxia, and used for microarray analysis (Tomasz Rzymski and Francesca Buffa, personal communication). In this way, the mRNA transcripts associated with multiple ribosomal subunits, were identified (Rzymski et al., 2010). These transcripts are undergoing active translation while most other translation is repressed (Wouters et al., 2005).

From this experiment, a list of such selectively translated transcripts was compiled. A portion of this data is included below, in Table 3.1.

Table 3.1. List of Genes Enriched in Polysomal Fractions of Hypoxic Cells

ID	Accession	Name	Symbol	p	FC
GI_21361917-S	NM_022356.2	leucine proline-enriched proteoglycan (leprecan) 1	LEPRE1	6.86E-09	3.114138385
GI_21269871-A	NM_139274.1	acyl-CoA synthetase short-chain family member 2	ACAS2	3.58E-07	3.064585734
GI_39930348-S	NM_015187.1	KIAA0746 protein	KIAA0746	6.41E-07	3.052902154
GI_9257230-S	NM_002538.2	occludin	OCLN	6.17E-05	3.039945624
Hs.356481-S	null	-	Hs.356481	3.57E-07	2.994918885
GI_16757969-I	NM_052966.1	chromosome 1 open reading frame 24	C1orf24	5.53E-08	2.973622799
GI_23957697-S	NM_153607.1	adult retina protein	LOC153222	6.41E-07	2.945852338
GI_8922666-S	NM_018217.1	chromosome 20 open reading frame 31	C20orf31	2.19E-06	2.922182049
GI_4503174-S	NM_003467.1	chemokine (C-X-C motif) receptor 4	CXCR4	6.83E-05	2.900439765
GI_40255072-S	NM_144717.2	fibronectin type III domain containing 6	MGC34923	6.07E-07	2.774095008
GI_14195617-A	NM_031845.1	microtubule-associated protein 2	MAP2	7.10E-06	2.765241537
GI_4504492-S	NM_003806.1	harakiri, BCL2 interacting protein (contains only BH3 domain)	HRK	2.52E-06	2.704222656
GI_13699861-S	NM_006389.2	hypoxia up-regulated 1	HYOU1	1.57E-06	2.689767083
GI_37546139-S	XM_210035.2	similar to putative UST1-like organic anion transporter	LOC286408	3.24E-05	2.655863561
GI_28372560-S	NM_174940.1	transmembrane protein 80	LOC283232	1.15E-06	2.637056885
GI_4557834-S	NM_000285.1	peptidase D	PEPD	9.47E-05	2.634728058
GI_38708325-S	NM_001896.2	casein kinase 2, alpha prime polypeptide	CSNK2A2	4.91E-05	2.623983869
GI_21396483-S	NM_003523.2	histone 1, H2be	HIST1H2BE	5.02E-05	2.599359723

As highlighted in the table, the mRNA transcript of the BH3-only protein HRK was 2.7-fold enriched in the polysomal fraction of cells exposed to severe hypoxia for 24 hours ($P = 2.52 \times 10^{-6}$). HRK was selected for further analysis because of its previously established role in apoptosis and its putative role in activating autophagy. The author hypothesized that HRK might play a role in the activation of cell death pathways in response to severe hypoxia.

3.2.4 Severe but not moderate hypoxia activates the integrated stress response and induces the expression of harakiri

To confirm the microarray data identifying HRK as a hypoxia-regulated gene, MCF7 and MDA-MB-231 cells were exposed to either moderate or severe hypoxia for 24 or 48 hours and protein and mRNA levels were assessed. Severe but not moderate hypoxia for 48 hours increased the expression of HRK mRNA to 35-fold the normoxic level in MCF7 cells and to 18-fold the normoxic level in MDA-MB-231 cells ($P<0.001$; N=3, one-way ANOVA) (Figure 3.8A). Blotting for markers of the HIF pathway (HIF1α, HIF2α, CAIX) and the integrated stress response (ATF4 and CHOP) showed that the kinetics of HRK mRNA induction matched those of the ISR target gene CHOP, rather than the HIF1-target gene CAIX (Figure 3.8C and Figure 3.8D).

It is worthy to note, however, that one can again observe significant heterogeneity in the hypoxic response, depending on the cell line examined. For example, HIF1α is robustly increased by both moderate and severe hypoxia in MCF7 cells, but only by moderate hypoxia in MDA-MB-231 cells (Figure 3.8C and D, respectively). This difference may be due to kinetic variability in the HIF response—that is HIF1α may be rapidly accumulated at earlier time points in severe hypoxia, and then is no longer translated at later time points. Indeed, there is evidence indicating that mediators of the ISR, such as PKR (which is activated by severe hypoxia) may in fact block the accumulation of HIF1α in certain cellular contexts (Papadakis et al., 2010).

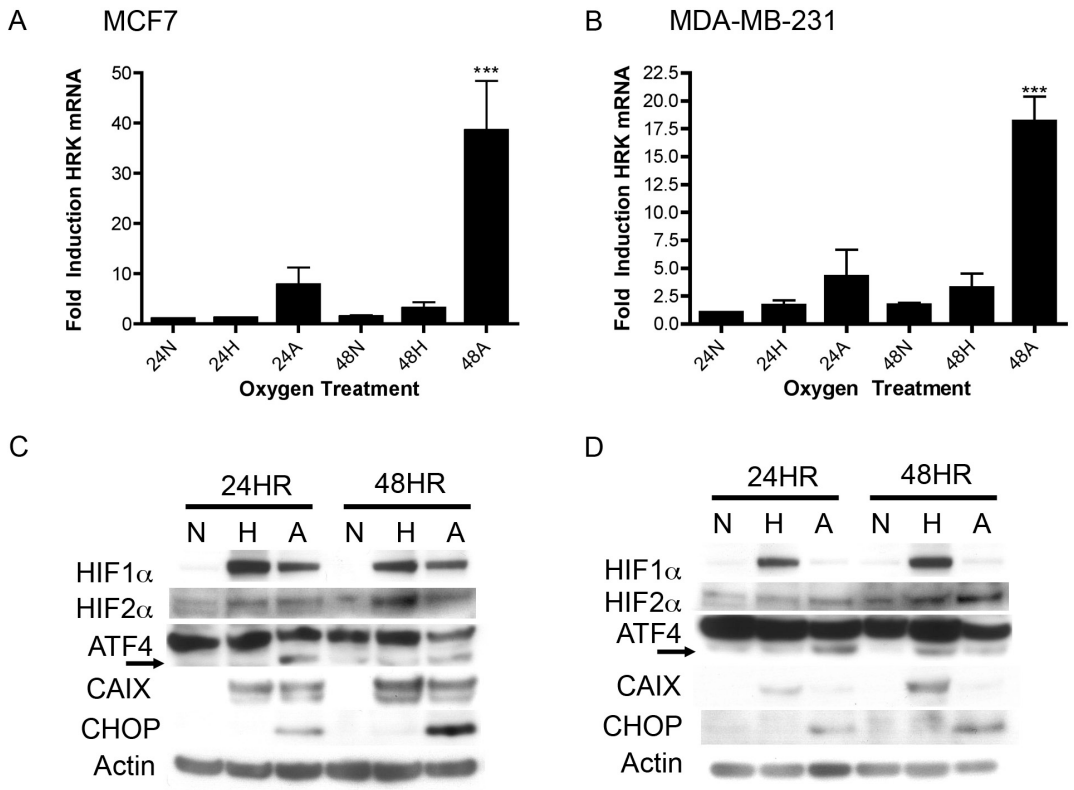

Figure 3.8 Severe hypoxia induces the expression of HRK mRNA and the accumulation of the ISR markers ATF4 and CHOP in both MCF7 and MDA-MB-231 breast cancer cell lines.

*MCF7 and MDA-MB-231 cells were exposed to normoxia, moderate hypoxia (H), or severe hypoxia (A) for 24 or 48 hours. Cells were harvested and analyzed by RT-qPCR (Part A and Part B) or by western blotting (Part C and Part D) with the indicated antibodies or primer sets. In parts A and B, *** indicates P<0.001 relative to 24N for at least N=3 independent experiments, with standard error shown. In parts C and D, representative images from at least N=2 independent experiments are shown.*

After substantial investment of time and money in commercial antibodies and the generation of new antibodies, the endogenous levels of HRK remained undetectable by western blotting. Forced expression of myc-tagged HRK and western blotting of

these lysates identified two antibodies that could detect HRK: an in-house antibody provided by another group (raised against a central peptide region) (Shinoe et al., 2001), and the N20 antibody from Santa Cruz Biotechnology (raised against an N-terminal peptide) (Figure 3.9). Unfortunately, neither of these antibodies could detect endogenous levels of HRK protein in any of the cell lines investigated (data not shown).

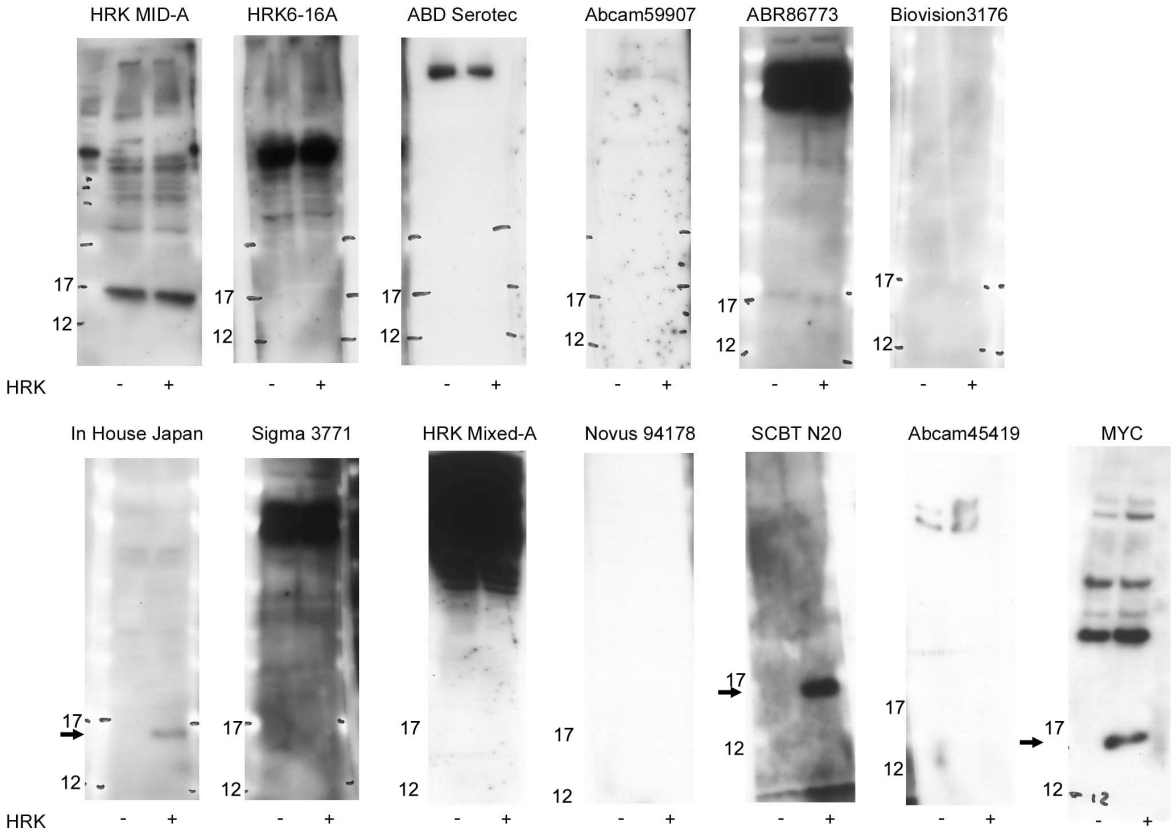

Figure 3.9 HRK antibody validation.

MCF7 cells were transfected with either an empty control vector or a vector encoding myc-tagged HRK for 48 hours. Cells were then harvested and analyzed by western blotting using the antibodies indicated at the top of each membrane slice. An anti-myc antibody was used to assess the expression of myc-tagged HRK. Note that the relative molecular weight of HRK is 13kDA, and that of the HRK-myc fusion protein is 14-15kDA. Arrows point to true positive immunoreactive bands.

3.2.5 Severe hypoxia activates the UPR and induces HRK expression in a variety of cell lines

To further investigate the expression of HRK and the activation of the ISR in cancer, MCF7, MDA-MBA-231, and HCT116 cells were exposed to severe hypoxia for zero, two, six, twelve, 24, or 48 hours and cells were harvested for analysis by RT-qPCR and western blotting. HCT116 cells have a well-documented autophagic response to severe hypoxia, and strong activation of the ISR, and thus were included from this point on. In each cell line examined, HRK mRNA was strongly induced (Figure 3.8A through C). This expression was highest after 48 hours in severe hypoxia, and the magnitude of this induction ranged from 7-fold in the HCT116 cells ($P<0.01$) to 93-fold in the MCF7 cells ($P<0.01$). Without exception, the maximal expression of HRK followed the phosphorylation of PERK (12 to 24HR) and accumulation of ATF4 protein (24HR), and matched the expression of the ATF4 target gene CHOP (Figure 3.10). This pattern of expression suggested that HRK might be an ATF4-dependent gene.

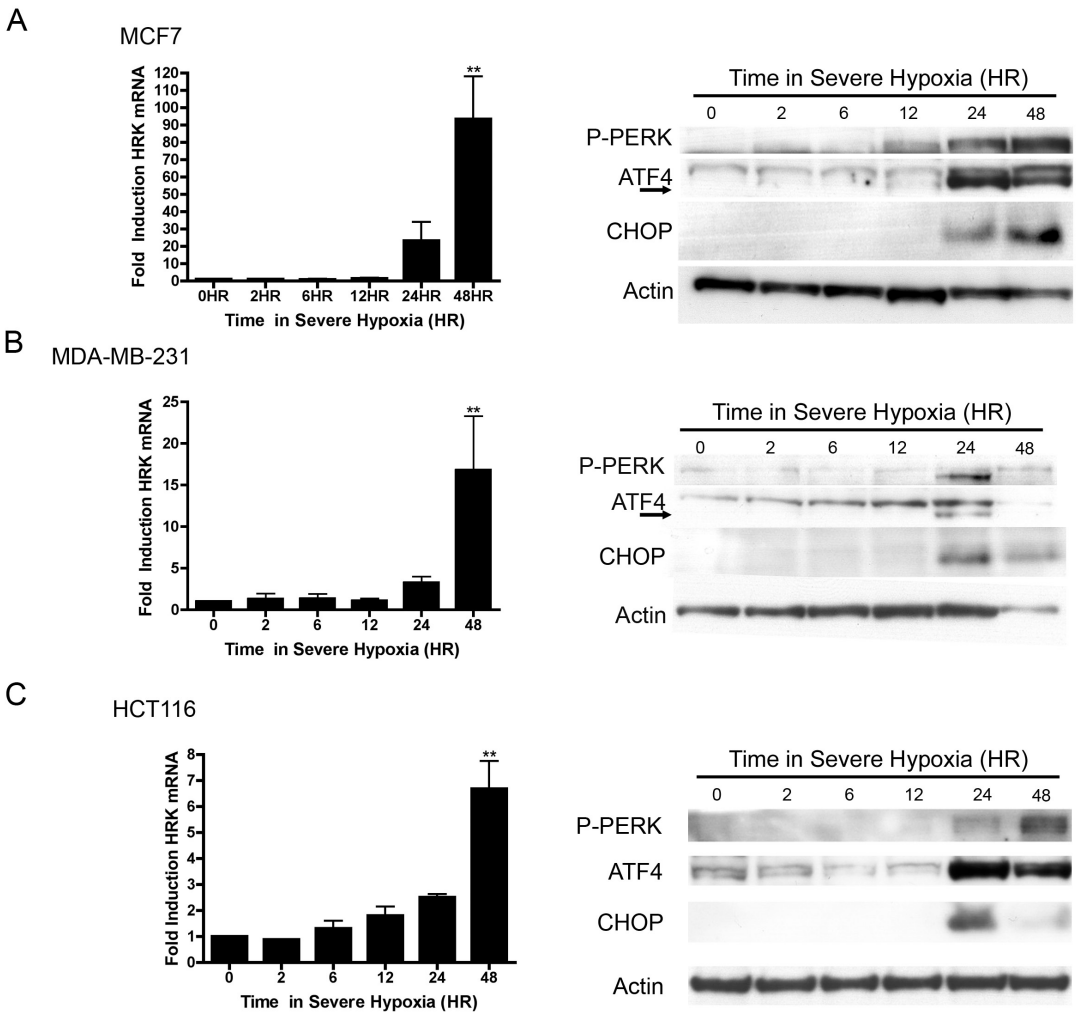

Figure 3.10 Severe hypoxia induces the expression of HRK mRNA over a timecourse that matches the phosphorlyation of PERK protein, and the accumulation of ATF4 and CHOP protein in MCF7, MDA-MB-231, and HCT116 cancer cell lines.

*MCF7, MDA-MB-231, and HCT116 cells were exposed to severe hypoxia for the indicated times. Cells were harvested and analyzed by western blotting or RT-qPCR using the denoted antibodies or PCR primers, respectively. For RT-qPCR, N=3 independent experiments were done and ** indicates P<0.01 by one-way-ANOVA. For western blotting, representative images from at least N=2 independent experiments are shown.*

To assess if this pattern of HRK expression is a standard response, several cell lines from other tissues were analyzed. When HEK293 (human embryonic kidney fibroblasts), HeLa (cervical cancer cells), MEF3T6 (mouse embryonic fibroblasts), and T47D (another ER+ breast cancer cell line) cell lines were exposed to severe hypoxia, the same pattern of HRK mRNA expression was observed (Figure 3.11).

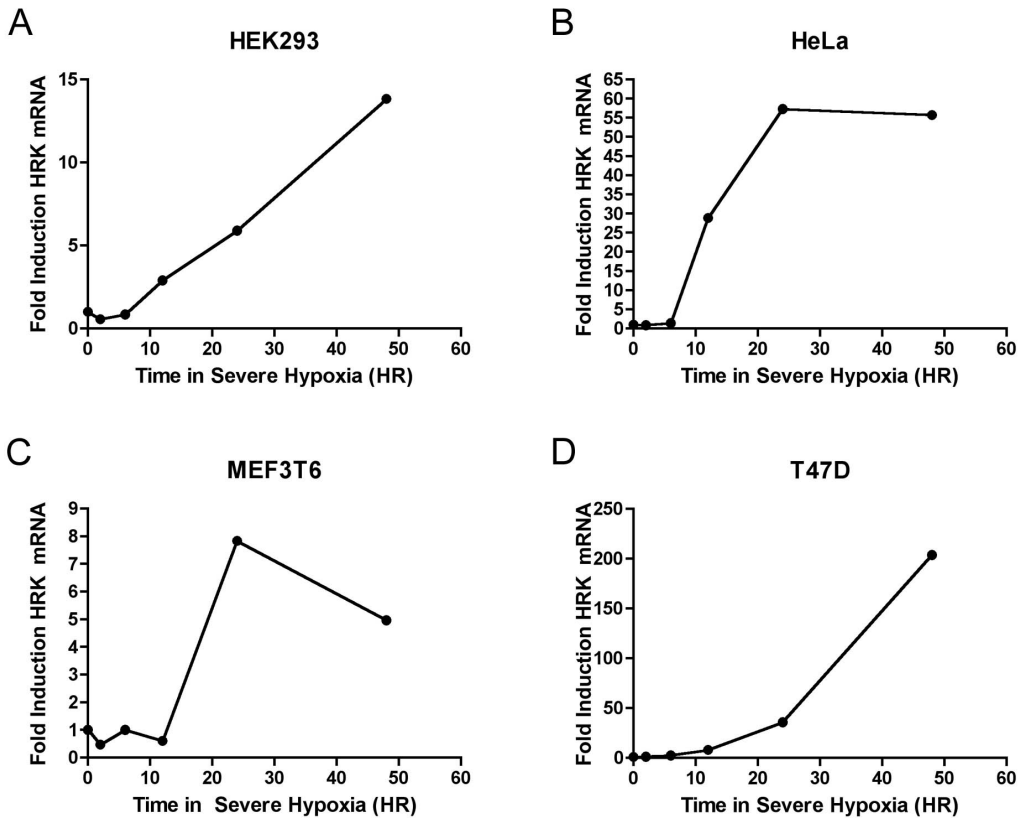

Figure 3.11 Severe hypoxia induces HRK mRNA expression in four other cell lines.

HEK293 (A), HeLa (B), MEF3T6 (C), or T47D (D) cells were exposed to severe hypoxia for the indicate times. Cells were harvested and analyzed by RT-qPCR using primers specific to HRK mRNA. N=1 independent experiment is shown in each case.

Interestingly, HRK could not be detected in the U87 glioblastoma cell line or the SW48 colon adenocarcinoma cell line, agreeing with previous work demonstrating that

silencing of HRK in these contexts may be important for tumour progression (Nakamura et al., 2005; Obata et al., 2003).

3.2.6 HRK mRNA expression is activated by ER stress-inducing drugs

As shown above, severe hypoxia was observed to activate the ISR and to induce the expression of HRK mRNA (Figure 3.10), implying that HRK is a target of the UPR. To ascertain whether hypoxic HRK mRNA expression is due to ER stress, MCF7 cells were treated with a panel of drugs in normoxia. These included the ER stressors thapsigargin (inhibits the ER calcium ATPase) and tunicamycin (blocks N-linked glycosylation of proteins), the proteasome inhibitors MG132, MG115, and bortezomib, the ROS inducer arsenite, and the so-called hypoxia mimetics $CoCl_2$ and DFO (inhibit the prolyl hydroxylases, stabilizing HIFα).

Treatment of cells with thapsigargin or tunicamycin resulted in more than 15-fold HRK mRNA induction ($P<0.05$) (Figure 3.12A). This induction was accompanied by phosphorylation of PERK and accumulation of ATF4 (Figure 3.12B). This result suggests that ER stress contributes to the upregulation of harakiri in severe hypoxia. It is interesting to note that treatment with proteasome inhibitors yielded a larger accumulation of ATF4 and HIF1α protein, but failed to significantly induce HRK. In agreement with previous work, this result demonstrates that both ATF4 and HIF1α are being rapidly turned over in normoxia. Interestingly, blocking the degradation of these factors is insufficient to drive HRK expression, indicating this pool of ATF4 and HIF1α is transcriptionally less active (Milani et al., 2009). Thus, though the accumulation of ATF4 caused by thapsigargin and tunicamycin treatment is less dramatic, it is likely that this pool of ATF4 is more functionally significant.

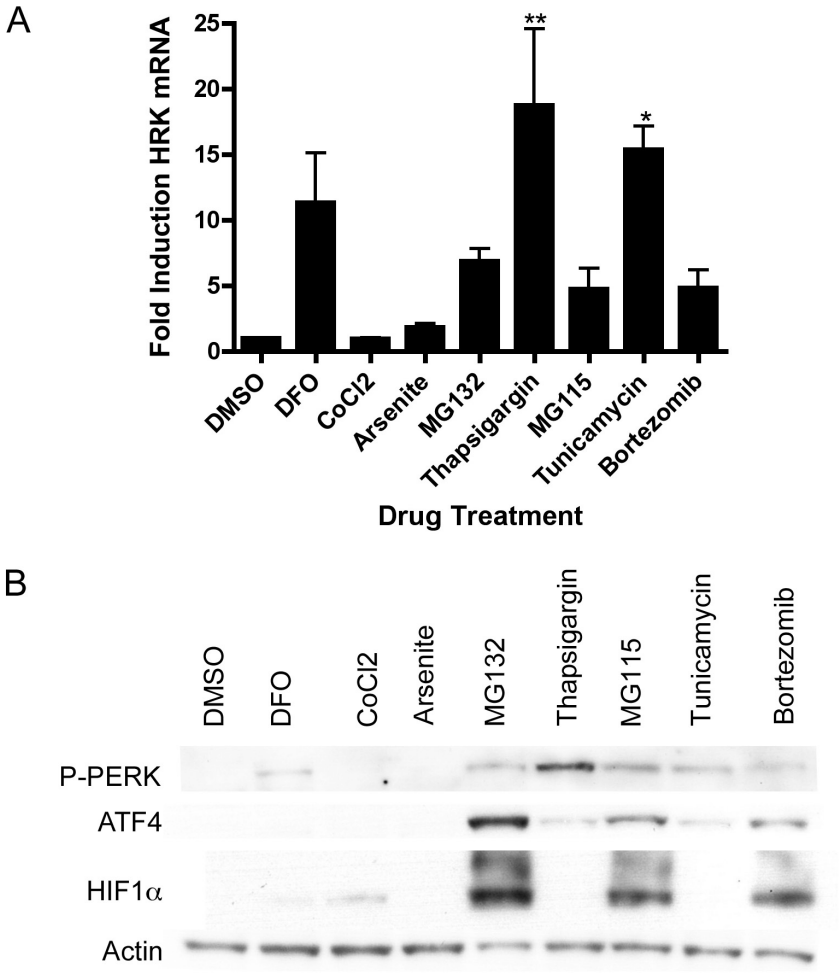

Figure 3.12 Treatment of MCF7 breast cancer cells with the ER-stress inducing agents thapsigargin or tunicamycin causes the induction of HRK mRNA and the accumulation of ATF4 protein.

*MCF7 cells were treated with 40μM deferoxamine mesylate (DFO), 100μM cobalt (II) chloride ($CoCl_2$), 5μM arsenite, 10μM MG132, 5μM MG115, 5μg/mL tunicamycin, 300nM thapsigargin, 100nM bortezomib, or DMSO. After 24 hours, cells were harvested for RT-qPCR (A), or western blotting (B) using the indicated primers and antibodies, respectively. For RT-qPCR, N=3 independent experiments were done; ** and * indicate P<0.01 or P<0.05 by one-way-ANOVA relative to the DMSO treated control, respectively. For western blotting, representative images from at least N=2 independent experiments are shown.*

3.2.7 Harakiri mRNA is rapidly degraded upon reoxygenation

Given that HRK was so strongly induced by severe hypoxia, and its reported role in death, the author next sought to assess the dynamics of HRK mRNA stability. When MCF7 cells were exposed to severe hypoxia for 24 hours and subsequently reoxygenated, HRK mRNA levels were observed to rapidly fall to normoxic levels, with a $t_{1/2}$ of approximately 1.5 hours (Figure 3.13). Thus, it is clear that HRK mRNA expression is oxygen sensitive.

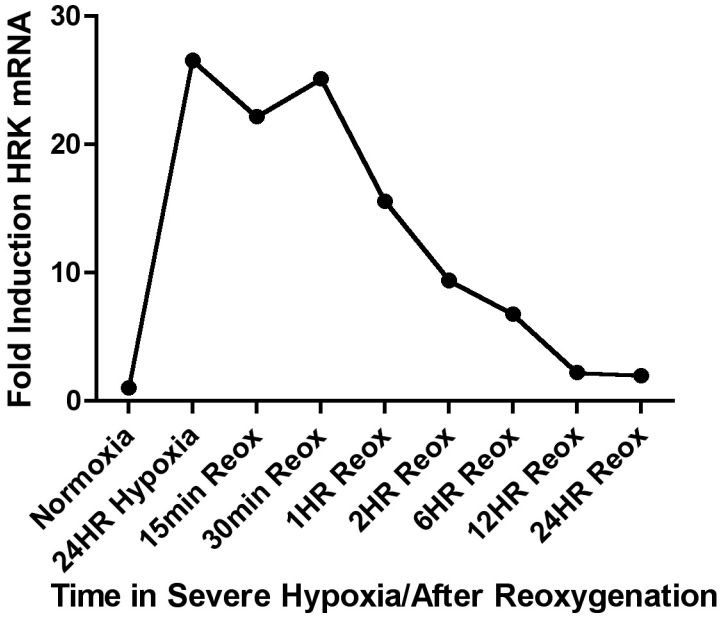

Figure 3.13 Harakiri mRNA levels decrease to normoxic levels following reoxygenation of MCF7 breast cancer cells.

MCF7 cells were exposed to severe hypoxia for 24 hours and then reoxygenated by returning them to the normal cell culture incubator for the indicated times. Cells were then harvested and analyzed by RT-qPCR for HRK mRNA with PCR primers specific to HRK. N=1 independent experiment was performed.

3.2.8 Severe hypoxia stimulates the expression of other BH3-only proteins

As described above, HRK is a member of the BCL2 family of proteins. These proteins are well known regulators of apoptosis and autophagy, and are subject to tight control at both the transcriptional and post-translational level. Since HRK is so strongly induced by severe hypoxia, RT-qPCR was done to determine if other members of the BCL2 family were similarly activated. MCF7 cells exposed to severe hypoxia for 48 hours were found to upregulate the expression of two other BH3-only proteins: PUMA and NOXA (Figure 3.14). In agreement with this finding, previous reports have implicated PUMA and NOXA expression in cell death due to ER stress and hypoxia (Armstrong et al., 2009; Cazanave et al., 2010; Hetz, 2007; Kim et al., 2004; Wang et al., 2009; Yu et al., 2003).

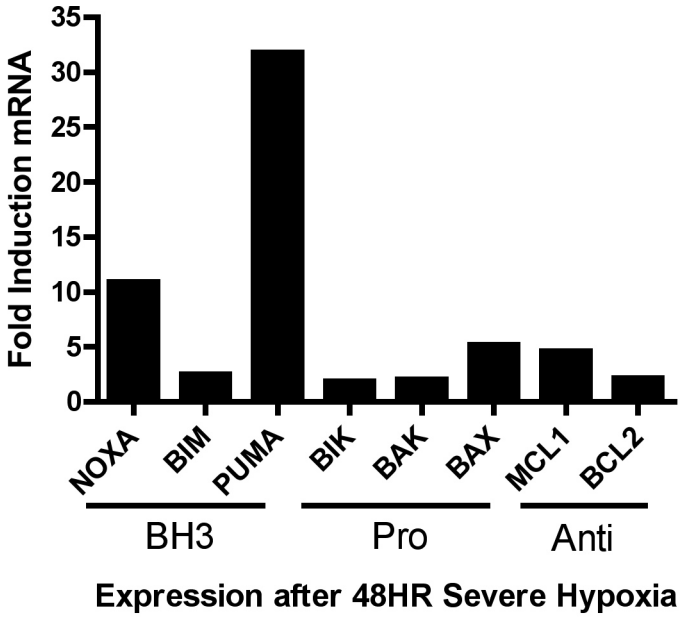

Figure 3.14 PUMA and NOXA mRNA accumulates in MCF7 breast cancer cells exposed to severe hypoxia for 48 hours.

MCF7 cells were exposed to severe hypoxia or normoxia for 48 hours and then harvested for RT-qPCR analysis using the primer sets indicated. NOXA, BIM, and PUMA

are BH3-only proteins; BIK, BAK, and BAX are multidomain pro-apoptotic proteins; MCL1 and BCL2 are multidomain antiapoptotic proteins. N=1 independent experiment.

To further assess the expression profile of PUMA and NOXA after exposure to severe hypoxia, a time course experiment was done. MCF7, MDA-MB-231, and HCT116 cells were exposed to severe hypoxia and both RT-qPCR and western blotting were done to measure PUMA and NOXA expression. In each cell line examined, the pattern of PUMA and NOXA mRNA expression closely mimicked that observed for HRK mRNA and the accumulation of ATF4 protein: induction occurred at 24 hours and reached a maximum after 48 hours in severe hypoxia (Figure 3.15A, Figure 3.16A, Figure 3.17A). The relative fold induction of HRK mRNA greatly exceeded that of PUMA, which in turn was greater than that of NOXA. The accumulation of PUMA and NOXA protein, on the other hand, did not always reflect the expression pattern at the mRNA level (summary in Table 3.2). In MCF7 and HCT116 cells, PUMA protein levels were high in normoxia, and decreased with hypoxic exposure (Figure 3.15B, Figure 3.17B). In MDA-MB-231 cells, PUMA protein accumulated with exposure to severe hypoxia, but this accumulation preceded the mRNA induction (Figure 3.16B). It is important to note that the RT-qPCR primers used for PUMA were designed to detect both the α and β isoforms. However, the PUMA band detected by western blotting had an apparent molecular weight of approximately 20kDA, implying that it is PUMA-β (Tampio et al., 2009). However, further study would be necessary to confirm this assertion and its functional relevance in severe hypoxia. It is also worthy to note that the expression of PUMA and NOXA protein at 48 hours in Figure 3.16B is likely much greater than observed, as the number of viable cells remaining at this time point was quite low.

By contrast, the regulation of NOXA protein more closely reflected the changes in mRNA. In MDA-MB-231 and HCT116 cells, NOXA protein accumulated with exposure

to severe hypoxia, though again preceding the mRNA induction (Figure 3.16B, Figure 3.17B). In MCF7 cells, NOXA protein was undetectable (Figure 3.15B).

The disconnect between the mRNA level of PUMA and NOXA and the expression of their proteins implies that they are being regulated at multiple levels, likely in a cell context-dependent manner. The common induction of mRNA after 24 hours of severe hypoxia implies a common mode of transcriptional regulation (perhaps through ATF4). However, the cell line-dependent differences in protein accumulation (or indeed degradation) are likely due to tissue-specific differences in the regulation of these genes, and additional mutations acquired by these specific cancer cells. For example, the rapid degradation of PUMA protein observed in MCF7 and HCT116 cells in severe hypoxia may be due to blockade of translation or specific proteasomal degradation pathways to protect these cancer cells from PUMA-mediated apoptosis. Similarly, the failure to detect NOXA protein in MCF7 cells despite high mRNA induction may be due to mutations in the gene that prevent its translation. Alternatively, the early accumulation of PUMA and NOXA protein seen in MDA-MB-231 cells could be due to post-transcriptional mechanisms that promote the selective translation of these transcripts in severe hypoxia.

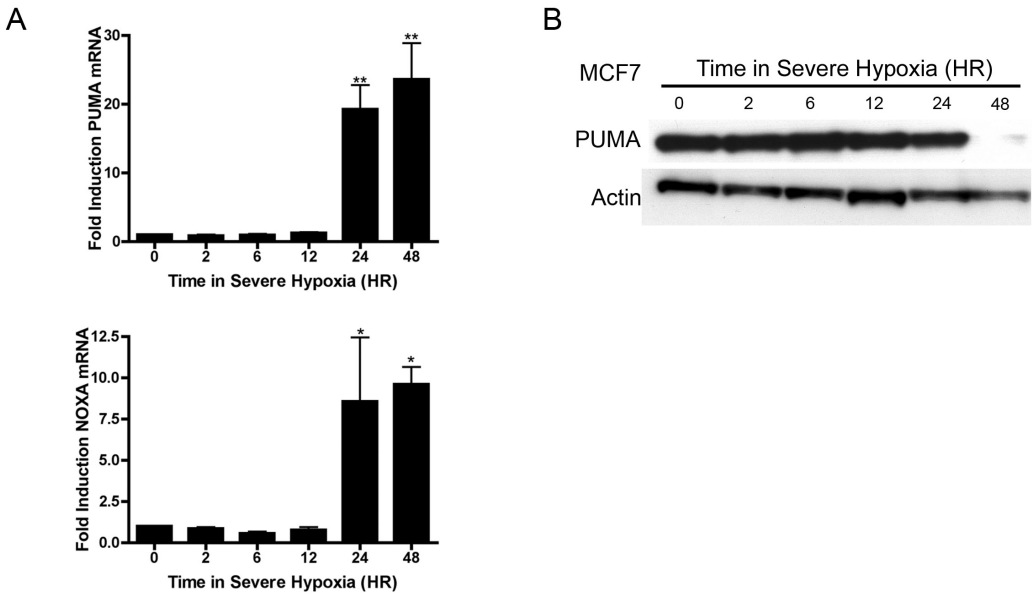

Figure 3.15 Severe hypoxia causes the accumulation of PUMA and NOXA mRNA in MCF7 cells.

*MCF7 cells were exposed to severe hypoxia for the times indicated. Cells were harvested and analyzed by RT-qPCR (A) and western blotting (B) using the primers and antibodies indicated, respectively. For RT-qPCR, N=3 independent experiments were done; ** and * indicate P<0.01 or P<0.05 by one-way-ANOVA relative to the normoxic control, respectively. For western blotting, representative images from at least N=2 independent experiments are shown.*

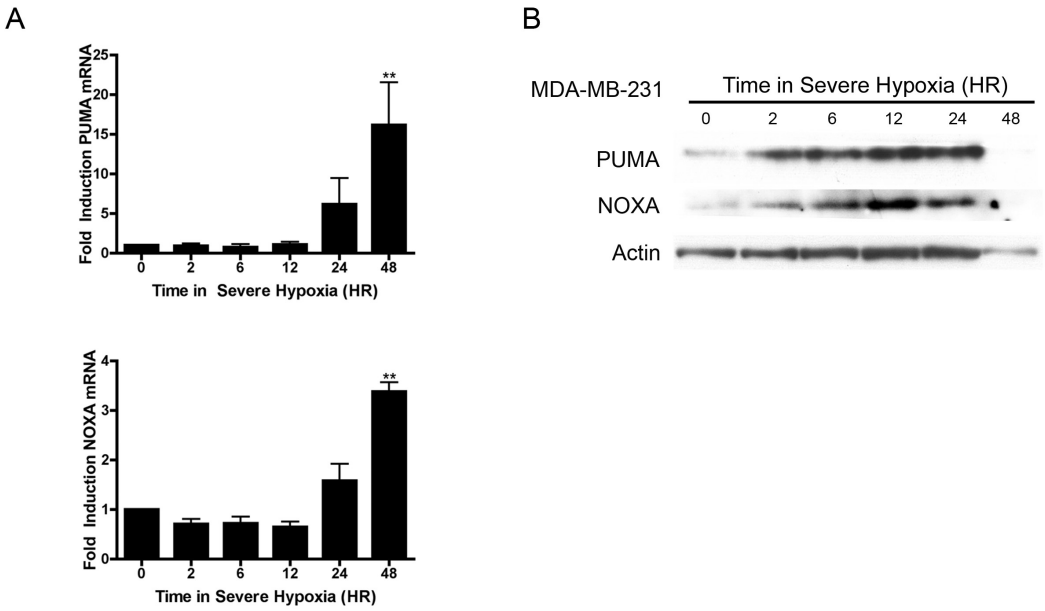

Figure 3.16 Severe hypoxia causes the accumulation of PUMA and NOXA mRNA and protein in MDA-MB-231 cells.

*MDA-MB-231 cells were exposed to severe hypoxia for the times indicated. Cells were harvested and analyzed by RT-qPCR (A) and western blotting (B) using the primers and antibodies indicated, respectively. For RT-qPCR, N=3 independent experiments were done; ** indicates P<0.01 by one-way-ANOVA relative to the normoxic control. For western blotting, representative images from at least N=2 independent experiments are shown.*

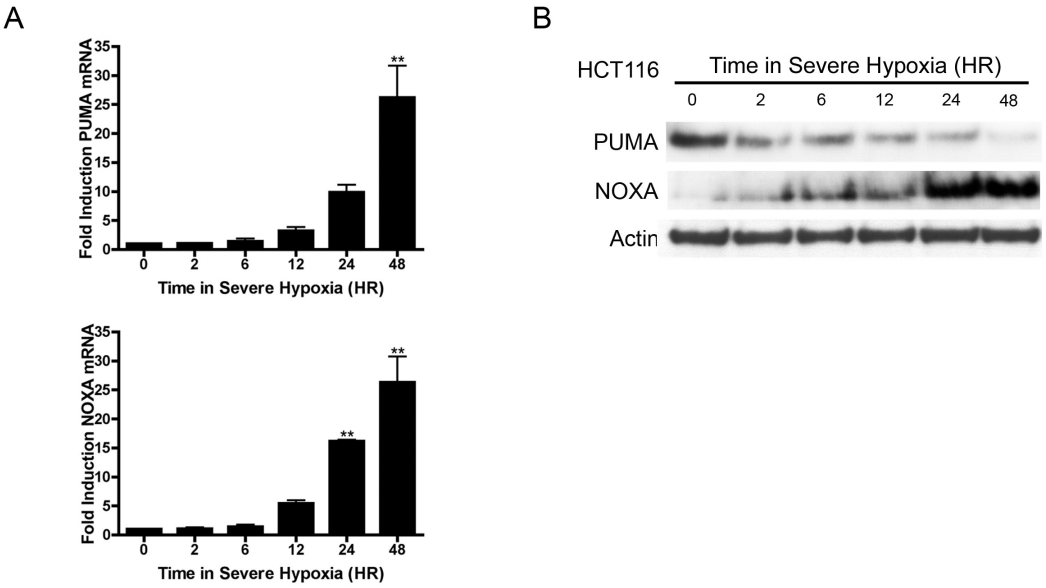

Figure 3.17 Severe hypoxia causes the accumulation of PUMA and NOXA mRNA and NOXA protein in HCT116 cells.

*HCT116 cells were exposed to severe hypoxia for the times indicated. Cells were harvested and analyzed by RT-qPCR (A) and western blotting (B) using the primers and antibodies indicated, respectively. For RT-qPCR, N=3 independent experiments were done; ** indicates P<0.01 by one-way-ANOVA relative to the normoxic control. For western blotting, representative images from at least N=2 independent experiments are shown.*

Table 3.2. Summary of PUMA and NOXA regulation in severe hypoxia.

Cell Line	ATF4 protein	PUMA mRNA	PUMA protein	NOXA mRNA	NOXA protein
MCF7	Up at 24hr	Up at 24hr	Down at 48hr	Up at 24hr	Not detected
MDA-MB-231	Up at 24hr	Up at 24hr	Up at 2hr	Up at 24hr	Up at 6hr
HCT116	Up at 24hr	Up at 24hr	Down at 2hr	Up at 24hr	Up at 6hr

3.2.9 The hypoxic induction of HRK, PUMA, and NOXA is ATF4-dependent

HRK, PUMA, and NOXA mRNA levels all exhibited a pattern of induction in severe hypoxia that mimics the UPR target gene CHOP (data not shown). Moderate hypoxia was insufficient to induce HRK mRNA to the levels observed in severe hypoxia. Additionally, the ER stress inducing agents thapsigargin and tunicamycin both induced high levels of HRK mRNA in normoxia. Thus, the transcription of these genes was suspected to be dependent on the UPR. Furthermore, examination of the promoter regions of HRK, PUMA, and NOXA predicted several putative ATF4-binding sites (Genomatix).

As an example, a schematic of the HRK promoter region is shown in the figure below (Figure 3.18). As can be observed in this figure, putative CREB sites were found on both the positive and negative strand, one of which was previously validated to regulate HRK expression (Towers et al, 2009). Moreover, sequence analysis identified putative binding sites for HIF, p53, and NFκB (not shown).

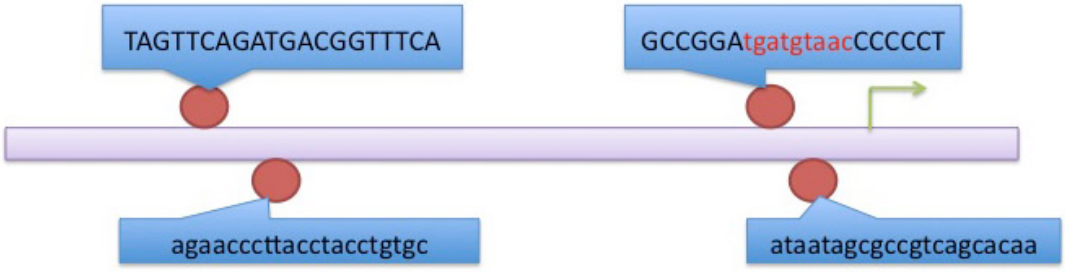

Figure 3.18 Putative CREB/ATF4 binding sites are predicted in the HRK promoter region.

Putative CREB/ATF4 binding sites (red circles) are indicated on the schematic diagram above. Transcription start is indicated by the green arrows, and callouts show the

sequences predicted as binding sites matching the TGACG core sequence. Transcription start was assumed to occur from the first codon of Exon 1, and was identified using NCBI gene browsing tools. Note that the sequence highlighted in red was validated in previous work (Towers et al, 2009).

To test this conjecture, short interfering RNA molecules specific to ATF4 (Rzymski et al., 2010) were used to ablate ATF4 protein and transcriptional activity, and MCF7 cells were exposed to severe hypoxia for 48 hours. The knockdown of ATF4 protein was confirmed by western blotting (Figure 3.19A), and two previously established ATF4 target genes, CHOP and LC3, were used to confirm reduced ATF4 activity (Figure 3.19A).

Knockdown of ATF4 in MCF7 cells reduced the level of HRK, PUMA, and NOXA mRNA transcripts to near normoxic levels (Figure 3.19B). This blunted response implies that ATF4 is indeed mediating the transcription of these BH3-only proteins in severe hypoxia. Similarly, the rate of PUMA protein degradation was greatly enhanced by knockdown of ATF4 (Figure 3.19A). Thus, despite there being no further increase in PUMA protein levels with exposure to hypoxia, ATF4 is clearly required to maintain PUMA protein levels under normoxic and hypoxic conditions.

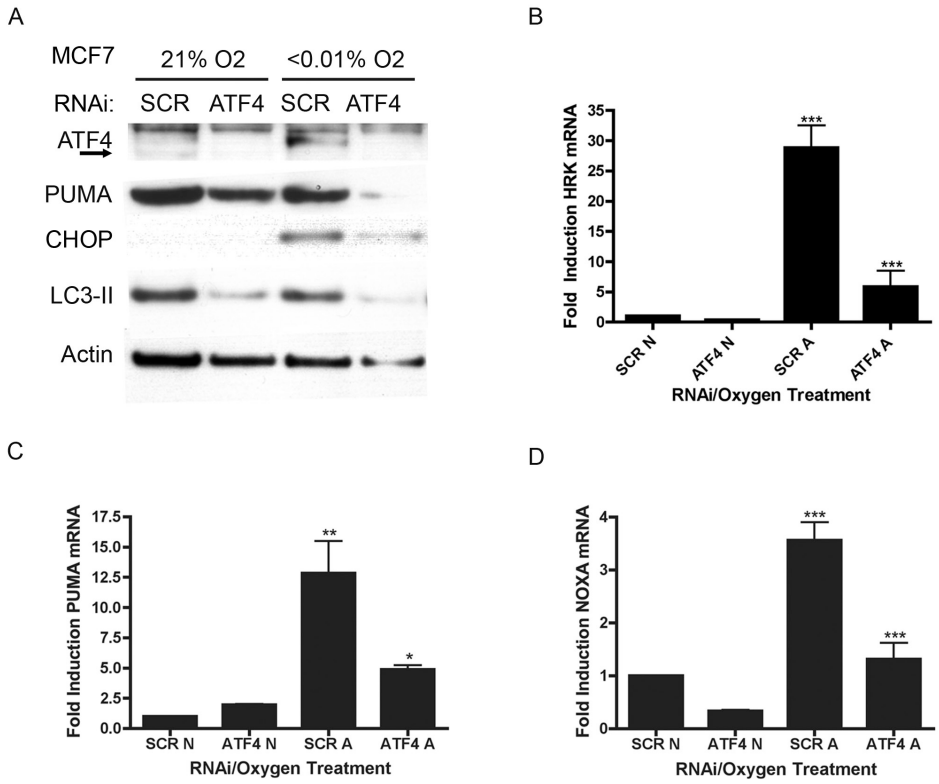

Figure 3.19 MCF7 cells treated with ATF4 siRNA show reduced HRK, PUMA, and NOXA mRNA accumulation upon exposure to severe hypoxia for 48 hours.

*MCF7 cells were transfected with siRNA against ATF4 (ATF4) or a scrambled control sequence (SCR) overnight and exposed to severe hypoxia (A) or normoxia (N) the following day. After 48 hours, cells were harvested for western blotting (A) or RT-qPCR (B-D) using the indicated antibodies and primers, respectively. For RT-qPCR, N=3 independent experiments were done; *, **, and *** indicate P<0.05, P<0.01, and P<0.001 by one-way-ANOVA for SCR A vs SCR N, and ATF4 A vs SCR A. For western blotting, representative images from at least N=2 independent experiments are shown.*

Similar results were obtained when MDA-MB-231 cells and HCT116 cells were treated with siRNA against ATF4 and exposed to severe hypoxia (Figure 3.20 and Figure 3.21). In MDA-MB-231 cells, HRK and PUMA both showed a strong dependence on ATF4, both on the protein level for PUMA and the transcript level for both PUMA and HRK

(Figure 3.20). By contrast, neither the NOXA protein nor transcript levels were reduced by ATF4 knockdown in these cells, and changes in NOXA mRNA were not statistically significant. In HCT116 cells, HRK but not PUMA or NOXA, appeared to depend on ATF4 for the induction of their mRNA transcripts, and for the maintenance of PUMA and NOXA protein levels (Figure 3.21). The latter discrepancy between PUMA and NOXA mRNA and protein may have been due to off-target effects of ATF4-knockdown. Thus, despite cell line specific differences, it is clear that ATF4 regulates a program of BH3-only protein expression in response to severe hypoxia. In particular, HRK appears to be particularly dependent on ATF4 for its expression.

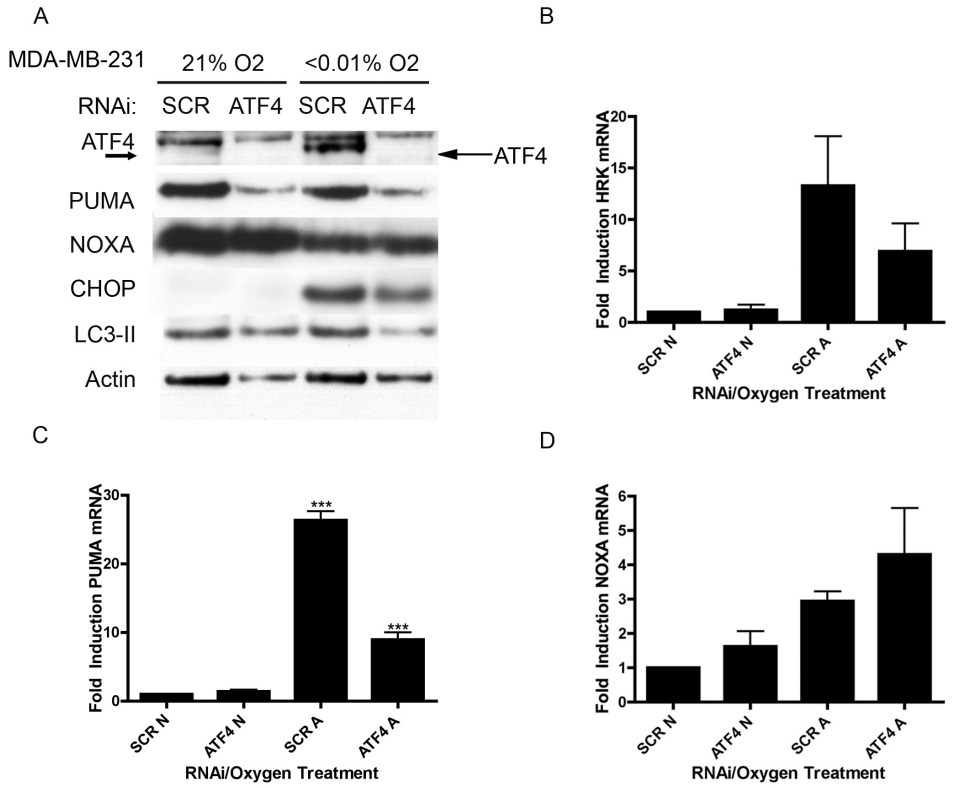

Figure 3.20 MDA-MB-231 cells treated with ATF4 siRNA show reduced HRK, and PUMA mRNA accumulation upon exposure to severe hypoxia for 48 hours.

MDA-MB-231 cells were transfected with siRNA against ATF4 (ATF4) or a scrambled control sequence (SCR) overnight and exposed to severe hypoxia (A) or normoxia (N)

*the following day. After 48 hours, cells were harvested for western blotting (A) or RT-qPCR (B-D) using the indicated antibodies and primers, respectively. For RT-qPCR, N=3 independent experiments were done; *** indicates P<0.001 by one-way-ANOVA for SCR A vs SCR N, and ATF4 A vs SCR A. For western blotting, representative images from at least N=2 independent experiments are shown.*

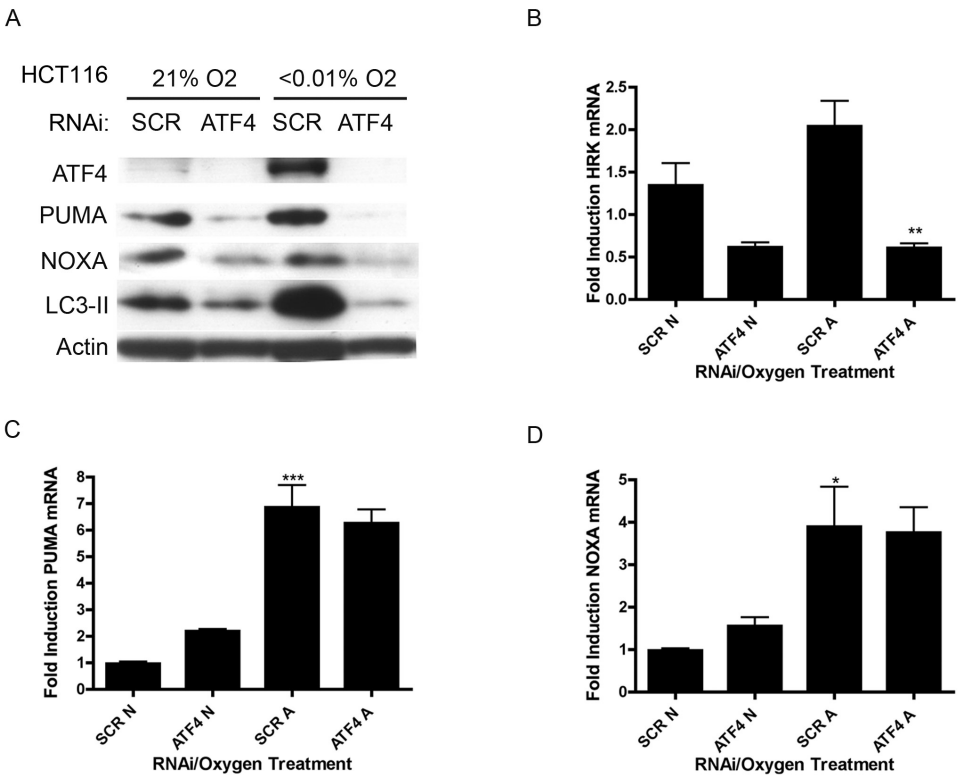

Figure 3.21 HCT116 cells treated with ATF4 siRNA show reduced HRK mRNA accumulation, as well as reduced PUMA and NOXA protein levels upon exposure to severe hypoxia for 48 hours.

*HCT116 cells were transfected with siRNA against ATF4 (ATF4) or a scrambled control sequence (SCR) overnight and exposed to severe hypoxia (A) or normoxia (N) the following day. After 48 hours, cells were harvested for western blotting (A) or RT-qPCR (B-D) using the indicated antibodies and primers, respectively. For RT-qPCR, N=3 independent experiments were done; *, **, and *** indicate P<0.05, P<0.01, and P<0.001 by one-way-ANOVA for SCR A vs SCR N, and ATF4 A vs SCR A. For western blotting, representative images from at least N=2 independent experiments are shown.*

As this work was underway, several other groups published results to confirm the reliance of PUMA and NOXA on ATF4 in several contexts. PUMA was shown to be upregulated by the PERK-ATF4 pathway and to mediate apoptosis in response to NSAID treatment in gastric cells (Ishihara et al., 2007) and in response to ER stress in neuronal cells (Galehdar et al., 2010). Interestingly, NOXA was induced by a heterodimer consisting of ATF4 and ATF3 in response to pharmacological blockade of ERAD (Wang et al., 2009). HRK, on the other hand, is still poorly characterized and its regulation by ATF4 has yet to be described in the literature. In light of these findings (or lack thereof for HRK), the work of this chapter is focused on the regulation and functional relevance of HRK in severe hypoxia.

3.2.10 Exogenous expression of ATF4 drives the transcription of HRK

Having established that RNAi-mediated knockdown of ATF4 protein prevents the hypoxic induction of HRK, a vector encoding the open reading frame of ATF4 was used to exogenously express ATF4 in MCF7 cells in both normoxia and severe hypoxia. Despite the well-established lability of ATF4 protein, transfection of 1000ng or 2000ng of DNA was sufficient to express high levels of ATF4 in normoxia (Figure 3.22A). HRK mRNA levels were found to increase in a dose-dependent manner with increasing amounts of transfected DNA, thus confirming the regulation of HRK by ATF4 (Figure 3.22B).

It is interesting to note that ATF4 alone was sufficient to drive the expression of HRK. This result differs from other data that have shown ATF4 to act as part of a heterodimeric in concord with UPR transcription factors to activate target genes. For example, XBP1 and ATF6 are both required for maximal CHOP induction (Oyadomari and Mori, 2004), and thus, overexpression of ATF4 failed to induce CHOP in this thesis (data not shown).

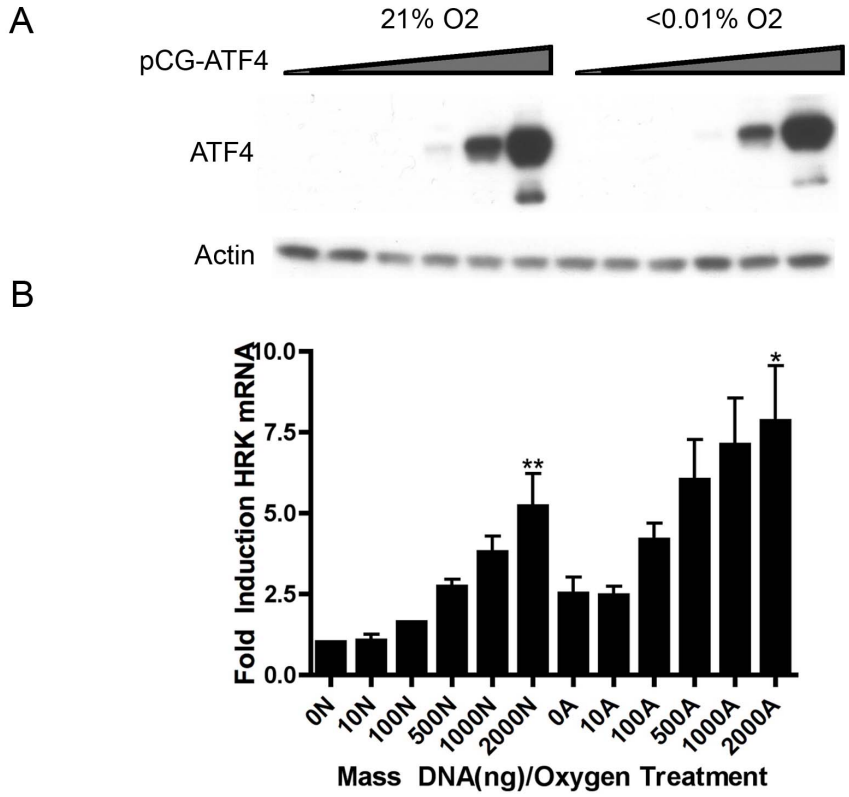

Figure 3.22 Exogenous expression of ATF4 drives causes the accumulation of HRK mRNA in MCF7 breast cancer cells exposed to normoxia or severe hypoxia for 24 hours.

*MCF7 cells were transfected with 0 to 2000ng of pCG-ATF4 and allowed to rest for 24 hours, before being exposed to normoxia (Xng N) or severe hypoxia (Xng A) for a further 24 hours. Cells were then harvested and analyzed by western blotting using the antibodies indicated (A) or by RT-qPCR using primers specific to HRK mRNA (B). For RT-qPCR, N=3 independent experiments were done; *, and ** indicate P<0.05, and P<0.01 by one-way-ANOVA for 2000N vs 0N, and 2000A vs 0A. For western blotting, representative images from at least N=2 independent experiments are shown.*

3.2.11 ATF4 binds directly to the promoter region of the HRK gene

To determine if ATF4 acts directly at the promoter region of HRK, a chromatin immunoprecipitation assay (ChIP) was performed using an antibody specific for ATF4. Using the Genomatix® online software suite, the putative CREB/ATF binding sites containing the TGACG core sequence were identified. By designing a set of PCR primers spanning the region 2000bp upstream of the transcription start site (Figure 3.22A), the likely ATF4 binding sites were narrowed down to those proximal to ChIP primer set #2 (Figure 3.23B). Thus, it is clear that ATF4 induces the transcription of HRK mRNA by direct action at the HRK promoter.

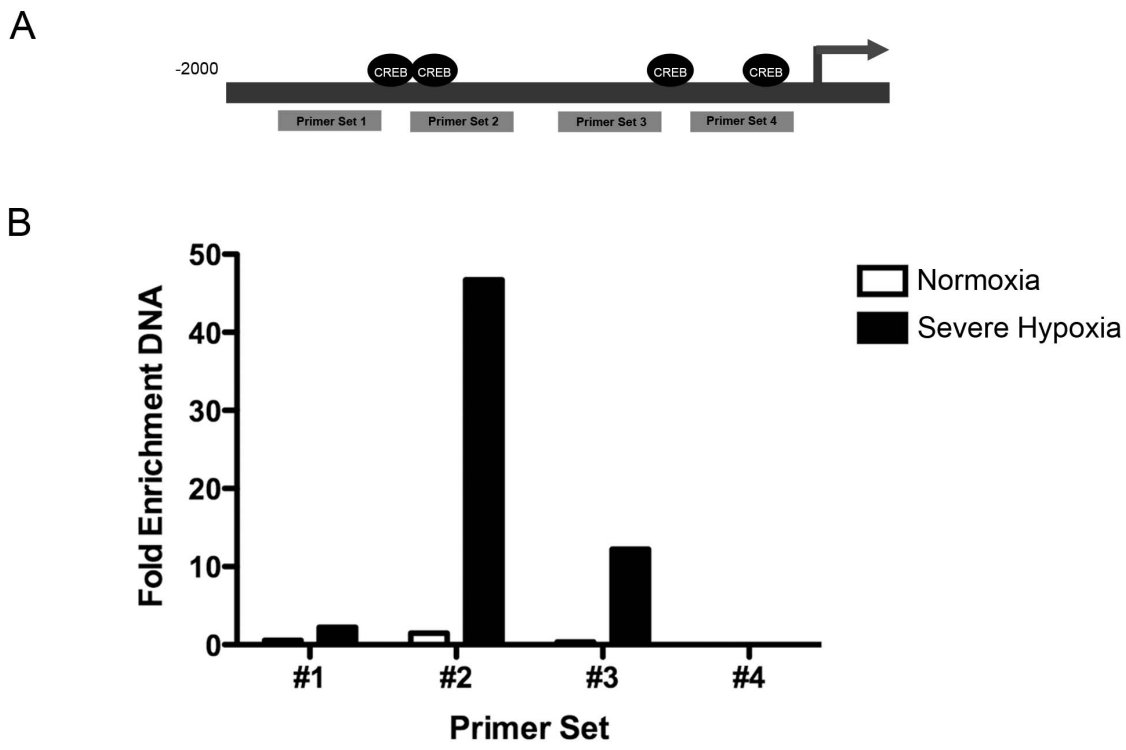

Figure 3.23 Chromatin immunoprecipitation using an ATF4-specific antibody enriches lysates from MCF7 cells exposed to severe hypoxia for 48 hours in DNA corresponding to the HRK promoter region.

MCF7 cells were exposed to normoxia or severe hypoxia for 48 hours and then fixed with paraformaldehyde. DNA was sheared and a chromatin immunoprecipitation

was performed. Primers sets were designed as a tiled set against a 2000bp region upstream of HRK transcription start containing four putative ATF/CREB binding sites (A). RT-qPCR was done to analyze to quantify the enrichment of these fragments in the normoxic and hypoxic samples (B). Arrow indicates direction and location of transcription start, +1. A representative experiment of two independent experiments is shown.

3.2.12 HRK expression is repressed by HIF2

The HIFs play a role in many aspects of hypoxia and tumourigenesis. Previous work has shown that HIF1 is involved in the suppression of proapoptotic Bid and Bax, and the induction of the autophagy-related BH3-only proteins BNIP3 and NIX (Erler et al., 2004; Sowter et al., 2001). Thus, HIF1α and HIF2α were knocked down in MCF7 cells to determine if the HIFs play a role in regulating HRK expression. Following transfection with siRNA molecules specific to HIF1α or HIF2α, cells were exposed to normoxia, moderate hypoxia, or severe hypoxia for 24 hours. In the scrambled controls, HIF1α and HIF2α were stabilized in both conditions of hypoxia and the accumulation of CAIX, a well-described HIF1 target, was observed (Figure 3.24A).

Ablation of HIF1α and HIF2α was confirmed by western blotting and reduced HIF1 transcriptional activity was confirmed by loss of CAIX expression (Figure 3.24A). Neither HIF1α nor HIF2α seemed to be important to HRK regulation in normoxia or moderate hypoxia. Similarly, in severe hypoxia, knockdown of HIF1α resulted in slightly reduced HRK induction (though not statistically significant) (Figure 3.24B). Unexpectedly, however, ablation of HIF2α increased the level of HRK mRNA induction to four times that stimulated by severe hypoxia alone ($P<0.01$) (Figure 3.24B). This result suggests that HIF2 may limit the expression of HRK mRNA. It is possible that HIF2 may directly repress HRK transcription by direct activity at the HRK promoter. The HIFs may interact with ATF4, either directly or indirectly, to reduce its activity at

the HRK promoter. When CHOP mRNA levels were analyzed in the same samples, the same effect was not observed (data not shown).

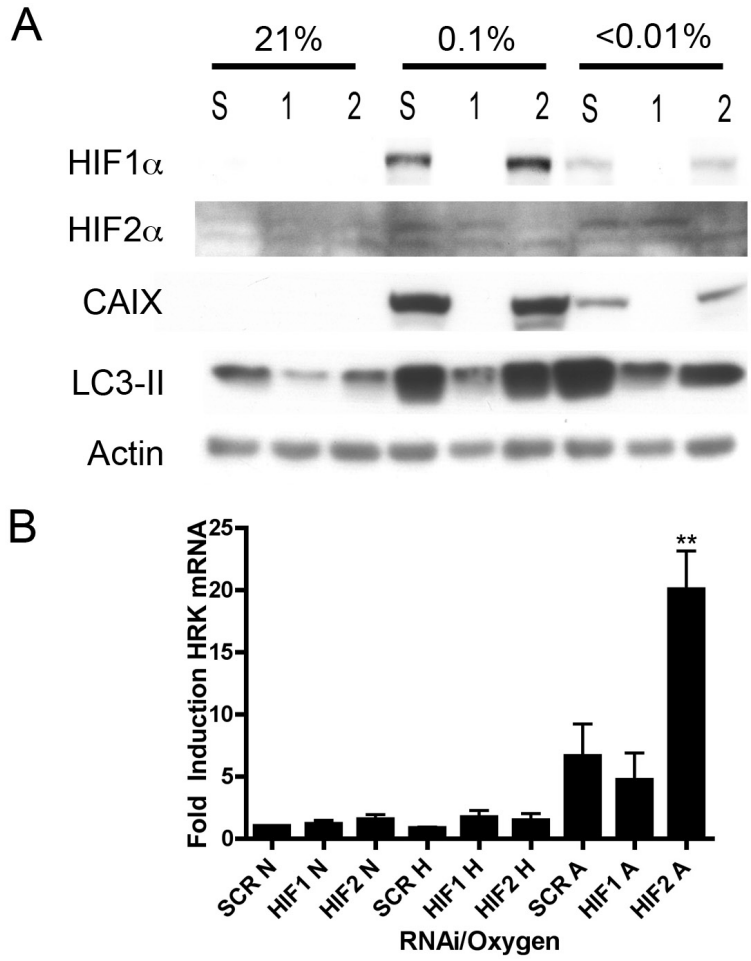

Figure 3.24 Treatment of MCF7 breast cancer cells with HIF2α siRNA increases HRK mRNA accumulation in severe hypoxia.

*MCF7 cells were transfected with siRNA molecules specific for HIF1α, HIF2α, or a scrambled control, and then exposed to normoxia, moderate hypoxia (H), or severe hypoxia (A). After 24 hours, cells were harvested and analyzed by western blotting (A) or RT-qPCR (B) using the specified antibodies and primers, respectively. For RT-qPCR, N=3 independent experiments were done. ** indicates P<0.01 by one-way-ANOVA for HIF2 A vs SCR A. For western blotting, representative images from at least N=2 independent experiments are shown.*

3.2.13 Short interfering RNA molecules specific to HRK reduce its expression in severe hypoxia

In order to study the function of HRK in cancer cells, short interfering RNA molecules specific to HRK were designed using Dharmacon's siDESIGN® Center. The top four rated siRNA sequences were selected and ordered from Eurogentec. These were rehydrated as a 20μM stock, and transfected into cells at a concentration of 200nM (50nM each). At three days post-transfection (including 48 hours in severe hypoxia), RT-qPCR showed substantial knockdown of HRK with sequences one (25% of SCR), three (14% of SCR), and four (17% of SCR) and as a pool (5.3% of SCR) (Figure 3.25). However, sequence one was also observed to affect the expression of the UPR target gene CHOP (data not shown). As a result, sequence three and four were prepared as a pool. RT-qPCR for OAS2 indicated that transfection with these siRNA sequences did not induce an interferon response (data not shown).

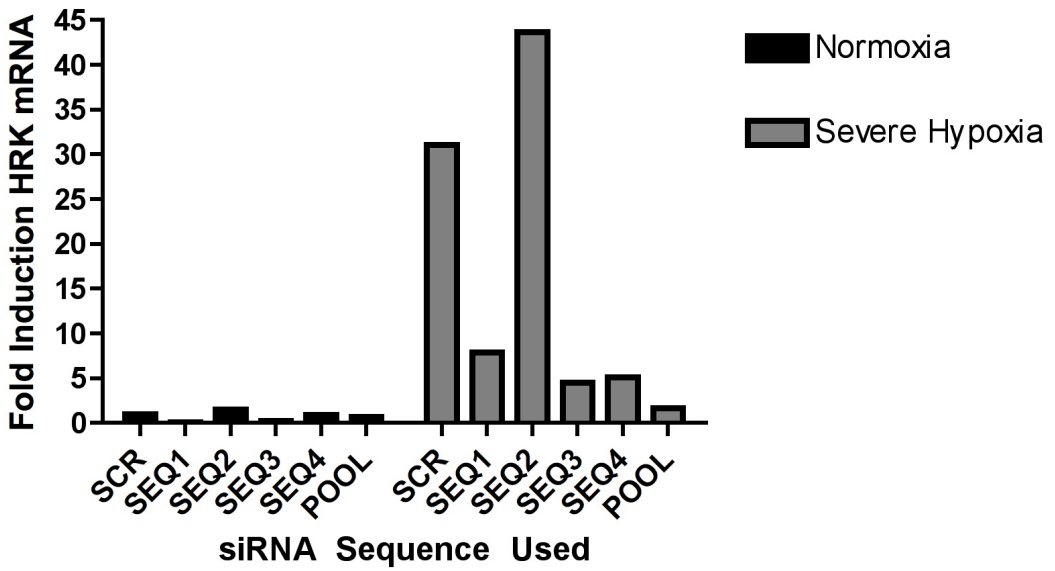

Figure 3.25 Treatment of MCF7 cells with siRNA sequences against HRK mRNA reduce its accumulation after 48 hours in severe hypoxia.

MCF7 cells were tranfected with siRNA against HRK for 24 hours and then exposed to severe hypoxia. 48 hours later, cells were harvested and analyzed by RT-qPCR using primers specific to HRK. N=1 independent experiment.

To confirm the efficacy of pooled sequence three and four at a lower concentration, another transfection was done for 24 hours at 20nM total siRNA. The pool (final conc of 10nM each) reduced the expression of HRK by to 20.6% of the SCR control (Figure 3.26).

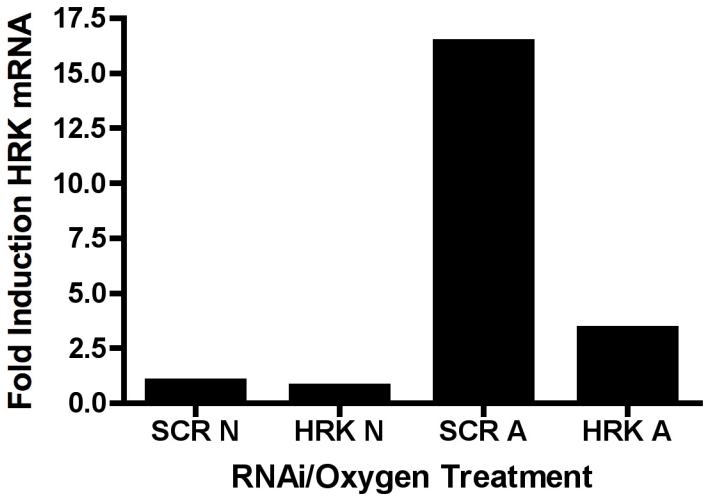

Figure 3.26 Treatment of MCF7 cells with pooled HRK siRNA sequences SEQ3 and SEQ4 reduce HRK mRNA accumulation after 48 hours in severe hypoxia. *MCF7 cells were transfected with a pool of sequence three and sequence four at a final concentration of 20nM (10nM of each). 24 hours later, cells were exposed to severe hypoxia for a further 48 hours. Cells were then harvested and analyzed by RT-qPCR using primers specific for HRK. N=1 independent experiment.*

3.2.14 HRK is required for hypoxia-induced autophagy

Several recent studies have shown that BH3-only proteins can trigger autophagy by releasing BCN1 from its inhibitory complex with BCL2 (Maiuri et al., 2007). BNIP3 and NIX, for example, have been shown to trigger mitochondrial autophagy in hypoxic cancer cells and in reticulocytes (Zhang et al., 2008; Zhang and Ney, 2008). Thus, the author hypothesized that HRK may play a role in initiating autophagy in severe hypoxia. Accordingly, when HRK was knocked down with RNAi, MDA-MB-231 and HCT116 cancer cells exposed to severe hypoxia for 24 hours showed a greatly reduced level of autophagy as assessed by LC3-II blotting (Figure 3.27). Interestingly, though this effect could not be observed by western blotting in MCF7 cells, staining for autophagosomes revealed that HRK knockdown greatly reduced hypoxia-induced LC3-

positive puncta formation (Figure 3.28). Thus, it is possible that in MCF7 cells LC3 is rapidly converted to the lipidated isoform following protein translation, even when not incorporated into autophagosomes. As such, loss of HRK failed to reduce the pool of LC3-II even though it obviously affected autophagosome formation as measured by immunocytochemistry. It must also be noted that knockdown of HRK failed to reduce autophagy in normoxia, a result that agrees with the specific induction of HRK in severe hypoxia.

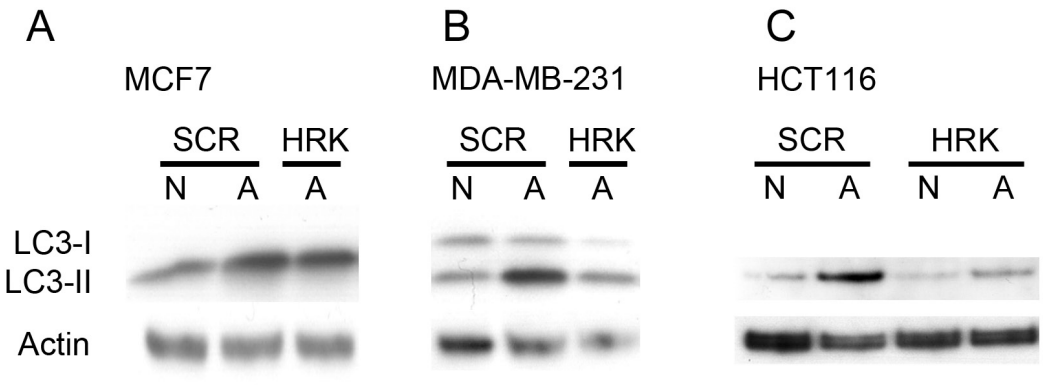

Figure 3.27 Treatment of MDA-MB-231 and HCT116 cells with HRK siRNA reduces LC3-II protein accumulation after 24 hours in severe hypoxia.
MCF7 (A), MDA-MB-231 (B), and HCT116 (C) cells were transfected with pooled siRNA molecules specific for HRK or a scrambled control. After 24 hours, cells were exposed to severe hypoxia for an additional 24 hours and then harvested for western blotting using the indicated antibodies. N indicates normoxia and A indicates severe hypoxia. Representative images from at least N=2 independent experiments are shown.

Previously, HRK has been shown to activate apoptosis in response to growth factor withdrawal or neuronal axotomy by freeing BAX and BAK from repression by BCL2 and BCL-X_L (Sanz et al., 2000; Wakabayashi et al., 2002). It is therefore likely that the observed increase in autophagy in severe hypoxia is due to depression of BCN1 activity.

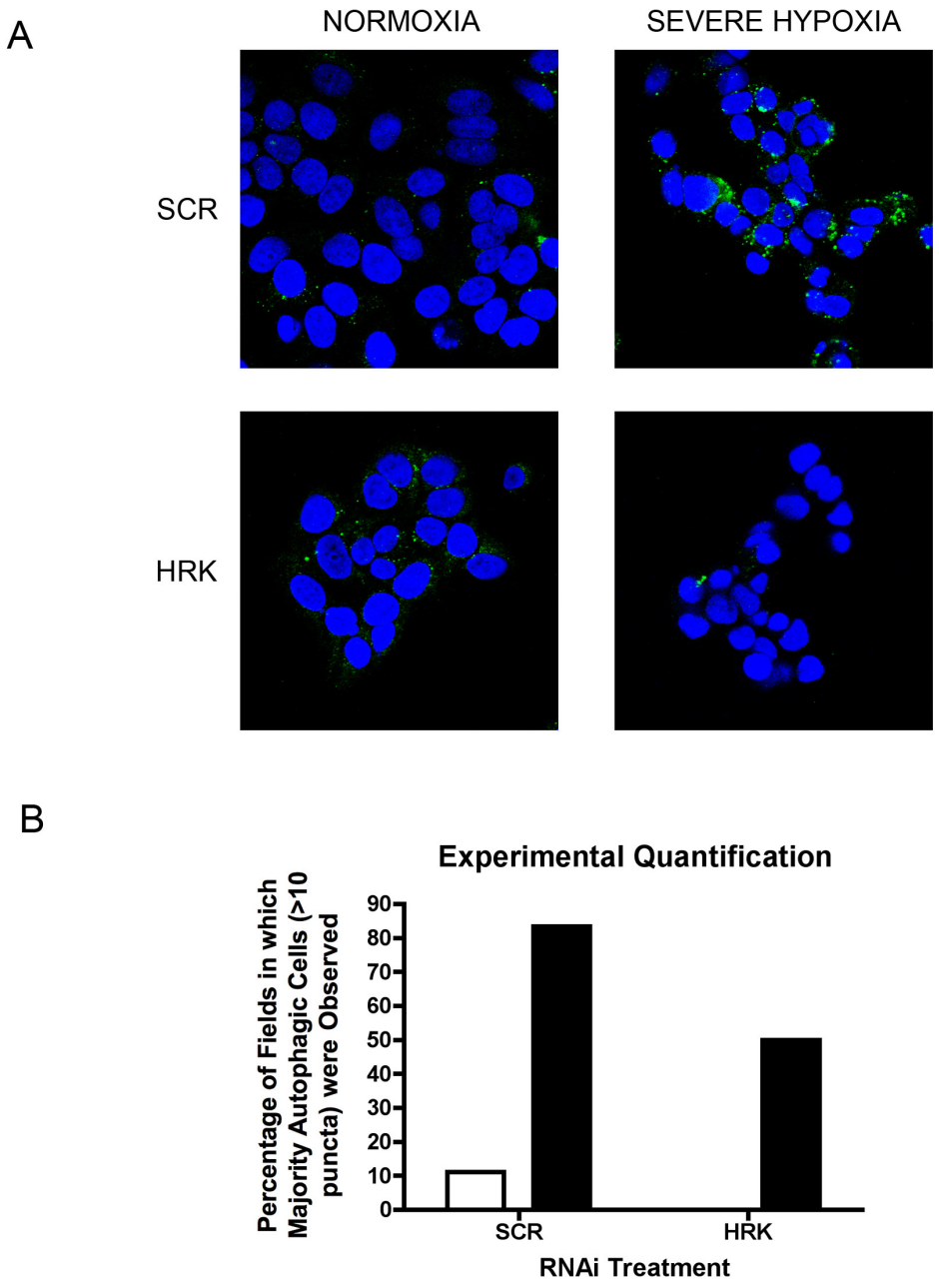

Figure 3.28 Treatment of MCF7 cells with HRK siRNA reduces the accumulation of LC3-positive puncta after 24 hours in severe hypoxia. *MCF7 cells were transfected with pooled siRNA molecules specific for HRK or a scrambled control. After 24 hours, cells were reseeded onto coverslips. 16 hours later, cells were exposed to severe hypoxia for an additional 24 hours and then fixed and*

stained for LC3 (green). DAPI (blue) was used to stain nuclei. (A) Representative images from N=3 independent experiments are shown. (B) The percentage of fields containing a majority autophagic cells was assessed and quantified for one such experiment.

To further confirm this result, Imagestream® analysis of autphagic flux was performed (Phadwal et al, 2011, submitted). In this assay, MCF7 cells were transfected with siRNA against HRK and exposed to severe hypoxia for 24 hours. Fixed cells were stained with antibodies against LC3 and with a lysosomal dye. The Imagestream® platform can be considered a combination of flow cytometry and fluorescence microscopy. As each cell moves through the system, up to six images in six different channels can be captured. After collecting 5000 events, the Imagestream® software can be used to analyze changes in localization, distribution, and intensity of particular markers. In this assay, developed by the Katja Simon group (with contributions from the author of this work), autophagic flux is measured directly by assessing the colocalization of LC3-positive puncta and lysosomes, thereby giving a direct indication of the number of autophagosomes fusing with lysosomes in each cell (Figure 3.29).

This experiment confirmed the previous results. As expected, the scrambled control demonstrated a high level of autophagy even in normoxia (colocalization was 5.2185 +/- 0.3470%) , and this level was increased by exposure to severe hypoxia (6.8173 +/- 0.3575%) (Figure 3.29B). Knockdown of HRK reduced the hypoxic increase in autophagy to near normoxic levels (4.9120 +/- 0.3352%), but was less effective in normoxia (4.439 5 +/- 0.3144%). Interestingly, though the percent colocalization between LC3 and lysosomes increased, the number of LC3-positive dots per cell did not change, as measured by this system (Figure 3.29E). It is likely, however, that this result is a consequence of the limited resolution of the system, and is indeed one reason why the developers of this technique chose to rely on colocalization as their metric.

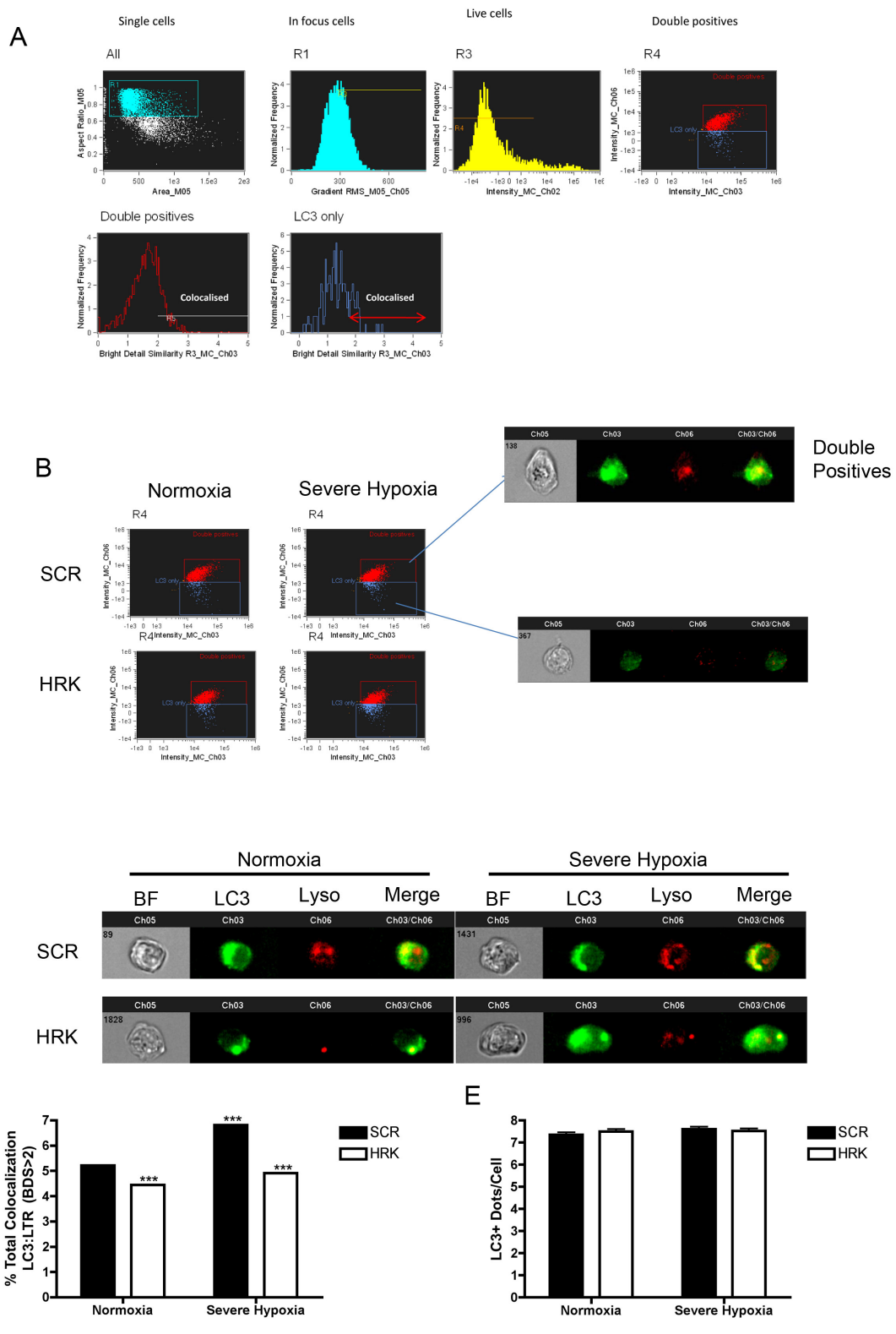
A
Single cells
In focus cells
Live cells
Double positives
All
R1
R3
R4
Aspect Ratio_M05
Area_M05
Normalized Frequency
Gradient RMS_M05_Ch05
Intensity_MC_Ch02
Intensity_MC_Ch06
Intensity_MC_Ch03
Double positives
LC3 only
Double positives
LC3 only
Colocalised
Colocalised
Bright Detail Similarity R3_MC_Ch03
B
Normoxia
Severe Hypoxia
R4
SCR
HRK
Double positives
LC3 only
Ch05
Ch03
Ch06
Ch03/Ch06
138
367
C
Normoxia
Severe Hypoxia
BF
LC3
Lyso
Merge
SCR
HRK
89
1431
1828
996
D
% Total Colocalization LC3:LTR (BDS>2)
***
SCR
HRK
Normoxia
Severe Hypoxia
E
LC3+ Dots/Cell
SCR
HRK
Normoxia
Severe Hypoxia

Figure 3.29 Treatment of MCF7 cells with HRK siRNA reduces the colocalization of LC3-positive and lysosomal puncta after 24 hours in severe hypoxia as measured by Imagestream® analysis.

*MCF7 cells were transfected with pooled siRNA molecules specific for HRK or a scrambled control. After 24 hours, cells were exposed to severe hypoxia for an additional 24 hours and then fixed and stained for Imagestream analysis. Gating strategy is shown in (A). This strategy can be summed up as follows: Single cells→ in focus cells→ live cells → double positive cells → double positives with BDS>2. Representative images of staining are shown in (C). Quantification of LC3:Lysosomal colocalization is shown in (D), where *** indicates P<0.001 by two-way ANOVA and N=5000. (E) The number of LC3-positive dots per cell, though not used as an experimental metric here, is shown for the benefit of the reader. A representative experiment of N=3 independent experiments is shown.*

The author next investigated the effect of HRK overexpression on cell survival and autophagy. When MCF7 cells were transfected with a vector encoding a myc-tagged HRK construct, no increase in PARP cleavage was observed in normoxia, and there was no apparent difference in HRK protein accumulation with caspase inhibition by ZVAD-FMK (Figure 3.30), indicating that even high levels of HRK were not able to induce apoptosis in this cell line. Interestingly, however, LC3-II levels increased markedly with caspase inhibition, agreeing with a previous report that implicated caspase activation as a "braking" mechanism for autophagy through the degradation of beclin 1 (Djavaheri-Mergny et al., 2010). Importantly, HRK expression failed to increase LC3-II levels, indicating that HRK is required for autophagy but not sufficient to initiate autophagy. On the other hand, the expression of HRK did appear to reduce the level of COXIV, a well-established mitochondrial marker. Thus, HRK may specifically promote the selection of mitochondria for autophagic degradation.

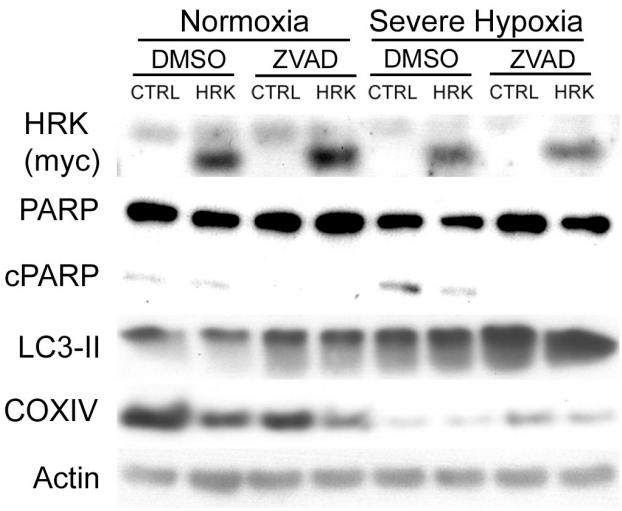

Figure 3.30 Exogenous expression of a myc-tagged HRK construct causes a reduction in PARP cleavage and COXIV protein in MCF7 cells exposed to severe hypoxia and/or caspase inhibitors.

MCF7 cells were transfected with a vector encoding either myc-tagged HRK or an empty vector control for 24 hours and then exposed to severe hypoxia for an additional 24 hours. Cells were then harvested and analyzed by western blotting using the antibodies indicated. Representative images from N=2 independent experiments are shown.

3.2.15 HRK protects against cell death in severe hypoxia

RNAi-mediated knockdown of HRK reduced autophagic flux in severe hypoxia. As discussed previously, autophagy is a mode of adaptation by which both normal and cancer cells survive stress. On the other hand, the BH3-only proteins are best known as effectors of apoptotic cell death, often in response to the same stressors that activate autophagy. The role of HRK in hypoxia-induced cell death has not yet been described. Thus, to determine the role of HRK in cell survival in severe hypoxia, cell death was assessed by staining with annexin V and propidium iodide, and analysis by flow cytometry. In contradiction to the known role of HRK in apoptotic cell death, loss

of HRK sensitized MCF7 cells to hypoxia-induced cell death (Figure 3.31). A small, but significant increase in the number of annexin V-positive cells was observed when cells were treated with siRNA against HRK in either normoxia or severe hypoxia, though the effect was two-fold greater in the latter condition (Figure 3.31A). Thus, it appears that in the context of severe hypoxia, HRK plays a role in autophagic survival rather than apoptotic death.

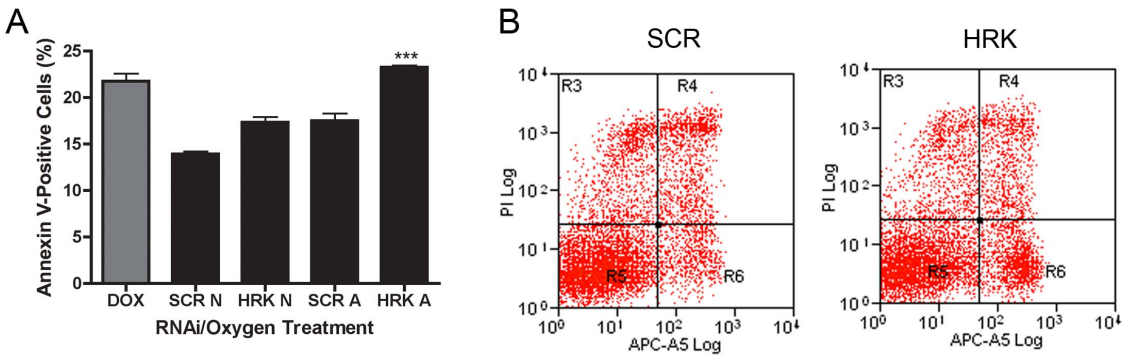

Figure 3.31 Treatment with HRK siRNA increases the population of annexin V-positive MCF7 cells following exposure to severe hypoxia for 48 hours.

*MCF7 cells were transfected with pooled siRNA molecules specific for HRK or a scrambled control. After 24 hours, cells were exposed to severe hypoxia for an additional 48 hours and then stained for annexin V and propidium iodide and analyzed by flow cytometry. Cells treated with 5μM doxorubicin for 48hr served as a positive control for cell death (DOX). A representative experiment of N=3 independent experiments is shown. Quantification of the percent cell death is shown in A. *** indicates P<0.001. Scatter plots of cells treated in severe hypoxia are shown in B. Y-axis is indicates PI staining, and X-axis indicates annexin V staining.*

3.2.16 Knockdown of HRK fails to block spheroid growth

Having established a role for HRK in cancer cell survival in severe hypoxia, it was hypothesized that HRK may be important in the formation and maintenance of a hypoxic tumour core. To answer this question, a three dimensional tumour spheroid model was used (Ivascu and Kubbies, 2006). Spheroids prepared from HRK or SCR knockdown cells (which maintain their silenced phenotype for at least four days) grew at a similar rate (Figure 3.32A and Figure 3.32B). Thus, though there is a small difference in viability with HRK knockdown in severe hypoxia, it appears that these differences are insufficient to affect spheroid growth in this model.

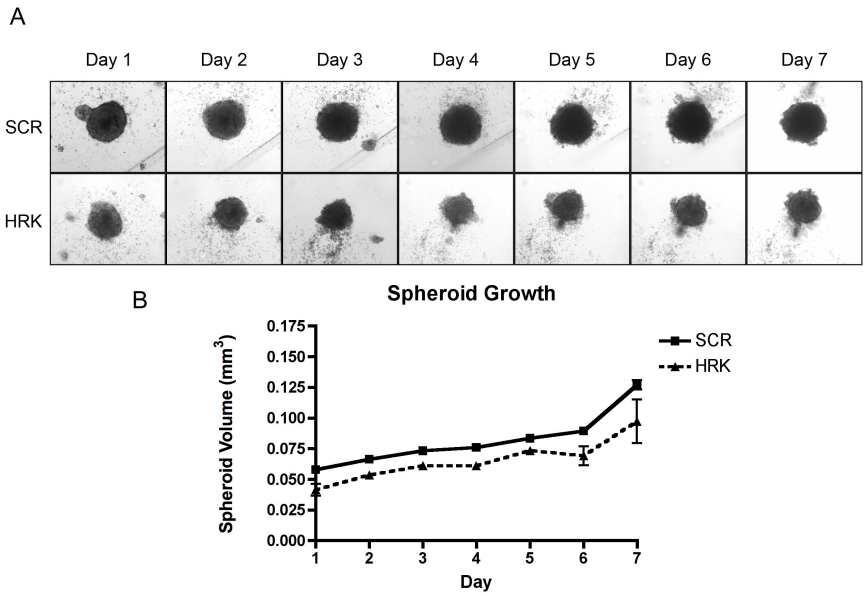

Figure 3.32 Spheroids derived from MCF7 cells first treated with HRK siRNA grow at a similar rate to those treated with a scrambled control.

MCF7 cells were transfected with pooled siRNA molecules specific for HRK or a scrambled control. After 24 hours, cells were reseeded 5000 cells/well to a round bottom 96 well format. After 24 hours more, spheroid-like structures form and begin to grow. Images were taken daily and volume measurements were calculated with ImageJ®. N=10 for each group. A representative experiment of N=3 independent experiments is shown.

3.3 Discussion

3.3.1 Severe hypoxia activates autophagy in cancer cells

The importance of autophagy as a mode of cell survival in the hypoxic tumour microenvironment is becoming increasingly apparent. Solid tumours experience extremes in pH, nutrient availability, and oxygen tension not commonly found in normal tissues. These stressors promote an aggressive cancer cell phenotype, selecting for clones with diminished apoptotic potential (Graeber et al., 1996), increased glycolytic flux, and enhanced acid tolerance (Cairns et al., 2011). Additionally, tumour cells can activate acute adaptive mechanisms such as the integrated stress response as a means of surviving the harsh microenvironmental stressors (Gillies and Gatenby, 2007; Hanahan and Weinberg, 2000; Ruan et al., 2009; Wouters and Koritzinsky, 2008). The ISR renders this adaptive response by through the expression of genes involved in protein folding, ER homeostasis, redox control, ERAD, amino acid metabolism, and autophagy (Kroemer et al., 2010). The importance of autophagy as a mode of resistance in cancer has been recently emphasized in a seminal review by Hanahan and Weinberg (Hanahan and Weinberg, 2011).

In agreement with this accumulating body of data, the author found that autophagic flux was rapidly increased in breast cancer cells exposed to severe hypoxia. Autophagy preceded cell death in this context, fitting with previous findings that, in most cases, autophagy is activated to protect cells from apoptosis and necrosis (Degenhardt et al., 2006; Mathew et al., 2007; Rabinowitz and White, 2011; Rouschop et al., 2009b; White et al., 2010).

3.3.2 HRK, PUMA, and NOXA are induced by ER stress and severe hypoxia

The BCL2 family of proteins has been extensively studied in a variety of contexts. In this chapter, the author demonstrated that the BH3-only proteins HRK, PUMA, and NOXA were induced at the mRNA level by severe hypoxia. Previous work has considered the role of PUMA and NOXA but not HRK in hypoxia-induced cell death. PUMA was shown to be upregulated by p53 in hypoxia and to induce apoptosis in colorectal cancer cells (Yu et al., 2003). Similarly, NOXA is expressed in a HIF1-dependent fashion to trigger apoptosis in hypoxic neuroblastoma cells or in a rat model of brain ischemia (Kim et al., 2004). A clear connection between hypoxia and HRK has not yet been published. However, in one report, it was shown that HRK was induced in a rat model of ischemia-reperfusion and that the association between BCL2 and HRK increases in this context (Guan et al., 2006). Thus, in the agreement with the literature, the author has demonstrated that the BH3-only proteins HRK, PUMA, and NOXA are highly induced at the mRNA level in breast and colorectal cancer cells in severe hypoxia.

The accumulation of PUMA and NOXA protein did not always correlate with the changes in the mRNA. For example, in MCF7 cells no NOXA protein could be detected despite a rapid increase in NOXA mRNA in severe hypoxia. Similarly, resting PUMA protein levels were high in this cell line, and declined rapidly after 48 hours in severe hypoxia. In MDA-MB-231 cells, early induction of both PUMA and NOXA protein was observed, preceding that of the mRNA expression. It is likely that PUMA and NOXA are subject to significant post-transcriptional and post-translation regulation. The failure to detect NOXA protein in MCF7 cells might reflect a post-transcriptional regulatory mechanism by which the translation of NOXA is prevented, or a post-translational mechanism by which NOXA protein is rapidly degraded. Recent work has shown that ubiquitination and proteasomal degradation of NOXA is an important regulatory mechanism in human leukemia cells *in vivo* (Baou et al., 2010).

The high level of PUMA protein in normoxia may be reflective of PUMA stabilization and/or constitutive PUMA translation. A recent publication showed that phosphorylation of PUMA at serine 10 is essential in the regulation of PUMA protein turnover by the proteasome and for its apoptotic activity (Fricker et al., 2010). Nonphosphorylatable PUMA was resistant to degradation by the proteasome and induced apoptosis to a greater extent in HeLa cells. Alternatively, it is possible that the constitutively high levels of PUMA in MCF7 cells are not toxic due to elevated expression of the BCL2 family members. The early accumulation of PUMA and NOXA protein in MDA-MB-231 cells is likely due to post-transcriptional regulation. It is very likely that these genes contain regulatory elements in their 5' and 3' UTRs that promote their selective translation in stress conditions. Indeed, this is often the case for many ISR target genes, such as ATF4 (Blais et al., 2004; Koritzinsky et al., 2006), LAMP3 (Mujcic et al., 2009), GADD34, CHOP, and CAIX (Koritzinsky et al., 2006). In agreement with this hypothesis, HRK was initially identified as being enriched in the polysome-associated mRNA of hypoxic cell, implying that it is selectively translated in this condition. The heterogeneity in the expression of PUMA and NOXA protein and mRNA indicates that in some circumstances these proteins might be potent killers, and thus are dysregulated or repressed by diverse means in the development of cancer.

HRK mRNA levels were found to increase significantly with exposure to severe hypoxia, but not moderate hypoxia, and to be strongly induced by treatment with thapsigargin or tunicamycin. Thus, the ER stress caused by severe hypoxia was hypothesized to be responsible for the induction of HRK. This pattern of expression implied that the integrated stress response might be involved in the expression of HRK. The timing of HRK mRNA expression correlated with that of PERK activation and ATF4 accumulation, implying a role for the integrated stress response in this process.

Only one study has directly linked the expression of HRK to ER stress. In this study, Gurzov and coworkers showed that Dp5 was induced by ER stress in a JNK-dependent fashion in pancreatic β-cells (Gurzov et al., 2009), and failed to identify the integrated stress response as a regulator of HRK. As described in section 3.1.3.1, HRK has been shown to be upregulated in response to a diverse array of stimuli, including NGF withdrawal (Coultas et al., 2007; Imaizumi et al., 1997), amyloid beta protein treatment (Chen et al., 2006; Imaizumi et al., 1999), potassium deprivation (Coultas et al., 2007; Ma et al., 2007), axotomy (Imaizumi et al., 2004; Wakabayashi et al., 2002), and the aggregation of polyQ-androgen receptor protein (Young et al., 2009). Provocatively, each of these pathologies has been shown to result in elevated levels of ER stress, and activation of the unfolded protein response (Aoki et al., 2002; Duennwald and Lindquist, 2008; Hoozemans et al., 2009; Lee do et al., 2010; Shimoke et al., 2004; Shimoke et al., 2011; Yu et al., 1999).

It is likely that HRK protein expression and activation is subject to extensive post-translational and post-transcriptional regulation. Unfortunately, the author was unable to obtain an effective antibody to assess changes in HRK protein expression.

3.3.3 HRK, PUMA, and NOXA comprise an ATF4-dependent program of BH3-only protein expression in severe hypoxia

The integrated stress response is activated by severe hypoxia, resulting in the translation of ATF4 and the transcription of genes involved in redox homeostasis, protein folding, amino acid transport, drug metabolism, angiogenesis, ER associated protein degradation, autophagy, and apoptosis (Blais et al., 2004; Harding et al., 2003; Kroemer et al., 2010). When siRNA molecules were used to ablate the expression and activity of ATF4 in MCF7, MDA-MB-231, and HCT116 cells, the transcriptional induction of HRK, PUMA, and NOXA was significantly

reduced. When PUMA and NOXA protein levels were analyzed by western blotting, it was found that this reduction in transcription resulted in less PUMA and NOXA protein, as well. At the same time that this work was underway, PUMA was shown to be upregulated by the PERK-ATF4 pathway and to mediate apoptosis in response to NSAID treatment in gastric cells (Ishihara et al., 2007) and in response to ER stress in neuronal cells (Galehdar et al., 2010). Similarly, NOXA expression was activated by a heterodimer consisting of ATF4 and ATF3 in response to pharmacological blockade of ERAD (Wang et al., 2009).

The dependence of HRK on ATF4 for its expression was further characterized in this study. It was found that ectopic expression of ATF4 was sufficient to drive the expression of HRK. This finding differs from that for other UPR targets, such as CHOP, whose expression requires ATF4 as well as additional factors, such as XBP1 and ATF6 (Harding et al., 2000). Thus, ATF4 might form a homodimer with itself or a heterodimer with another abundant factor to drive the transcription of HRK (Gombart et al., 2007; Hai and Curran, 1991; Podust et al., 2001).

The author demonstrated that ATF4 binds directly to the promoter region of HRK. This analysis revealed, interestingly, that ATF4 acted at the CREB/ATF sites most distant from the transcription start site. By contrast, it has previously been shown that NGF withdrawal promotes the activity of c-Jun and ATF2 at a different CREB/ATF site on the HRK promoter, 96bp upstream of transcription start (Towers et al., 2009). In order to determine which of these elements are required for ATF4-mediated HRK regulation, site-directed mutagenesis of the HRK promoter in a luciferase construct would need to be done.

Interestingly, when RNAi was used to reduce the level of HIF2α protein, the expression of HRK mRNA in severe hypoxia increased dramatically. This result suggests that the HIFs may compete with ATF4 at the promoter region of HRK, or otherwise suppress the expression of HRK in some way. Indeed, there are several

established HIF target genes that are also induced in an ATF4-dependent manner. For example, treatment of human retinal pigment cells or MEFs with arsenite induced the expression of the HIF1 target gene VEGF via direct transcriptional activity of ATF4 at the promoter 1767bp downstream of transcription start (Roybal et al., 2005). Similarly, CAIX expression in U373 cells exposed to severe hypoxia was found to be dependent on direct transcriptional activation by ATF4 (van den Beucken et al., 2009). Thus, there is overlap between the transcriptional targets of ATF4 and HIF1. It remains to be seen, however, whether the binding of HIF1 or HIF2 to the promoter region of HRK can inhibit the transcriptional activity of ATF4. Alternatively, HIF2 may drive the expression of another factor to repress the expression of HRK in *trans*. Such factors might include an ATF-like transcription factor, an ATF4-binding protein, or a microRNA that can bind and degrade the HRK transcript directly.

3.3.4 Loss of HRK reduces autophagy and cancer cell survival in severe hypoxia

The BH3-only proteins can act as potent inducers of autophagy. The ectopic expression of PUMA activates autophagy and apoptosis in cancer cells (Yee et al., 2009). NOXA promotes H-Ras-driven autphagy by releasing BCN1 from its repression by MCL-1 (Elgendy et al., 2011). Similarly, the BAD mimetic ABT737 has been shown to activate autophagy by freeing BCN1 from BCL2 or BCL-X_L (Maiuri et al., 2007). In this work, when specific siRNA molecules against HRK were used to ablate its expression in severe hypoxia, the level of LC3-II protein, LC3-positive puncta, and LC3:Lysosomal colocalization were reduced, indicating that HRK is an important inducer of hypoxia-induced autophagy. Given that HRK is thought to bind to and inhibit BCL2 and BCL-X_L in a fashion similar to BAD (Inohara et al., 1997), it is not surprising that HRK is required for hypoxia-induced autophagy.

Provocatively, RNAi-mediated knockdown of HRK resulted in decreased tumour cell survival in severe hypoxia. Despite the established role of HRK in neuronal cell death through apoptosis, it thus appears that in human cancer cells HRK can act to promote hypoxic survival through autophagy. This result agrees with the growing body of work highlighting autophagy as an important cell survival mechanism in hypoxia.

Interestingly, when myc-tagged HRK was ectopically expressed in MCF7 cells, cell death was not activated. In fact, the expression of HRK appeared to slightly reduce PARP cleavage in severe hypoxia, indicating a slight reduction in cell death. This failure is likely a reflection of the cellular context. HRK can bind to and inactivate BCL2 and BCL-X_L, but binding of the full-length protein to MCL-1 or A1 has not been shown. MCF7 cells, which contain high basal levels of MCL-1 (Dhillon and Mudryj, 2003), are therefore unlikely to undergo apoptosis due to expression of HRK alone.

Alternatively, if we consider the direct activator hypothesis, *in vitro* binding assays have indicated that HRK binds to and inhibits BCL2 and BCL-X_L but is unable to directly interact with BAX or BAK (Willis et al., 2007). Thus, the expression of HRK alone may release BAX and BAK, BCN1, or other BH3-only proteins from complexes with BCL2 or BCL-X_L, but will not activate BAX or BAK oligomerization directly. Unless there are high levels of active BIM or BID present (ie the cells are "primed for death"), then one would not expect HRK expression alone to be sufficient to activate apoptosis.

Finally, the interaction of HRK with BCL2 or BCL-X_L might be sufficiently potent to disrupt BCN1-BCL2 interactions, but not BAX-BCL2 interactions. Indeed, it has been shown that HRK BH3 peptides have a much lower affinity for BCL2 than the BH3s of BIM, PUMA, BMF, or BAD and as a consequence viral transfection of full length HRK fails to kill MEFs (Chen et al., 2005). Thus, such differences in binding

affinities might permit a "window" in which HRK could selectively release BCN1 but not BAX from complexes with BCL2.

A deeper investigation would therefore be necessary to determine the binding of HRK to BCL2 or BCL-X_L and detailed protein profiling would be required to determine the relative levels of the BCL2 family members in this context, both of which are beyond the scope of this thesis.

Surprisingly, the level of LC3-II was unchanged by the ectopic expression of HRK, indicating that HRK is required for but not sufficient to trigger autophagy, and that further elevation of HRK in severe hypoxia was redundant. There are many levels of autophagy regulation. HRK probably activates autophagy by releasing BCN1 from inhibition by BCL2 or BCL-X_L, increasing the PI3K activity of the Vps34 complex. However, ULK1-mediated release of AMBRA1 from dynein complexes is also required for the activation of autophagy (Fimia et al., 2010). Many such inputs are likely required for the initiation of autophagy, and thus it is not surprising that HRK expression on its own failed to induce autophagy in normoxia and made little difference in autophagy levels in severe hypoxia.

Despite the fact that HRK was insufficient to induce higher levels of macroautophagy, it was observed that ectopic expression of HRK resulted in a decrease in COXIV protein levels. This result implies that HRK may act to promote selective mitochondrial autophagy. This effect might occur in a manner similar to BNIP3, parkin, PINK1, or yeast ATG32, which have been shown to behave as specific targeting molecules for mitophagy (Kanki and Klionsky, 2009; Kanki et al., 2009; Narendra and Youle, 2011; Youle and Narendra, 2011; Zhang et al., 2008; Zhang and Ney, 2008). Thus, while HRK expression might not increase flux through autophagy, it may target mitochondria for degradation by basal autophagy.

Spheroids derived from MCF7 cells lacking HRK appeared to grow normally. Thus, although HRK protects MCF7 cells from cell death severe hypoxia, the magnitude of this change was not sufficient to affect gross spheroid growth. Further work is required to assess the role of HRK in tumour cell survival in other cell contexts.

3.4 Summary and conclusions

Autophagy is an important pathway by which tumour cells survive the hypoxic microenvironment of the tumour. In recent years, it has become increasingly clear that the integrated stress response can mediate cell survival by upregulating the autophagic machinery MAP1LC3B and ATG5(Kroemer et al., 2010; Rouschop et al., 2009b; Rzymski and Harris, 2007). ATF4 orchestrates a program of BH3-only protein expression in response to severe hypoxia. ATF4-mediated HRK expression was demonstrated to be required for autophagy in severe hypoxia. Importantly, this study provides the first evidence that transcription can trigger *de novo* autophagy induction, rather than simply upregulating the molecular machinery to maintain flux through the pathway. Furthermore, ATF4-mediated upregulation of HRK was important for cancer cell survival in severe hypoxia, and may play a role in selective mitochondrial autophagy.

The BH3-only proteins have well-established roles as inducers of apoptotic cell death in a variety of cellular contexts. In this study, the author has described a program of BH3-only protein expression regulated by the crucial ISR transcription factor ATF4. HRK, PUMA, and NOXA have each been ascribed roles in autophagy in apoptosis. The ISR is primarily a cell survival mechanism, but after prolonged or insurmountable stress, it can also promote apoptotic cell death. Thus, ATF4-mediated induction of HRK, PUMA, and NOXA is a manifestation of the "double-edged" nature of the ISR: early induction of these BH3s might activate autophagy to protect cells from hypoxic stress. Prolonged stress, however, might lead to excessive BH3 expression and the activation of additional pro-apoptotic genes,

tipping the balance towards cell death. These effects will be highly dependent on the cellular context. ATF4-mediated induction of HRK in untransformed neurons would likely kill these cells outright. However, in the context of highly transformed cancer cell lines that are partially defective for apoptosis (Ex. MCF7s lack caspase 3 and NOXA protein), it is likely that HRK expression would trigger autophagy but not apoptosis. In other contexts, the reality may lie somewhere in between these two extremes (Figure 3.33).

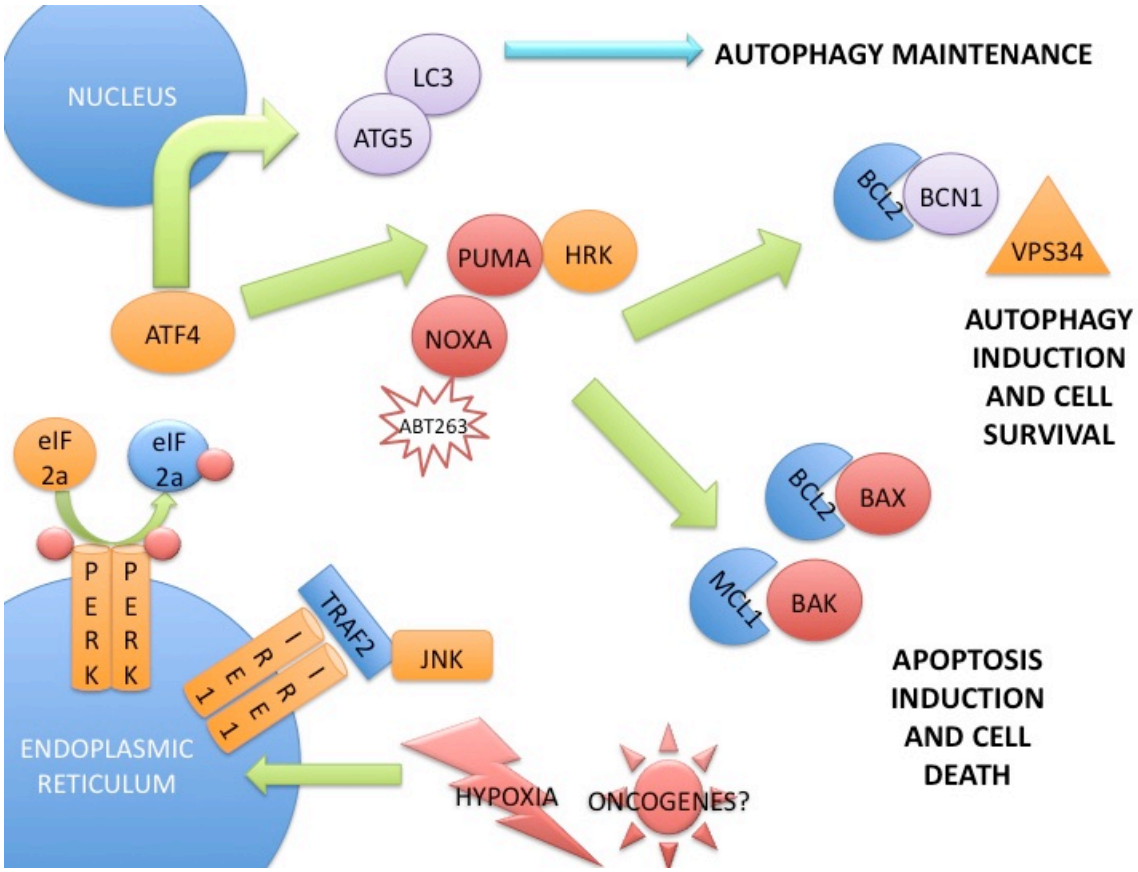

Figure 3.33 Proposed model for ATF4 regulation of program of BH3-only proteins.

Recent advances in the mechanistic understanding of apoptosis have led to the development of BH3-mimetics, such as the BAD-mimetics ABT737 and ABT263. Surprisingly, screening of these compounds revealed that they potently activate apoptosis in cancer cells but not in normal cells, and cause regression of

lymphomas as well as solid tumours (Oltersdorf et al., 2005). More than 17 clinical trials using ABT263 are underway or completed in leukemias and a variety of solid tumours (www.clinicaltrials.gov). As discussed earlier in this chapter, cancer cells treated with ABT737 activate autophagy through a BCN1-dependent mechanism (Armstrong et al., 2011; Maiuri et al., 2007). Thus, it will be interesting to see if the effect of ABT263 or ABT737 as a single agent or in combination with standard chemotherapy protocols might be enhanced by combinatorial inhibition of autophagy.

Chapter 4 ATF4 drives cell survival and autophagy through transcriptional upregulation of UNC51-like kinase 1

This chapter elucidates yet another link between the integrated stress response and autophagy. ULK1 protein and mRNA are increased in cancer cells by exposure to severe hypoxia, ER stress, and moderate hypoxia, and by the stressors present in the tumour microenvironment. ULK1 is a direct target of ATF4 transcriptional activity. ULK1 expression leads to increased ULK1 kinase activity and autophagy in severe hypoxia, and is required for mitochondrial autophagy. Knockdown of ULK1 or ATF4 causes cancer cell death in both normoxia and severe hypoxia, through necrosis and apoptosis, respectively. ULK1 expression is associated with reduced relapse-free survival in breast cancer patients. Thus, ULK1 is a potential target for cancer therapy.

4.1 Introduction

4.1.1 UNC51-like kinase 1 and autophagy

The autophagy process can be divided into three phases: the initiation of phagophore formation, the elongation of the nascent autophagosome, and the maturation of the autophagosome and its fusion with acidic lysosomes to form an autophagolysosome. Following digestion of intravesicular contents, macronutrients are released to the cytosol by lysosomal permeases. The mechanistic details of this process are still not well understood. However, it is known that the initiation of autophagy requires the activation of the class III phosphatidylinositol 3-kinase Vps34 (Kihara et al., 2001). Vps34 activation requires interaction with the BH3-only protein BCN1 (Zeng et al., 2006), which in turn is released from its inhibition by the antiapoptotic BCL2 family members

through the binding of other BH3-only proteins such as BAD, BIM, PUMA, or NOXA (Maiuri et al., 2007). Activation of Vps34 results in the production of phosphatidylinositol-3-phosphate (PI3P), which becomes incorporated into the membranes of the initiating phagophore at the endoplasmic reticulum (Axe et al., 2008; Walker et al., 2008). In chapter three, the author demonstrated that the BH3-only protein HRK is a target of ATF4 transcriptional upregulation in severe hypoxia and is important for hypoxia-induced autophagy.

Autophagy initiation also requires the activity of the serine/threonine kinase UNC51-like kinase 1 (ULK1). ULK1 is one of five mammalian orthologs of yeast ATG1 (the others being ULK2, ULK3, ULK4, and Fused) (Chan and Tooze, 2009; Kuroyanagi et al., 1998; Yan et al., 1998). ULK1 and ULK2 are the two most highly conserved ATG1 orthologs with 57% sequence homology in the kinase domain. In 2007, siRNA screening of the kinome identified the mammalian ATG1 ortholog ULK1 as a multidomain modulator of autophagy (Chan et al., 2007). Importantly, ULK1 but not ULK2 was required for autophagy in HEK293 cells exposed to amino acid starvation.

The function of ULK1 in autophagy is likely pleiotropic (Figure 4.1). A number of studies have indicated that ULK1 and ATG1 play an essential role in the formation of the pre-autophagosomal structure (PAS) (Cheong and Klionsky, 2008; Cheong et al., 2008). In yeast, ATG1 has been shown to play a role in both the biosynthetic cytoplasm to vesicle (CVT) pathway, and in the regulation of nonspecific macroautphagy. In mammals, the kinase activity of ULK1 is essential for the induction of macroautophagy in a variety of contexts. In both systems, it has been shown that ATG1/ULK1 plays an important role in the cycling of ATG9 between the PAS and the trans-Golgi network (TGN) through the phosphorylation of ZIP kinase and activation of actin-associated motor protein myosin II, presumably to aid in membrane delivery to the growing phagophore in the process of elongation (Reggiori et al., 2004; Tang et al., 2011; Young et al., 2006). Provocatively, ULK1 was recently shown to regulate the PI3K activity of Vps34 through AMBRA1.

Direct phosphorylation of dynein light chain 1 (DLC1) by ULK1 allowed the release of AMBRA1-DLC1 from dynein motor complexes. AMBRA1 was then able to relocalize to the ER and join the Vps34/BCN1 complex, allosterically enhancing the PI3K activity of Vps34 and autophagy initiation (Di Bartolomeo et al., 2010). In both yeast and flies, ATG1/UNC51 has been shown to negatively regulate cell growth and viability, in part through the negative regulation of S6K, though the mechanistic details of this pathway and its relevance to mammalian systems are unclear (Lee et al., 2007b; Scott et al., 2007).

Several studies have demonstrated that mammalian ULK1 but not ULK2 plays a crucial role in the survival of amino acid deprivation and glucose deprivation through nonspecific macroautophagy (Chan et al., 2007; Di Bartolomeo et al., 2010; Ganley et al., 2009; Kim et al., 2011; Lee et al., 2010; Mercer et al., 2009). However, recent work has also indicated that in some contexts ULK1 is crucial for the specific elimination of mitochondria. Elegant work from Craig Thompson's group demonstrated that ULK1-mediated mitophagy is necessary for reticulocyte maturation in mice (Kundu et al., 2008a). More recently, Rubin Shaw's group released data demonstrating that ULK1 plays an essential role in surviving nutrient deprivation through mitophagy in the murine liver, primary hepatocytes, and mouse embryonic fibroblasts (Egan et al., 2011).

As of yet, only a handful of ULK1 kinase substrates have been identified. A recent opinion piece in "Autophagy" highlighted the need to identify the physiologically-relevant targets of ULK1 in order to fully understand the mechanics of autophagy and its relevance to cellular function and pathology (Deminoff and Herman, 2007). Thus, the identification of ZIPK (Tang et al., 2011) and DLC1 (Di Bartolomeo et al., 2010) as ULK1 substrates is a significant step in the right direction.

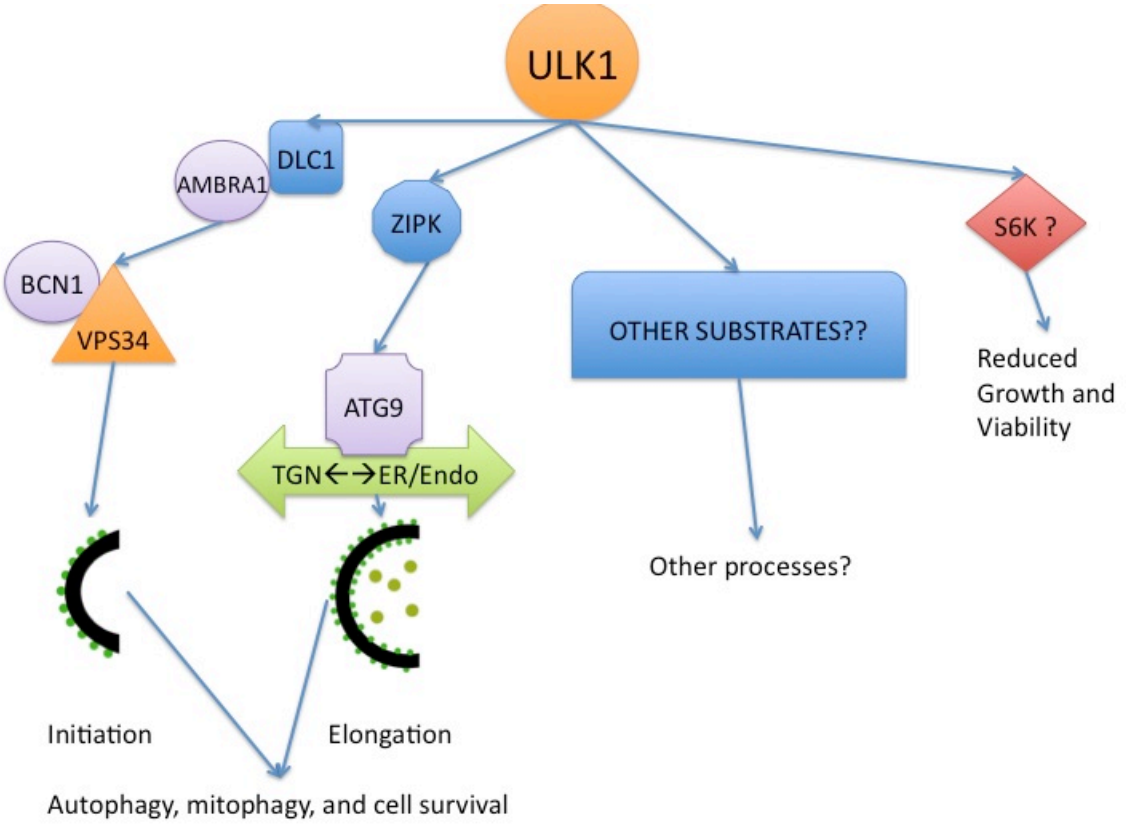

Figure 4.1 ULK1 regulates autophagy in mammals through multiple downstream effectors.

The regulation of ATG1/ULK1 activity is complex. In the yeast system, nutrient deprivation (amino acids or glucose) causes ATG1 to form a protein complex with ATG13 and ATG17 that is essential for the kinase activity of ATG1, its translocation to the PAS, and autophagy initiation (Cheong et al., 2008; Kabeya et al., 2005; Reggiori et al., 2004). In fed conditions, phosphorylation of ATG13 by TOR blocks this process (Kamada et al., 2010; Stephan et al., 2009).

In mammals, ULK1 activity is regulated in a manner similar to ATG1 (Figure 4.2). ULK1 forms large (approximately 3MDa) protein complexes that include mammalian ATG13 and FIP200 (the mammalian ortholog of ATG17). However, in contrast to the yeast model where ATG13 and 17 bind to ATG1 in response to starvation, the mammalian complexes appear to be stable in the fed condition (Hosokawa et al., 2009). Additionally, in the fed state, active mTORC1 is

incorporated into these ULK1-ATG13-FIP200-containing megacomplexes, where it phosphorylates both ULK1 and ATG13, preventing their association at the PAS and the activation of the kinase activity of ULK1 (Ganley et al., 2009; Hosokawa et al., 2009). Furthermore, it was shown that the interaction of ATG13 and FIP200 with ULK1 was essential for the stability of the ULK1 protein. Knockdown of ATG13 or FIP200 resulted in increased degradation of the ULK1 protein (Ganley et al., 2009). The stability of the ATG13 protein, in turn, seems to be dependent on its association with ATG101, yet another member of this complex (Mercer et al., 2009).

More recent work has revealed that ULK1 is also regulated through phosphorylation by AMP kinase (AMPK). Lee and coworkers showed that AMPK binds to the PS domain of ULK1, and inactivates mTORC1 by phosphorylation of raptor at Ser792 (Lee et al., 2010). In addition, Egan and coworkers elegantly showed that in mice AMPK activates the ULK1 kinase by direct phosphorylation of ULK1 at Ser555 and Ser467 (Egan et al., 2011). Work from the Guan lab demonstrated that AMPK can also activate ULK1 by phosphorylation at Ser317 and Ser777 in starvation, while mTORC1 inhibits ULK1 activity in the fed state by specifically phosphorylating Ser757, preventing the interaction of ULK1 with AMPK (Kim et al., 2011). Interestingly, a more recent study has demonstrated that ULK1 undergoes dramatic dephosphorylation at thirteen serine residues upon starvation, confirming the work from 2009 by two other groups (Ganley et al., 2009; Hosokawa et al., 2009; Shang et al., 2011). In particular, in the fed state mTOR maintains phosphorylation at Ser638 of human ULK1, preventing AMPK-mediated phosphorylation of ULK1 at Ser758, its activation, and the induction of autophagy (Shang et al., 2011). To confound these results further, it has been previously established that ULK1 undergoes essential autophoshorylation *in vivo* and *in vitro* (Hara et al., 2008; Kijanska et al., 2010; Yan et al., 1998; Yeh et al., 2010). In the yeast system, ATG1 may also be a target of PKA (Stephan et al., 2009).

Thus, though it remains to be seen which of these phosphorylation events are most important in the activation of autophagy, it is clear that ULK1 activity is regulated at several levels: allosteric activation by ATG13 and ATG17, localization to 3MDa megacomplexes, proteasomal degradation, association with mTOR and AMPK and specific phosphorylation by each, and autophosphorylation. The sheer complexity of ULK1 control underscores its tremendous importance in cellular homeostasis.

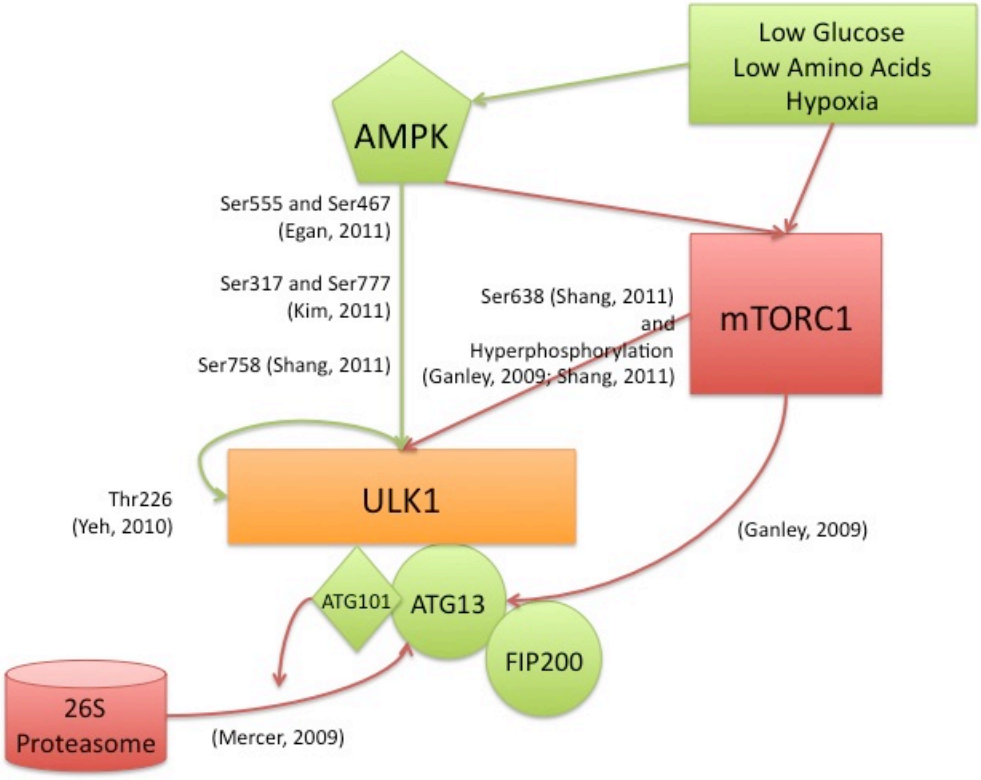

Figure 4.2 ULK1 is subject to complex post-translational regulation.

The work in this chapter demonstrates for the first time that ULK1 activity and autophagy induction can also be regulated by transcriptional induction. The author presents convincing evidence showing that in certain contexts ULK1 protein and autophagy in normoxia and severe hypoxia can be regulated by the transcriptional activity of essential ISR transcription factor ATF4. Furthermore, the author provides data to support an essential role for ULK1-mediated

autophagy and mitophagy in cancer cell survival in both “stressed” and “unstressed” conditions, validating ULK1 as a potential target for cancer therapy.

4.2 Results

4.2.1 Microarray analysis identified ULK1 as an ATF4 target gene

In previous work done by this group, ATF4 target genes were identified through the use of microarray analysis (Rzymski et al., 2010). In this study, siRNA molecules specific for ATF4 were used to ablate its expression and activity in MCF7 cells. After 24 hours exposure to severe hypoxia, cells were harvested and mRNA isolated for microarray analysis. 355 genes were found to have changed expression following severe hypoxia and ATF4 knockdown. The top 25 of these genes were validated by RT-qPCR analysis and published (Rzymski et al., 2010). In this report, the authors identified MAP1LC3B as an ATF4 target gene, and showed that ATF4-dependent upregulation of MAP1LC3B was essential for autophagy maintenance and the survival of cancer cells in severe hypoxia. Though not published simultaneously, this microarray experiment also showed that ULK1 mRNA was induced 1.76-fold by severe hypoxia (P=0.001), and then reduced to 0.60-fold after knockdown of ATF4 (P=0.004).

Table 4.1 List of Genes with Changed Expression Following ATF4 Knockdown

ID	Accession	Name	Symbol	24hr Severe Hypoxia		siRNA vs ATF4	
				P	FC	P	FC
GI_27481123-S	XM_036589.3	-	KIAA1078	0.000	1.59	0.009	0.58
GI_40018630-A	NM_017572.2	MAP kinase interacting serine/threonine kinase 2	MKNK2	0.000	3.58	0.002	0.58
GI_37540765-S	XM_208108.3	-	LOC283698	0.000	0.51	0.002	0.59
GI_21361968-S	NM_025144.2	alpha-kinase 1	LAK	0.013	1.23	0.002	0.59
GI_34577109-I	NM_184041.1	aldolase A, fructose-bisphosphate	ALDOA	0.005	2.07	0.001	0.59
GI_16306547-S	NM_006513.2	seryl-tRNA synthetase	SARS	0.050	1.41	0.001	0.59
GI_7661869-S	NM_014685.1	homocysteine-inducible, endoplasmic reticulum stress-inducible, ubiquitin-like domain member 1	HERPUD1	0.000	6.60	0.000	0.59
GI_4506782-S	NM_003864.1	Sin3A-associated protein, 30kDa	SAP30	0.000	2.60	0.000	0.60
GI_4507830-S	**NM_003565.1**	**unc-51-like kinase 1 (C. elegans)**	**ULK1**	**0.001**	**1.76**	**0.004**	**0.60**
GI_4885638-S	NM_005486.1	target of myb1-like 1 (chicken)	TOM1L1	0.007	1.36	0.000	0.60
GI_5174508-S	NM_005900.1	SMAD, mothers against DPP homolog 1 (Drosophila)	MADH1	0.010	0.66	0.001	0.60
GI_14249551-S	NM_032839.1	disrupted in renal carcinoma 2	DIRC2	0.007	0.70	0.000	0.60
GI_7770073-A	NM_002161.2	isoleucine-tRNA synthetase	IARS	0.000	1.57	0.000	0.61
GI_37546901-S	XM_059415.4	-	KIAA2028	0.000	1.26	0.001	0.61
GI_41393611-A	NM_006054.2	reticulon 3	RTN3	0.000	1.34	0.001	0.61
GI_8922276-S	NM_018022.1	transmembrane protein 51	FLJ10199	0.000	0.49	0.001	0.61

4.2.2 ULK1 expression is induced by severe hypoxia

Given the emerging and important role of ULK1 in mammalian autophagy, its identification as a hypoxia-regulated gene was an exciting result. Thus, the author first sought to validate the hypoxic induction of ULK1. A panel of five cancer cell lines were exposed to severe hypoxia and then harvested for analysis by western blotting. ULK1 protein displayed three patterns of expression. In A431 and HT29 cells, ULK1 protein accumulated after twelve hours in severe hypoxia and remained elevated, in a manner that followed the accumulation of ATF4 and mimicked the expression of CHOP (Figure 4.3A and Figure 4.3B). Alternatively, in MCF7 cells ULK1 protein was found to be expressed in normoxia, and then decreased after 48 hours in severe hypoxia (Figure 4.3C). Finally, HCT116 and U87 cells showed a slight accumulation of ULK1 protein after six to twelve hours in severe hypoxia, but these levels also fell after 48 hours in severe hypoxia (Figure 4.3D and Figure 4.3E). In each cell line examined, autophagy induction, as measured by LC3-II protein levels, increased markedly after 12 to 24 hours in severe hypoxia. This was followed in most cases with PARP cleavage after 24 to 48 hours in severe hypoxia, indicating that autophagy precedes cell death. Thus, it seems that autophagy is first activated to protect cells from severe hypoxia, and failing recovery or reoxygenation, apoptosis becomes activated.

In contrast to the varied expression profiles of ULK1 protein, the induction of ULK1 mRNA was similar in each cell line examined. A431, HT29, and MCF7 cells were exposed to severe hypoxia for the same times and cells were harvested for analysis by RT-qPCR. In each case, ULK1 mRNA was seen to increase after 12 hours in severe hypoxia and to reach a maximum after 48 hours, correlating with the accumulation of ATF4 protein (Figure 4.4). A431 and HT29 cells exhibited close to 30-fold increases in ULK1 mRNA ($P<0.05$, and $P<0.01$ respectively), while MCF7 cells exhibited a more modest increase of five-fold ($P<0.01$).

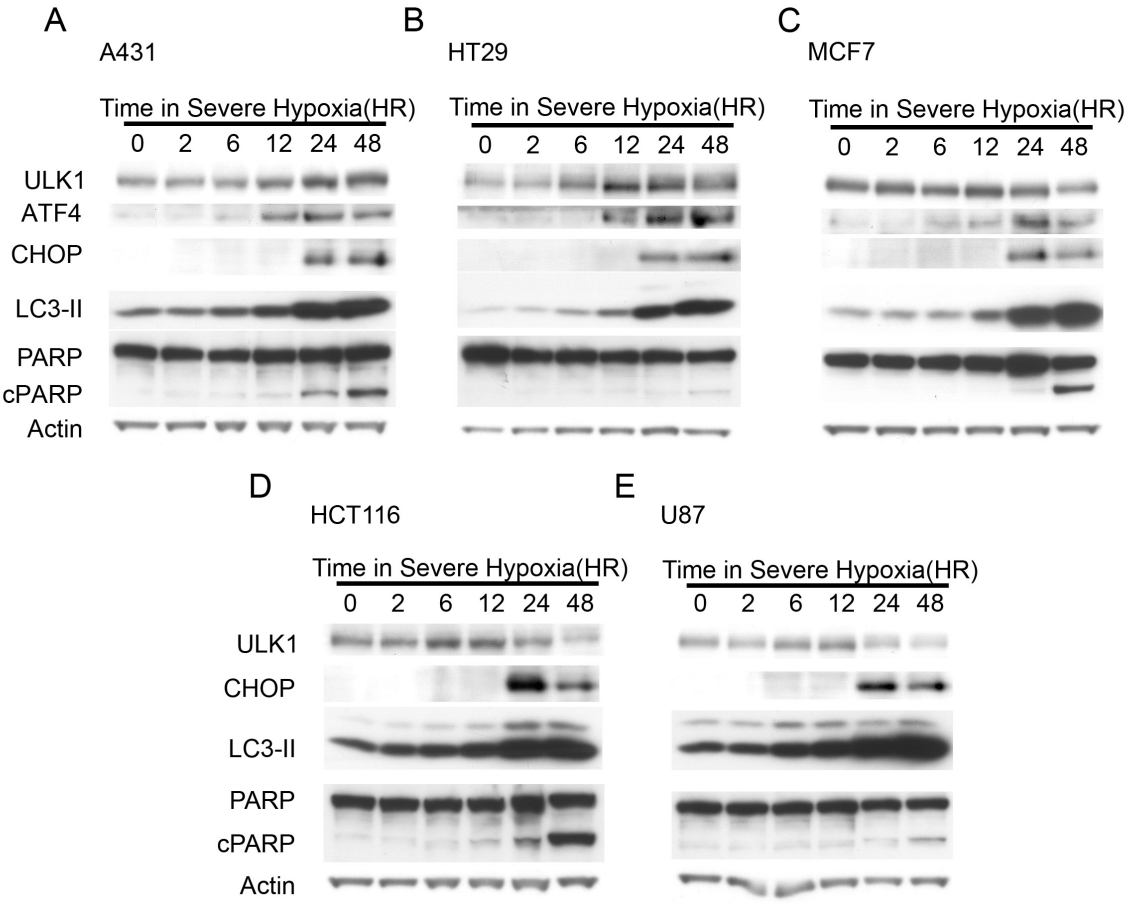

Figure 4.3 ULK1 protein accumulates in A431 and HT29 cells exposed to severe hypoxia in a timecourse similar to accumulation of the ISR markers CHOP and ATF4.

A431 (A), HT29 (B), MCF7 (C), HCT116 (D), and U87 (E) cells were exposed to severe hypoxia for the denoted periods, after which cells were harvested and analyzed by western blotting using the indicated antibodies. Representative images from at least N=2 independent experiments are shown.

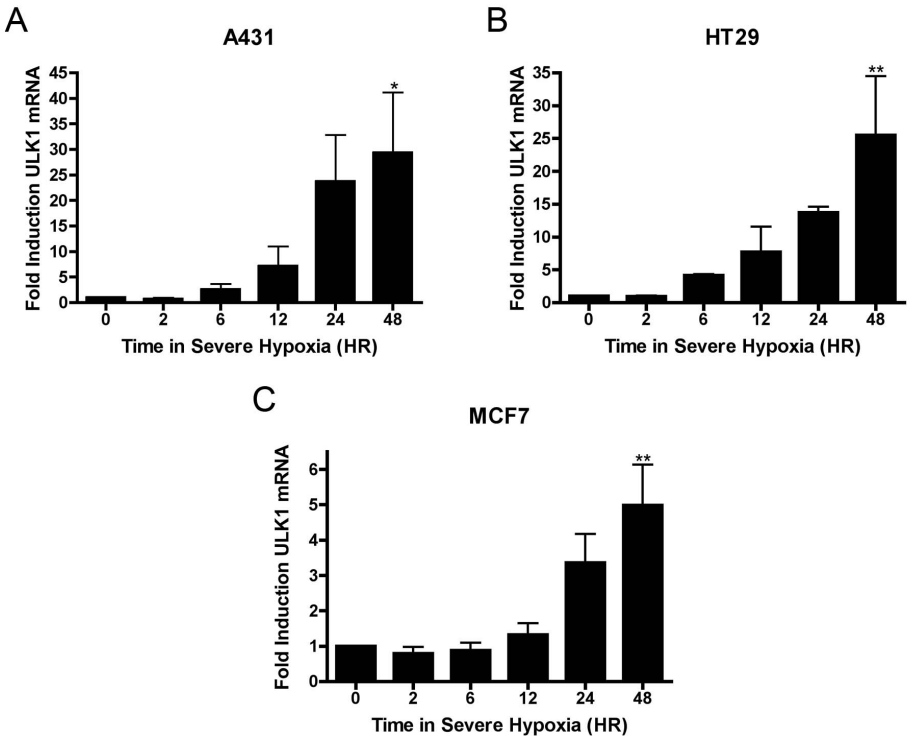

Figure 4.4 Exposure of A431, HT29, and MCF7 cancer cells to severe hypoxia leads to the accumulation of ULK1 mRNA by 48 hours.

*A431 (A), HT29 (B), and MCF7 (C) cells were exposed to severe hypoxia for the denoted periods, after which cells were harvested and analyzed by RT-qPCR using primers specific for ULK1 mRNA. N=3 independent experiments were done; *, and ** indicate P<0.05, and P<0.01 by one-way-ANOVA vs 0HR control.*

4.2.3 ER stressors, moderate hypoxia, intratumoural hypoxia, and anti-angiogenic therapy also induce ULK1 expression

The author next hypothesized that the induction of ULK1 mRNA and protein by severe hypoxia was due to ER stress and the ISR. Indeed, ULK1 protein accumulated in A431 cells treated with the ER stress-inducing drugs thapsigargin and tunicamycin (Figure 4.5). As in severe hypoxia, the accumulation of ATF4

preceded that of ULK1, and ULK1 protein accrued at a similar rate to CHOP protein.

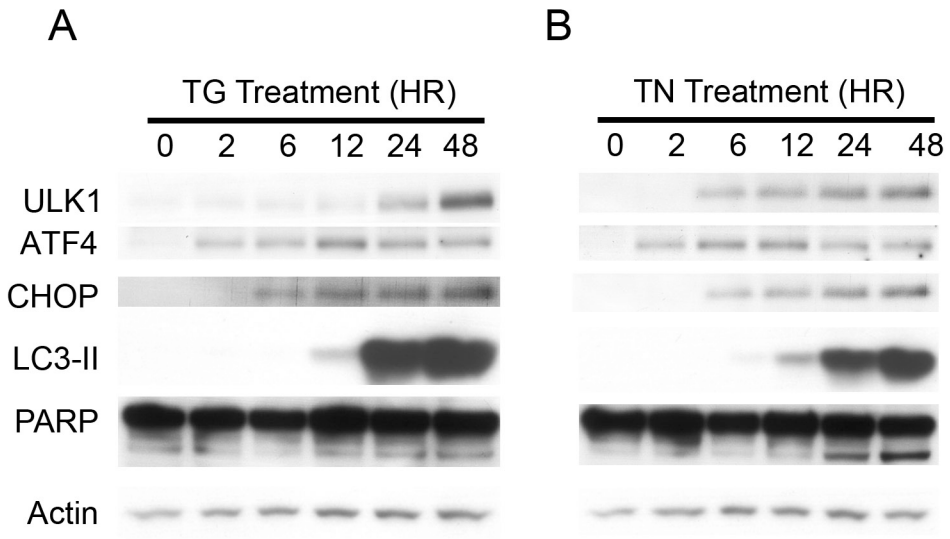

Figure 4.5 Treatment A431 cancer cells with the ER stress-inducing drugs thapsigargin or tunicamycin leads to the accumulation of ULK1 protein and the ISR markers ATF4 and CHOP.

A431 cells were treated with 300nM thapsigargin (A) or 5μg/mL tunicamycin for the denoted periods, after which cells were harvested and analyzed by western blotting using the indicated antibodies. Representative images from at least N=2 independent experiments are shown.

In addition to severe hypoxia, moderate hypoxia was also sufficient to increase ULK1 expression in these cells (Figure 4.6). ULK1 protein levels increased after slightly after 12 hours and reached a maximum after 48 hours in moderate hypoxia, though ATF4 levels did not increase significantly until 24 hours in moderate hypoxia. CHOP protein expression was not observed at all. HIF1α, on the other hand, was stabilized as early as 2 hours in moderate hypoxia, and the expression profile of the HIF1-dependent gene CAIX closely resembled that of ULK1.

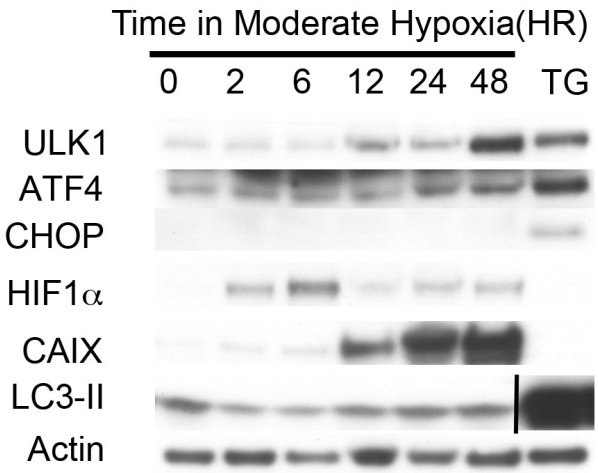

Figure 4.6 Exposure of A431 cancer cells to moderate hypoxia leads to the accumulation of ULK1 protein by 48 hours.

A431 cells were exposed to moderate hypoxia (0.1% O_2) for the denoted periods, after which cells were harvested and analyzed by western blotting using the indicated antibodies. Representative images from at least N=2 independent experiments are shown. TG indicates treatment with 300nM thapsigargin for 24 hours as a positive control for ER stress but not hypoxia. NB. LC3-II image was cropped to remove intervening lanes, indicated by vertical bar (though still from the same experiment and from the same gel).

To determine if ULK1 was upregulated in a three-dimensional model of tumour growth, A431 spheroids were grown (Ivascu and Kubbies, 2006). After one, three, six, or nine days growth, spheroids were collected and analyzed by western blotting (Figure 4.7). ATF4, HIF1α, and CAIX were induced after three days, indicating that these spheroids contained hypoxic cells. ULK1 protein also accumulated after three days growth and increased further by day six. Additionally, LC3-II protein levels were seen to increase by day six, indicating that autophagy is activated in this model.

Nine-day-old A431 spheroids were stained for the hypoxia markers pimonidazole, CAIX, and CHOP (Figure 4.7B). The patterns of pimonidazole and CAIX staining suggest that these spheroids contain a steep oxygen gradient, with moderate hypoxia beginning within 3-4 cell layers of the surface. CHOP staining in the perinecrotic region near the core indicated that there were also regions of severe hypoxia. Thus, the elevated levels of ULK1 protein observed by western blotting were likely triggered by the hypoxic spheroid microenvironment. Note. ULK1 staining was attempted with several different antibodies and a variety of staining protocols, but was unsuccessful.

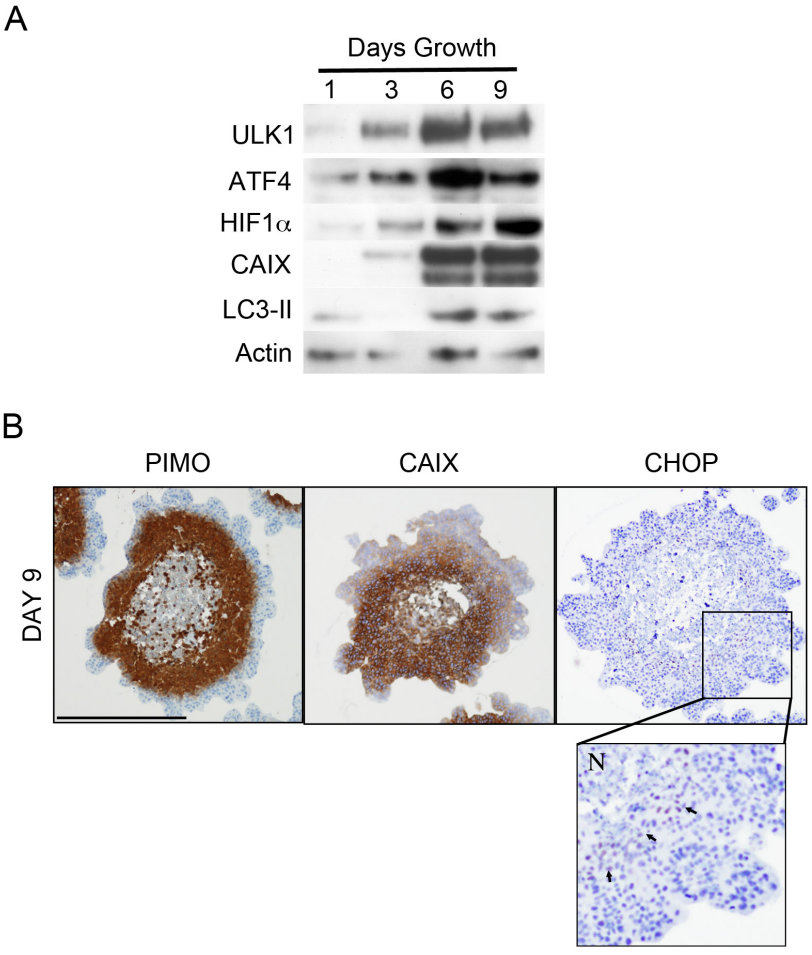

Figure 4.7 ULK1 protein accumulates in pimonidazole- and CAIX-positive spheroids derived from A431 cancer cells after 3 days growth.

A431 cells were seeded 5000 cells/well to a round bottom 96 well format with Matrigel®. After 24 hours, spheroid-like structures form and begin to grow (DAY 1). Spheroids were collected and harvested for western blotting on the indicated days with the specified antibodies (A) or after nine days growth fixed in formalin and stained with the indicated antibodies (B). Bar = 500μm. Representative images from at least N=2 independent experiments are shown. N denotes necrotic area and arrows point to positive CHOP staining.

To assess the expression of ULK1 *in vivo*, U87 xenografts harvested from mice treated with the humanized anti-VEGF antibody bevacizumab (Avastin® trade name) were analyzed for ULK1 mRNA expression by RT-qPCR (Figure 4.8). Previous work has shown that anti-angiogenic therapy increases intratumoural hypoxia *in vivo*, and thus the activation of hypoxia-responsive adaptive pathways is a major mode of resistance (Casanovas et al., 2005; Paez-Ribes et al., 2009). Bevacizumab treatment increased ULK1 expression compared to the PBS control treatment (N=5, P<0.001). CHOP mRNA levels were similarly elevated (P<0.001), indicating that the ISR was activated by bevacizumab treatment.

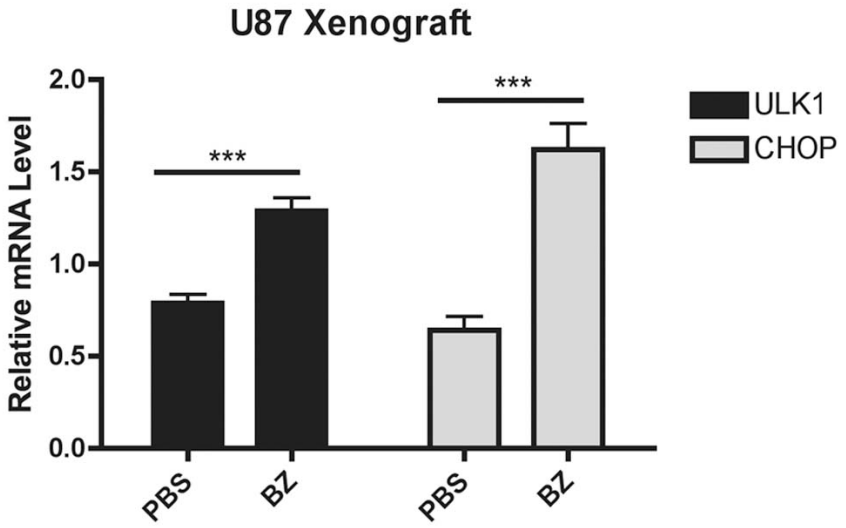

Figure 4.8 ULK1 and CHOP mRNA levels are higher in U87 xenografts grown in mice treated with the humanized anti-VEGF antibody bevacizumab.

*U87 cells were subcutaneously injected into the flanks of SCID mice. Starting on the day of implantation, mice were treated with 10mg/kg bevacizumab (BZ) or PBS (5 each group) every three days. After tumours reached 0.6 cm^3, mice were sacrificed and tumours were harvested and mRNA extracted for analysis with the indicated primers. *** denotes P<0.001 by Student's t-test of BZ treatment vs PBS control. Mouse work and RNA extraction was done by Dr. Ji-Liang Li. cDNA prep and RT-qPCR by the author of this work.*

4.2.4 ULK1 degradation in hypoxic MCF7 cells is mediated by the proteasome

In section 4.2.2, it was noted that ULK1 protein levels decrease over time in MCF7 cells, U87 cells, and HCT116 cells during exposure to severe hypoxia despite an increase in ULK1 mRNA. To investigate the mechanism of this reduction in ULK1 protein, MCF7 cells were exposed to severe hypoxia and treated with inhibitors of the proteasome (bortezomib and MG115), of the lysosome (chloroquine, bafilomycin A1, and E64D with pepstatin A), and of the caspases (ZVAD-FMK). Lysosomal inhibitors (Figure 4.9B and Figure 4.9C) and caspase inhibitors (Figure 4.9C) failed to prevent the degradation of ULK1. However, proteasome inhibition by bortezomib or MG115, partially blocked the reduction in ULK1 protein caused by prolonged exposure to severe hypoxia (Figure 4.9A). Unfortunately, it is difficult to discern between the effects of the proteasome on the ULK1 protein directly and the indirect effects of the proteasome on the ISR. Work previously published by this group has shown that bortezomib treatment results in ATF4 accumulation, and thus some of the observed rescue of ULK1 may in fact be due to enhanced transcription (Milani et al., 2009). Further studies are required to more fully understand the mechanism behind this change in expression.

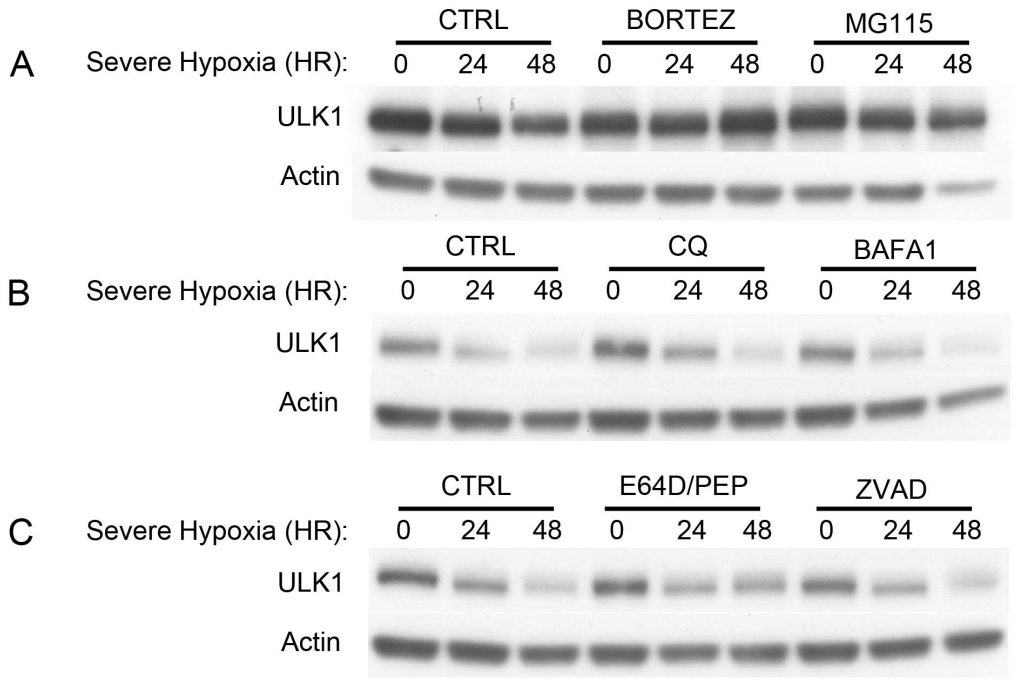

Figure 4.9 Treatment with MG115 or bortezomib causes the maintenance of ULK1 protein levels in MCF7 cells exposed to severe hypoxia for 24 or 48 hours relative to the untreated control.

MCF7 cells were treated with (A) 100nM bortezomib, 5μM MG115, (B) 25μM chloroquine, 0.1μM bafilomycin A1, (C) 10μg/mL of each E64D and pepstatin A, or 50μM ZVAD-FMK and then exposed to severe hypoxia for the indicated times. Cells were harvested and analyzed by western blotting using the indicated antibodies. Representative images from N=1 independent experiment are shown.

4.2.5 Severe hypoxia increases cellular ULK1 activity by both transcriptional and post-translational mechanisms

The figures above show clearly that ULK1 mRNA and protein expression are induced by severe hypoxia and ER stress. However, recent studies have demonstrated that the activity of the ULK1 kinase is highly regulated at the post-translational level by serine phosphorylation. In growth conditions (high glucose,

amino acids, oxygen, etc), mTOR phosphorylates both ULK1 and ATG13 at specific serine residues, reducing the activity of the complex. Starvation or rapamycin treatment results in dramatic dephosphorylation of ULK1 and increased autophagy through the ULK1-ATG13-FIP200 complex (Ganley et al., 2009). This event can be observed as a band shift on a low percentage gel. Adding a further level of complexity, AMPK has been shown to play a crucial role in ULK1 regulation. Starvation has been shown to promote AMPK association with ULK1 and mTOR. In contrast to the inhibitory phosphorylation events catalyzed by mTOR, AMPK promotes ULK1 activity and autophagy through specific phosphorylation of Ser317 and Ser777 or Ser467 and Ser555 while at the same time reducing mTOR activity through TSC2 (Egan et al., 2011; Kim et al., 2011; Lee et al.; Shang et al., 2011; Zhao and Klionsky, 2011).

Thus, having established that severe hypoxia causes the accumulation of ULK1 protein in A431 cells and results in the degradation of ULK1 protein in MCF7 cells, the author next sought to assess whether these changes in protein expression translated to altered cellular ULK1 activity. Cell lysates were prepared from A431 or MCF7 cells exposed to severe hypoxia for 12 or 24 hours. In collaboration with Dr. James Murray of the Center for Cancer Research and Cell Biology in Belfast, endogenous ULK1 was immunoprecipitated using these samples, and assessed for MBP phosphorylation as a measure of ULK1 activity (Kamada et al., 2000; Kamada et al., 1995). Interestingly, in the A431 cells the specific activity of ULK1 actually decreased by 35% ($P=0.0509$) after 24 hours in severe hypoxia (Figure 4.10B). However, due to the accumulation of ULK1 protein in this line, the total cellular ULK1 activity of ULK1 increased by 103% ($P=0.0991$) (Figure 4.10C). In MCF7 cells, on the other hand, though ULK1 protein does not accumulate in severe hypoxia, its specific activity increased by 115% after 12 hours in severe hypoxia ($P<0.05$) (Figure 4.10B), yielding an overall increase in total ULK1 activity of nearly 81% at this time point ($P<0.05$) (Figure 4.10C). Interestingly, this increase in ULK1 activity was transient, and by 24 hours in severe hypoxia both specific

and total ULK1 activity had decreased to normoxic levels (Figure 4.10B and Figure 4.10C).

A

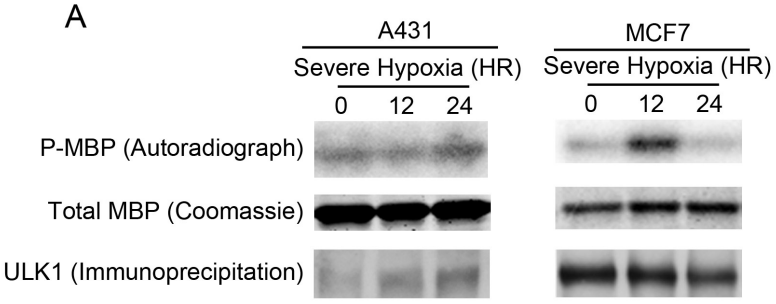
A431
Severe Hypoxia (HR)
0 12 24
MCF7
Severe Hypoxia (HR)
0 12 24
P-MBP (Autoradiograph)
Total MBP (Coomassie)
ULK1 (Immunoprecipitation)

B

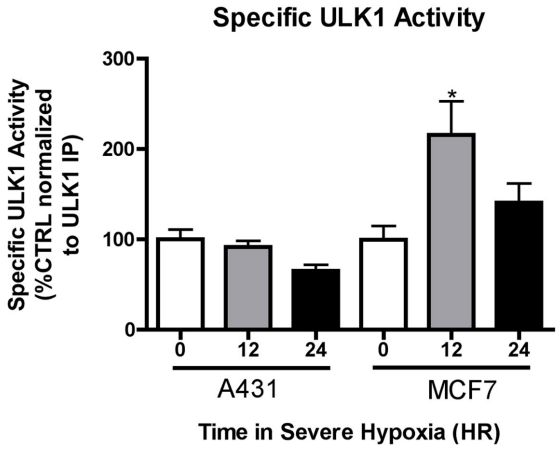
Specific ULK1 Activity
Specific ULK1 Activity (%CTRL normalized to ULK1 IP)
300
200
100
0
*
0 12 24 0 12 24
A431
MCF7
Time in Severe Hypoxia (HR)

C

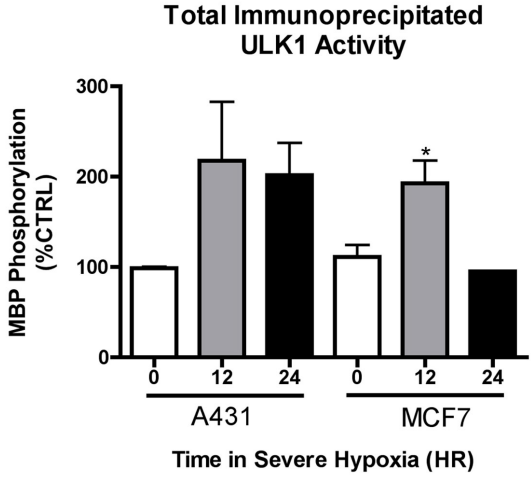
Total Immunoprecipitated ULK1 Activity
MBP Phosphorylation (%CTRL)
300
200
100
0
*
0 12 24 0 12 24
A431
MCF7
Time in Severe Hypoxia (HR)

Figure 4.10 Immunoprecipitated ULK1 protein from MCF7 cells exposed to severe hypoxia for 12 hours shows elevated kinase activity, as measured by MBP phosphorylation.

*A431 cells were exposed to severe hypoxia for twelve or 24 hours, after which cells were harvested and lysates prepared. A specific antibody was used to immunoprecipitate ULK1, and autoradiography for ULK1 kinase activity was done using myelin basic protein as a substrate (A). Coomassie staining was done to quantify MBP levels, and western blotting for ULK1 was done to confirm successful pulldown. Representative images from N=3 independent experiments are shown. (B) Specific ULK1 activity was calculated as the ratio of MBP phosphorylation to ULK1 protein (densitometry). (C) Total ULK1 activity, irrespective of ULK1 protein level is also shown. * indicates P<0.05 vs 0HR control by Student's T-test (N=3).*

The activation of the mTOR and AMPK pathways was next assessed. In both cell lines, there is a downward band shift of ULK1 (Figure 4.11). This shift was similar to that observed with rapamycin treatment and matched that observed by Ganley and coworkers due to the de-repressing dephophorylation of ULK1 in starvation, suggesting that this is also occurring in severe hypoxia. This event was accompanied by increased activity of AMPK, as ascertained by activating phosphorylation of AMPKα at Thr172, and downstream phosphorylation of AMPK target proteins ACC and Raptor at Ser79 and Ser792, respectively. Likewise, there is a clear decrease in mTOR activity: the phosphorylation of mTOR target p70 S6 kinase at Ser371 drops markedly with exposure to severe hypoxia or rapamycin. Thus, severe hypoxia activates not only the transcription and translation of ULK1 protein but also its post-translational modification, likely through the AMPK and mTOR pathways. In the MCF7 cell line, these changes appear to increase the specific activity of the ULK1 kinase. However, in A431 cells, increased AMPK signaling and decreased mTOR signaling appear to have no effect on the specific activity of ULK1. As such, to maintain high levels of autophagic flux in severe hypoxia, ULK1 mRNA and protein are strongly upregulated.

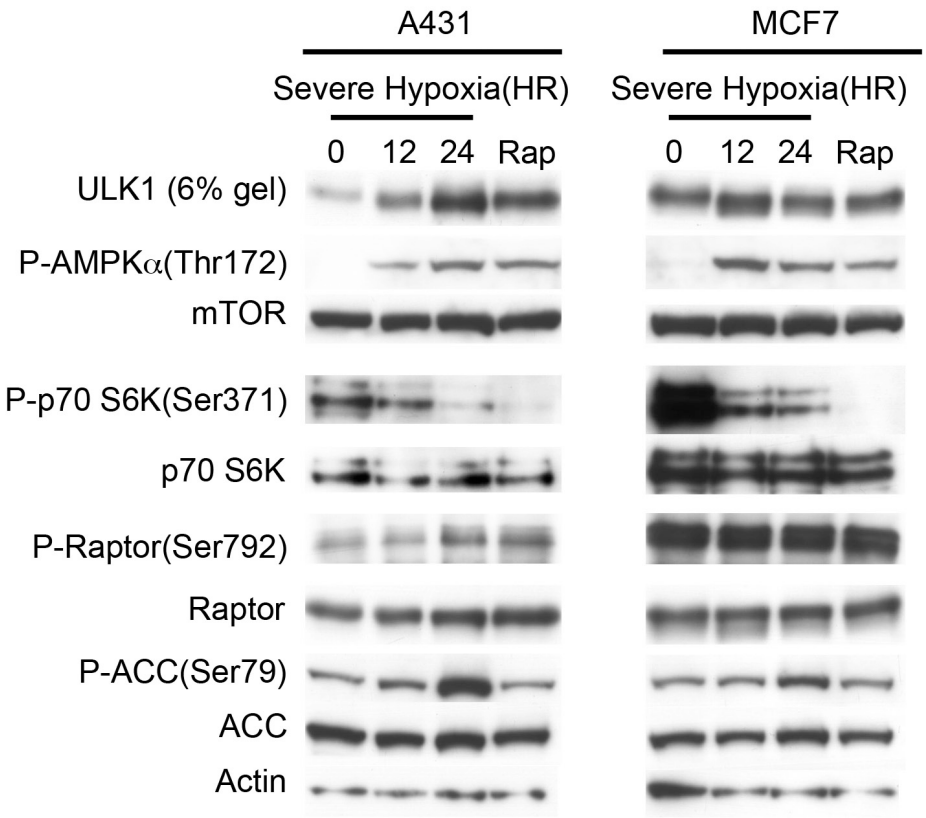

Figure 4.11 Exposure of A431 or MCF7 cancer cells to severe hypoxia causes a downward bandshift in ULK1 protein, increased phosphorlyation of AMPK and its target ACC, and decreased phosphorylation of the mTOR target S6K. *A431 or MCF7 cells were exposed to severe hypoxia for twelve or 24 hours, or to 100nM rapamycin for 24 hours and then harvested for analysis by western blotting with the indicated antibodies. Representative images from at least N=2 independent experiments are shown.*

4.2.6 Severe hypoxia induces ULK1 in an ATF4-dependent manner

The microarray data discussed in section 4.2.1 revealed that ULK1 mRNA was induced 1.76-fold in severe hypoxia in MCF7 cells. Additionally, knockdown of

ATF4 by RNAi reduced this expression to 0.60-fold relative to the level in normoxia. To validate the latter result, a siRNA sequence specific for ATF4 was used to deplete ATF4 protein in normoxia and severe hypoxia. In both A431 and MCF7 cells, siRNA knockdown reduced ATF4 protein levels at least 50% after exposure to severe hypoxia (Figure 4.12A and Figure 4.12B). The hypoxic induction of ULK1 protein in A431 cells was suppressed by this treatment, and the hypoxic degradation of ULK1 protein in MCF7 cells was expedited, and basal ULK1 protein levels were diminished. Similarly, knockdown of ATF4 resulted in a greater than 50% reduction in ULK1 mRNA after 48 hours in severe hypoxia, in both the A431 and MCF7 cell lines ($P<0.05$ and $P<0.01$, respectively). Thus, ULK1 is upregulated in severe hypoxia through an ATF4-dependent mechanism.

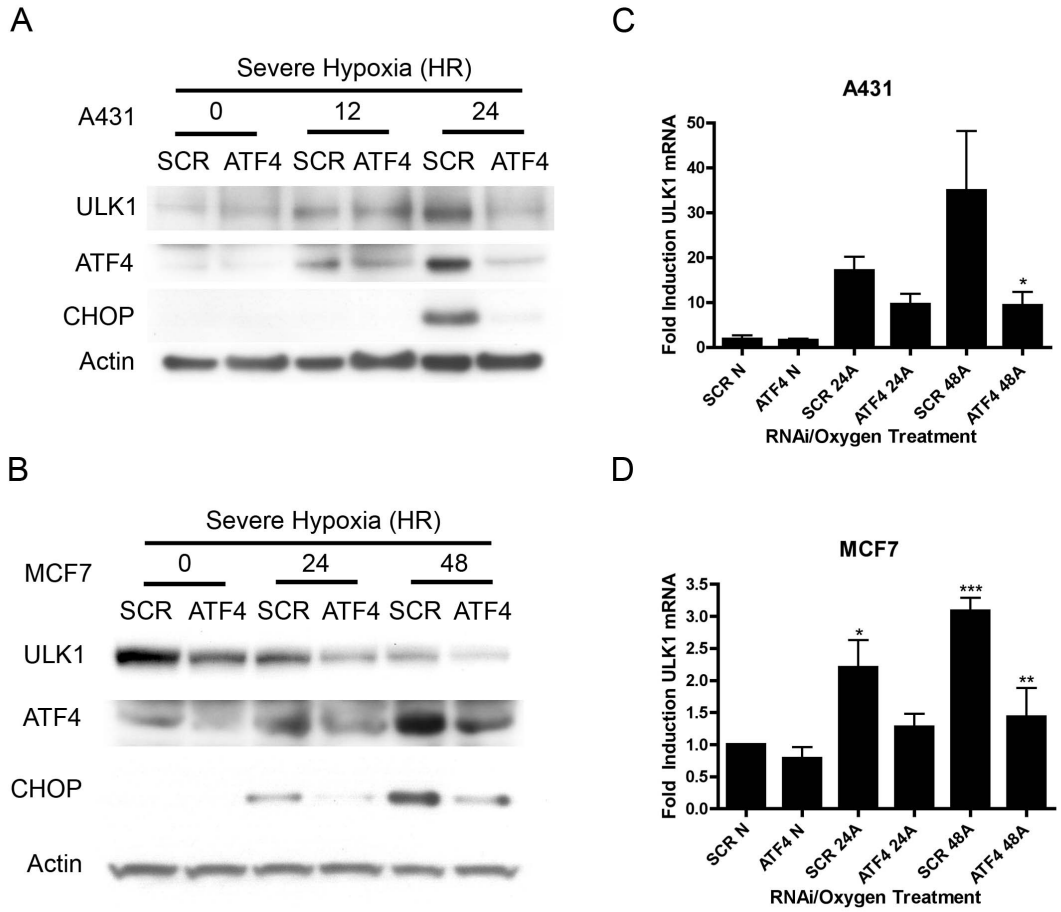

Figure 4.12 Treatment of A431 and MCF7 cancer cells with ATF4 siRNA reduces the accumulation of ULK1 mRNA and protein in severe hypoxia.

*A431 (A and C) or MCF7 (B and D) cells were transfected with siRNA against ATF4 (ATF4) or a scrambled control sequence (SCR) overnight and exposed to severe hypoxia (A) or normoxia (N) the following day. After 12, 24 or 48 hours, cells were harvested for analysis by western blotting or RT-qPCR using the indicated antibodies and primers, respectively. For western blotting, representative images from at least N=2 independent experiments are shown. For RT-qPCR, N=3 independent experiments were done and *, **, and *** indicate P<0.05, P<0.01, and P<0.001, respectively, by one-way-ANOVA for SCR A vs SCR N or ATF4 A vs SCR A.*

4.2.7 ER stress induces ULK1 in an ATF4-dependent manner

To assess whether ULK1 induction by ER stress is also mediated by ATF4, A431 cells were transfected with siRNA against ATF4 and treated with tunicamycin or thapsigargin for 24 hours. In each case, ATF4 protein was almost completely ablated by this treatment, and the accumulation of ULK1 protein was blocked accordingly (Figure 4.13). Thus, ER stress incites the accumulation of ULK1 protein in an ATF4-dependent manner.

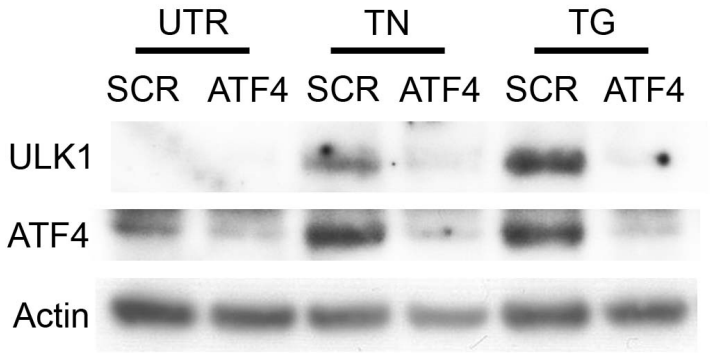

Figure 4.13 Treatment of A431 cancer cells with ATF4 siRNA reduces the accumulation of ULK1 protein following treatment with thapsigargin or tunicamycin for 24 hours.

A431 cells were transfected with siRNA against ATF4 (ATF4) or a scrambled control sequence (SCR) overnight and treated with or 5μg/mL tunicamycin (TN) or 300nM thapsigargin (TG) the following day. After 24 hours, cells were harvested for analysis by western blotting using the indicated antibodies. Representative images from at least N=2 independent experiments are shown.

4.2.8 Exogenous expression of ATF4 is not sufficient to drive the expression of ULK1

Given that knockdown of ATF4 prevented the expression of ULK1 mRNA and protein in response to severe hypoxia and ER stress, the effect of ATF4

overexpression on ULK1 was examined. A vector encoding the open reading frame of ATF4 was used to express ATF4 in normoxic A431 cells at a high level, and the expression of ULK1 was assessed by western blotting (Figure 4.14). ULK1 protein levels did appear to be slightly upregulated, but this change was subtle relative to that observed in severe hypoxia. It is therefore likely that ATF4 requires the presence of other (hypoxia-induced) factors to activate ULK1 transcription, such as is the case for CHOP (Oyadomari and Mori, 2004).

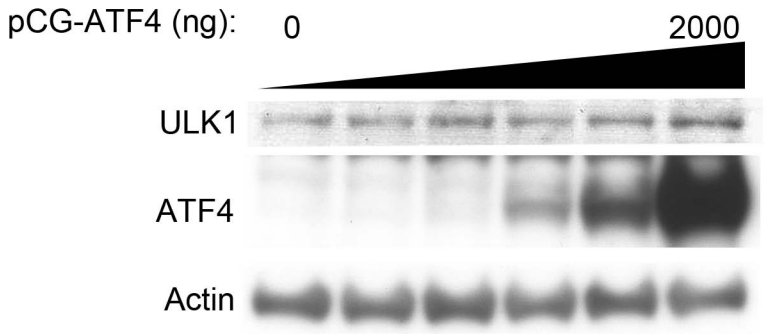

Figure 4.14 Exogenous expression of ATF4 protein fails to increase the expression of ULK1 protein in A431 cells in normoxia.
A431 cells were transfected with 0 to 2000ng of pCG-empty vector or pCG-ATF4. 48 hours later, cells were harvested and analyzed by western blotting using the indicated antibodies. Representative images from N=1 independent experiment are shown.

4.2.9 ATF4 binds directly to the promoter region of ULK1

To determine if ATF4 acts in *cis* to promote the expression of ULK1, a chromatin immunoprecipitation assay (ChIP) was performed using antibodies specific for ATF4. Using the Genomatix® online software suite, several putative CREB/ATF binding sites containing the TGACG core sequence were identified in the promoter

region of ULK1. Next, a set of qPCR primers were designed, spanning the region 2000bp upstream of the transcription start site, the first exon, and 500bp downstream of translation start (Figure 4.15A). Primers were also designed against a region of chromosome 12 well upstream of the ULK1 gene (negative control), as well as a previously published set of primers designed against the CHOP promoter (positive control) (Rouschop et al., 2009b). qPCR of the ATF4 ChIP samples showed the greatest enrichment of those fragments corresponding to primer set #3 (Figure 4.15B), corresponding to the CREB site spanning -306bp to -285bp (relative to ATG in exon one). Furthermore, the signal obtained from this primer set increased with exposure to severe hypoxia, reflecting increased ATF4 binding with severe hypoxia (Figure 4.15C). These results indicate that this CREB/ATF element is a site of direct interaction for ATF4.

It must be noted, however, that this latter conclusion depends on the assumption that each primer pair is roughly equally efficient and thus that the observed signal is proportional to the relative abundance of DNA in the sample. As such, primer set #3 may simply be more efficient than set #1, which would lead to the false assumption that the proximal CREB site is the *bona fide* ATF4 binding element.

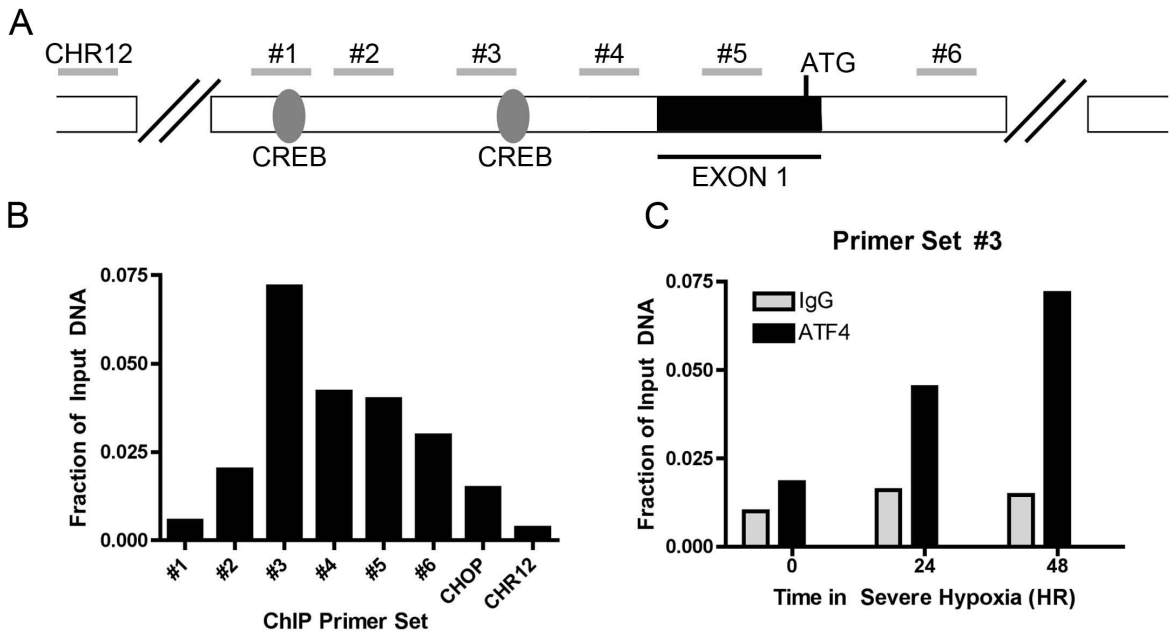

Figure 4.15 Chromatin immunoprecipitation using an ATF4-specific antibody enriches lysates from MCF7 cells in DNA corresponding to the ULK1 promoter in a hypoxia-dependent manner.

MCF7 cells were exposed to severe hypoxia for the indicated times and then fixed with paraformaldehyde. DNA was sheared and a chromatin immunoprecipitation was performed. Primers sets (represented by gray bars) were designed spanning the region 2000bp upstream of the transcription start site, the first exon, and 500bp downstream of translation start containing two putative ATF/CREB binding sites (A). QPCR was done to analyze the enrichment of these fragments in the hypoxic samples (B). qPCR against the region corresponding to primer set #3 showed hypoxia-dependent enrichment of the ATF4 pulldown samples relative to the IgG controls (C). Data shown are representative of three independent experiments.

4.2.10 ULK1 is essential for hypoxia-induced autophagy

Recent work has established ULK1 as being a key regulator of mammalian autophagy in a variety of contexts. An siRNA screen of the kinome first identified ULK1 as an important modulator of autophagy during amino acid deprivation

(Chan et al., 2007). A hierarchial proteomic analysis of the ATG proteins demonstrated that ATG1/ULK1 is the most upstream ATG protein involved in glucose starvation-induced autophagy (Behrends et al., 2010). Similarly, recent studies have shown ULK1 to be directly phosphorylated and activated by the crucial energy-sensing AMPK, and to play a key role in AMPK-mediated mitophagy (Egan et al., 2011; Kim et al., 2011). Thus, given the profound upregulation and activation of ULK1 in severe hypoxia, the author hypothesized that ULK1 is essential for autophagy in the context of cancer cells in severe hypoxia. To test this hypothesis, siRNA sequences specific for ULK1 were used to deplete its expression and cells were exposed to severe hypoxia. Indeed, knockdown of ULK1 reduced both the accumulation of LC3-II protein (Figure 4.16A) and the formation of LC3-positive puncta in A431 cells exposed to severe hypoxia (Figure 4.16C). Knockdown of ULK1 also reduced autophagy induction in MCF7 cells, although the effect was less remarkable (Figure 4.16B and Figure 4.16D).

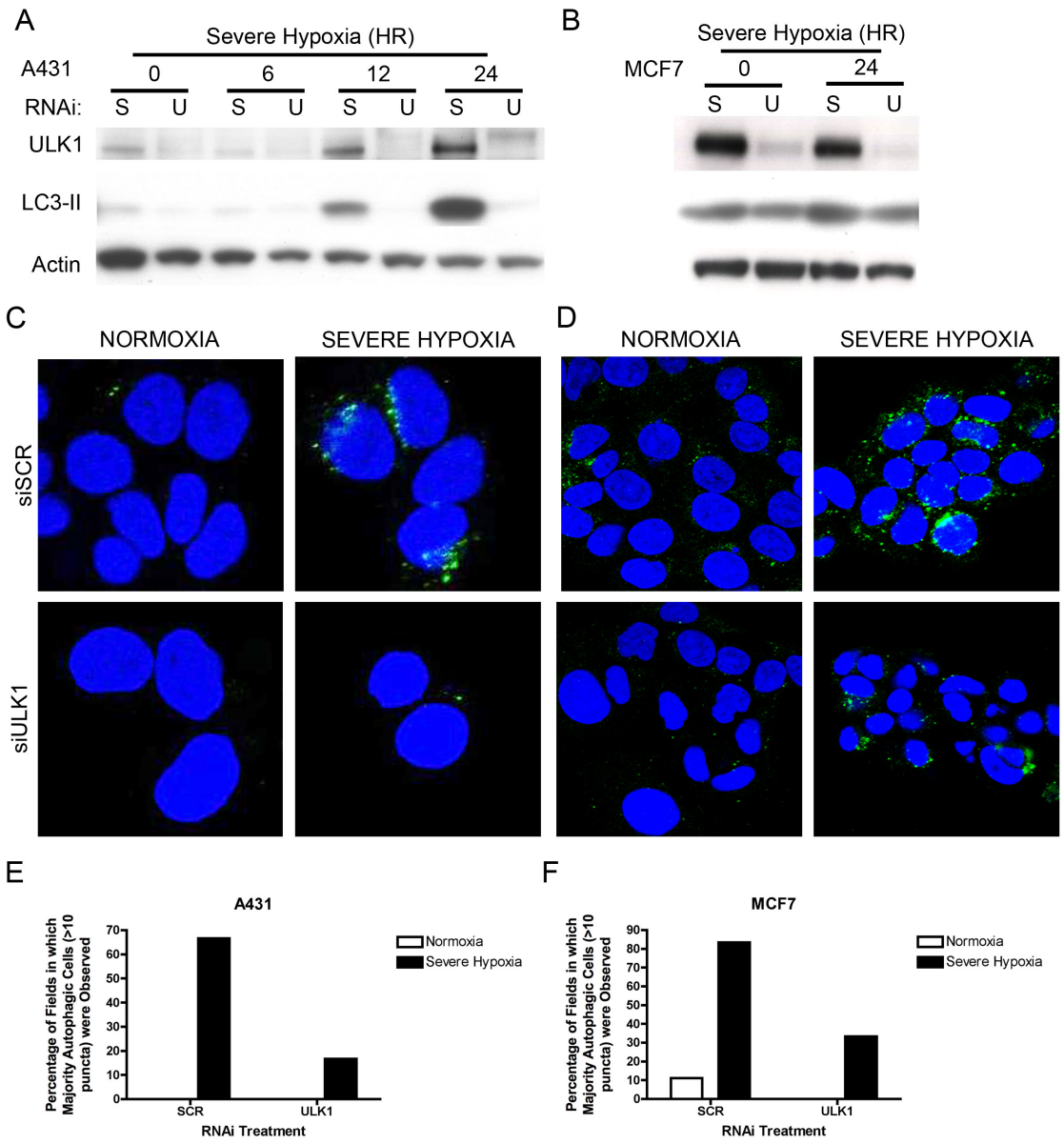

Figure 4.16 Treatment of A431 or MCF7 cells with ULK1 siRNA reduces LC3-II protein accumulation and LC3-positive puncta accumulation following exposure to severe hypoxia for 24 hours.

A431 (A and C) or MCF7 (B and D) cells were transfected with siRNA against ULK1 (U) or a scrambled control sequence (S) overnight and exposed to severe hypoxia the next day for the indicated times. (A and B) Cells were harvested for analysis by western blotting using the indicated antibodies. (C and D) Cells were fixed and stained for LC3 (green) and counterstained with DAPI (blue). Representative images

from at least N=3 independent experiments are shown. (E and F)) The percentage of fields containing a majority autophagic cells was assessed and quantified for one such experiment.

4.2.11 Loss of ULK1 in reduces flux through the autophagy pathway in both normoxia and severe hypoxia

As described in Chapter 3, the accumulation of LC3 protein and LC3-positive puncta can indicate that autophagic flux is occurring at a higher rate as a result of increased autophagy induction or alternatively that autophagosome fusion with lysosomes has been blocked. Thus to confirm that ULK1 knockdown results in a reduction in autophagy induction rather than an increased rate of degradation, lysosomal inhibitors were added to A431 cells following RNAi-mediated ablation of ULK1 protein. As expected, LC3-positive puncta were detected at a high level in cells treated with choloroquine in normoxia and to an even greater extent after exposure to severe hypoxia, indicating that severe hypoxia increases autophagy induction and flux in these cells (Figure 4.17). However, in cells lacking ULK1 this accumulation was almost completely blocked in both normoxia and severe hypoxia. Thus, ULK1 is essential for autophagic flux in both normoxia and severe hypoxia.

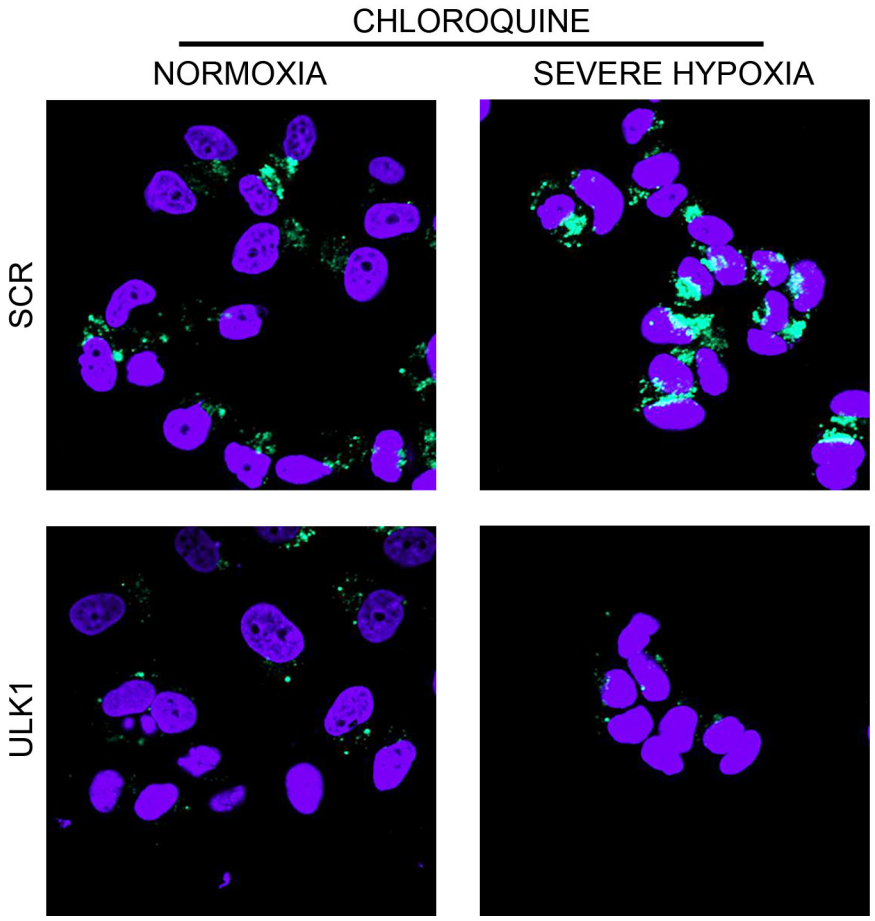

Figure 4.17 Treatment of MCF7 cells with ULK1 siRNA reduces LC3-positive puncta accumulation following exposure to severe hypoxia and chloroquine for 24 hours.

MCF7 cells were transfected with siRNA against ULK1 or a scrambled control sequence (SCR) overnight and reseeded onto coverslips the next day. Cells were treated with 25μM chloroquine and exposed to severe hypoxia for 24 hours and then fixed and stained for LC3 (green) and counterstained with DAPI (blue). Representative images from at least N=2 independent experiments are shown.

To further confirm this result, Imagestream® analysis of autophagic flux was performed (Pike, Chapter 3; Phadwal et al., 2011, submitted). The scrambled control demonstrated a high level of autophagy even in normoxia, and this level

was increased by exposure to severe hypoxia (Figure 4.18A). In contrast, loss of ULK1 expression resulted in a more than 80% decrease in autophagic flux in normoxia (P<0.001) and nearly 90% in severe hypoxia (P<0.001), thereby confirming a role for ULK1 in the regulation of autophagy in cancer cells in both normoxia and severe hypoxia.

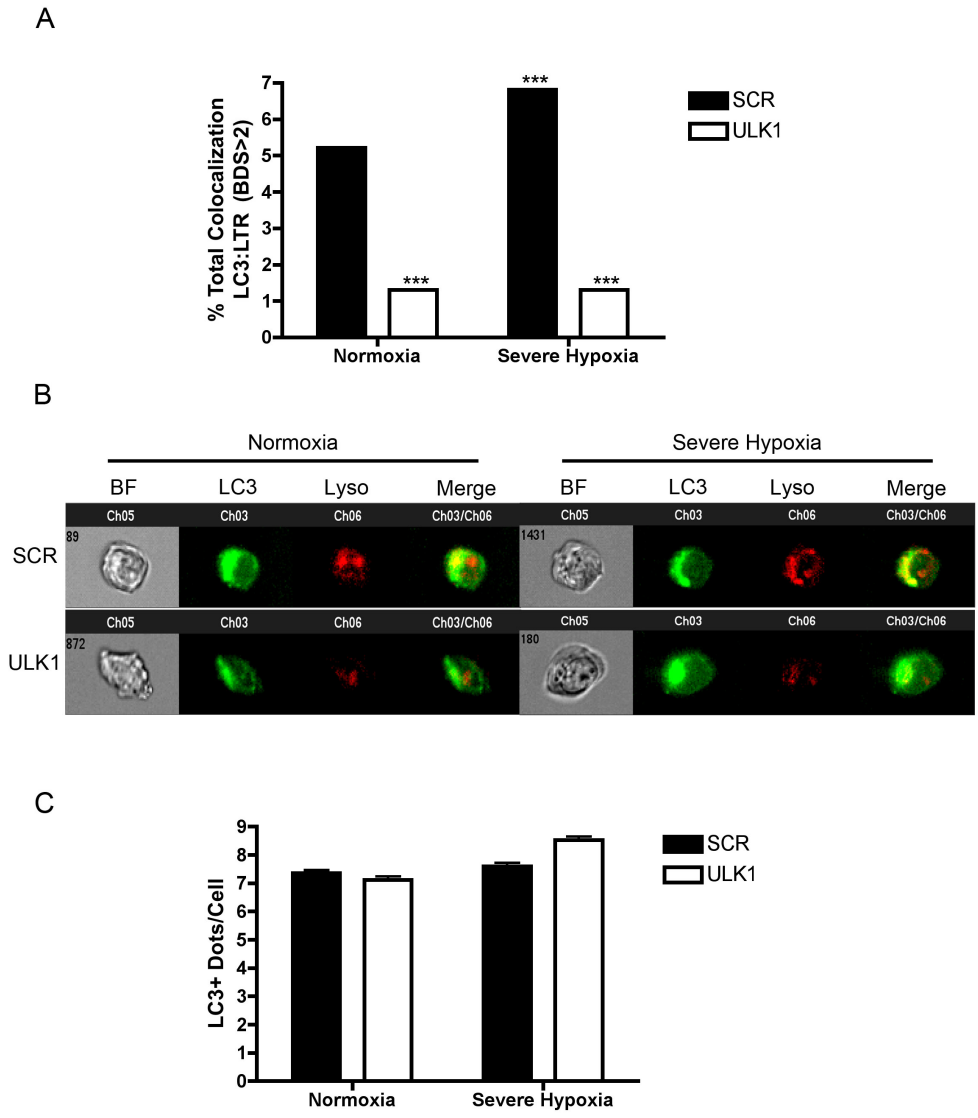

Figure 4.18 Treatment of MCF7 cells with ULK1 siRNA reduces the colocalization of LC3-positive puncta with lysosomal puncta following exposure to severe hypoxia for 24 hours.

*MCF7 cells were transfected with siRNA against ULK1 or a scrambled control sequence (SCR) overnight and exposed to severe hypoxia the next day. 24 hours later, cells were stained for LC3 (green) and lysosomes (red), and fixed for Imagestream® analysis. *** indicates P<0.001 by two-way ANOVA, where N=5000 in (A). Representative images from N=3 independent experiments are shown in (B). Number of LC3+ dots per cell are shown in (C) for the benefit of the reader.*

4.2.12 Loss of ULK1 or ATF4 reduces mitophagy in cancer cells

Having established a role for ULK1 and ATF4 in autophagy in cancer cells in normoxia and severe hypoxia, the author next hypothesized that ULK1 might play a role in mitophagy. This hypothesis follows from previous work in mouse fibroblasts, primary hepatocytes, and in reticulocytes, which showed that ULK1 is essential for mitophagy in a variety of physiological contexts (Egan et al., 2011; Kundu et al., 2008b). Thus, to determine if ULK1 plays a similar role in cancer, A431 cells were depleted of ULK1 or ATF4 and exposed to severe hypoxia. Cells were stained with Mitotracker Red FM, a specific mitochondrial dye, and analyzed by flow cytometry. Indeed, knockdown of ULK1 resulted in an increase in the mean mitochondrial fluorescence by 40% (P<0.001) in both normoxia and severe hypoxia (Figure 4.19) to an equal degree in each case. ATF4 knockdown had a similar effect, though smaller in magnitude, increasing the mean mitochondrial fluorescence by 20% (P<0.001) (Figure 4.19).

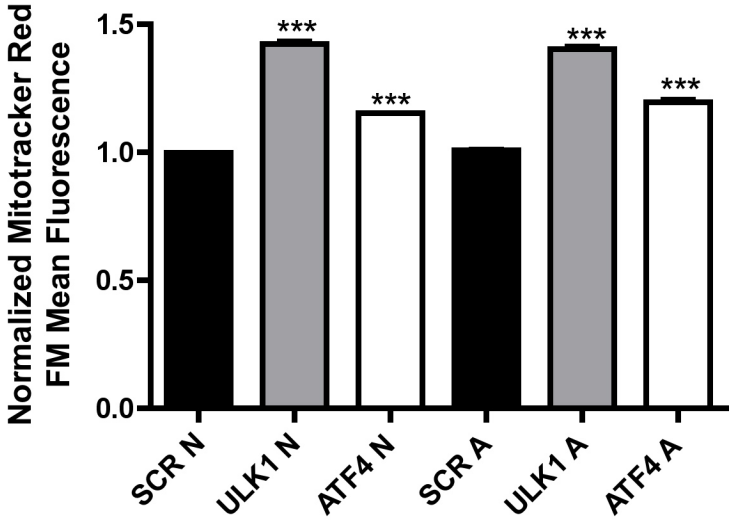

Figure 4.19 Treatment of A431 cells with ULK1 or ATF4 siRNA reduces mean Mitotracker FM fluorescence® as measured by FACS in normoxia and after exposure to severe hypoxia for 24 hours.

*A431 cells were transfected with siRNA against ULK1, ATF4, or a scrambled control sequence (SCR) overnight. The next day, cells were exposed to severe hypoxia. After 24 hours, Mitotracker Red FM® dye was added and cells were analyzed by flow cytometry. N=1 independent experiments were done with N=3 replicates. *** indicates P<0.001 by one-way-ANOVA for ULK1 or ATF4 treatments relative to the SCR control in the same oxygen tension.*

In collaboration with Professor David Ferguson, TEM analysis of cellular morphology was next done to look for signs of mitochondrial autophagy. In the scrambled control cells many of the mitochondria appeared to be enclosed by ER-like membranes (Figure 4.20A). In some instances, lysosomal structures containing what appeared to be partially digested organelles were also seen. Knockdown of ULK1 and to a lesser extent, ATF4, reduced the number of mitochondria enclosed by ER (Figure 4.20B). Instead, ER appeared linear and sometimes adjacent to mitochondria, but was rarely seen to encircle them, suggesting that ULK1 plays a role in mitophagy. For an example of an enclosed and an unenclosed mitochondrion see Figure 4.20A (bottom right panel).

A

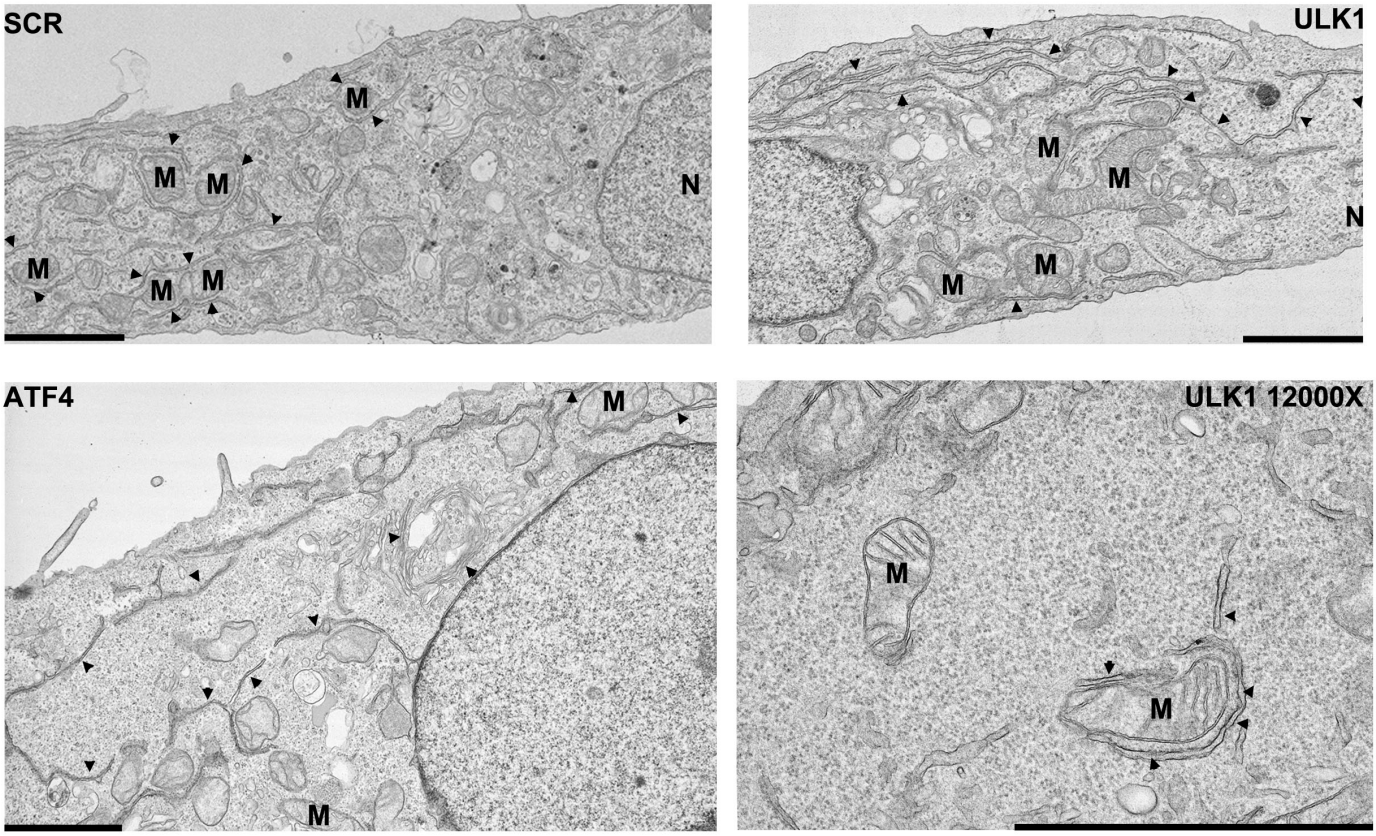
SCR
M
M
M
N
M
M
M
ULK1
M
M
N
M
M
M
ATF4
M
M
ULK1 12000X
M
M

B

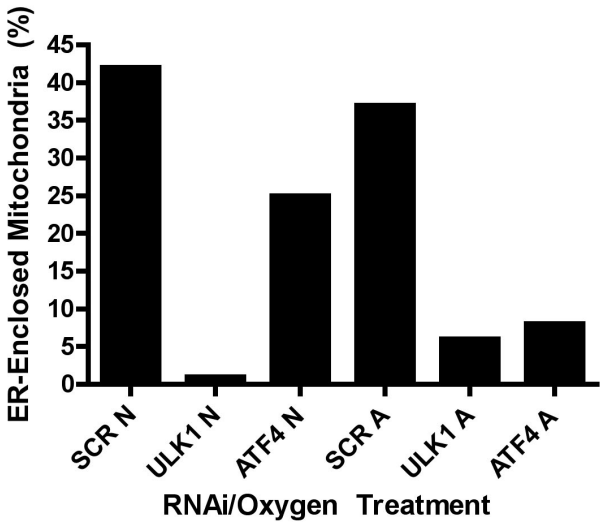
ER-Enclosed Mitochondria (%)
45
40
35
30
25
20
15
10
5
0
SCR N
ULK1 N
ATF4 N
SCR A
ULK1 A
ATF4 A
RNAi/Oxygen Treatment

Figure 4.20 Treatment with ULK1 or ATF4 siRNA reduces the number of ER-enclosed mitochondria in A431 cells exposed to severe hypoxia or not for 24 hours as measured by TEM.

A431 cells were transfected with siRNA against ULK1, ATF4, or a scrambled control sequence (SCR) overnight. The next day, cells were exposed to severe hypoxia. After 24 hours, cells were fixed and prepared for transmission electron microscopy (A). Images are labeled with N for nuclei, M for mitochondria, L for autophagosomal/lysosomal-like structures containing organelles, and with arrowheads for reticular membranes. Quantitation of the described phenotype is provided in (B). Representative images from N=1 independent experiment are shown, with N=100 cells analyzed in each group of this experiment. TEM done by Professor David Ferguson.

4.2.13 ULK1 and ATF4 are required for cancer cell survival in both normoxia and severe hypoxia

There is a substantial body of work to support the role of autophagy in the adaptation to and survival of nutrient deprivation and hypoxia. Several recent studies have demonstrated that ULK1 is instrumental for cell survival in amino acid or glucose starvation. Work from this group and others has shown that cancer cells adapt to and survive hypoxia *in vitro* and *in vivo* through increased autophagy (Degenhardt et al., 2006; Milani et al., 2009; Rouschop et al., 2009a; Rzymski et al., 2010). Thus, it was hypothesized that ULK1 is essential for cancer cell survival in severe hypoxia. To test this hypothesis, A431 and MCF7 cells were transfected with siRNA against ULK1 and exposed to severe hypoxia. Western blot analysis revealed high levels of cleaved PARP following ULK1 knockdown in severe hypoxia (Figure 4.21), indicating elevated levels of apoptosis or necrosis (Otsuki et al., 2003; Shah et al., 1996).

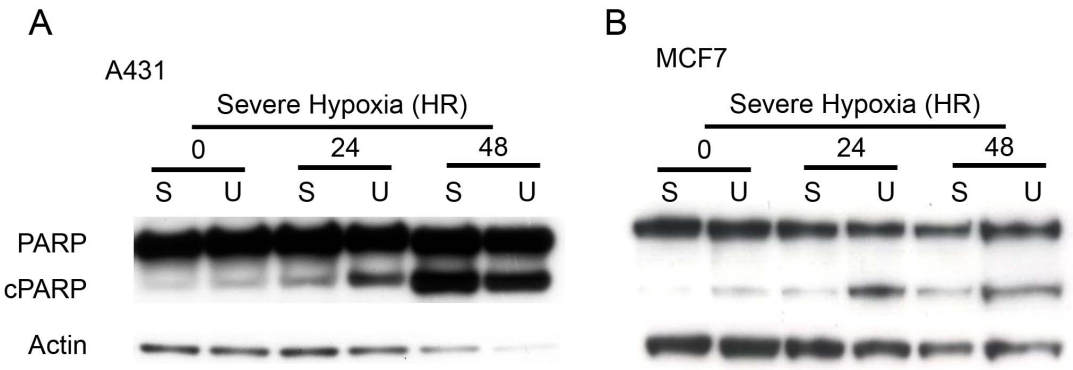

Figure 4.21 Treatment of A431 or MCF7 cells with ULK1 siRNA results in increased PARP cleavage after 24 hours in severe hypoxia.

A431 (A) or MCF7 (B) cells were transfected with siRNA against ULK1 (U) or a scrambled control sequence (S) overnight and exposed to severe hypoxia the next day. 24 or 48 hours later, cells were harvested and analyzed by western blotting with antibodies against total PARP. Representative images from at least N=2 independent experiments are shown.

Furthermore, knockdown of ULK1 by RNAi increased annexin-V staining in A431 cells exposed to severe hypoxia to 63% ($P<0.001$ vs SCR A), indicating that cancer cells depend on ULK1 for survival in severe hypoxia (Figure 4.22A). Knockdown of ULK1 in normoxic cells also caused upwards an increase in annexin-V staining to 40% (16% in the SCR control) ($P<0.001$ vs SCR N) (Figure 4.22A). Severe hypoxia itself was sufficient to increase annexin-V staining to 39% ($P<0.001$ vs SCR N). Similar results were obtained when ULK1 was silenced in MCF7 cells. Knockdown of ULK1 in normoxia was sufficient to increase annexin-V staining from 14% in the scrambled control to 36% ($P<0.001$) (Figure 4.22B). This staining was further increased in severe hypoxia: ULK1 knockdown increased the proportion of annexin-V-positive cell from 18% to 51% ($P<0.001$). When ATF4 was reduced by RNAi in A431 cells, a similar result was obtained. Loss of ATF4 compromised cell survival in both severe hypoxia and in "unstressed" conditions, increasing annexin-V staining from 10% in the control cells to 36% in the ATF4-

knockdown cells in normoxia (P<0.001) and from 55% to 65% in severe hypoxia (not significant)(Figure 4.22C).

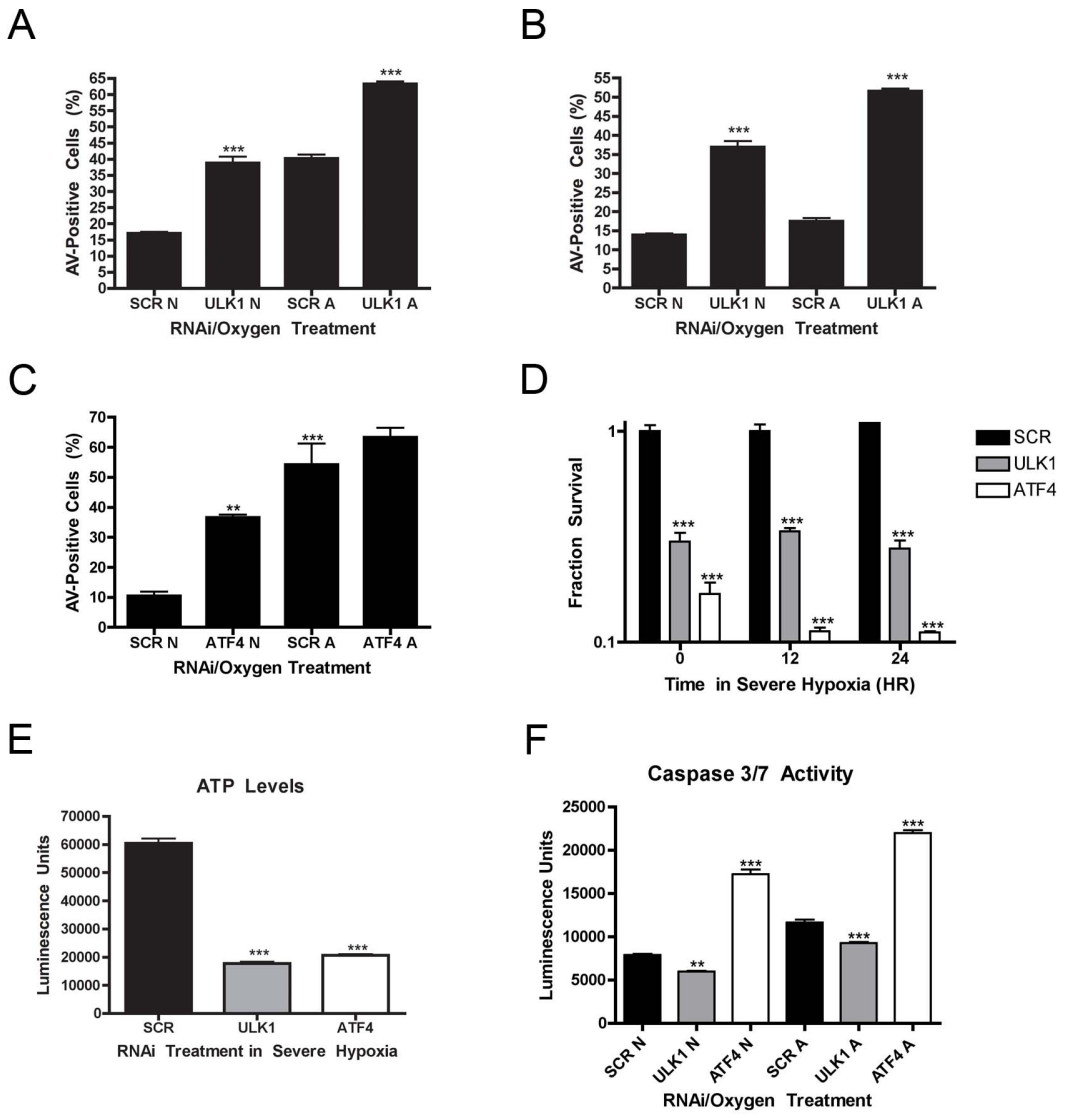

Figure 4.22 Treatment of A431 or MCF7 cells with ULK1 or ATF4 siRNA increases cell death in both normoxia and severe hypoxia as measured by FACS, clonogenic survival, ATP levels, and caspase 3/7 activity.

A431 (A, C, D, E, and F) or MCF7 (B) cells were transfected with siRNA against ULK1, ATF4, or a scrambled control sequence (SCR) overnight and exposed to severe hypoxia the next day. After 36 hours, A431 (A and C) or MCF7 (B) cells were stained with

*annexinV-AlexaFluor647 and analyzed by flow cytometry. Clonogenicity was assessed by seeding serial dilutions of A431 cells into 60mm dishes and exposure them to severe hypoxia for 12 or 24 hours (D). Changes in ATP in severe hypoxia were assessed after exposure to severe hypoxia for 36 hours (E). Caspase 3/7 activity was determined after 24 hours in severe hypoxia (F). In each panel, the results of one experiment with at least N=3 replicates is shown, representative of at least N=3 independent experiments. *, **, and *** indicate P<0.05, P<0.01, and P<0.001, respectively, by one-way ANOVA for ULK1 RNAi or ATF4 RNAi treatments vs the SCR control at the same oxygen tension, or for SCR A vs SCR N.*

The effect of ULK1 or ATF4 depletion on clonogenic survival was next assessed. Knockdown of ULK1 reduced the surviving fraction in both normoxia and after exposure to severe hypoxia for either 12 or 24 hours by 65% (P<0.001) (Figure 4.22D). Loss of ATF4 reduced the surviving fraction by 80% in normoxia (P<0.001), and 90% after 12 or 24 hours in severe hypoxia (P<0.001). ATP levels were also assessed and it was seen that loss of either ULK1 or ATF4 resulted in a reduction of cellular ATP (Figure 4.22E). Hence, ATF4 and ULK1 are likely important for maintaining high levels of cellular ATP in both normoxia and severe hypoxia.

Finally, the mechanism of cell death was investigated by measuring caspase activity. Caspase 3/7 activity increased to 1.47-fold the normoxic level after exposure to severe hypoxia (P<0.001) (Figure 4.22F). As expected, knockdown of ATF4 increased caspase activity by 2.2-fold and 2.8-fold in normoxia and severe hypoxia, respectively (P<0.001 vs SCR N or SCR A, respectively). Surprisingly, ULK1 depletion decreased caspase activity to 0.8-fold and 1.2-fold in normoxia and severe hypoxia, respectively (P<0.001 vs SCR N or SCR A, respectively). Thus, despite having similar effects on cell viability, cell death due to ULK1 knockdown may occur through a nonapoptotic mechanism while that following ATF4 knockdown likely occurs through apoptosis.

These results imply that ULK1 is necessary for cell function and homeostasis in A431 cancer cells not only in the stressful condition of severe hypoxia, but also in normoxia. This effect differs from results in untransformed cells. For example, ULK1-/- mice are viable, and hepatocytes or fibroblasts from such mice are fully viable until put in stressful conditions (Egan et al., 2011). Thus, it may be that the oncogenic mutations that lead to an aggressive cancer cell phenotype put these same cells in a state of perpetual stress, resulting in a sort of "autophagy addiction". Indeed, as this work was in progress, two articles were published demonstrating that autophagy is required for maintaining oxidative metabolism and cell survival in H-Ras expressing and pancreatic tumours, both *in vitro* and *in vivo* (Guo et al., 2011; Yang et al., 2011).

4.2.14 Loss of ULK1 enhances cell death due to ER stress

To assess the importance of ULK1 in the survival of ER stress in normoxia, cell death was measured in ULK1 knockdown cells treated with tunicamycin or thapsigargin. In agreement with the results in severe hypoxia, loss of ULK1 caused cell death in both untreated and drug treated cells (Figure 4.23). Additionally, it appears the combined treatment of tunicamycin and ULK1 knockdown may have a greater than additive effect, implying that ULK1 might have a specific role in the removal of aggregates of unfolded proteins accumulating due to blockade of N-linked glycosylation.

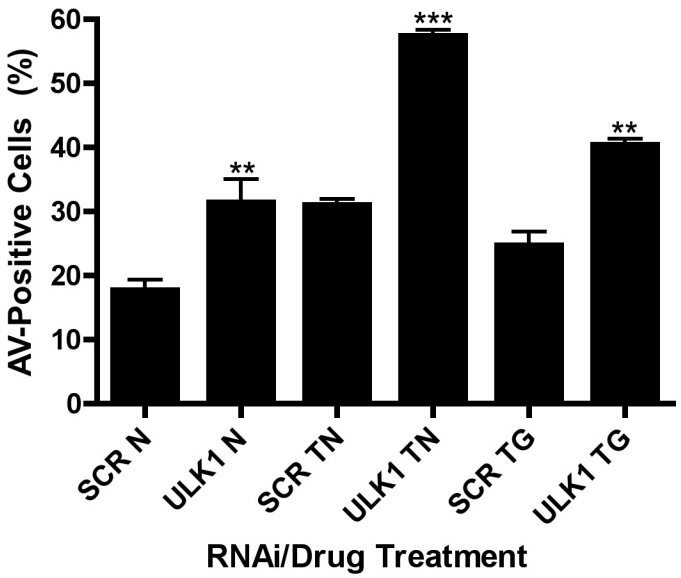

Figure 4.23 Treatment of A431 cells with ULK1 siRNA increases the population of annexin V-positive cells following treatment with thapsigargin or tunicamycin for 24 hours.

*A431 cells were transfected with siRNA against ULK1, ATF4, or a scrambled control sequence (SCR) overnight. The next day, cells were exposed to 5μg/mL tunicamycin (TN) or 300nM thapsigargin (TG). After 24 hours, cells were stained with annexinV-AlexaFluor647 and analyzed by flow cytometry. The result of one experiment with at least N=3 replicates is shown, representative of N=2 independent experiments. **, and *** indicate P<0.01 and P<0.001, respectively, by one-way ANOVA for ULK1 vs SCR in same treatment group.*

4.2.15 Knockdown of ULK1 or ATF4 dramatically reduces spheroid growth

Having established that ablation of ULK1 or ATF4 reduces cell viability in normoxia or severe hypoxia simulated by an anaerobic incubator, the author next assessed the effect of ULK1 or ATF4 knockdown on growth in a three-dimensional spheroid model. A431 cells were transfected with siRNA sequences specific for ULK1 or ATF4, or a scrambled control and then reseeded to 96-well format for the

formation of spheroids, as described previously (Ivascu and Kubbies, 2006). Knockdown of ULK1 or ATF4 reduced spheroid growth (Figure 4.24). No increase in size in the ULK1 or ATF4-deficient spheroids was observed until more than four days post-transfection. Importantly, previous analysis by RT-qPCR has shown gene silencing of ULK1 using these sequences to last at least three days. As such, it is likely that the observed recovery and continued spheroid growth following day four was due to exhaustion of cellular siRNA levels. However, to further validate this conclusion, one would need to collect spheroids each day and analyze for RNAi-mediated knockdown of ULK1 by RT-qPCR or western blotting.

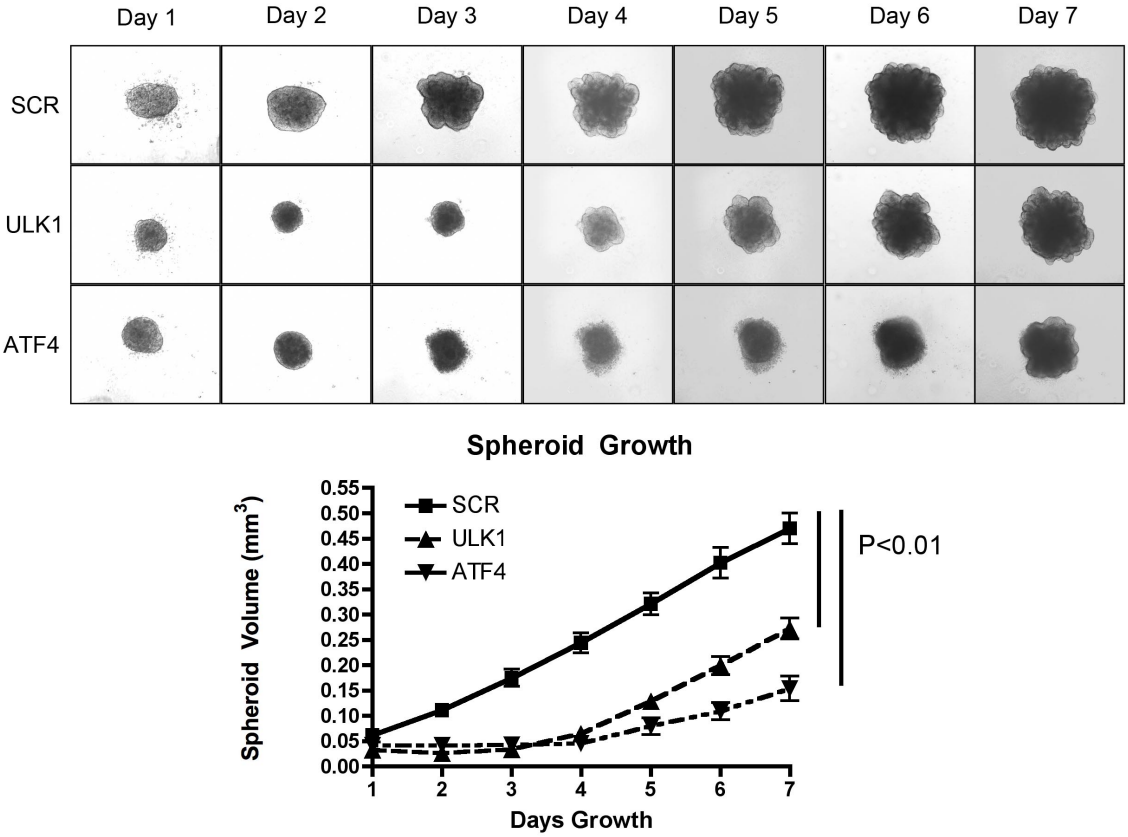

Figure 4.24 Spheroids derived from A431 cells treated with ULK1 or ATF4 siRNA a reduced growth rate.

A431 cells were transfected with siRNA sequences specific for ULK1, ATF4, or a scrambled control (SCR). The next day, cells were reseeded into round bottom 96-well plates at 5000 cells/well. After 24 hours more, spheroid-like structures formed and began to grow (DAY 1). Images were taken daily and volume measurements were

calculated with ImageJ®. Representative images from N=4 independent experiments are shown, with N=10 spheroids in each group of each experiment. Regression analysis was applied to calculate the slope of each curve and P-values were calculated by one-way ANOVA.

Cell death in the spheroids was assessed on day three by annexin-V staining. ULK1- and ATF4-depleted spheroids contained 84% and 90% dying cells, while control spheroids contained 26% dying cells ($P<0.01$) (Figure 4.25). Additionally, immunohistochemical staining for pimonidazole, CAIX, and CHOP indicated that the ULK1- and ATF4-knockdown spheroids were much less hypoxic than the SCR controls (Figure 4.26). Thus, it is likely these spheroids were unable to support a hypoxic core, were unable to grow large enough to become hypoxic due to the normoxic effects of ULK1 and ATF4 knockdown, or some combination of both.

Similarly, spheroids derived from ATF4-knockdown cells were highly positive for cleaved caspase 3, particularly in the central hypoxic regions, indicating high levels of apoptosis were taking place. The spheroids derived from the scrambled control transfection were only slightly positive for cleaved caspase 3, and these cells were located in the severely hypoxic core. In contrast, knockdown of ULK1 resulted in reduced cleaved caspase 3, a result that agrees with that seen in Figure 4.22F. It is also worthy to note that staining for Ki67, a marker that is absent from cells in G_0 of the cell cycle, was nearly the same with each treatment. Thus, the differences in spheroid volume appeared to be due to enhanced cell death rather than decreased proliferation.

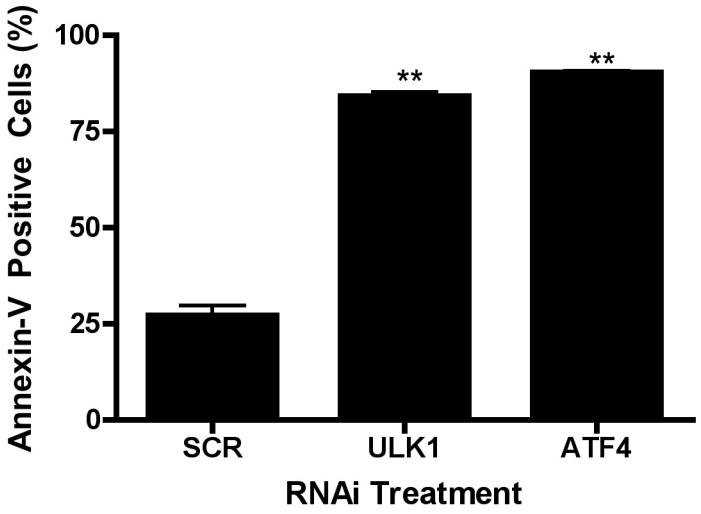

Figure 4.25 Spheroids derived from A431 cells treated with ULK1 or ATF4 siRNA show an increased population of annexin V-positive cells as measured by FACS after three days.

*Spheroids formed from ULK1-, ATF4-, or control-knockdown spheroids were harvested on day three and dissociated using Accutase®. Following staining for annexinV-AlexaFluor647, cells were analyzed by flow cytometry. N=3 groups of three or four spheroids were analyzed. ** indicates P<0.01 by one-way ANOVA for ULK1 or ATF4 vs SCR.*

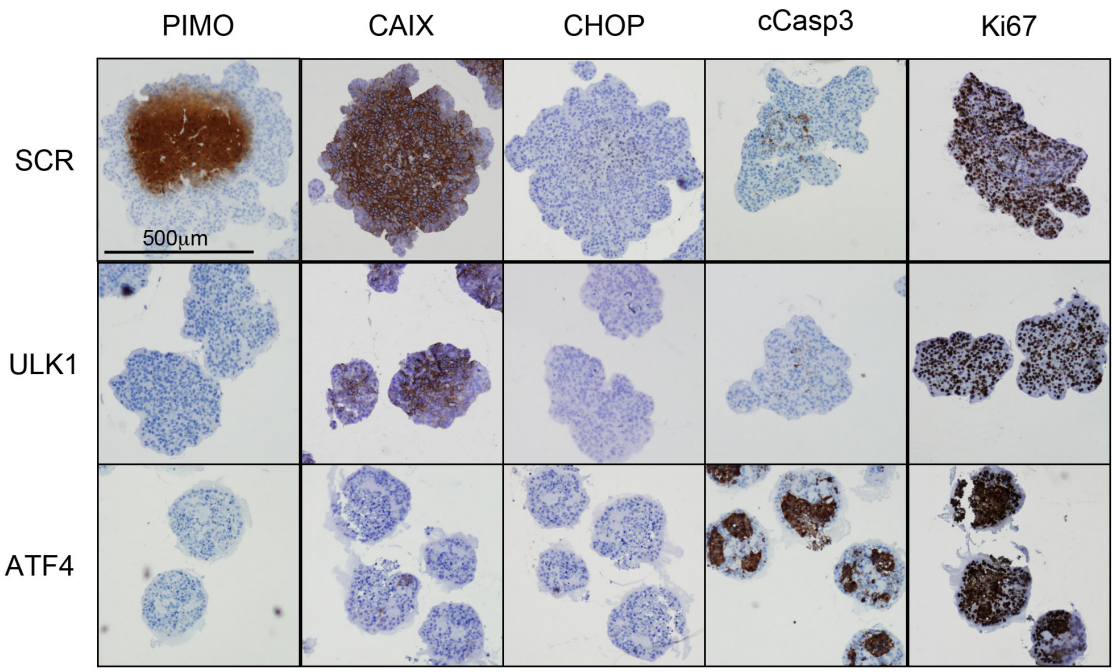

Figure 4.26 Three-day-old spheroids derived from A431 cells treated with ULK1 or ATF4 siRNA show decreased staining for pimonidazole, CAIX, and CHOP, and those derived from A431 cells treated with ATF4 siRNA show increased staining for cleaved caspase 3, as determined by immunohistochemistry.

A431 spheroids lacking ULK1 or ATF4, or controls were harvested on day three and fixed over night in formalin. Immunohistochemical analysis was done using the markers indicated. Spheroids were treated for at least four hours in pimonidazole prior to harvesting and staining with the indicated antibodies. Representative images from N=3 independent experiments are shown, with N=10 spheroids in each group of each experiment. Black scale bar indicates 500μm.

To determine if a similar effect could be observed by pharmacological inhibition of autophagy, A431 spheroids were prepared and treated with a single dose of chloroquine or bafilomycin A1. Spheroids treated in this way showed a significant though less complete growth delay, confirming the results obtained from ULK1 knockdown (Figure 4.27). The rebound in growth following day four is likely due

to partial exhaustion of the drug in the media and upregulation of intracellular drug pumps.

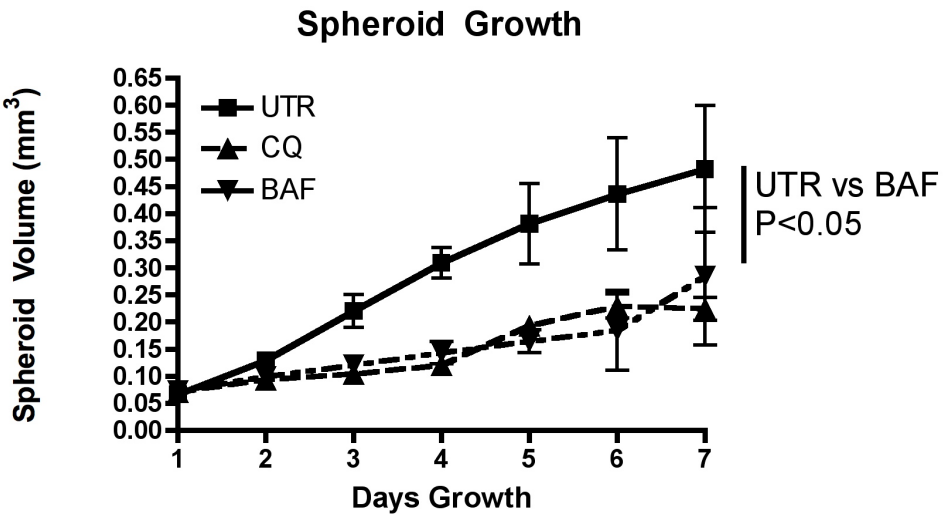

Figure 4.27 Treatment of spheroids derived from A431 cells with a single dose of chloroquine or bafilomycin at the time of seeding retards their growth.

A431 cells were seeded 5000 cells/well to a round bottom 96 well format with Matrigel®. After 24 hours, spheroid-like structures formed and began to grow (DAY 1). A single dose of 25μM chloroquine or 0.1μM bafilomycin A1 was administered to spheroids on day 1. Images were taken daily and volume measurements were calculated with ImageJ®. N=10 spheroids in each group. Regression analysis was applied to calculate the slope of each curve and P-values were calculated by one-way ANOVA.

4.2.16 ULK1 protects cells from necrotic cell death

In Figure 4.22, it was demonstrated that knockdown of ATF4 increased caspase 3/7 activity in normoxia and hypoxia, while knockdown of ULK1 appeared to reduce caspase activity, despite the fact that loss of either ULK1 or ATF4 had

similar effects on overall cell viability in normoxia and severe hypoxia. This difference implies that ULK1 activity is required for caspase-dependent cell death, or apoptosis.

Apoptosis is considered to be the default form of cell death. In a series of tightly regulated steps, cells activate intracellular proteases called caspases that effect organized cellular demolition. Apoptosis is an energy-requiring, active process. Morphological hallmarks of apoptosis include nuclear condensation and plasma membrane blebbing, as the nucleus and cytoplasm are effectively "chopped up and shipped off" into apoptotic bodies for engulfment by phagocytic cells. Intracellular components are not released into the extracellular milieu. It is worth mentioning, however, that if an apoptotic cell is not engulfed by immune cells or its surrounding neighbors (as would be the case living tissue), then secondary necrosis can occur.

Necrosis, unlike apoptosis, is a passive process. Apoptosis-deficient cells can undergo necrosis following a cytotoxic insult. As opposed to apoptosis, cells fail to undergo nuclear condensation and packaging into apoptotic bodies. The plasma membrane becomes compromised in necrosis, and cells rupture, spilling intracellular components into the environment, causing inflammation. One such component is HMGB1.

HMGB1, or high mobility group box protein 1, acts as an architectural chromatin-binding factor that bends DNA and promotes protein assembly on specific DNA targets (Bustin, 1999). Necrotic cells passively release HMGB1 as the integrity of the plasma membrane fails, causing inflammation *in vivo* (Muller et al., 2001; Scaffidi et al., 2002). Thus, HMGB1 release to the media is a useful assay for measuring necrosis.

To determine if loss of ULK1 forces cancer cells to die by necrosis, A431 cells were treated with RNAi against ULK1, ATF4, or a scrambled control, and exposed to

severe hypoxia for 36 hours. The culture medium was collected and both adherent and floating cells were harvested for analysis by western blotting. The concentration of HMGB1 in the media was quantified using an ELISA kit. Severe hypoxia alone was sufficient to slightly increase the amount of HMGB1 released, though not significantly (Figure 4.28A). However, knockdown of either ULK1 or ATF4 increased the amount of HMGB1 released to the medium in normoxia (10-12ng/mL, $P<0.01$) and in severe hypoxia (almost 15ng/mL; $P<0.05$). Note that a positive control was included with the ELISA kit, shown in the figure (4.28A). However, a more appropriate control might be the use of a mild detergent (to lyse cell membranes and allow HMGB1 release).

These results were matched by western blotting for HMGB1 in the adherent and dead cells, which showed that knockdown of ULK1 or ATF4 in severe hypoxia led to loss of intracellular HMGB1 (Figure 4.28B).

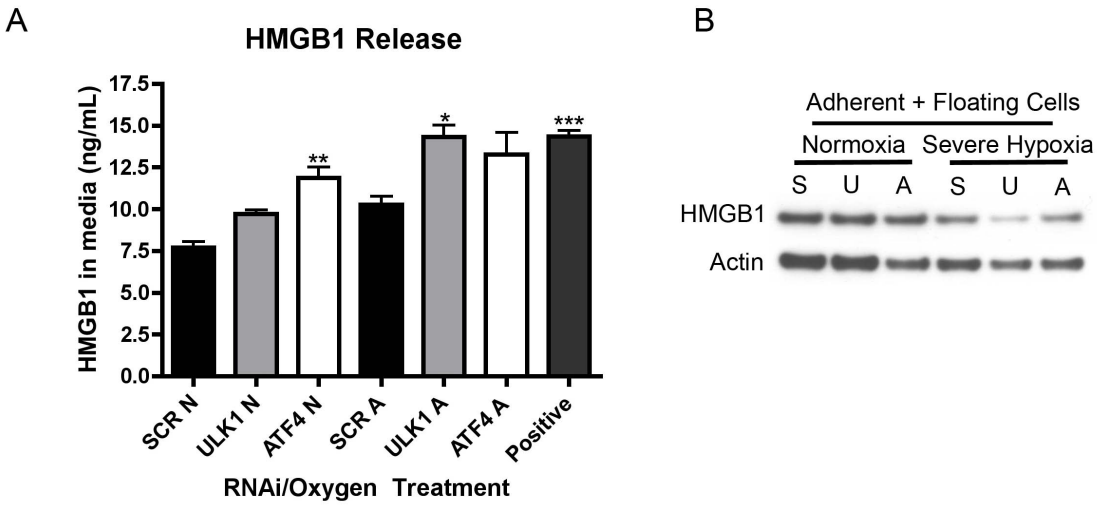

Figure 4.28 Treatment of A431 cells with ULK1 or ATF4 siRNA increases HMGB1 protein levels in the media, as measured by ELISA, and decreases HMGB1 protein levels in adherent cells, as measured by western blotting, following exposure to severe hypoxia for 36 hours.

*A431 cells were transfected with siRNA against ULK1, ATF4, or a scrambled control sequence (SCR) overnight. The next day, cells were exposed to severe hypoxia. After 36 hours, the medium was collected and analyzed by HMGB1 ELISA (A) and the floating and adherent cells were collected and analyzed by western blotting for the indicated antibodies (B). For ELISA, N=6 samples from N=3 independent experiments were analyzed. *, **, and *** indicate P<0.05, P<0.01, and P<0.001, respectively, by one-way ANOVA for ULK1 or ATF4 vs SCR in the same oxygen tension, or Positive control vs SCR N. For western blotting, representative images from N=3 independent experiments are shown.*

These results demonstrate that knockdown of either ULK1 or ATF4 in severe hypoxia results in cell permeability and spillage of intracellular components into the medium. ULK1 knockdown promoted HMGB1 release in the absence of caspase activation, implying that loss of ULK1 leads to necrotic cell death. The increased release of HMGB1 observed with loss of ATF4, on the other hand, is likely due to secondary necrosis, since this release coincides with the activation of the effector caspases 3 and 7.

Morphological evidence for this mode of cell death was observed by transmission electron microscopy (TEM). A431 cells were transfected with siRNA against ULK1 or ATF4 and exposed to severe hypoxia for 24 hours. In both normoxia and severe hypoxia, SCR and ULK1 knockdown cells showed relatively normal gross cell architecture. No nuclear condensation, cell rounding, or membrane blebbing could be observed in these cells (Figure 4.29A, top panels). In contrast, loss of ATF4 resulted in a strikingly different phenotype. These cells were rounded, and intracellular organelles appeared tightly packed and condensed (Figure 4.29A, bottom panels). Membrane blebbing was observed in some cells (denoted with B in Figure 4.29A bottom left panel). In addition, the reticular membranes appeared dysfunctional and tightly bound, as opposed to the discrete filamentous membranes seen in the control or ULK1 knockdown cells. The quantification of

this phenotype showed that the effect was enhanced in ATF4 knockdown cells exposed to severe hypoxia (Figure 4.29B). It was not apparent, however, that the nucleus had undergone condensation. Thus, this phenotype may be the early stages of apoptosis.

It is worthy of note that the magnitude of cell death observed following ATF4 knockdown shown in Figure 4.22 was significantly larger than that quantified in terms of the morphological features assessed in Figure 4.29. However, this discrepancy can be explained in two ways. First, TEM analysis was done after only 24 hours in severe hypoxia, while the FACS analysis shown in Figure 4.22 was done after 36 hours in severe hypoxia—thus, the magnitude of death due to ATF4 knockdown alone or ATF4 knockdown with severe hypoxia would be expected to be greater in the latter case. Second, the change in morphology quantified in Figure 4.29 is likely an indicator of early apoptosis and fails to account for necrotic cell death. That is, it is likely that a fraction of the ATF4-depleted cells are dying by necrosis as well as apoptosis, and thus will make up the difference in magnitude of cell death observed in Figure 4.22 (which includes both modes).

A

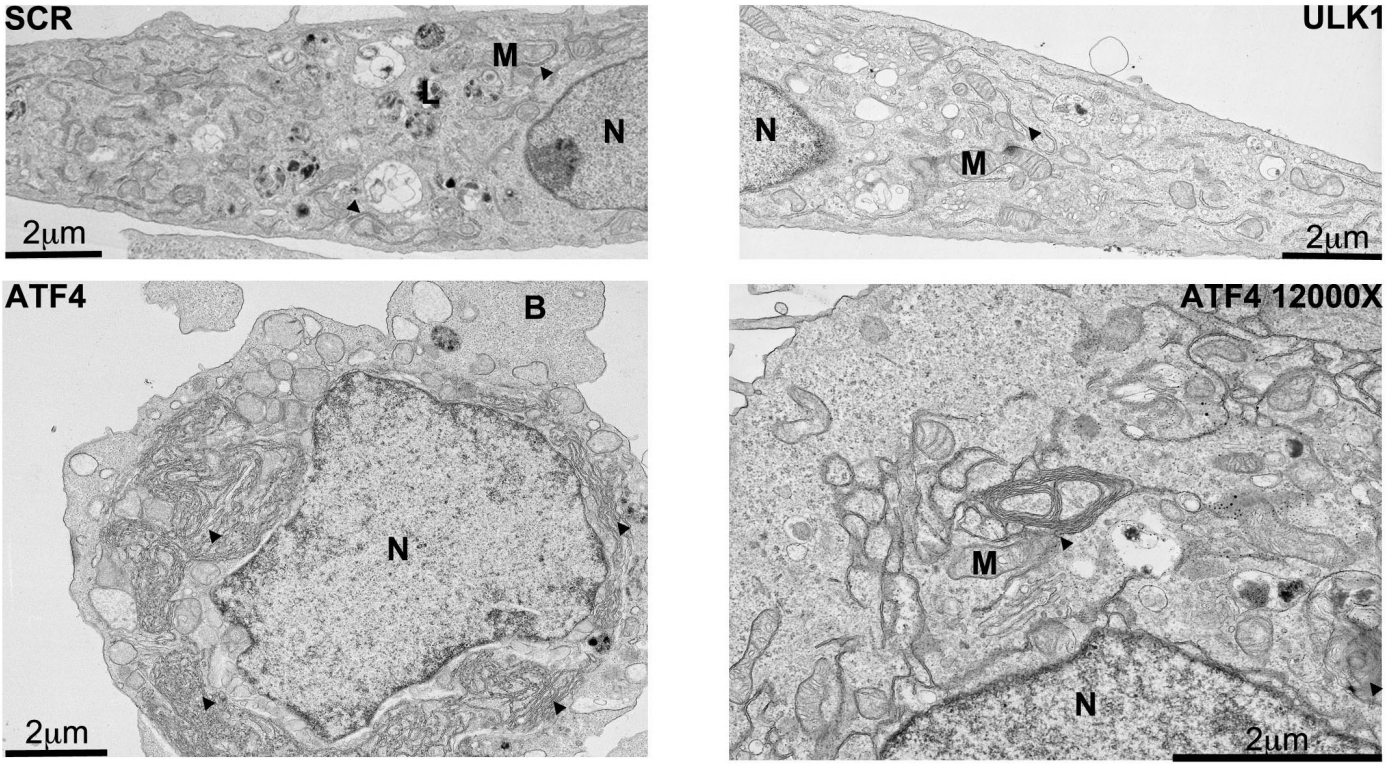
SCR
M
L
N
2μm
ULK1
N
M
2μm
ATF4
B
N
2μm
ATF4 12000X
M
N
2μm

B

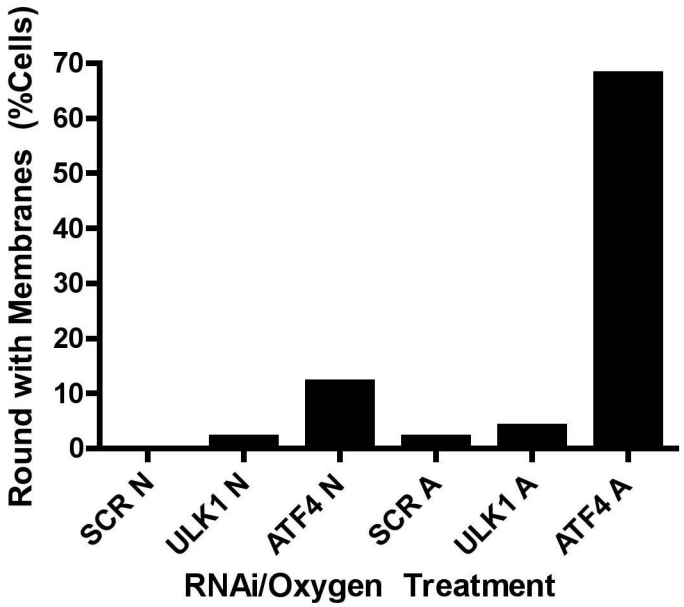
Round with Membranes (%Cells)
70
60
50
40
30
20
10
0
SCR N
ULK1 N
ATF4 N
SCR A
ULK1 A
ATF4 A
RNAi/Oxygen Treatment

Figure 4.29 Treatment of A431 cells with siRNA for ATF4 but not ULK1 increases the number of rounded cells with blebbing and organelle accumulation, as measured by TEM, following exposure to severe hypoxia for 24 hours.

A431 cells were transfected with siRNA against ULK1, ATF4, or a scrambled control sequence (SCR) overnight. The next day, cells were exposed to severe hypoxia. After 24 hours, cells were fixed and prepared for transmission electron microscopy (A). Images are labeled with N for nuclei, M for mitochondria, L for autophagosomal/lysosomal-like structures containing organelles, and with arrowheads for reticular membranes. Quantitation of the described phenotype is provided in (B). Representative images from at least N=1 independent experiments are shown, with more N=100 cells analyzed within this experiment. TEM images courtesy of Professor David Ferguson.

As mentioned in section 4.2.16, A431 spheroids derived from ATF4-depleted cells displayed high levels of cleaved caspase 3, while those derived from cells lacking ULK1 or the knockdown cells showed very little. Interestingly, when these cells were examined under higher zoom, morphological differences were also observed. When the structure of individual nuclei in the ULK1- or ATF4-knockdown spheroids were compared, it was clear that cells lacking ULK1 had intact nuclei, similar to those in the SCR controls, while those lacking ATF4 showed nuclear fragmentation, a hallmark of apoptosis (Figure 4.30).

Thus, loss of ULK1 promotes cell death and HMGB1 release in the absence of caspase activity, membrane blebbing, or nuclear fragmentation. ATF4 knockdown cells, on the other hand, showed all of these hallmarks of apoptosis. Hence, it appears that ULK1 is essential for cell death through apoptosis in this context, and that loss of ULK1 instead forces cells to undergo death by necrosis.

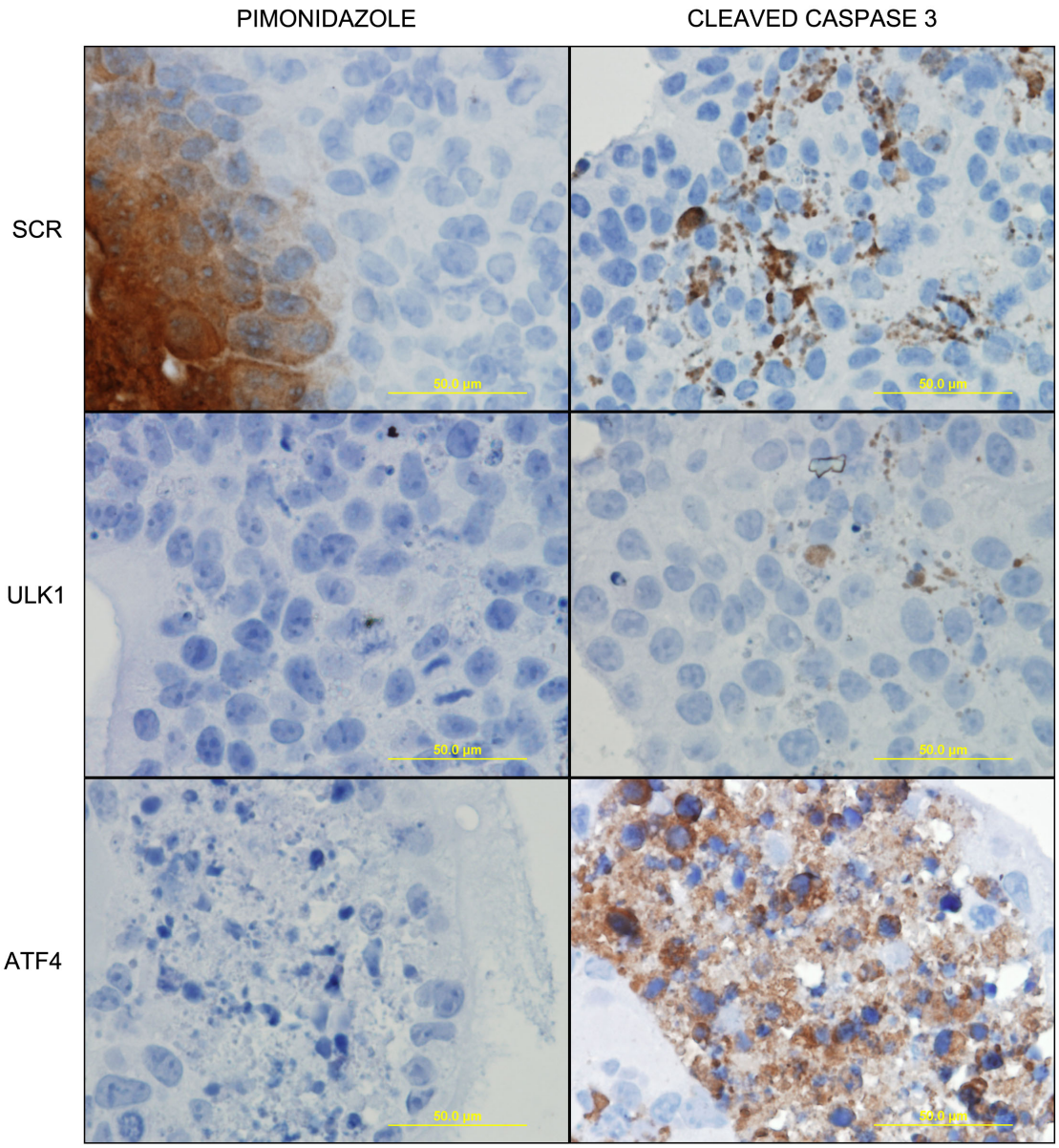

Figure 4.30 Three-day-old spheroids derived from A431 cells treated with ATF4 siRNA show increased nuclear fragmentation and caspase 3 cleavage, as measured by immunohistochemistry.

A431 spheroids lacking ULK1 or ATF4, or controls were harvested on day three and fixed over night in formalin. Immunohistochemical analysis was done using the markers indicated. Spheroids were treated for at least four hours in pimonidazole prior to harvesting. Cells were counterstained with hematoxylin. Representative images from N=3 independent experiments are shown, with N=10 spheroids in each

group of each experiment.

4.2.17 High levels of ULK1 correlate with a poor prognosis in cancer

Much recent work has focused on the role of ULK1 in mammalian autophagy, and several studies have considered the importance of autophagy in cancer cell survival *in vivo*. In the sections above, the author demonstrated that ULK1 plays an important role in cancer cell survival in normoxia, severe hypoxia, and ER stress *in vitro* and in a three dimensional model of tumour growth.

To examine the potential importance of ULK1 in cancer prognosis and treatment, the expression of ULK1 mRNA was examined in a cohort of 152 breast cancer patients. Tumour samples were obtained from retrospective series of patients with primary breast cancer who were treated in Oxford, UK, between 1990 and 1992. Patients received adjuvant chemotherapy and/or adjuvant hormone therapy, or no adjuvant treatment. This series of is part of a published series (Loi et al., 2008); and full treatment details and demographics has been previous described (Higgins et al., 2010). Total RNA was isolated from tumour samples and mRNA expression was measured using Affimetrix U133 arrays, as described previously (Loi et al., 2008). *Please note that these data were collected and analyzed by Dr. Francesca Buffa, Oxford University, and are included here for the interest of the reader.*

When the association of ULK1 mRNA with clinical and molecular covariates was analyzed, it was determined that ULK1 expression was positively associated with ERBB2/HER2 signaling (Wirapati et al., 2008) and negatively associated with an apoptosis signature (Desmedt et al., 2008) (Figure 4.31).

Association with clinical and molecular covariates:

Continuous/ordinal covariates:

Spearman Rank Test	Tumour grade	Tumour size	Proliferation	ESR11 Signalling	ERBB2Signalling	Invasion	Immune Response	Apoptosis	Hypoxia
Correlation Coefficient	0.0461	0.1278	0.1406	0.1116	0.3520	-0.0090	-0.1125	-0.2390	0.0412
Sig. (2-tailed)	0.6041	0.1166	0.0840	0.1710	0.0000	0.9124	0.1675	0.0030	0.6140
N	129	152	152	152	152	152	152	152	152

Plot of significant associations:

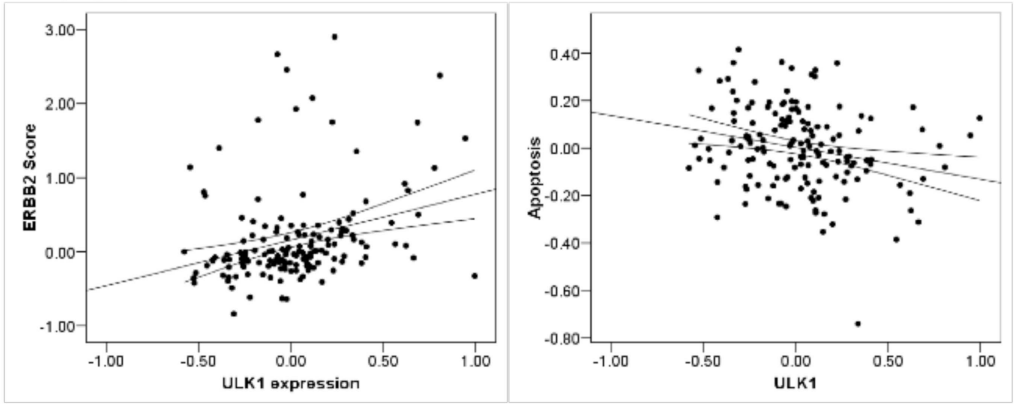

Figure 4.31 ULK1 mRNA expression is positively associated with HER2 signaling and negatively associated with an apoptosis signature in a cohort of breast cancer patients, as measured by metagene analysis.

Univariate analysis of ULK1 expression with common clinical and molecular covariates was done. Correlation coefficients and P-values are found in the table (top panel), and significant associations are highlighted in red. A plot of significiant associations is shown in the lower panel. Analyses were done by Spearman Rank correlation test and ANOVA. N=152. Courtesy of Dr. Francesca Buffa.

Strikingly, univariate analysis revealed that patients with the highest level of ULK1 mRNA had significantly lower relapse-free survival (P=0.021, N=152) (Figure 4.32).

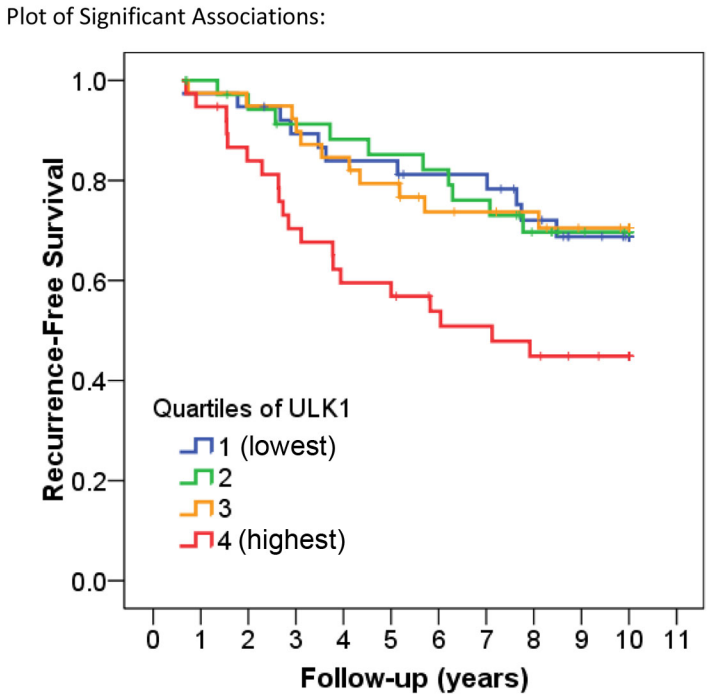

Figure 4.32 Univariate analysis shows that breast cancer patients with high ULK1 mRNA have significantly lower relapse-free survival.

ULK1 gene expression was considered and patient samples were ranked from low to high expression, normalized from 0 to 1, and divided into quartiles. Analyses were done by Spearman Rank correlation test and ANOVA. N=152. Courtesy of Dr. Francesca Buffa.

When multivariate analysis was done to include estrogen receptor status, patient age, nodal status, tumour size, and tumour grade, the association of ULK1 with reduced relapse-free survival remained (Figure 4.33) ($P<0.0335$). When ERBB2/HER2 signaling was included in the analysis, the results were similar and remained significant (data not shown). Thus, ULK1 expression is prognostic in breast cancer, independent of other clinical or molecular variables.

Multivariate analysis including ER status, patient age, Nodal status, Tumour Size and grade:

Covariates	HR	p	95.0% CI for Exp(B)	
			Lower	Upper
ULK1 expression (fractional rank)	3.5137	0.0335	1.1035	11.1882
ER positive	0.5574	0.2171	0.2204	1.4100
Age (binary)	0.8722	0.7604	0.3622	2.1004
Grade	1.2056	0.4792	0.7182	2.0236
Tumour Size	1.2439	0.0356	1.0148	1.5248
Nodes involved	0.9913	0.9088	0.8535	1.1513

Backward Likelihood Reduced model :

Covariates	HR	p	95.0% CI for Exp(B)	
			Lower	Upper
ULK1 expression (fractional rank)	3.4038	0.0358	1.0850	10.6787
ER positive	0.4683	0.0289	0.2372	0.9247
Tumour Size	1.2592	0.0106	1.0553	1.5024

Figure 4.33 Multivariate analysis indicates that elevated ULK1 mRNA expression is associated with decreased relapse-free survival independent of common clinical and molecular variables in a cohort of breast cancer patients.

ULK1 gene expression was considered and patient samples were ranked from low to high expression, normalized from 0 to 1, and divided into quartiles. Cox analysis was done and the P-values for significant associations are highlighted in red. HR indicates hazard ratio. N=152. Courtesy of Dr. F. Buffa, Oxford University.

4.3 Discussion

4.3.1 ULK1 expression is induced by severe hypoxia, ER stress, moderate hypoxia, and intratumoural hypoxia

The regulation of ULK1 activity and its function in mammalian cells is a topic of increasing interest. Literature on this topic has focused on the regulation of ULK1 activity by a series of complex post-translational phosphorylation events and protein-protein interactions. To date, no other group has conducted a detailed study of ULK1 protein and RNA expression as a means by which cells increase ULK1 activity. In this chapter, the author has demonstrated that severe hypoxia induces the expression of ULK1 mRNA in several cancer cell lines. In the A431 cell line, the expression of ULK1 protein correlated with that of ULK1 mRNA, indicating that transcriptional induction is a means by which total ULK1 kinase activity could be increased in cells.

ULK1 protein was similarly increased in A431 cells exposed to ER stress inducers, indicating that severe hypoxia may increase ULK1 expression via the integrated stress response, as was suggested from microarray analysis. Additionally, even moderate hypoxia was sufficient to promote the accumulation of ULK1 protein, despite the fact that the same condition did not result in CHOP accumulation. ULK1 was not dependent on HIF1α for its induction. The accumulation of ULK1 in moderate hypoxia might be explained by a stronger interaction of ATF4 with the ULK1 promoter site than with the CHOP promoter site (a result later confirmed by ChIP) or reduced degradation by the ubiquitin-proteasome system. Finally, when A431 cells were grown as spheroids, or when U87 cells were grown as xenografts, the intratumoural hypoxia of either environ was sufficient to cause ULK1 protein and mRNA accumulation, respectively. These results, taken as a whole, indicate that the transcriptional induction of ULK1 may be an avenue by which cancer cells

increase total ULK1 kinase activity and autophagy to survive ER stress and hypoxia.

As was the case with PUMA and NOXA in chapter three, in different cell lines the changes in ULK1 protein did not always correlate with those in its mRNA transcript. In most cases, after 48 hours in severe hypoxia, the amount of ULK1 protein decreased, despite the fact that ULK1 mRNA levels were at their highest at this time point. There are several reasons why this change may have occurred. One possibility is that despite the strong induction of ULK1 mRNA transcription, these transcripts are being inefficiently translated into proteins due to the global inhibition of mRNA translation incurred by activation of the ISR (Koumenis et al., 2002). Alternatively, ULK1 may be degraded by the proteasome, as treatment with proteasome inhibitors resulted in a partial rescue of ULK1 protein. Indeed, several publications have demonstrated that ULK1 may be actively degraded by the proteasome, and that the essential autophagy genes ATG101 and ATG13 play a protective role in ULK1 complexes (Ganley et al., 2009; Mercer et al., 2009). Moreover, autophosphorylation of ULK1 has been shown to be essential for its stability and activity (Dorsey et al., 2009). Thus, the observation that proteasome inhibition protected ULK1 from degradation but was not permissive for enhanced expression indicates that a combination of degradation and translational repression appears to be occurring.

4.3.2 Severe hypoxia increases cellular ULK1 activity

A plethora of work has been published on the post-translational mechanisms by which ULK1/ATG1 activity and autophagy are regulated (reviewed in (Mizushima, 2010)). Though the molecular details are still unsettled, it has been shown that ULK1 kinase activity is negatively regulated by mTORC1 phosphorylation and positively regulated by AMPK phosphorylation at distinct serine residues.

In A431 cells, total ULK1 activity increases in severe hypoxia, but the specific activity of the enzyme is decreased (conducted in collaboration with Dr. James Murray, Queen's University, Belfast). Hence, despite AMPK activation and mTOR inhibition, the specific activity of the ULK1 decreased in severe hypoxia in this cell line. Due to ATF4-mediated induction of ULK1 mRNA and protein, however, the total cellular activity of ULK1 increased in this context, increasing autophagic flux in severe hypoxia.

In MCF7 cells, on the other hand, both the specific and total activity of ULK1 kinase was increased by severe hypoxia, indicating that post-translational signaling is intact in this system. Transcriptional induction of ULK1 by ATF4 failed to enhance ULK1 protein expression in this context, but rather maintained high levels of ULK1 throughout the hypoxic stress.

Hence, this data demonstrates for the first time that autophagy initiation and flux can be transcriptionally and as well as post-translationally induced.

4.3.3 ULK1 is a direct target of ATF4 transcriptional activity

Many links between the ISR and autophagy have been uncovered (reviewed in (Kroemer et al., 2010)). Work from this group and others has demonstrated that ATF4 can maintain autophagic flux in severe hypoxia by transcriptionally upregulating MAP1LC3B and ATG5, two key components of the autophagy machinery (Rouschop et al., 2009b; Rzymski et al., 2010). In chapter three, the author demonstrated for the first time that ATF4 can initiate autophagy through the transcriptional induction of the BH3-only protein harakiri. In this chapter, it was demonstrated that ATF4 could also activate the transcription of the autophagy-initiating kinase ULK1 as a means of increasing ULK1 kinase activity and autophagy.

Indeed, when a specific siRNA sequence for ATF4 was used to ablate its expression and transcriptional activity, A431 cells failed to induce ULK1 mRNA or protein upon exposure to severe hypoxia, or ER stressors, and in MCF7 cells ULK1 protein was rapidly degraded. The transcription of ULK1 was found to be a consequence of direct binding by ATF4 at a CREB/ATF element in the ULK1 promoter. It was shown, furthermore, that HIF1α and HIF2α were dispensable for the accumulation of ULK1 protein in severe hypoxia. Thus, the work of this thesis has uncovered two novel mechanisms by which ATF4 can transcriptionally *initiate* autophagy in cancer cells.

4.3.4 ULK1 is essential for autophagy and mitophagy in cancer cells

Previous work has indicated that ULK1 plays an essential role in mammalian autophagy due to amino acid (Chan et al., 2007; Ganley et al., 2009; Hosokawa et al., 2009; Mercer et al., 2009; Young et al., 2006), glucose (Kim et al., 2011; Shang et al., 2011), and serum starvation (Hosokawa et al., 2009; Mercer et al., 2009; Shang et al., 2011), or in response to AMPK activation by metformin (Lee et al., 2010) or mTOR inhibition by rapamycin (Ganley et al., 2009; Hosokawa et al., 2009). Given the convincing evidence implicating ULK1 as an "essential" autophagy gene, one would expect that ULK1 is also required for autophagy in severe hypoxia.

Indeed, knockdown of ULK1 in A431 and MCF7 cells resulted in a dramatic reduction in LC3-II levels by western blotting, and much fewer LC3-positive puncta by immunocytochemistry. Additionally, it was shown that ULK1 was required for flux through the autophagy pathway, as knockdown of ULK1 reduced LC3-puncta in chloroquine treated cells measured by immunocytochemistry, and autophagolysosmes measured by Imagestream® analysis in both normoxia and severe hypoxia. These data fit with the established roles of ULK1/ATG1 in starvation conditions in promoting PAS formation at the ER (Cheong and Klionsky,

2008; Ganley et al., 2009), in enhancing the activity of the Vps34-BCN1 complex (Di Bartolomeo et al., 2010), and in the elongation of the phagophore by ATG9 cycling between the ER or late endosomes and TGN (Tang et al., 2011; Young et al., 2006).

In addition to starvation-induced macroautophagy, ULK1 has been shown to play a role in the specific autophagic degradation of mitochondria. In particular, ULK1 is crucial for the elimination of mitochondria during normal reticulocyte maturation (Kundu et al., 2008a) and for mitochondrial homeostasis in the liver (Egan et al., 2011). In agreement with these results, the work of this chapter demonstrated that ULK1 and ATF4 are important for mitophagy in A431 cancer cells in both normoxia and in severe hypoxia. Knockdown of either ULK1 or ATF4 resulted in an accumulation of mitochondria that could be detected by increased mitotracker red staining.

Furthermore, TEM analysis of cells treated with ULK1 or ATF4 RNAi showed a marked difference in the association of ER membranes with mitochondria. It is thought that the ER may be the source of the isolation membrane during autophagy initiation whereby cradle-like structures emerging from the ER can encapsulate cytoplasm to form autophagosomes (Hayashi-Nishino et al., 2009). Structures consistent with this model were observed to specifically encircle mitochondria in the control cells. However, when cells were treated with RNAi against ULK1 or ATF4, the ER seemed to associate with mitochondria laterally, rather than to encircle them. These morphological data are, unfortunately, not sufficient to rigorously identify these structures.

It is important to note that the TEM analysis of mitophagy did not consider the total number of mitochondria in each cell and, strictly speaking, is semi-quantitative at best. As such, the small differences in the number of enclosed mitochondria between normoxia and severe hypoxia are likely of little significance. It is convincing, however, that both ULK1 and ATF4 knockdown

yielded a similar increase in both mitochondria staining (by FACS) and decrease in ER-enclosed mitochondria (by TEM) in both normoxia and severe hypoxia. As such, it is clear that ULK1 and ATF4 play crucial roles in autophagy and mitophagy in cancer cells in both normoxia and severe hypoxia.

4.3.5 ULK1 and ATF4 are required for cancer cell survival in both normoxia and severe hypoxia, and in a spheroid model of tumour growth

Interestingly, in contrast to ATG7, ATG5, or BCN1 knockout mice, which die during embryogenesis or within one day of birth (Komatsu et al., 2005; Kuma et al., 2004; Yue et al., 2003), ULK1 knockout mice are viable and show no overt developmental defects (Kundu et al., 2008a). This apparent contradiction may be due to the expression of other ATG1 orthologs, such as ULK2, which can fulfill the role of ULK1 during development.

Despite its apparent redundancy during development, it has been shown that ULK1 plays an important role in the survival of starvation. ULK1 genetic knockout MEFs (ULK1-/-) stably expressing an shRNA sequence against ULK2 were viable in normal culture conditions but were sensitized to nutrient deprivation (no serum, amino acids, or glucose). The cells were almost fully rescued by reconstitution with wild type but not kinase-dead or AMPK-nonphosphorylatable ULK1 (Egan et al., 2011), indicating that ULK1 but not ULK2 is essential for the survival of nutrient deprivation. Thus, in untransformed cells it appears that ULK1 is required for the survival stress, but superfluous in the fed state.

Despite the tremendous interest in the regulation of ULK1 protein, and the growing understanding of its essential role in mammalian autophagy, the author of this thesis failed to find any work in the literature that assessed the role of ULK1 in human cancer. We demonstrated that knockdown of ULK1 was sufficient to kill 40% of A431 and cancer cells in normoxia, as measured by annexin-V positivity.

Similarly, treatment with ULK1 RNAi increased PARP cleavage, and diminished ATP levels and clonogenicity of A431 cells by more than 50%. When cells were exposed to severe hypoxia or the ER stressors thapsigargin or tunicamycin, cell death was further increased. When A431 cells were treated with siRNA against ATF4, a similar result was obtained. Spheroids produced from A431 cells deficient in ULK1 or ATF4 failed to grow for four days, and cell death was increased from 25% with control siRNA treatment to more than 80% with ULK1 or ATF4 siRNA treatment. Similar results were obtained with untransfected A431 spheroids treated with the lysosomal inhibitors chloroquine or bafilomycin A1.

Thus, contrary to the apparently dispensable role of ULK1 in growth and survival in untransformed cells in fed conditions, it appears that ULK1 is required in at least a subset of cancer cells. The observation that loss of ULK1 resulted in the death of "unstressed" cancer cells, implies that these cells depend on ULK1-driven autophagy and mitophagy for homeostasis.

It is well known that the oncogenic mutations that are essential for cancer progression are highly stressful for the transformed cell. Oncogene-induced apoptosis is well described (Harrington et al., 1994; White, 1993). Recent work indicates that H-Ras and V-Ras can increase basal autophagy in cancer cells, and that in a subset of cancers, autophagy is required for normal growth and homeostasis—so called "autophagy addiction" (Elgendy et al., 2011; Guo et al., 2011). There is even more profound evidence that pancreatic cancer cells also require autophagy for cell growth and homeostasis (Yang et al., 2011). Thus, in rapidly dividing cancers, it is likely that autophagy plays a key role in maintaining viable mitochondria and energetic homeostasis. The work shown in this chapter therefore highlights this phenomenon further, and demonstrates for the first time that specific targeting of the essential autophagy gene ULK1 not only slows the growth of cancer cells but also kills them outright. Thus, targeting of the ULK1 kinase is a potentially fruitful strategy for cancer therapy.

4.3.6 ULK1 protects cells from necrotic cell death

It is commonly accepted that in most cellular contexts autophagy serves to protect cells from nutrient deprivation and hypoxia. However, a number of workers have reported instances of cell death by autophagy. These reports need sometimes be questioned, however, as autophagy is activated by many of the same stressors that activate apoptosis, and thus many examples of "autophagic cell death" may in fact be cell death with autophagic features (Kroemer and Levine, 2008). Nonetheless, there is significant interplay between the pathways of autophagy and apoptosis. For example, the antiapoptotic BCL2 family proteins BCL2, BCL-X_L, and MCL-1 inhibit both apoptosis and autophagy. Recent work has also indicated that essential autophagy genes such as BCN1 may be specifically cleaved by activated caspases during apoptosis, providing a negative feedback loop to block autophagy.

The emerging picture portrays autophagy primarily as a protective mechanism (Kroemer et al., 2010; Levine and Kroemer, 2008; Mizushima et al., 2008; White et al., 2010). When nutrients are limited or when dysfunctional organelles or protein aggregates accumulate, autophagy is activated to generate additional nutrients and destroy these afflictions. However, excessive activation of autophagy may result in the elimination of organelles and proteins that are critical for survival, thereby activating cell death (Azad et al., 2008; Chen et al., 2008; Elgendy et al., 2011; Lenardo et al., 2009; Park et al., 2009; Shimizu et al., 2010; Yu et al., 2004; Yu et al., 2006b). Numerous studies have identified apoptosis as the "default" mode of cell death. When apoptosis fails to be activated, such as in the case when ATP levels drop precariously low or when essential apoptosis genes are inactivated, then cell death occurs by the passive process of necrosis. Reports have demonstrated that inhibition of autophagy in apoptosis-deficient cells causes necrotic cell death *in vivo* (Degenhardt et al., 2006). Interestingly, there is also some evidence to support a role of autophagy in promoting apoptosis. Apoptosis

due to the ectopic expression of PUMA and BAX, for example, is blocked by the depletion of essential autophagy genes ATG5, ATG7, or ATG10 (Yee et al., 2009).

In this chapter, the author demonstrated that ULK1 was required for survival in both normoxia and severe hypoxia, and that loss of ULK1 resulted in necrotic cell death rather than apoptotic cell death. By contrast, loss of ATF4, which was also required for survival, resulted in an apoptotic mode of cell death. Thus, it may be that loss of ULK1 results in a near-complete abrogation of autophagy, while loss of ATF4 reduces autophagy and other UPR survival pathways, but is not complete. In the rapidly dividing A431 cells, the near complete loss of autophagy may thus result in a reduction of cellular ATP levels, and prevent the activation of the effector caspases, leading to a necrotic cell death phenotype. Loss of ATF4, on the other hand, reduces autophagy and other cell survival mechanisms to a critical point of no return, but still affords enough autophagic activity to promote the activation of the apoptotic pathway.

4.3.7 ULK1 expression is associated with poor relapse-free survival and HER2 signaling in breast cancer patients

When the level of ULK1 mRNA in clinical samples from breast cancer patients was analyzed, an association between ULK1 and reduced relapse-free survival was found. Furthermore, ULK1 expression was found to be strongly associated with HER2 signaling and anticorrelated with apoptotic signaling. These results imply that ULK1 may be upregulated in breast cancer as a mode of cell survival and tumour progression. Tumours with high ULK1 had reduced apoptotic signaling, which indicates that ULK1 may be protecting tumour cells from death *in vivo*. Furthermore, ULK1 was highly upregulated in tumours with high HER2 signaling, indicating that HER2-positive cells may depend on ULK1 for survival similarly to H-Ras tumour cells or pancreatic tumour cells require ATG5 and autophagy for growth *in vivo* (Guo et al., 2011; Yang et al., 2011). In fact, it has previously been

reported that Herceptin®-resistant cells depend on elevated autophagy for growth and survival (Vazquez-Martin et al., 2009). Thus, it is tantalizing to speculate that ULK1 inhibition could selectively kill HER2-positive breast cancer cells. A collaboration with Dr. Dean Singleton has been established to investigate the potential efficacy of targeting ULK1 in mouse xenograft models using inducible shRNA systems.

4.4 Summary and Conclusions

The integrated stress response is a well-known mediator of cell survival in stressful conditions. Recent work has described a role for the ISR in upregulating the autophagic machinery MAP1LC3B and ATG5 through the transcription factor ATF4 (Rouschop et al., 2009b; Rzymski et al., 2010). The work of this chapter uncovered an exciting new link between the ISR and autophagy: namely, that ATF4 can increase autophagy by direct transcriptional activation of the essential autophagy gene, ULK1. Loss of ULK1 blocked autophagy and mitophagy in both normoxia and severe hypoxia. Furthermore, the activity of ULK1 was shown to be crucial not only for the survival of cancer cells in the stressful condition of severe hypoxia, but also under normal growth conditions. The analysis of clinical samples demonstrated that ULK1 expression is associated with reduced relapse-free survival and HER2 signaling in breast cancer patients. Thus, ULK1 is a potential target for cancer therapy (Figure 4.34).

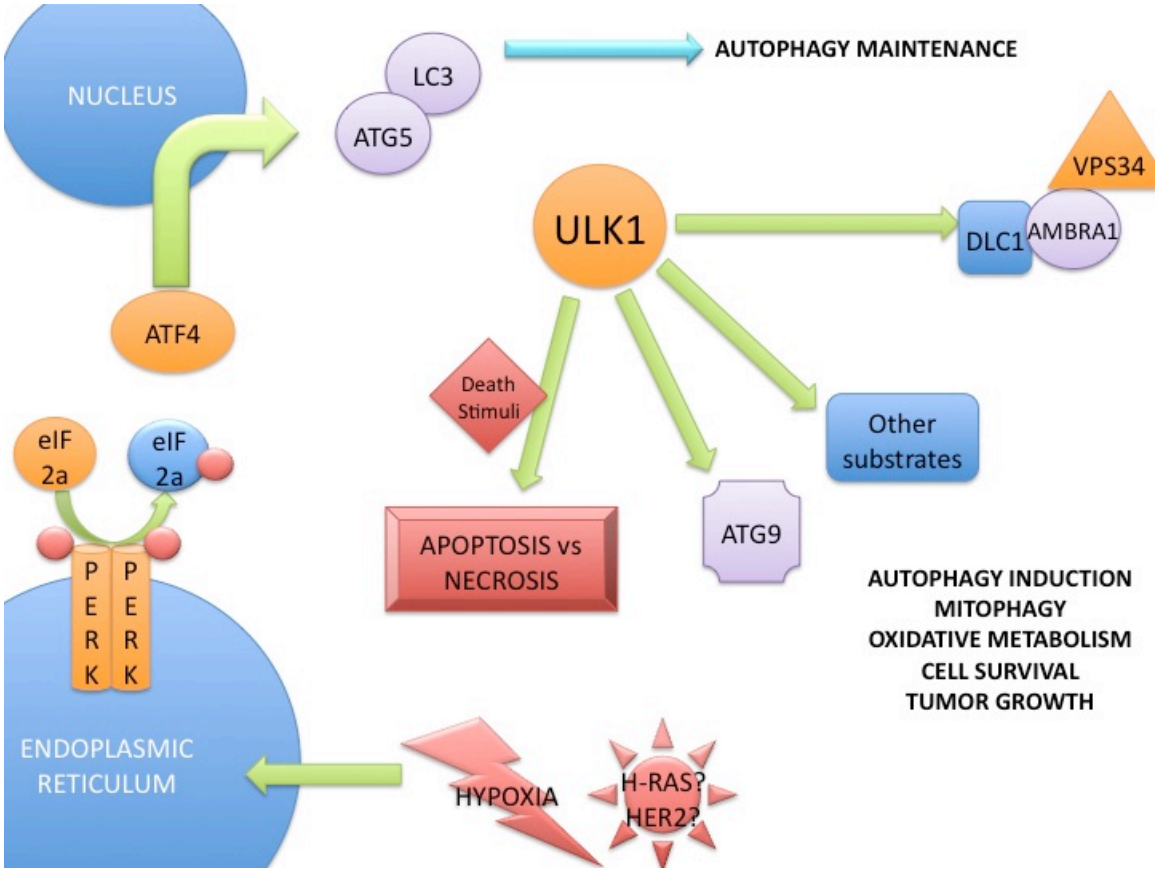

Figure 4.34 ATF4 drives cancer cell survival and autophagy through transcriptional upregulation of UNC51-like kinase 1.

Chapter 5 Thesis summary and conclusions

5.1 ATF4 regulates a program of BH3-only protein expression in response to severe hypoxia

Cancer cells survive the harsh oxygen and nutrient deprivation of the tumour microenvironment through the selection of apoptosis-resistant and glycolytic clones, and the activation of cellular adaptive mechanisms in those clones (Cairns et al., 2011; Graeber et al., 1996). In particular, the integrated stress response has been shown to be pivotal in cancer cell survival *in vivo* and the resistance of cancer cells to therapy (Harding et al., 2003). In recent years, it has become more and more apparent that increased autophagy is one mechanism by which the ISR can confer resistance to stress (Kroemer et al., 2010).

In chapter three, the author demonstrated that the ISR transcription factor ATF4 regulates a program of BH3-only protein expression in response to severe hypoxia. ATF4 transcriptionally activates the expression of HRK, PUMA, and NOXA in severe hypoxia. Others have demonstrated that ATF4-mediated PUMA and NOXA induction can result in apoptotic cell death (Galehdar et al., 2010; Ishihara et al., 2007; Wang et al., 2009). In this chapter, the author demonstrated that the poorly described BH3-only protein HRK is a direct target of transcriptional activation by ATF4, and that HRK induces autophagy in severe hypoxia. Previous work from this lab and others has shown that ATF4 upregulates the expression of the autophagy machinery to maintain high levels of autophagic flux in severe hypoxia, but failed to establish a direct link between ATF4 and the induction of autophagy (Rouschop et al., 2009b; Rzymski et al., 2010).

In contrast to the previously described role of HRK in apoptosis, this thesis has demonstrated that HRK can play a pro-survival role in the context of breast cancer cells. Thus, this work expands our understanding of the integrated stress response and of hypoxia-induced autophagy, and provides the first evidence that the integrated stress response can transcriptionally trigger the autophagy process.

5.2 ATF4 drives cell survival and autophagy through transcriptional upregulation of UNC51-like kinase 1

The ULK1 kinase has been identified as an essential mediator of autophagy in mammals (Kuroyanagi et al., 1998; Yan et al., 1998). In recent years, ULK1 has attracted great interest; a body of work is quickly forming which demonstrates that ULK1 plays a pivotal role in several aspects of autophagy initiation and progression, as well as selective mitophagy processes (reviewed in (Mizushima, 2010)). To date, no group has described the transcriptional regulation of ULK1 or its role in the survival of cancer cells.

The work presented in chapter four substantially expanded upon the literature. In this chapter, the author demonstrated that the expression of ULK1 in cancer cells is transcriptionally regulated by ATF4. The author went on to identify ULK1 as a crucial regulator of autophagy and mitophagy in both normoxia and severe hypoxia. Furthermore, it was shown that ULK1 plays a pivotal role in cancer cell survival not only in severe hypoxia, but also in normoxia, and that human breast cancer patients with high levels of ULK1 relapsed earlier than those with low levels of ULK1. The author has thus revealed a new mechanism of autophagy regulation and cancer cell survival.

5.3 Working model of ISR regulation of autophagy

A working model of ISR regulation of autophagy is presented in Figure 5.1 below. The author has demonstrated that severe hypoxia activates ATF4, which in turn upregulates the expression of the BH3-only proteins HRK, PUMA, and NOXA and the essential kinase ULK1. Previous work has shown that ATF4 drives the expression of MAP1LC3B and ATG5 in severe hypoxia to maintain high levels of autophagic flux (Rouschop et al., 2009b; Rzymski et al., 2010). HRK is likely to bind to and inhibit the repressive activity of BCL2 or BCL-X_L on BCN1 (Inohara et al., 1997; Maiuri et al., 2007), permitting greater Vps34 PI3K activity and the induction of autophagy. PUMA and NOXA have been shown to play a similar role in autophagy induction (Elgendy et al., 2011; Yee et al., 2009). Alternatively, IRE1-mediated JNK activation can induce autophagy via BCN1 in ER stress (Park et al., 2009; Shimizu et al., 2010). It is known that the ULK1 kinase can phosphorylate DLC1 to free AMBRA1 from the dynein motor complex (Fimia et al., 2010), allowing it to colocalize with BCN1/Vps34 complexes at the ER and induce autophagy. In addition, ULK1 is essential for ATG9 cycling between the ER and TGN (Young et al., 2006), permitting phagophore elongation. It is likely, furthermore, that the ULK1 kinase phosphorylates other as yet unknown substrates to initiate or maintain autophagy (Deminoff and Herman, 2007). Thus, ATF4 activates the transcription of a complex program of BH3-only proteins, kinases, and structural proteins that can both initiate and maintain high levels of autophagy in cancer cells. The work of this thesis and that of other groups has demonstrated that cancer cells rely on autophagy to survive environmental stress, and to grow through the oncogenic mutations that make them so dangerous (Degenhardt et al., 2006; Guo et al., 2011; Mathew and White, 2011; Rabinowitz and White, 2011; Rouschop et al., 2009b; Rzymski et al., 2010; Rzymski et al., 2009; White et al., 2010).

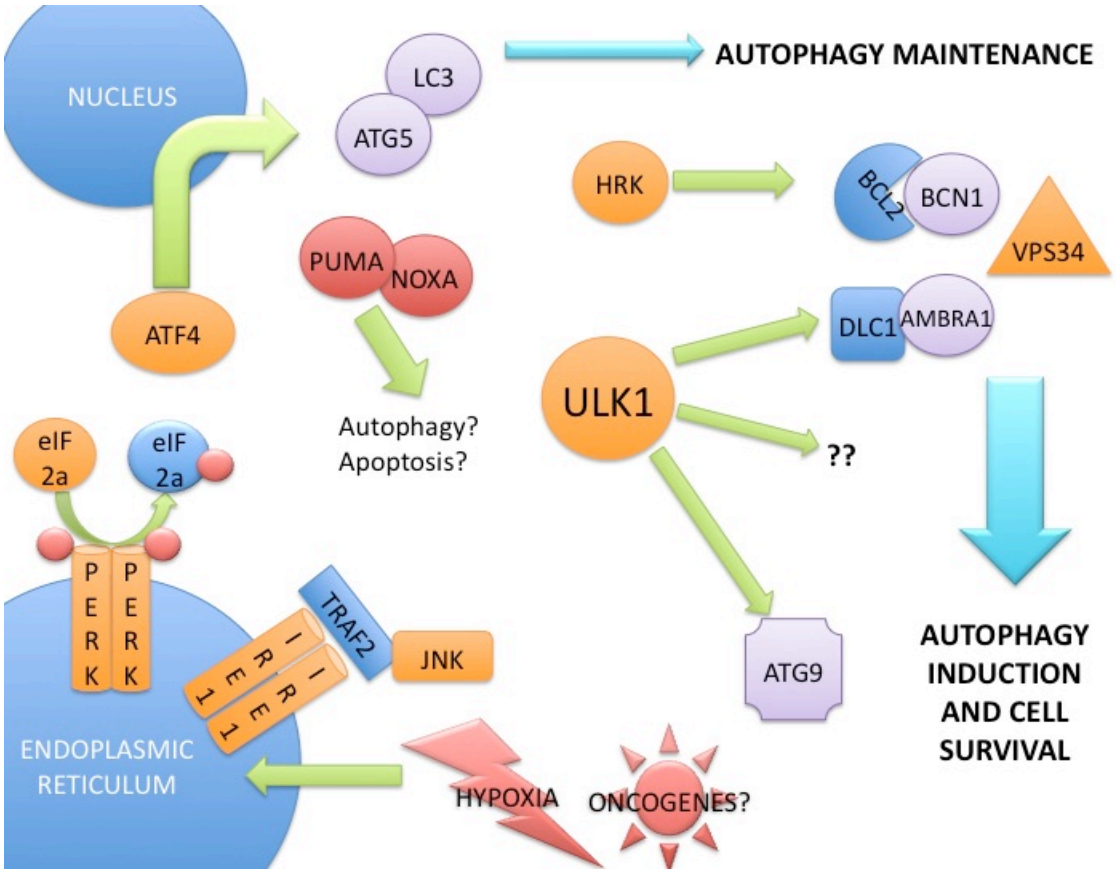

Figure 5.1 Proposed model for ISR regulation of autophagy.

5.4 Clinical implications

As is clear from the work of this thesis and the literature discussed herein, autophagy is an exceptionally complex pathway with broad and dramatic influence over many core cellular processes and disease pathologies. Autophagy plays two apparently opposing roles in human cancer. The first of these roles is the suppression of tumourigenesis. Mice with reduced expression of BCN1, for example, develop spontaneous tumours (Aita et al., 1999; Liang et al., 1999; Qu et al., 2003). Autophagy defects lead to the accumulation of ubiquitinated proteins and abnormal mitochondria in tissues, which are linked to increased production of reactive oxygen species, DNA damage, and necrotic cell death that causes chronic inflammation, leading in turn to enhanced tumour progression *in vivo*

(Degenhardt et al., 2006; Komatsu et al., 2007; Komatsu et al., 2005; Kongara et al., 2010; Mathew et al., 2009; Mathew et al., 2007; Rouschop et al., 2009a).

On the other hand, autophagy seems to be essential for the continued growth and survival of established tumours (Degenhardt et al., 2006; Rouschop et al., 2009b), and recent work has demonstrated that the oncogenic changes that make cancer cells so promiscuous and unrelenting may cause them to become dependent upon autophagy for normal growth and survival—so-called "autophagy addiction" (Guo et al., 2011; Yang et al., 2011).

Many of the treatment regimens applied to kill cancer cells also activate autophagy. In many cases, it appears that autophagy may be a mode by which cancer cells can survive cytotoxic assaults of chemotherapy or radiation. As such, targeted therapy against autophagy in combination with conventional radiation, chemotherapy, or other targeted agents is an exciting new avenue of clinical cancer research. For example, a phase three trial in glioblastoma patients treated with radiation and carmustine demonstrated that the administration of daily chloroquine increased the median survival from 11 to 24 months, though the power of this study was insufficient to yield a significant difference in survival (Sotelo et al., 2006). Preclinical models have demonstrated that autophagy inhibition can improve the efficacy of a variety of anticancer agents (Amaravadi et al., 2007; Carew et al., 2007; Katayama et al., 2007).

Molecular studies have informed rational therapeutic approaches to cancer treatment. In mouse models, for example, mTOR inhibitors failed to produce any clinical benefit in many cancers, largely due to concomitant activation of upstream PI3K signaling and downstream autophagy. However, while dual inhibition of PI3K and mTOR yielded a largely cytostatic response, the addition of chloroquine to the treatment regime resulted in complete tumour regression (Degtyarev et al., 2008). It will be interesting to see if the anti-tumourigenic effects of metformin

can be enhanced by inhibition of AMPK-ULK1-induced autophagy (Ben Sahra et al., 2010; Egan et al., 2011; Iliopoulos et al., 2011; Sahra et al., 2010).

In a similar vein, recent clinical trials to investigate anti-angiogenic agents have failed. Phase three trial results indicate that the administration of bevacizumab or sunitinib to breast cancer patients in combination with standard chemotherapy results an increased overall survival of one to two months in many cases (Lord and Harris, 2011). One mode of resistance is thought to exist via the hypoxic activation of adaptive pathways, such as the integrated stress response and autophagy. Thus, combinatorial therapy of anti-angiogenic agents and autophagy inhibitors may be beneficial.

Likewise, proteasome inhibition as a mode of cancer therapy is an area of intense research. The ubiquitin proteasome system (UPS) forms the major pathway for the degradation of short-lived and soluble proteins. Autophagy, on the other hand, mediates degradation of long-lived and membrane-bound proteins, in addition to large protein aggregates. Recent work from this laboratory has demonstrated that proteasome inhibition with bortezomib causes activation of the integrated stress response and resistance through autophagy. RNAi-mediated ablation of ATF4 or of the essential autophagy genes MAP1LC3B or BCN1 resulted in enhanced cell death with bortezomib treatment (Milani et al., 2009). Intriguingly, this effect seems to be enhanced in cancer cells, perhaps reflecting a higher metabolic rate and stress status in cancer relative to normal cells (Ding et al., 2009).

In this thesis, the author demonstrated that the hypoxic induction of autophagy is mediated in part by the BH3-only protein HRK. Preclinical studies indicate that oral administration of the BAD-mimetics ABT737 and ABT263 result in complete tumour regression by activating apoptosis (Tse et al., 2008), and clinical trials are ongoing. However, it remains to be seen whether BH3-mediated activation of autophagy will cause resistance in a subset of these patients (Maiuri et al., 2007). In the final sections of this work, a connection was revealed between ULK1 and

HER2 status in breast cancer patients, implying that ULK1 may be involved in surviving the stress of constitutive HER2 activation. Intriguingly, elevated autophagy has also been linked to Herceptin® resistance (Vazquez-Martin et al., 2009). Assessing the role of ULK1 in HER2-positive breast cancer will thus be an important avenue of investigation.

Clinical trials designed to test the effect of autophagy inhibition in combination with standard therapies are still ongoing. There are more than twenty trials underway which use hydroxychloroquine as a single agent for therapy or in combination with radiation therapy, standard chemotherapeutic agents, mTOR inhibitors, the VEGF inhibitor bevacizumab, the proteasome inhibitor bortezomib, or other targeted therapeutics (www.clinicaltrials.gov).

Hydroxychloroquine represents the first generation of autophagy inhibitors. Like bafilomycin or other chloroquine derivatives, it disrupts the vacuolar H^+ ATPase responsible for acidifying lysosomes, thereby blocking autophagy in its final step (Gonzalez-Polo et al., 2005; Marceau et al., 2009; Poole and Ohkuma, 1981). Unfortunately, chloroquine and even the more tolerable derivative hydroxychloroqine have several effects unrelated to lysosomal inhibition (can inhibit MDR proteins, for example) (Henry et al., 2006). Hydroxychloroquine also has a long half-life, meaning weeks of dosing are required to achieve efficacious concentrations *in vivo*. Furthermore, its low potency requires the use of micromolar concentrations (Carmichael et al., 2003). A more specific, potent, and well-tolerated inhibitor of autophagy is needed.

The latter work of this thesis demonstrated the potential efficacy of targeting UNC51-like kinase 1 as a mode of cancer therapy *in vitro*. The current literature and the data shown here indicate that a specific inhibitor against ULK1 or a pan-ULK inhibitor that also targets ULK2 (and possibly ULK3, ULK4, and FUSED)

should effectively block autophagy, and induce death in cancer cells that depend on autophagy for survival.

A PubMed search yields more than 3225 articles published on the topic of autophagy. The mechanistic details of this essential cellular process are becoming better understood by the day. It is clear that in some contexts autophagy plays a crucial role in the survival of cancer cells; however, in other contexts, it appears that autophagy may be an active player in cell death. The future of autophagy inhibition as a mode of cancer therapy will depend on the development of potent and specific inhibitors of ULK1 or other essential autophagy genes. More importantly, however, the efficacy of autophagy inhibition as a mode of therapy will require the appropriate identification of those stressors, mutations, or therapies that prompt cancer cells to rely on autophagy as a survival mechanism.

References

Adachi, Y., Yamamoto, K., Okada, T., Yoshida, H., Harada, A., and Mori, K. (2008). ATF6 is a transcription factor specializing in the regulation of quality control proteins in the endoplasmic reticulum. Cell Struct Funct *33*, 75-89.

Aita, V.M., Liang, X.H., Murty, V.V., Pincus, D.L., Yu, W., Cayanis, E., Kalachikov, S., Gilliam, T.C., and Levine, B. (1999). Cloning and genomic organization of beclin 1, a candidate tumor suppressor gene on chromosome 17q21. Genomics *59*, 59-65.

Alves, N.L., Derks, I.A., Berk, E., Spijker, R., van Lier, R.A., and Eldering, E. (2006). The Noxa/Mcl-1 axis regulates susceptibility to apoptosis under glucose limitation in dividing T cells. Immunity *24*, 703-716.

Amaravadi, R.K., Yu, D., Lum, J.J., Bui, T., Christophorou, M.A., Evan, G.I., Thomas-Tikhonenko, A., and Thompson, C.B. (2007). Autophagy inhibition enhances therapy-induced apoptosis in a Myc-induced model of lymphoma. J Clin Invest *117*, 326-336.

Ameri, K., Lewis, C.E., Raida, M., Sowter, H., Hai, T., and Harris, A.L. (2004). Anoxic induction of ATF-4 through HIF-1-independent pathways of protein stabilization in human cancer cells. Blood *103*, 1876-1882.

Aoki, S., Su, Q., Li, H., Nishikawa, K., Ayukawa, K., Hara, Y., Namikawa, K., Kiryu-Seo, S., Kiyama, H., and Wada, K. (2002). Identification of an axotomy-induced glycosylated protein, AIGP1, possibly involved in cell death triggered by endoplasmic reticulum-Golgi stress. J Neurosci *22*, 10751-10760.

Armstrong, J.L., Corazzari, M., Martin, S., Pagliarini, V., Falasca, L., Hill, D.S., Ellis, N., Al Sabah, S., Redfern, C.P., Fimia, G.M.*, et al.* (2011). Oncogenic B-RAF signalling in melanoma impairs the therapeutic advantage of autophagy inhibition. Clin Cancer Res *17*, 2216-2226.

Armstrong, J.L., Flockhart, R., Veal, G.J., Lovat, P.E., and Redfern, C.P. (2009). Regulation of endoplasmic reticulum stress-induced cell death by ATF4 in neuroectodermal tumor cells. J Biol Chem *285*, 6091-6100.

Armstrong, J.L., Flockhart, R., Veal, G.J., Lovat, P.E., and Redfern, C.P. (2010). Regulation of endoplasmic reticulum stress-induced cell death by ATF4 in neuroectodermal tumor cells. J Biol Chem *285*, 6091-6100.

Axe, E.L., Walker, S.A., Manifava, M., Chandra, P., Roderick, H.L., Habermann, A., Griffiths, G., and Ktistakis, N.T. (2008). Autophagosome formation from membrane compartments enriched in phosphatidylinositol 3-phosphate and dynamically connected to the endoplasmic reticulum. J Cell Biol *182*, 685-701.

Azad, M.B., Chen, Y., Henson, E.S., Cizeau, J., McMillan-Ward, E., Israels, S.J., and Gibson, S.B. (2008). Hypoxia induces autophagic cell death in apoptosis-competent cells through a mechanism involving BNIP3. Autophagy *4*, 195-204.

Azuma, C., Raleigh, J.A., and Thrall, D.E. (1997). Longevity of pimonidazole adducts in spontaneous canine tumors as an estimate of hypoxic cell lifetime. Radiat Res *148*, 35-42.

Baou, M., Kohlhaas, S.L., Butterworth, M., Vogler, M., Dinsdale, D., Walewska, R., Majid, A., Eldering, E., Dyer, M.J., and Cohen, G.M. (2010). Role of NOXA and its ubiquitination in proteasome inhibitor-induced apoptosis in chronic lymphocytic leukemia cells. Haematologica *95*, 1510-1518.

Behrends, C., Sowa, M.E., Gygi, S.P., and Harper, J.W. (2010). Network organization of the human autophagy system. Nature *466*, 68-76.

Ben Sahra, I., Laurent, K., Giuliano, S., Larbret, F., Ponzio, G., Gounon, P., Le Marchand-Brustel, Y., Giorgetti-Peraldi, S., Cormont, M., Bertolotto, C.*, et al.* (2010). Targeting cancer cell metabolism: the combination of metformin and 2-deoxyglucose induces p53-dependent apoptosis in prostate cancer cells. Cancer Res *70*, 2465-2475.

Bernales, S., Papa, F.R., and Walter, P. (2006). Intracellular signaling by the unfolded protein response. Annu Rev Cell Dev Biol *22*, 487-508.

Bernardi, R., Guernah, I., Jin, D., Grisendi, S., Alimonti, A., Teruya-Feldstein, J., Cordon-Cardo, C., Simon, M.C., Rafii, S., and Pandolfi, P.P. (2006). PML inhibits HIF-1alpha translation and neoangiogenesis through repression of mTOR. Nature *442*, 779-785.

Bernier, J., Hall, E.J., and Giaccia, A. (2004). Radiation oncology: a century of achievements. Nat Rev Cancer *4*, 737-747.

Bertolotti, A., Zhang, Y., Hendershot, L.M., Harding, H.P., and Ron, D. (2000). Dynamic interaction of BiP and ER stress transducers in the unfolded-protein response. Nat Cell Biol *2*, 326-332.

Bertout, J.A., Patel, S.A., and Simon, M.C. (2008). The impact of O2 availability on human cancer. Nat Rev Cancer *8*, 967-975.

Bi, M., Naczki, C., Koritzinsky, M., Fels, D., Blais, J., Hu, N., Harding, H., Novoa, I., Varia, M., Raleigh, J.*, et al.* (2005). ER stress-regulated translation increases tolerance to extreme hypoxia and promotes tumor growth. EMBO J *24*, 3470-3481.

Blais, J.D., Filipenko, V., Bi, M., Harding, H.P., Ron, D., Koumenis, C., Wouters, B.G., and Bell, J.C. (2004). Activating transcription factor 4 is translationally regulated by hypoxic stress. Mol Cell Biol *24*, 7469-7482.

Bobrovnikova-Marjon, E., Grigoriadou, C., Pytel, D., Zhang, F., Ye, J., Koumenis, C., Cavener, D., and Diehl, J.A. PERK promotes cancer cell proliferation and tumor growth by limiting oxidative DNA damage. Oncogene *29*, 3881-3895.

Bobrovnikova-Marjon, E., Hatzivassiliou, G., Grigoriadou, C., Romero, M., Cavener, D.R., Thompson, C.B., and Diehl, J.A. (2008). PERK-dependent regulation of lipogenesis during mouse mammary gland development and adipocyte differentiation. Proc Natl Acad Sci U S A *105*, 16314-16319.

Boya, P., Gonzalez-Polo, R.A., Casares, N., Perfettini, J.L., Dessen, P., Larochette, N., Metivier, D., Meley, D., Souquere, S., Yoshimori, T.*, et al.* (2005). Inhibition of macroautophagy triggers apoptosis. Mol Cell Biol *25*, 1025-1040.

Brizel, D.M., Rosner, G.L., Prosnitz, L.R., and Dewhirst, M.W. (1995). Patterns and variability of tumor oxygenation in human soft tissue sarcomas, cervical carcinomas, and lymph node metastases. Int J Radiat Oncol Biol Phys *32*, 1121-1125.

Browne, G.J., and Proud, C.G. (2004). A novel mTOR-regulated phosphorylation site in elongation factor 2 kinase modulates the activity of the kinase and its binding to calmodulin. Mol Cell Biol *24*, 2986-2997.

Brugarolas, J., Lei, K., Hurley, R.L., Manning, B.D., Reiling, J.H., Hafen, E., Witters, L.A., Ellisen, L.W., and Kaelin, W.G., Jr. (2004). Regulation of mTOR function in response to hypoxia by REDD1 and the TSC1/TSC2 tumor suppressor complex. Genes Dev *18*, 2893-2904.

Bustin, M. (1999). Regulation of DNA-dependent activities by the functional motifs of the high-mobility-group chromosomal proteins. Mol Cell Biol *19*, 5237-5246.

Cairns, R.A., Harris, I.S., and Mak, T.W. (2011). Regulation of cancer cell metabolism. Nat Rev Cancer *11*, 85-95.

Calfon, M., Zeng, H., Urano, F., Till, J.H., Hubbard, S.R., Harding, H.P., Clark, S.G., and Ron, D. (2002). IRE1 couples endoplasmic reticulum load to secretory capacity by processing the XBP-1 mRNA. Nature *415*, 92-96.

Carew, J.S., Nawrocki, S.T., Kahue, C.N., Zhang, H., Yang, C., Chung, L., Houghton, J.A., Huang, P., Giles, F.J., and Cleveland, J.L. (2007). Targeting autophagy augments the anticancer activity of the histone deacetylase inhibitor SAHA to overcome Bcr-Abl-mediated drug resistance. Blood *110*, 313-322.

Carmichael, S.J., Charles, B., and Tett, S.E. (2003). Population pharmacokinetics of hydroxychloroquine in patients with rheumatoid arthritis. Ther Drug Monit *25*, 671-681.

Cartron, P.F., Gallenne, T., Bougras, G., Gautier, F., Manero, F., Vusio, P., Meflah, K., Vallette, F.M., and Juin, P. (2004). The first alpha helix of Bax plays a necessary role in its ligand-induced activation by the BH3-only proteins Bid and PUMA. Mol Cell *16*, 807-818.

Casanovas, O., Hicklin, D.J., Bergers, G., and Hanahan, D. (2005). Drug resistance by evasion of antiangiogenic targeting of VEGF signaling in late-stage pancreatic islet tumors. Cancer Cell *8*, 299-309.

Cazanave, S.C., Elmi, N.A., Akazawa, Y., Bronk, S.F., Mott, J.L., and Gores, G.J. (2010). CHOP and AP-1 cooperatively mediate PUMA expression during lipoapoptosis. Am J Physiol Gastrointest Liver Physiol *299*, G236-243.

Certo, M., Del Gaizo Moore, V., Nishino, M., Wei, G., Korsmeyer, S., Armstrong, S.A., and Letai, A. (2006). Mitochondria primed by death signals determine cellular addiction to antiapoptotic BCL-2 family members. Cancer Cell *9*, 351-365.

Chan, E.Y., Kir, S., and Tooze, S.A. (2007). siRNA screening of the kinome identifies ULK1 as a multidomain modulator of autophagy. J Biol Chem *282*, 25464-25474.

Chan, E.Y., and Tooze, S.A. (2009). Evolution of Atg1 function and regulation. Autophagy *5*, 758-765.

Chan, N., Koritzinsky, M., Zhao, H., Bindra, R., Glazer, P.M., Powell, S., Belmaaza, A., Wouters, B., and Bristow, R.G. (2008). Chronic hypoxia decreases synthesis of homologous recombination proteins to offset chemoresistance and radioresistance. Cancer Res *68*, 605-614.

Chen, L., Willis, S.N., Wei, A., Smith, B.J., Fletcher, J.I., Hinds, M.G., Colman, P.M., Day, C.L., Adams, J.M., and Huang, D.C. (2005). Differential targeting of prosurvival Bcl-2

proteins by their BH3-only ligands allows complementary apoptotic function. Mol Cell *17*, 393-403.

Chen, S., Lee, J.M., Zeng, C., Chen, H., Hsu, C.Y., and Xu, J. (2006). Amyloid beta peptide increases DP5 expression via activation of neutral sphingomyelinase and JNK in oligodendrocytes. J Neurochem *97*, 631-640.

Chen, Y., McMillan-Ward, E., Kong, J., Israels, S.J., and Gibson, S.B. (2008). Oxidative stress induces autophagic cell death independent of apoptosis in transformed and cancer cells. Cell Death Differ *15*, 171-182.

Cheong, H., and Klionsky, D.J. (2008). Dual role of Atg1 in regulation of autophagy-specific PAS assembly in Saccharomyces cerevisiae. Autophagy *4*, 724-726.

Cheong, H., Nair, U., Geng, J., and Klionsky, D.J. (2008). The Atg1 kinase complex is involved in the regulation of protein recruitment to initiate sequestering vesicle formation for nonspecific autophagy in Saccharomyces cerevisiae. Mol Biol Cell *19*, 668-681.

Chipuk, J.E., Bouchier-Hayes, L., Kuwana, T., Newmeyer, D.D., and Green, D.R. (2005). PUMA couples the nuclear and cytoplasmic proapoptotic function of p53. Science *309*, 1732-1735.

Churchill-Davidson, I. (1964a). High-Pressure Oxygen and Radiotherapy. Anglo Ger Med Rev *2*, 519-523.

Churchill-Davidson, I. (1964b). Oxygenation in Radiotherapy of Malignant Disease of the Upper Air Passages. The Oxygen Effect of Radiotherapy. Proc R Soc Med *57*, 635-638.

Cockman, M.E., Masson, N., Mole, D.R., Jaakkola, P., Chang, G.W., Clifford, S.C., Maher, E.R., Pugh, C.W., Ratcliffe, P.J., and Maxwell, P.H. (2000). Hypoxia inducible factor-alpha binding and ubiquitylation by the von Hippel-Lindau tumor suppressor protein. J Biol Chem *275*, 25733-25741.

Comerford, K.M., Wallace, T.J., Karhausen, J., Louis, N.A., Montalto, M.C., and Colgan, S.P. (2002). Hypoxia-inducible factor-1-dependent regulation of the multidrug resistance (MDR1) gene. Cancer Res *62*, 3387-3394.

Coultas, L., Terzano, S., Thomas, T., Voss, A., Reid, K., Stanley, E.G., Scott, C.L., Bouillet, P., Bartlett, P., Ham, J.*, et al.* (2007). Hrk/DP5 contributes to the apoptosis of select neuronal populations but is dispensable for haematopoietic cell apoptosis. J Cell Sci *120*, 2044-2052.

Cox, J.S., Shamu, C.E., and Walter, P. (1993). Transcriptional induction of genes encoding endoplasmic reticulum resident proteins requires a transmembrane protein kinase. Cell *73*, 1197-1206.

Credle, J.J., Finer-Moore, J.S., Papa, F.R., Stroud, R.M., and Walter, P. (2005). On the mechanism of sensing unfolded protein in the endoplasmic reticulum. Proc Natl Acad Sci U S A *102*, 18773-18784.

Degenhardt, K., Mathew, R., Beaudoin, B., Bray, K., Anderson, D., Chen, G., Mukherjee, C., Shi, Y., Gelinas, C., Fan, Y.*, et al.* (2006). Autophagy promotes tumor cell survival and restricts necrosis, inflammation, and tumorigenesis. Cancer Cell *10*, 51-64.

Degtyarev, M., De Maziere, A., Orr, C., Lin, J., Lee, B.B., Tien, J.Y., Prior, W.W., van Dijk, S., Wu, H., Gray, D.C.*, et al.* (2008). Akt inhibition promotes autophagy and sensitizes PTEN-null tumors to lysosomotropic agents. J Cell Biol *183*, 101-116.

Deminoff, S.J., and Herman, P.K. (2007). Identifying Atg1 substrates: four means to an end. Autophagy *3*, 667-673.

Desmedt, C., Haibe-Kains, B., Wirapati, P., Buyse, M., Larsimont, D., Bontempi, G., Delorenzi, M., Piccart, M., and Sotiriou, C. (2008). Biological processes associated with breast cancer clinical outcome depend on the molecular subtypes. Clin Cancer Res *14*, 5158-5165.

DeYoung, M.P., Horak, P., Sofer, A., Sgroi, D., and Ellisen, L.W. (2008). Hypoxia regulates TSC1/2-mTOR signaling and tumor suppression through REDD1-mediated 14-3-3 shuttling. Genes Dev *22*, 239-251.

Dhillon, N.K., and Mudryj, M. (2003). Cyclin E overexpression enhances cytokine-mediated apoptosis in MCF7 breast cancer cells. Genes Immun *4*, 336-342.

Di Bartolomeo, S., Corazzari, M., Nazio, F., Oliverio, S., Lisi, G., Antonioli, M., Pagliarini, V., Matteoni, S., Fuoco, C., Giunta, L.*, et al.* (2010). The dynamic interaction of AMBRA1 with the dynein motor complex regulates mammalian autophagy. J Cell Biol *191*, 155-168.

Ding, W.X., Ni, H.M., Gao, W., Chen, X., Kang, J.H., Stolz, D.B., Liu, J., and Yin, X.M. (2009). Oncogenic transformation confers a selective susceptibility to the combined suppression of the proteasome and autophagy. Mol Cancer Ther *8*, 2036-2045.

Djavaheri-Mergny, M., Maiuri, M.C., and Kroemer, G. (2010). Cross talk between apoptosis and autophagy by caspase-mediated cleavage of Beclin 1. Oncogene *29*, 1717-1719.

Doroudgar, S., Thuerauf, D.J., Marcinko, M.C., Belmont, P.J., and Glembotski, C.C. (2009). Ischemia activates the ATF6 branch of the endoplasmic reticulum stress response. J Biol Chem *284*, 29735-29745.

Dorsey, F.C., Rose, K.L., Coenen, S., Prater, S.M., Cavett, V., Cleveland, J.L., and Caldwell-Busby, J. (2009). Mapping the phosphorylation sites of Ulk1. J Proteome Res *8*, 5253-5263.

Dubois, L., Magagnin, M.G., Cleven, A.H., Weppler, S.A., Grenacher, B., Landuyt, W., Lieuwes, N., Lambin, P., Gorr, T.A., Koritzinsky, M.*, et al.* (2009). Inhibition of 4E-BP1 sensitizes U87 glioblastoma xenograft tumors to irradiation by decreasing hypoxia tolerance. Int J Radiat Oncol Biol Phys *73*, 1219-1227.

Duennwald, M.L., and Lindquist, S. (2008). Impaired ERAD and ER stress are early and specific events in polyglutamine toxicity. Genes Dev *22*, 3308-3319.

Egan, D.F., Shackelford, D.B., Mihaylova, M.M., Gelino, S., Kohnz, R.A., Mair, W., Vasquez, D.S., Joshi, A., Gwinn, D.M., Taylor, R.*, et al.* (2011). Phosphorylation of ULK1 (hATG1) by AMP-activated protein kinase connects energy sensing to mitophagy. Science *331*, 456-461.

Elgendy, M., Sheridan, C., Brumatti, G., and Martin, S.J. (2011). Oncogenic Ras-Induced Expression of Noxa and Beclin-1 Promotes Autophagic Cell Death and Limits Clonogenic Survival. Mol Cell. *42*, 23-35.

Erler, J.T., Cawthorne, C.J., Williams, K.J., Koritzinsky, M., Wouters, B.G., Wilson, C., Miller, C., Demonacos, C., Stratford, I.J., and Dive, C. (2004). Hypoxia-mediated down-regulation of Bid and Bax in tumors occurs via hypoxia-inducible factor 1-dependent and -independent mechanisms and contributes to drug resistance. Mol Cell Biol *24*, 2875-2889.

Erlich, S., Mizrachy, L., Segev, O., Lindenboim, L., Zmira, O., Adi-Harel, S., Hirsch, J.A., Stein, R., and Pinkas-Kramarski, R. (2007). Differential interactions between Beclin 1 and Bcl-2 family members. Autophagy *3*, 561-568.

Fei, P., Bernhard, E.J., and El-Deiry, W.S. (2002). Tissue-specific induction of p53 targets in vivo. Cancer Res *62*, 7316-7327.

Fimia, G.M., Di Bartolomeo, S., Piacentini, M., and Cecconi, F. (2010). Unleashing the Ambra1-Beclin 1 complex from dynein chains: Ulk1 sets Ambra1 free to induce autophagy. Autophagy *7*, 115-117.

Flinterman, M., Guelen, L., Ezzati-Nik, S., Killick, R., Melino, G., Tominaga, K., Mymryk, J.S., Gaken, J., and Tavassoli, M. (2005). E1A activates transcription of p73 and Noxa to induce apoptosis. J Biol Chem *280*, 5945-5959.

Fricker, M., O'Prey, J., Tolkovsky, A.M., and Ryan, K.M. (2010). Phosphorylation of Puma modulates its apoptotic function by regulating protein stability. Cell Death Dis *1*, e59.

Furuya, N., Yu, J., Byfield, M., Pattingre, S., and Levine, B. (2005). The evolutionarily conserved domain of Beclin 1 is required for Vps34 binding, autophagy and tumor suppressor function. Autophagy *1*, 46-52.

Galehdar, Z., Swan, P., Fuerth, B., Callaghan, S.M., Park, D.S., and Cregan, S.P. (2010). Neuronal apoptosis induced by endoplasmic reticulum stress is regulated by ATF4-CHOP-mediated induction of the Bcl-2 homology 3-only member PUMA. J Neurosci *30*, 16938-16948.

Ganley, I.G., Lam du, H., Wang, J., Ding, X., Chen, S., and Jiang, X. (2009). ULK1.ATG13.FIP200 complex mediates mTOR signaling and is essential for autophagy. J Biol Chem *284*, 12297-12305.

Ghosh, R., Lipson, K.L., Sargent, K.E., Mercurio, A.M., Hunt, J.S., Ron, D., and Urano, F. Transcriptional regulation of VEGF-A by the unfolded protein response pathway. PLoS One *5*, e9575.

Gillies, R.J., and Gatenby, R.A. (2007). Hypoxia and adaptive landscapes in the evolution of carcinogenesis. Cancer Metastasis Rev *26*, 311-317.

Goldman, S.J., Taylor, R., Zhang, Y., and Jin, S. Autophagy and the degradation of mitochondria. Mitochondrion *10*, 309-315.

Gombart, A.F., Grewal, J., and Koeffler, H.P. (2007). ATF4 differentially regulates transcriptional activation of myeloid-specific genes by C/EBPepsilon and C/EBPalpha. J Leukoc Biol *81*, 1535-1547.

Gonzalez-Polo, R.A., Boya, P., Pauleau, A.L., Jalil, A., Larochette, N., Souquere, S., Eskelinen, E.L., Pierron, G., Saftig, P., and Kroemer, G. (2005). The apoptosis/autophagy paradox: autophagic vacuolization before apoptotic death. J Cell Sci *118*, 3091-3102.

Gordan, J.D., and Simon, M.C. (2007). Hypoxia-inducible factors: central regulators of the tumor phenotype. Curr Opin Genet Dev *17*, 71-77.

Graeber, T.G., Osmanian, C., Jacks, T., Housman, D.E., Koch, C.J., Lowe, S.W., and Giaccia, A.J. (1996). Hypoxia-mediated selection of cells with diminished apoptotic potential in solid tumours. Nature *379*, 88-91.

Grau, C., and Overgaard, J. (1992). Effect of etoposide, carmustine, vincristine, 5-fluorouracil, or methotrexate on radiobiologically oxic and hypoxic cells in a C3H mouse mammary carcinoma in situ. Cancer Chemother Pharmacol *30*, 277-280.

Guan, Q.H., Pei, D.S., Xu, T.L., and Zhang, G.Y. (2006). Brain ischemia/reperfusion-induced expression of DP5 and its interaction with Bcl-2, thus freeing Bax from Bcl-2/Bax dimmers are mediated by c-Jun N-terminal kinase (JNK) pathway. Neurosci Lett *393*, 226-230.

Guertin, D.A., and Sabatini, D.M. (2007). Defining the role of mTOR in cancer. Cancer Cell *12*, 9-22.

Guo, J.Y., Chen, H.Y., Mathew, R., Fan, J., Strohecker, A.M., Karsli-Uzunbas, G., Kamphorst, J.J., Chen, G., Lemons, J.M., Karantza, V.*, et al.* (2011). Activated Ras requires autophagy to maintain oxidative metabolism and tumorigenesis. Genes Dev *25*, 460-470.

Gurzov, E.N., Ortis, F., Cunha, D.A., Gosset, G., Li, M., Cardozo, A.K., and Eizirik, D.L. (2009). Signaling by IL-1beta+IFN-gamma and ER stress converge on DP5/Hrk activation: a novel mechanism for pancreatic beta-cell apoptosis. Cell Death Differ *16*, 1539-1550.

Gutierrez, M.G., Munafo, D.B., Beron, W., and Colombo, M.I. (2004). Rab7 is required for the normal progression of the autophagic pathway in mammalian cells. J Cell Sci *117*, 2687-2697.

Hai, T., and Curran, T. (1991). Cross-family dimerization of transcription factors Fos/Jun and ATF/CREB alters DNA binding specificity. Proc Natl Acad Sci U S A *88*, 3720-3724.

Hallaert, D.Y., Spijker, R., Jak, M., Derks, I.A., Alves, N.L., Wensveen, F.M., de Boer, J.P., de Jong, D., Green, S.R., van Oers, M.H.*, et al.* (2007). Crosstalk among Bcl-2 family members in B-CLL: seliciclib acts via the Mcl-1/Noxa axis and gradual exhaustion of Bcl-2 protection. Cell Death Differ *14*, 1958-1967.

Hanahan, D., and Weinberg, R.A. (2000). The hallmarks of cancer. Cell *100*, 57-70.

Hanahan, D., and Weinberg, R.A. (2011). Hallmarks of cancer: the next generation. Cell *144*, 646-674.

Hara, K., Maruki, Y., Long, X., Yoshino, K., Oshiro, N., Hidayat, S., Tokunaga, C., Avruch, J., and Yonezawa, K. (2002). Raptor, a binding partner of target of rapamycin (TOR), mediates TOR action. Cell *110*, 177-189.

Hara, T., and Mizushima, N. (2009). Role of ULK-FIP200 complex in mammalian autophagy: FIP200, a counterpart of yeast Atg17? Autophagy *5*, 85-87.

Hara, T., Takamura, A., Kishi, C., Iemura, S., Natsume, T., Guan, J.L., and Mizushima, N. (2008). FIP200, a ULK-interacting protein, is required for autophagosome formation in mammalian cells. J Cell Biol *181*, 497-510.

Harada, H., Kizaka-Kondoh, S., Li, G., Itasaka, S., Shibuya, K., Inoue, M., and Hiraoka, M. (2007). Significance of HIF-1-active cells in angiogenesis and radioresistance. Oncogene *26*, 7508-7516.

Harding, H.P., Novoa, I., Zhang, Y., Zeng, H., Wek, R., Schapira, M., and Ron, D. (2000). Regulated translation initiation controls stress-induced gene expression in mammalian cells. Mol Cell *6*, 1099-1108.

Harding, H.P., Zhang, Y., and Ron, D. (1999). Protein translation and folding are coupled by an endoplasmic-reticulum-resident kinase. Nature *397*, 271-274.

Harding, H.P., Zhang, Y., Zeng, H., Novoa, I., Lu, P.D., Calfon, M., Sadri, N., Yun, C., Popko, B., Paules, R.*, et al.* (2003). An integrated stress response regulates amino acid metabolism and resistance to oxidative stress. Mol Cell *11*, 619-633.

Harrington, E.A., Fanidi, A., and Evan, G.I. (1994). Oncogenes and cell death. Curr Opin Genet Dev *4*, 120-129.

Harris, A.L. (2002). Hypoxia--a key regulatory factor in tumour growth. Nat Rev Cancer *2*, 38-47.

Hayashi-Nishino, M., Fujita, N., Noda, T., Yamaguchi, A., Yoshimori, T., and Yamamoto, A. (2009). A subdomain of the endoplasmic reticulum forms a cradle for autophagosome formation. Nat Cell Biol *11*, 1433-1437.

Haze, K., Yoshida, H., Yanagi, H., Yura, T., and Mori, K. (1999). Mammalian transcription factor ATF6 is synthesized as a transmembrane protein and

activated by proteolysis in response to endoplasmic reticulum stress. Mol Biol Cell *10*, 3787-3799.

Henry, M., Alibert, S., Orlandi-Pradines, E., Bogreau, H., Fusai, T., Rogier, C., Barbe, J., and Pradines, B. (2006). Chloroquine resistance reversal agents as promising antimalarial drugs. Curr Drug Targets *7*, 935-948.

Hetz, C., Bernasconi, P., Fisher, J., Lee, A.H., Bassik, M.C., Antonsson, B., Brandt, G.S., Iwakoshi, N.N., Schinzel, A., Glimcher, L.H.*, et al.* (2006). Proapoptotic BAX and BAK modulate the unfolded protein response by a direct interaction with IRE1alpha. Science *312*, 572-576.

Hetz, C.A. (2007). ER stress signaling and the BCL-2 family of proteins: from adaptation to irreversible cellular damage. Antioxid Redox Signal *9*, 2345-2355.

Higgins, G.S., Harris, A.L., Prevo, R., Helleday, T., McKenna, W.G., and Buffa, F.M. (2010). Overexpression of POLQ confers a poor prognosis in early breast cancer patients. Oncotarget *1*, 175-184.

Higuchi, T., Nakamura, M., Shimada, K., Ishida, E., Hirao, K., and Konishi, N. (2008). HRK inactivation associated with promoter methylation and LOH in prostate cancer. Prostate *68*, 105-113.

Hijikata, M., Kato, N., Sato, T., Kagami, Y., and Shimotohno, K. (1990). Molecular cloning and characterization of a cDNA for a novel phorbol-12-myristate-13-acetate-responsive gene that is highly expressed in an adult T-cell leukemia cell line. J Virol *64*, 4632-4639.

Hockel, M., Schlenger, K., Aral, B., Mitze, M., Schaffer, U., and Vaupel, P. (1996). Association between tumor hypoxia and malignant progression in advanced cancer of the uterine cervix. Cancer Res *56*, 4509-4515.

Hockel, M., Vorndran, B., Schlenger, K., Baussmann, E., and Knapstein, P.G. (1993). Tumor oxygenation: a new predictive parameter in locally advanced cancer of the uterine cervix. Gynecol Oncol *51*, 141-149.

Hoozemans, J.J., van Haastert, E.S., Nijholt, D.A., Rozemuller, A.J., Eikelenboom, P., and Scheper, W. (2009). The unfolded protein response is activated in pretangle neurons in Alzheimer's disease hippocampus. Am J Pathol *174*, 1241-1251.

Hosokawa, N., Hara, T., Kaizuka, T., Kishi, C., Takamura, A., Miura, Y., Iemura, S., Natsume, T., Takehana, K., Yamada, N.*, et al.* (2009). Nutrient-dependent mTORC1

association with the ULK1-Atg13-FIP200 complex required for autophagy. Mol Biol Cell *20*, 1981-1991.

Iliopoulos, D., Hirsch, H.A., and Struhl, K. (2011). Metformin decreases the dose of chemotherapy for prolonging tumor remission in mouse xenografts involving multiple cancer cell types. Cancer Res. *71(9)*, 3196-201.

Imaizumi, K., Benito, A., Kiryu-Seo, S., Gonzalez, V., Inohara, N., Lieberman, A.P., Kiyama, H., and Nunez, G. (2004). Critical role for DP5/Harakiri, a Bcl-2 homology domain 3-only Bcl-2 family member, in axotomy-induced neuronal cell death. J Neurosci *24*, 3721-3725.

Imaizumi, K., Morihara, T., Mori, Y., Katayama, T., Tsuda, M., Furuyama, T., Wanaka, A., Takeda, M., and Tohyama, M. (1999). The cell death-promoting gene DP5, which interacts with the BCL2 family, is induced during neuronal apoptosis following exposure to amyloid beta protein. J Biol Chem *274*, 7975-7981.

Imaizumi, K., Tsuda, M., Imai, Y., Wanaka, A., Takagi, T., and Tohyama, M. (1997). Molecular cloning of a novel polypeptide, DP5, induced during programmed neuronal death. J Biol Chem *272*, 18842-18848.

Inohara, N., Ding, L., Chen, S., and Nunez, G. (1997). harakiri, a novel regulator of cell death, encodes a protein that activates apoptosis and interacts selectively with survival-promoting proteins Bcl-2 and Bcl-X(L). EMBO J *16*, 1686-1694.

Inoue, S., Riley, J., Gant, T.W., Dyer, M.J., and Cohen, G.M. (2007). Apoptosis induced by histone deacetylase inhibitors in leukemic cells is mediated by Bim and Noxa. Leukemia *21*, 1773-1782.

Ishihara, T., Hoshino, T., Namba, T., Tanaka, K., and Mizushima, T. (2007). Involvement of up-regulation of PUMA in non-steroidal anti-inflammatory drug-induced apoptosis. Biochem Biophys Res Commun *356*, 711-717.

Itakura, E., Kishi, C., Inoue, K., and Mizushima, N. (2008). Beclin 1 forms two distinct phosphatidylinositol 3-kinase complexes with mammalian Atg14 and UVRAG. Mol Biol Cell *19*, 5360-5372.

Ivan, M., Kondo, K., Yang, H., Kim, W., Valiando, J., Ohh, M., Salic, A., Asara, J.M., Lane, W.S., and Kaelin, W.G., Jr. (2001). HIFalpha targeted for VHL-mediated destruction by proline hydroxylation: implications for O2 sensing. Science *292*, 464-468.

Ivascu, A., and Kubbies, M. (2006). Rapid generation of single-tumor spheroids for high-throughput cell function and toxicity analysis. J Biomol Screen *11*, 922-932.

Jaakkola, P., Mole, D.R., Tian, Y.M., Wilson, M.I., Gielbert, J., Gaskell, S.J., Kriegsheim, A., Hebestreit, H.F., Mukherji, M., Schofield, C.J.*, et al.* (2001). Targeting of HIF-alpha to the von Hippel-Lindau ubiquitylation complex by O2-regulated prolyl hydroxylation. Science *292*, 468-472.

Jacinto, E., Loewith, R., Schmidt, A., Lin, S., Ruegg, M.A., Hall, A., and Hall, M.N. (2004). Mammalian TOR complex 2 controls the actin cytoskeleton and is rapamycin insensitive. Nat Cell Biol *6*, 1122-1128.

Kabeya, Y., Kamada, Y., Baba, M., Takikawa, H., Sasaki, M., and Ohsumi, Y. (2005). Atg17 functions in cooperation with Atg1 and Atg13 in yeast autophagy. Mol Biol Cell *16*, 2544-2553.

Kabeya, Y., Mizushima, N., Ueno, T., Yamamoto, A., Kirisako, T., Noda, T., Kominami, E., Ohsumi, Y., and Yoshimori, T. (2000). LC3, a mammalian homologue of yeast Apg8p, is localized in autophagosome membranes after processing. EMBO J *19*, 5720-5728.

Kaelin, W.G., Jr., and Ratcliffe, P.J. (2008). Oxygen sensing by metazoans: the central role of the HIF hydroxylase pathway. Mol Cell *30*, 393-402.

Kaeser, M.D., and Iggo, R.D. (2002). Chromatin immunoprecipitation analysis fails to support the latency model for regulation of p53 DNA binding activity in vivo. Proc Natl Acad Sci U S A *99*, 95-100.

Kalinec, G.M., Fernandez-Zapico, M.E., Urrutia, R., Esteban-Cruciani, N., Chen, S., and Kalinec, F. (2005). Pivotal role of Harakiri in the induction and prevention of gentamicin-induced hearing loss. Proc Natl Acad Sci U S A *102*, 16019-16024.

Kamada, Y., Funakoshi, T., Shintani, T., Nagano, K., Ohsumi, M., and Ohsumi, Y. (2000). Tor-mediated induction of autophagy via an Apg1 protein kinase complex. J Cell Biol *150*, 1507-1513.

Kamada, Y., Jung, U.S., Piotrowski, J., and Levin, D.E. (1995). The protein kinase C-activated MAP kinase pathway of Saccharomyces cerevisiae mediates a novel aspect of the heat shock response. Genes Dev *9*, 1559-1571.

Kamada, Y., Yoshino, K., Kondo, C., Kawamata, T., Oshiro, N., Yonezawa, K., and Ohsumi, Y. (2010). Tor directly controls the Atg1 kinase complex to regulate autophagy. Mol Cell Biol *30*, 1049-1058.

Kamura, T., Sato, S., Iwai, K., Czyzyk-Krzeska, M., Conaway, R.C., and Conaway, J.W. (2000). Activation of HIF1alpha ubiquitination by a reconstituted von Hippel-Lindau (VHL) tumor suppressor complex. Proc Natl Acad Sci U S A *97*, 10430-10435.

Kanazawa, K., Imaizumi, K., Mori, T., Honma, Y., Tojo, M., Tanno, Y., Yokoya, S., Niwa, S., Tohyama, M., Takagi, T.*, et al.* (1998). Expression pattern of a novel death-promoting gene, DP5, in the developing murine nervous system. Brain Res Mol Brain Res *54*, 316-320.

Kanki, T., and Klionsky, D.J. The molecular mechanism of mitochondria autophagy in yeast. Mol Microbiol *75*, 795-800.

Kanki, T., and Klionsky, D.J. (2009). Atg32 is a tag for mitochondria degradation in yeast. Autophagy *5*, 1201-1202.

Kanki, T., Wang, K., Cao, Y., Baba, M., and Klionsky, D.J. (2009). Atg32 is a mitochondrial protein that confers selectivity during mitophagy. Dev Cell *17*, 98-109.

Karantza-Wadsworth, V., Patel, S., Kravchuk, O., Chen, G., Mathew, R., Jin, S., and White, E. (2007). Autophagy mitigates metabolic stress and genome damage in mammary tumorigenesis. Genes Dev *21*, 1621-1635.

Katayama, M., Kawaguchi, T., Berger, M.S., and Pieper, R.O. (2007). DNA damaging agent-induced autophagy produces a cytoprotective adenosine triphosphate surge in malignant glioma cells. Cell Death Differ *14*, 548-558.

Kihara, A., Noda, T., Ishihara, N., and Ohsumi, Y. (2001). Two distinct Vps34 phosphatidylinositol 3-kinase complexes function in autophagy and carboxypeptidase Y sorting in Saccharomyces cerevisiae. J Cell Biol *152*, 519-530.

Kijanska, M., Dohnal, I., Reiter, W., Kaspar, S., Stoffel, I., Ammerer, G., Kraft, C., and Peter, M. (2010). Activation of Atg1 kinase in autophagy by regulated phosphorylation. Autophagy *6*, 1168-1178.

Kim, D.H., Sarbassov, D.D., Ali, S.M., King, J.E., Latek, R.R., Erdjument-Bromage, H., Tempst, P., and Sabatini, D.M. (2002). mTOR interacts with raptor to form a nutrient-sensitive complex that signals to the cell growth machinery. Cell *110*, 163-175.

Kim, H., Rafiuddin-Shah, M., Tu, H.C., Jeffers, J.R., Zambetti, G.P., Hsieh, J.J., and Cheng, E.H. (2006). Hierarchical regulation of mitochondrion-dependent apoptosis by BCL-2 subfamilies. Nat Cell Biol *8*, 1348-1358.

Kim, H., Tu, H.C., Ren, D., Takeuchi, O., Jeffers, J.R., Zambetti, G.P., Hsieh, J.J., and Cheng, E.H. (2009). Stepwise activation of BAX and BAK by tBID, BIM, and PUMA initiates mitochondrial apoptosis. Mol Cell *36*, 487-499.

Kim, J., Kundu, M., Viollet, B., and Guan, K.L. (2011). AMPK and mTOR regulate autophagy through direct phosphorylation of Ulk1. Nat Cell Biol *13*, 132-141.

Kim, J.Y., Ahn, H.J., Ryu, J.H., Suk, K., and Park, J.H. (2004). BH3-only protein Noxa is a mediator of hypoxic cell death induced by hypoxia-inducible factor 1alpha. J Exp Med *199*, 113-124.

Klionsky, D.J., Abeliovich, H., Agostinis, P., Agrawal, D.K., Aliev, G., Askew, D.S., Baba, M., Baehrecke, E.H., Bahr, B.A., Ballabio, A.*, et al.* (2008). Guidelines for the use and interpretation of assays for monitoring autophagy in higher eukaryotes. Autophagy *4*, 151-175.

Knowles, H.J., and Harris, A.L. (2001). Hypoxia and oxidative stress in breast cancer. Hypoxia and tumourigenesis. Breast Cancer Res *3*, 318-322.

Komatsu, M., Waguri, S., Koike, M., Sou, Y.S., Ueno, T., Hara, T., Mizushima, N., Iwata, J., Ezaki, J., Murata, S.*, et al.* (2007). Homeostatic levels of p62 control cytoplasmic inclusion body formation in autophagy-deficient mice. Cell *131*, 1149-1163.

Komatsu, M., Waguri, S., Ueno, T., Iwata, J., Murata, S., Tanida, I., Ezaki, J., Mizushima, N., Ohsumi, Y., Uchiyama, Y.*, et al.* (2005). Impairment of starvation-induced and constitutive autophagy in Atg7-deficient mice. J Cell Biol *169*, 425-434.

Kongara, S., Kravchuk, O., Teplova, I., Lozy, F., Schulte, J., Moore, D., Barnard, N., Neumann, C.A., White, E., and Karantza, V. (2010). Autophagy regulates keratin 8 homeostasis in mammary epithelial cells and in breast tumors. Mol Cancer Res *8*, 873-884.

Koritzinsky, M., Magagnin, M.G., van den Beucken, T., Seigneuric, R., Savelkouls, K., Dostie, J., Pyronnet, S., Kaufman, R.J., Weppler, S.A., Voncken, J.W.*, et al.* (2006). Gene expression during acute and prolonged hypoxia is regulated by distinct mechanisms of translational control. EMBO J *25*, 1114-1125.

Koritzinsky, M., Rouschop, K.M., van den Beucken, T., Magagnin, M.G., Savelkouls, K., Lambin, P., and Wouters, B.G. (2007). Phosphorylation of eIF2alpha is required for mRNA translation inhibition and survival during moderate hypoxia. Radiother Oncol *83*, 353-361.

Koumenis, C., Naczki, C., Koritzinsky, M., Rastani, S., Diehl, A., Sonenberg, N., Koromilas, A., and Wouters, B.G. (2002). Regulation of protein synthesis by hypoxia via activation of the endoplasmic reticulum kinase PERK and phosphorylation of the translation initiation factor eIF2alpha. Mol Cell Biol *22*, 7405-7416.

Kraft, C., Peter, M., and Hofmann, K. Selective autophagy: ubiquitin-mediated recognition and beyond. Nat Cell Biol *12*, 836-841.

Kroemer, G., and Levine, B. (2008). Autophagic cell death: the story of a misnomer. Nat Rev Mol Cell Biol *9*, 1004-1010.

Kroemer, G., Marino, G., and Levine, B. (2010). Autophagy and the integrated stress response. Mol Cell *40*, 280-293.

Kuma, A., Hatano, M., Matsui, M., Yamamoto, A., Nakaya, H., Yoshimori, T., Ohsumi, Y., Tokuhisa, T., and Mizushima, N. (2004). The role of autophagy during the early neonatal starvation period. Nature *432*, 1032-1036.

Kundu, M., Lindsten, T., Yang, C.Y., Wu, J., Zhao, F., Zhang, J., Selak, M.A., Ney, P.A., and Thompson, C.B. (2008a). Ulk1 plays a critical role in the autophagic clearance of mitochondria and ribosomes during reticulocyte maturation. Blood *112*, 1493-1502.

Kundu, M., Lindsten, T., Yang, C.Y., Wu, J.M., Zhao, F.P., Zhang, J., Selak, M.A., Ney, P.A., and Thompson, C.B. (2008b). Ulk1 plays a critical role in the autophagic clearance of mitochondria and ribosomes during reticulocyte maturation. Blood *112*, 1493-1502.

Kuroyanagi, H., Yan, J., Seki, N., Yamanouchi, Y., Suzuki, Y., Takano, T., Muramatsu, M., and Shirasawa, T. (1998). Human ULK1, a novel serine/threonine kinase related to UNC-51 kinase of Caenorhabditis elegans: cDNA cloning, expression, and chromosomal assignment. Genomics *51*, 76-85.

Lee do, Y., Lee, K.S., Lee, H.J., Kim do, H., Noh, Y.H., Yu, K., Jung, H.Y., Lee, S.H., Lee, J.Y., Youn, Y.C.*, et al.* (2010). Activation of PERK signaling attenuates Abeta-mediated ER stress. PLoS One *5*, e10489.

Lee, J.A., Beigneux, A., Ahmad, S.T., Young, S.G., and Gao, F.B. (2007a). ESCRT-III dysfunction causes autophagosome accumulation and neurodegeneration. Curr Biol *17*, 1561-1567.

Lee, J.A., and Gao, F.B. (2008). Roles of ESCRT in autophagy-associated neurodegeneration. Autophagy *4*, 230-232.

Lee, J.W., Park, S., Takahashi, Y., and Wang, H.G. The association of AMPK with ULK1 regulates autophagy. PLoS One *5*, e15394.

Lee, J.W., Park, S., Takahashi, Y., and Wang, H.G. (2010). The association of AMPK with ULK1 regulates autophagy. PLoS One *5*, e15394.

Lee, S.B., Kim, S., Lee, J., Park, J., Lee, G., Kim, Y., Kim, J.M., and Chung, J. (2007b). ATG1, an autophagy regulator, inhibits cell growth by negatively regulating S6 kinase. EMBO Rep *8*, 360-365.

Lee, Y.Y., Cevallos, R.C., and Jan, E. (2009). An upstream open reading frame regulates translation of GADD34 during cellular stresses that induce eIF2alpha phosphorylation. J Biol Chem *284*, 6661-6673.

Lenardo, M.J., McPhee, C.K., and Yu, L. (2009). Autophagic cell death. Methods Enzymol *453*, 17-31.

Letai, A., Bassik, M.C., Walensky, L.D., Sorcinelli, M.D., Weiler, S., and Korsmeyer, S.J. (2002). Distinct BH3 domains either sensitize or activate mitochondrial apoptosis, serving as prototype cancer therapeutics. Cancer Cell *2*, 183-192.

Levine, B., and Kroemer, G. (2008). Autophagy in the pathogenesis of disease. Cell *132*, 27-42.

Levine, B., Sinha, S., and Kroemer, G. (2008). Bcl-2 family members: dual regulators of apoptosis and autophagy. Autophagy *4*, 600-606.

Li, J., Lee, B., and Lee, A.S. (2006). Endoplasmic reticulum stress-induced apoptosis: multiple pathways and activation of p53-up-regulated modulator of apoptosis (PUMA) and NOXA by p53. J Biol Chem *281*, 7260-7270.

Li, Y., Wang, Y., Kim, E., Beemiller, P., Wang, C.Y., Swanson, J., You, M., and Guan, K.L. (2007). Bnip3 mediates the hypoxia-induced inhibition on mammalian target of rapamycin by interacting with Rheb. J Biol Chem *282*, 35803-35813.

Liang, G., and Hai, T. (1997). Characterization of human activating transcription factor 4, a transcriptional activator that interacts with multiple domains of cAMP-responsive element-binding protein (CREB)-binding protein. J Biol Chem *272*, 24088-24095.

Liang, X.H., Jackson, S., Seaman, M., Brown, K., Kempkes, B., Hibshoosh, H., and Levine, B. (1999). Induction of autophagy and inhibition of tumorigenesis by beclin 1. Nature *402*, 672-676.

Liu, J., Zhang, J., Wang, X., Li, Y., Chen, Y., Li, K., Yao, L., and Guo, G. HIF-1 and NDRG2 contribute to hypoxia-induced radioresistance of cervical cancer Hela cells. Exp Cell Res *316*, 1985-1993.

Liu, L., Cash, T.P., Jones, R.G., Keith, B., Thompson, C.B., and Simon, M.C. (2006). Hypoxia-induced energy stress regulates mRNA translation and cell growth. Mol Cell *21*, 521-531.

Liu, L., Sun, L., Zhang, H., Li, Z., Ning, X., Shi, Y., Guo, C., Han, S., Wu, K., and Fan, D. (2009). Hypoxia-mediated up-regulation of MGr1-Ag/37LRP in gastric cancers occurs via hypoxia-inducible-factor 1-dependent mechanism and contributes to drug resistance. Int J Cancer *124*, 1707-1715.

Liu, X., Dai, S., Zhu, Y., Marrack, P., and Kappler, J.W. (2003). The structure of a Bcl-xL/Bim fragment complex: implications for Bim function. Immunity *19*, 341-352.

Loewith, R., Jacinto, E., Wullschleger, S., Lorberg, A., Crespo, J.L., Bonenfant, D., Oppliger, W., Jenoe, P., and Hall, M.N. (2002). Two TOR complexes, only one of which is rapamycin sensitive, have distinct roles in cell growth control. Mol Cell *10*, 457-468.

Loi, S., Haibe-Kains, B., Desmedt, C., Wirapati, P., Lallemand, F., Tutt, A.M., Gillet, C., Ellis, P., Ryder, K., Reid, J.F*., et al.* (2008). Predicting prognosis using molecular profiling in estrogen receptor-positive breast cancer treated with tamoxifen. BMC Genomics *9*, 239.

Lomonosova, E., and Chinnadurai, G. (2008). BH3-only proteins in apoptosis and beyond: an overview. Oncogene *27 Suppl 1*, S2-19.

Loncaster, J.A., Harris, A.L., Davidson, S.E., Logue, J.P., Hunter, R.D., Wycoff, C.C., Pastorek, J., Ratcliffe, P.J., Stratford, I.J., and West, C.M. (2001). Carbonic anhydrase (CA IX) expression, a potential new intrinsic marker of hypoxia: correlations with tumor oxygen measurements and prognosis in locally advanced carcinoma of the cervix. Cancer Res *61*, 6394-6399.

Lord, S., and Harris, A.L. (2011). Angiogenesis - still a worthwhile target for breast cancer therapy? Breast Cancer Res *12 Suppl 4*, S19.

Lu, P.D., Harding, H.P., and Ron, D. (2004a). Translation reinitiation at alternative open reading frames regulates gene expression in an integrated stress response. J Cell Biol *167*, 27-33.

Lu, P.D., Jousse, C., Marciniak, S.J., Zhang, Y., Novoa, I., Scheuner, D., Kaufman, R.J., Ron, D., and Harding, H.P. (2004b). Cytoprotection by pre-emptive conditional phosphorylation of translation initiation factor 2. EMBO J *23*, 169-179.

Luo, D., He, Y., Zhang, H., Yu, L., Chen, H., Xu, Z., Tang, S., Urano, F., and Min, W. (2008). AIP1 is critical in transducing IRE1-mediated endoplasmic reticulum stress response. J Biol Chem *283*, 11905-11912.

Lyng, H., Sundfor, K., and Rofstad, E.K. (1997). Oxygen tension in human tumours measured with polarographic needle electrodes and its relationship to vascular density, necrosis and hypoxia. Radiother Oncol *44*, 163-169.

Ma, C., Ying, C., Yuan, Z., Song, B., Li, D., Liu, Y., Lai, B., Li, W., Chen, R., Ching, Y.P.*, et al.* (2007). dp5/HRK is a c-Jun target gene and required for apoptosis induced by potassium deprivation in cerebellar granule neurons. J Biol Chem *282*, 30901-30909.

Ma, Y., and Hendershot, L.M. (2003). Delineation of a negative feedback regulatory loop that controls protein translation during endoplasmic reticulum stress. J Biol Chem *278*, 34864-34873.

Maiuri, M.C., Le Toumelin, G., Criollo, A., Rain, J.C., Gautier, F., Juin, P., Tasdemir, E., Pierron, G., Troulinaki, K., Tavernarakis, N.*, et al.* (2007). Functional and physical interaction between Bcl-X(L) and a BH3-like domain in Beclin-1. EMBO J *26*, 2527-2539.

Majmundar, A.J., Wong, W.J., and Simon, M.C. (2010). Hypoxia-inducible factors and the response to hypoxic stress. Mol Cell *40*, 294-309.

Marceau, F., Bawolak, M.T., Bouthillier, J., and Morissette, G. (2009). Vacuolar ATPase-mediated cellular concentration and retention of quinacrine: a model for the distribution of lipophilic cationic drugs to autophagic vacuoles. Drug Metab Dispos *37*, 2271-2274.

Marciniak, S.J., Yun, C.Y., Oyadomari, S., Novoa, I., Zhang, Y., Jungreis, R., Nagata, K., Harding, H.P., and Ron, D. (2004). CHOP induces death by promoting protein

synthesis and oxidation in the stressed endoplasmic reticulum. Genes Dev *18*, 3066-3077.

Marino, G., Salvador-Montoliu, N., Fueyo, A., Knecht, E., Mizushima, N., and Lopez-Otin, C. (2007). Tissue-specific autophagy alterations and increased tumorigenesis in mice deficient in Atg4C/autophagin-3. J Biol Chem *282*, 18573-18583.

Martindale, J.J., Fernandez, R., Thuerauf, D., Whittaker, R., Gude, N., Sussman, M.A., and Glembotski, C.C. (2006). Endoplasmic reticulum stress gene induction and protection from ischemia/reperfusion injury in the hearts of transgenic mice with a tamoxifen-regulated form of ATF6. Circ Res *98*, 1186-1193.

Mathew, R., Karp, C.M., Beaudoin, B., Vuong, N., Chen, G., Chen, H.Y., Bray, K., Reddy, A., Bhanot, G., Gelinas, C.*, et al.* (2009). Autophagy suppresses tumorigenesis through elimination of p62. Cell *137*, 1062-1075.

Mathew, R., Kongara, S., Beaudoin, B., Karp, C.M., Bray, K., Degenhardt, K., Chen, G., Jin, S., and White, E. (2007). Autophagy suppresses tumor progression by limiting chromosomal instability. Genes Dev *21*, 1367-1381.

Mathew, R., and White, E. (2011). Autophagy in tumorigenesis and energy metabolism: friend by day, foe by night. Curr Opin Genet Dev *21*, 113-119.

Matthews, N.E., Adams, M.A., Maxwell, L.R., Gofton, T.E., and Graham, C.H. (2001). Nitric oxide-mediated regulation of chemosensitivity in cancer cells. J Natl Cancer Inst *93*, 1879-1885.

Maxwell, P.H., Wiesener, M.S., Chang, G.W., Clifford, S.C., Vaux, E.C., Cockman, M.E., Wykoff, C.C., Pugh, C.W., Maher, E.R., and Ratcliffe, P.J. (1999). The tumour suppressor protein VHL targets hypoxia-inducible factors for oxygen-dependent proteolysis. Nature *399*, 271-275.

Mercer, C.A., Kaliappan, A., and Dennis, P.B. (2009). A novel, human Atg13 binding protein, Atg101, interacts with ULK1 and is essential for macroautophagy. Autophagy *5*, 649-662.

Milani, M., Rzymski, T., Mellor, H.R., Pike, L., Bottini, A., Generali, D., and Harris, A.L. (2009). The role of ATF4 stabilization and autophagy in resistance of breast cancer cells treated with Bortezomib. Cancer Res *69*, 4415-4423.

Minchinton, A.I., and Tannock, I.F. (2006). Drug penetration in solid tumours. Nat Rev Cancer *6*, 583-592.

Mizushima, N. The role of the Atg1/ULK1 complex in autophagy regulation. Curr Opin Cell Biol *22*, 132-139.

Mizushima, N. (2005). The pleiotropic role of autophagy: from protein metabolism to bactericide. Cell Death Differ *12 Suppl 2*, 1535-1541.

Mizushima, N. (2010). The role of the Atg1/ULK1 complex in autophagy regulation. Curr Opin Cell Biol *22*, 132-139.

Mizushima, N., Levine, B., Cuervo, A.M., and Klionsky, D.J. (2008). Autophagy fights disease through cellular self-digestion. Nature *451*, 1069-1075.

Mizushima, N., Noda, T., Yoshimori, T., Tanaka, Y., Ishii, T., George, M.D., Klionsky, D.J., Ohsumi, M., and Ohsumi, Y. (1998a). A protein conjugation system essential for autophagy. Nature *395*, 395-398.

Mizushima, N., Sugita, H., Yoshimori, T., and Ohsumi, Y. (1998b). A new protein conjugation system in human. The counterpart of the yeast Apg12p conjugation system essential for autophagy. J Biol Chem *273*, 33889-33892.

Morales, A.A., Gutman, D., Lee, K.P., and Boise, L.H. (2008). BH3-only proteins Noxa, Bmf, and Bim are necessary for arsenic trioxide-induced cell death in myeloma. Blood *111*, 5152-5162.

Muchmore, S.W., Sattler, M., Liang, H., Meadows, R.P., Harlan, J.E., Yoon, H.S., Nettesheim, D., Chang, B.S., Thompson, C.B., Wong, S.L.*, et al.* (1996). X-ray and NMR structure of human Bcl-xL, an inhibitor of programmed cell death. Nature *381*, 335-341.

Mujcic, H., Rzymski, T., Rouschop, K.M., Koritzinsky, M., Milani, M., Harris, A.L., and Wouters, B.G. (2009). Hypoxic activation of the unfolded protein response (UPR) induces expression of the metastasis-associated gene LAMP3. Radiother Oncol *92*, 450-459.

Muller, S., Scaffidi, P., Degryse, B., Bonaldi, T., Ronfani, L., Agresti, A., Beltrame, M., and Bianchi, M.E. (2001). New EMBO members' review: the double life of HMGB1 chromatin protein: architectural factor and extracellular signal. EMBO J *20*, 4337-4340.

Nakamura, M., Ishida, E., Shimada, K., Nakase, H., Sakaki, T., and Konishi, N. (2005). Frequent HRK inactivation associated with low apoptotic index in secondary glioblastomas. Acta Neuropathol *110*, 402-410.

Nakamura, M., Ishida, E., Shimada, K., Nakase, H., Sakaki, T., and Konishi, N. (2006). Defective expression of HRK is associated with promoter methylation in primary central nervous system lymphomas. Oncology *70*, 212-221.

Nakano, K., and Vousden, K.H. (2001). PUMA, a novel proapoptotic gene, is induced by p53. Mol Cell *7*, 683-694.

Narendra, D.P., and Youle, R.J. (2011). Targeting Mitochondrial Dysfunction: Role for PINK1 and Parkin in Mitochondrial Quality Control. Antioxid Redox Signal.

Nijhawan, D., Fang, M., Traer, E., Zhong, Q., Gao, W., Du, F., and Wang, X. (2003). Elimination of Mcl-1 is required for the initiation of apoptosis following ultraviolet irradiation. Genes Dev *17*, 1475-1486.

Noda, T., and Ohsumi, Y. (1998). Tor, a phosphatidylinositol kinase homologue, controls autophagy in yeast. J Biol Chem *273*, 3963-3966.

Novoa, I., Zeng, H., Harding, H.P., and Ron, D. (2001). Feedback inhibition of the unfolded protein response by GADD34-mediated dephosphorylation of eIF2alpha. J Cell Biol *153*, 1011-1022.

Nowell, P.C. (1976). The clonal evolution of tumor cell populations. Science *194*, 23-28.

Obata, T., Toyota, M., Satoh, A., Sasaki, Y., Ogi, K., Akino, K., Suzuki, H., Murai, M., Kikuchi, T., Mita, H.*, et al.* (2003). Identification of HRK as a target of epigenetic inactivation in colorectal and gastric cancer. Clin Cancer Res *9*, 6410-6418.

Oberstein, A., Jeffrey, P.D., and Shi, Y. (2007). Crystal structure of the Bcl-XL-Beclin 1 peptide complex: Beclin 1 is a novel BH3-only protein. J Biol Chem *282*, 13123-13132.

Oda, E., Ohki, R., Murasawa, H., Nemoto, J., Shibue, T., Yamashita, T., Tokino, T., Taniguchi, T., and Tanaka, N. (2000). Noxa, a BH3-only member of the Bcl-2 family and candidate mediator of p53-induced apoptosis. Science *288*, 1053-1058.

Ogata, M., Hino, S., Saito, A., Morikawa, K., Kondo, S., Kanemoto, S., Murakami, T., Taniguchi, M., Tanii, I., Yoshinaga, K.*, et al.* (2006). Autophagy is activated for cell survival after endoplasmic reticulum stress. Mol Cell Biol *26*, 9220-9231.

Ohh, M., Park, C.W., Ivan, M., Hoffman, M.A., Kim, T.Y., Huang, L.E., Pavletich, N., Chau, V., and Kaelin, W.G. (2000). Ubiquitination of hypoxia-inducible factor

requires direct binding to the beta-domain of the von Hippel-Lindau protein. Nat Cell Biol *2*, 423-427.

Okunieff, P., Fenton, B., and Chen, Y. (2005). Past, present, and future of oxygen in cancer research. Adv Exp Med Biol *566*, 213-222.

Olive, P.L., Banath, J.P., and Durand, R.E. (2002). The range of oxygenation in SiHa tumor xenografts. Radiat Res *158*, 159-166.

Oltersdorf, T., Elmore, S.W., Shoemaker, A.R., Armstrong, R.C., Augeri, D.J., Belli, B.A., Bruncko, M., Deckwerth, T.L., Dinges, J., Hajduk, P.J.*, et al.* (2005). An inhibitor of Bcl-2 family proteins induces regression of solid tumours. Nature *435*, 677-681.

Oltvai, Z.N., Milliman, C.L., and Korsmeyer, S.J. (1993). Bcl-2 heterodimerizes in vivo with a conserved homolog, Bax, that accelerates programmed cell death. Cell *74*, 609-619.

Opferman, J.T., Letai, A., Beard, C., Sorcinelli, M.D., Ong, C.C., and Korsmeyer, S.J. (2003). Development and maintenance of B and T lymphocytes requires antiapoptotic MCL-1. Nature *426*, 671-676.

Otsuki, Y., Li, Z., and Shibata, M.A. (2003). Apoptotic detection methods--from morphology to gene. Prog Histochem Cytochem *38*, 275-339.

Oyadomari, S., and Mori, M. (2004). Roles of CHOP/GADD153 in endoplasmic reticulum stress. Cell Death Differ *11*, 381-389.

Pacheco-Torres, J., Lopez-Larrubia, P., Ballesteros, P., and Cerdan, S. (2010). Imaging tumor hypoxia by magnetic resonance methods. NMR Biomed.

Paez-Ribes, M., Allen, E., Hudock, J., Takeda, T., Okuyama, H., Vinals, F., Inoue, M., Bergers, G., Hanahan, D., and Casanovas, O. (2009). Antiangiogenic therapy elicits malignant progression of tumors to increased local invasion and distant metastasis. Cancer Cell *15*, 220-231.

Papa, F.R., Zhang, C., Shokat, K., and Walter, P. (2003). Bypassing a kinase activity with an ATP-competitive drug. Science *302*, 1533-1537.

Papadakis, A.I., Paraskeva, E., Peidis, P., Muaddi, H., Li, S., Raptis, L., Pantopoulos, K., Simos, G., and Koromilas, A.E. (2010). eIF2{alpha} Kinase PKR modulates the hypoxic response by Stat3-dependent transcriptional suppression of HIF-1{alpha}. Cancer Res *70*, 7820-7829.

Park, K.J., Lee, S.H., Lee, C.H., Jang, J.Y., Chung, J., Kwon, M.H., and Kim, Y.S. (2009). Upregulation of Beclin-1 expression and phosphorylation of Bcl-2 and p53 are involved in the JNK-mediated autophagic cell death. Biochem Biophys Res Commun *382*, 726-729.

Pattingre, S., Tassa, A., Qu, X., Garuti, R., Liang, X.H., Mizushima, N., Packer, M., Schneider, M.D., and Levine, B. (2005). Bcl-2 antiapoptotic proteins inhibit Beclin 1-dependent autophagy. Cell *122*, 927-939.

Podust, L.M., Krezel, A.M., and Kim, Y. (2001). Crystal structure of the CCAAT box/enhancer-binding protein beta activating transcription factor-4 basic leucine zipper heterodimer in the absence of DNA. J Biol Chem *276*, 505-513.

Poole, B., and Ohkuma, S. (1981). Effect of weak bases on the intralysosomal pH in mouse peritoneal macrophages. J Cell Biol *90*, 665-669.

Powers, W.E., and Tolmach, L.J. (1964). Demonstration of an Anoxic Component in a Mouse Tumor-Cell Population by in Vivo Assay of Survival Following Irradiation. Radiology *83*, 328-336.

Prostko, C.R., Dholakia, J.N., Brostrom, M.A., and Brostrom, C.O. (1995). Activation of the double-stranded RNA-regulated protein kinase by depletion of endoplasmic reticular calcium stores. J Biol Chem *270*, 6211-6215.

Qu, X., Yu, J., Bhagat, G., Furuya, N., Hibshoosh, H., Troxel, A., Rosen, J., Eskelinen, E.L., Mizushima, N., Ohsumi, Y.*, et al.* (2003). Promotion of tumorigenesis by heterozygous disruption of the beclin 1 autophagy gene. J Clin Invest *112*, 1809-1820.

Rabinowitz, J.D., and White, E. (2011). Autophagy and metabolism. Science *330*, 1344-1348.

Ramaiah, K.V., Dhindsa, R.S., Chen, J.J., London, I.M., and Levin, D. (1992). Recycling and phosphorylation of eukaryotic initiation factor 2 on 60S subunits of 80S initiation complexes and polysomes. Proc Natl Acad Sci U S A *89*, 12063-12067.

Rashmi, R., Pillai, S.G., Vijayalingam, S., Ryerse, J., and Chinnadurai, G. (2008). BH3-only protein BIK induces caspase-independent cell death with autophagic features in Bcl-2 null cells. Oncogene *27*, 1366-1375.

Ravikumar, B., Imarisio, S., Sarkar, S., O'Kane, C.J., and Rubinsztein, D.C. (2008). Rab5 modulates aggregation and toxicity of mutant huntingtin through

macroautophagy in cell and fly models of Huntington disease. J Cell Sci *121*, 1649-1660.

Ravikumar, B., Vacher, C., Berger, Z., Davies, J.E., Luo, S., Oroz, L.G., Scaravilli, F., Easton, D.F., Duden, R., O'Kane, C.J.*, et al.* (2004). Inhibition of mTOR induces autophagy and reduces toxicity of polyglutamine expansions in fly and mouse models of Huntington disease. Nat Genet *36*, 585-595.

Reggiori, F., Tucker, K.A., Stromhaug, P.E., and Klionsky, D.J. (2004). The Atg1-Atg13 complex regulates Atg9 and Atg23 retrieval transport from the pre-autophagosomal structure. Dev Cell *6*, 79-90.

Ren, D., Tu, H.C., Kim, H., Wang, G.X., Bean, G.R., Takeuchi, O., Jeffers, J.R., Zambetti, G.P., Hsieh, J.J., and Cheng, E.H. (2010). BID, BIM, and PUMA are essential for activation of the BAX- and BAK-dependent cell death program. Science *330*, 1390-1393.

Romero-Ramirez, L., Cao, H., Nelson, D., Hammond, E., Lee, A.H., Yoshida, H., Mori, K., Glimcher, L.H., Denko, N.C., Giaccia, A.J.*, et al.* (2004). XBP1 is essential for survival under hypoxic conditions and is required for tumor growth. Cancer Res *64*, 5943-5947.

Ron, D., and Hubbard, S.R. (2008). How IRE1 reacts to ER stress. Cell *132*, 24-26.

Ron, D., and Walter, P. (2007). Signal integration in the endoplasmic reticulum unfolded protein response. Nat Rev Mol Cell Biol *8*, 519-529.

Rouschop, K.M., Ramaekers, C.H., Schaaf, M.B., Keulers, T.G., Savelkouls, K.G., Lambin, P., Koritzinsky, M., and Wouters, B.G. (2009a). Autophagy is required during cycling hypoxia to lower production of reactive oxygen species. Radiother Oncol *92*, 411-416.

Rouschop, K.M., van den Beucken, T., Dubois, L., Niessen, H., Bussink, J., Savelkouls, K., Keulers, T., Mujcic, H., Landuyt, W., Voncken, J.W.*, et al.* (2009b). The unfolded protein response protects human tumor cells during hypoxia through regulation of the autophagy genes MAP1LC3B and ATG5. J Clin Invest *120*, 127-141.

Rouschop, K.M., van den Beucken, T., Dubois, L., Niessen, H., Bussink, J., Savelkouls, K., Keulers, T., Mujcic, H., Landuyt, W., Voncken, J.W.*, et al.* (2010). The unfolded protein response protects human tumor cells during hypoxia through regulation of the autophagy genes MAP1LC3B and ATG5. J Clin Invest *120*, 127-141.

Roybal, C.N., Hunsaker, L.A., Barbash, O., Vander Jagt, D.L., and Abcouwer, S.F. (2005). The oxidative stressor arsenite activates vascular endothelial growth factor mRNA transcription by an ATF4-dependent mechanism. J Biol Chem *280*, 20331-20339.

Ruan, K., Song, G., and Ouyang, G. (2009). Role of hypoxia in the hallmarks of human cancer. J Cell Biochem *107*, 1053-1062.

Rzymski, T., and Harris, A.L. (2007). The unfolded protein response and integrated stress response to anoxia. Clin Cancer Res *13*, 2537-2540.

Rzymski, T., Milani, M., Pike, L., Buffa, F., Mellor, H.R., Winchester, L., Pires, I., Hammond, E., Ragoussis, I., and Harris, A.L. (2010). Regulation of autophagy by ATF4 in response to severe hypoxia. Oncogene *29*, 4424-4435.

Rzymski, T., Milani, M., Singleton, D.C., and Harris, A.L. (2009). Role of ATF4 in regulation of autophagy and resistance to drugs and hypoxia. Cell Cycle *8*, 3838-3847.

Sahra, I.B., Tanti, J.F., and Bost, F. (2010). The combination of metformin and 2-deoxyglucose inhibits autophagy and induces AMPK dependent apoptosis in prostate cancer cells. Autophagy *6(5),* 670-671.

Sanz, C., Benito, A., Inohara, N., Ekhterae, D., Nunez, G., and Fernandez-Luna, J.L. (2000). Specific and rapid induction of the proapoptotic protein Hrk after growth factor withdrawal in hematopoietic progenitor cells. Blood *95*, 2742-2747.

Sanz, C., Horita, M., and Fernandez-Luna, J.L. (2002). Fas signaling and blockade of Bcr-Abl kinase induce apoptotic Hrk protein via DREAM inhibition in human leukemia cells. Haematologica *87*, 903-907.

Sanz, C., Mellstrom, B., Link, W.A., Naranjo, J.R., and Fernandez-Luna, J.L. (2001). Interleukin 3-dependent activation of DREAM is involved in transcriptional silencing of the apoptotic Hrk gene in hematopoietic progenitor cells. EMBO J *20*, 2286-2292.

Sattler, M., Liang, H., Nettesheim, D., Meadows, R.P., Harlan, J.E., Eberstadt, M., Yoon, H.S., Shuker, S.B., Chang, B.S., Minn, A.J.*, et al.* (1997). Structure of Bcl-xL-Bak peptide complex: recognition between regulators of apoptosis. Science *275*, 983-986.

Scaffidi, P., Misteli, T., and Bianchi, M.E. (2002). Release of chromatin protein HMGB1 by necrotic cells triggers inflammation. Nature *418*, 191-195.

Scherz-Shouval, R., Shvets, E., Fass, E., Shorer, H., Gil, L., and Elazar, Z. (2007). Reactive oxygen species are essential for autophagy and specifically regulate the activity of Atg4. EMBO J *26*, 1749-1760.

Scheuner, D., Song, B., McEwen, E., Liu, C., Laybutt, R., Gillespie, P., Saunders, T., Bonner-Weir, S., and Kaufman, R.J. (2001). Translational control is required for the unfolded protein response and in vivo glucose homeostasis. Mol Cell *7*, 1165-1176.

Schroder, M., and Kaufman, R.J. (2005). The mammalian unfolded protein response. Annu Rev Biochem *74*, 739-789.

Scott, R.C., Juhasz, G., and Neufeld, T.P. (2007). Direct induction of autophagy by Atg1 inhibits cell growth and induces apoptotic cell death. Curr Biol *17*, 1-11.

Semenza, G.L. (2000). Hypoxia, clonal selection, and the role of HIF-1 in tumor progression. Crit Rev Biochem Mol Biol *35*, 71-103.

Semenza, G.L. (2007). Evaluation of HIF-1 inhibitors as anticancer agents. Drug Discov Today *12*, 853-859.

Semenza, G.L. (2009). Regulation of cancer cell metabolism by hypoxia-inducible factor 1. Semin Cancer Biol *19*, 12-16.

Semenza, G.L., and Wang, G.L. (1992). A nuclear factor induced by hypoxia via de novo protein synthesis binds to the human erythropoietin gene enhancer at a site required for transcriptional activation. Mol Cell Biol *12*, 5447-5454.

Shah, G.M., Shah, R.G., and Poirier, G.G. (1996). Different cleavage pattern for poly(ADP-ribose) polymerase during necrosis and apoptosis in HL-60 cells. Biochem Biophys Res Commun *229*, 838-844.

Shamu, C.E., and Walter, P. (1996). Oligomerization and phosphorylation of the Ire1p kinase during intracellular signaling from the endoplasmic reticulum to the nucleus. EMBO J *15*, 3028-3039.

Shang, L., Chen, S., Du, F., Li, S., Zhao, L., and Wang, X. (2011). Nutrient starvation elicits an acute autophagic response mediated by Ulk1 dephosphorylation and its subsequent dissociation from AMPK. Proc Natl Acad Sci U S A, *108(12)*, 4788-4793.

Shimizu, S., Konishi, A., Nishida, Y., Mizuta, T., Nishina, H., Yamamoto, A., and Tsujimoto, Y. (2010). Involvement of JNK in the regulation of autophagic cell death. Oncogene *29*, 2070-2082.

Shimoke, K., Amano, H., Kishi, S., Uchida, H., Kudo, M., and Ikeuchi, T. (2004). Nerve growth factor attenuates endoplasmic reticulum stress-mediated apoptosis via suppression of caspase-12 activity. J Biochem *135*, 439-446.

Shimoke, K., Sasaya, H., and Ikeuchi, T. (2011). Analysis of the role of nerve growth factor in promoting cell survival during endoplasmic reticulum stress in PC12 cells. Methods Enzymol *490*, 53-70.

Shinoe, T., Wanaka, A., Nikaido, T., Kanazawa, K., Shimizu, J., Imaizumi, K., and Kanazawa, I. (2001). Upregulation of the pro-apoptotic BH3-only peptide harakiri in spinal neurons of amyotrophic lateral sclerosis patients. Neurosci Lett *313*, 153-157.

Sotelo, J., Briceno, E., and Lopez-Gonzalez, M.A. (2006). Adding chloroquine to conventional treatment for glioblastoma multiforme: a randomized, double-blind, placebo-controlled trial. Ann Intern Med *144*, 337-343.

Sowter, H.M., Ratcliffe, P.J., Watson, P., Greenberg, A.H., and Harris, A.L. (2001). HIF-1-dependent regulation of hypoxic induction of the cell death factors BNIP3 and NIX in human tumors. Cancer Res *61*, 6669-6673.

Srivastava, S.P., Davies, M.V., and Kaufman, R.J. (1995). Calcium depletion from the endoplasmic reticulum activates the double-stranded RNA-dependent protein kinase (PKR) to inhibit protein synthesis. J Biol Chem *270*, 16619-16624.

Srivastava, S.P., Kumar, K.U., and Kaufman, R.J. (1998). Phosphorylation of eukaryotic translation initiation factor 2 mediates apoptosis in response to activation of the double-stranded RNA-dependent protein kinase. J Biol Chem *273*, 2416-2423.

Stainsby, W.N., and Eitzman, P.D. (1988). Roles of CO2, O2, and acid in arteriovenous [H+] difference during muscle contractions. J Appl Physiol *65*, 1803-1810.

Stephan, J.S., Yeh, Y.Y., Ramachandran, V., Deminoff, S.J., and Herman, P.K. (2009). The Tor and PKA signaling pathways independently target the Atg1/Atg13 protein kinase complex to control autophagy. Proc Natl Acad Sci U S A *106*, 17049-17054.

Sudhakar, A., Ramachandran, A., Ghosh, S., Hasnain, S.E., Kaufman, R.J., and Ramaiah, K.V. (2000). Phosphorylation of serine 51 in initiation factor 2 alpha (eIF2 alpha) promotes complex formation between eIF2 alpha(P) and eIF2B and causes inhibition in the guanine nucleotide exchange activity of eIF2B. Biochemistry *39*, 12929-12938.

Sun, Q., Fan, W., Chen, K., Ding, X., Chen, S., and Zhong, Q. (2008). Identification of Barkor as a mammalian autophagy-specific factor for Beclin 1 and class III phosphatidylinositol 3-kinase. Proc Natl Acad Sci U S A *105*, 19211-19216.

Sunayama, J., Ando, Y., Itoh, N., Tomiyama, A., Sakurada, K., Sugiyama, A., Kang, D., Tashiro, F., Gotoh, Y., Kuchino, Y.*, et al.* (2004). Physical and functional interaction between BH3-only protein Hrk and mitochondrial pore-forming protein p32. Cell Death Differ *11*, 771-781.

Suzuki, K., and Ohsumi, Y. (2007). Molecular machinery of autophagosome formation in yeast, Saccharomyces cerevisiae. FEBS Lett *581*, 2156-2161.

Tampio, M., Markkanen, P., Puttonen, K.A., Hagelberg, E., Heikkinen, H., Huhtinen, K., Loikkanen, J., Hirvonen, M.R., and Vahakangas, K.H. (2009). Induction of PUMA-alpha and down-regulation of PUMA-beta expression is associated with benzo(a)pyrene-induced apoptosis in MCF-7 cells. Toxicol Lett *188*, 214-222.

Tang, H.W., Wang, Y.B., Wang, S.L., Wu, M.H., Lin, S.Y., and Chen, G.C. (2011). Atg1-mediated myosin II activation regulates autophagosome formation during starvation-induced autophagy. EMBO J *30*, 636-651.

Tanida, I., Ueno, T., and Kominami, E. (2004a). Human light chain 3/MAP1LC3B is cleaved at its carboxyl-terminal Met121 to expose Gly120 for lipidation and targeting to autophagosomal membranes. J Biol Chem *279*, 47704-47710.

Tanida, I., Ueno, T., and Kominami, E. (2004b). LC3 conjugation system in mammalian autophagy. Int J Biochem Cell Biol *36*, 2503-2518.

Tanimoto, K., Makino, Y., Pereira, T., and Poellinger, L. (2000). Mechanism of regulation of the hypoxia-inducible factor-1 alpha by the von Hippel-Lindau tumor suppressor protein. EMBO J *19*, 4298-4309.

Taylor, R.C., Cullen, S.P., and Martin, S.J. (2008). Apoptosis: controlled demolition at the cellular level. Nat Rev Mol Cell Biol *9*, 231-241.

Thomlinson, R.H., and Gray, L.H. (1955). The histological structure of some human lung cancers and the possible implications for radiotherapy. Br J Cancer *9*, 539-549.

Towers, E., Gilley, J., Randall, R., Hughes, R., Kristiansen, M., and Ham, J. (2009). The proapoptotic dp5 gene is a direct target of the MLK-JNK-c-Jun pathway in sympathetic neurons. Nucleic Acids Res *37*, 3044-3060.

Tracy, K., Dibling, B.C., Spike, B.T., Knabb, J.R., Schumacker, P., and Macleod, K.F. (2007). BNIP3 is an RB/E2F target gene required for hypoxia-induced autophagy. Mol Cell Biol *27*, 6229-6242.

Tracy, K., and Macleod, K.F. (2007). Regulation of mitochondrial integrity, autophagy and cell survival by BNIP3. Autophagy *3*, 616-619.

Tse, C., Shoemaker, A.R., Adickes, J., Anderson, M.G., Chen, J., Jin, S., Johnson, E.F., Marsh, K.C., Mitten, M.J., Nimmer, P.*, et al.* (2008). ABT-263: a potent and orally bioavailable Bcl-2 family inhibitor. Cancer Res *68*, 3421-3428.

Tsuboi, Y., Kurimoto, M., Nagai, S., Hayakawa, Y., Kamiyama, H., Hayashi, N., Kitajima, I., and Endo, S. (2009). Induction of autophagic cell death and radiosensitization by the pharmacological inhibition of nuclear factor-kappa B activation in human glioma cell lines. J Neurosurg *110*, 594-604.

Tu, B.P., and Weissman, J.S. (2002). The FAD- and O(2)-dependent reaction cycle of Ero1-mediated oxidative protein folding in the endoplasmic reticulum. Mol Cell *10*, 983-994.

Tu, B.P., and Weissman, J.S. (2004). Oxidative protein folding in eukaryotes: mechanisms and consequences. J Cell Biol *164*, 341-346.

Uma, S., Thulasiraman, V., and Matts, R.L. (1999). Dual role for Hsc70 in the biogenesis and regulation of the heme-regulated kinase of the alpha subunit of eukaryotic translation initiation factor 2. Mol Cell Biol *19*, 5861-5871.

Urano, F., Wang, X., Bertolotti, A., Zhang, Y., Chung, P., Harding, H.P., and Ron, D. (2000). Coupling of stress in the ER to activation of JNK protein kinases by transmembrane protein kinase IRE1. Science *287*, 664-666.

van den Beucken, T., Koritzinsky, M., Niessen, H., Dubois, L., Savelkouls, K., Mujcic, H., Jutten, B., Kopacek, J., Pastorekova, S., van der Kogel, A.J.*, et al.* (2009). Hypoxia-induced expression of carbonic anhydrase 9 is dependent on the unfolded protein response. J Biol Chem *284*, 24204-24212.

van den Beucken, T., Koritzinsky, M., and Wouters, B.G. (2006). Translational control of gene expression during hypoxia. Cancer Biol Ther *5*, 749-755.

Vander Haar, E., Lee, S.I., Bandhakavi, S., Griffin, T.J., and Kim, D.H. (2007). Insulin signalling to mTOR mediated by the Akt/PKB substrate PRAS40. Nat Cell Biol *9*, 316-323.

Vattem, K.M., and Wek, R.C. (2004). Reinitiation involving upstream ORFs regulates ATF4 mRNA translation in mammalian cells. Proc Natl Acad Sci U S A *101*, 11269-11274.

Vaupel, P., Kallinowski, F., and Okunieff, P. (1989a). Blood flow, oxygen and nutrient supply, and metabolic microenvironment of human tumors: a review. Cancer Res *49*, 6449-6465.

Vaupel, P., Okunieff, P., Kallinowski, F., and Neuringer, L.J. (1989b). Correlations between 31P-NMR spectroscopy and tissue O2 tension measurements in a murine fibrosarcoma. Radiat Res *120*, 477-493.

Vaupel, P., Schlenger, K., and Hoeckel, M. (1992). Blood flow and tissue oxygenation of human tumors: an update. Adv Exp Med Biol *317*, 139-151.

Vazquez-Martin, A., Oliveras-Ferraros, C., and Menendez, J.A. (2009). Autophagy facilitates the development of breast cancer resistance to the anti-HER2 monoclonal antibody trastuzumab. PLoS One *4*, e6251.

Vogelstein, B., and Kinzler, K.W. (2004). Cancer genes and the pathways they control. Nat Med *10*, 789-799.

Wakabayashi, T., Kosaka, J., and Hommura, S. (2002). Up-regulation of Hrk, a regulator of cell death, in retinal ganglion cells of axotomized rat retina. Neurosci Lett *318*, 77-80.

Walker, S., Chandra, P., Manifava, M., Axe, E., and Ktistakis, N.T. (2008). Making autophagosomes: localized synthesis of phosphatidylinositol 3-phosphate holds the clue. Autophagy *4*, 1093-1096.

Wang, G.L., Jiang, B.H., Rue, E.A., and Semenza, G.L. (1995). Hypoxia-inducible factor 1 is a basic-helix-loop-helix-PAS heterodimer regulated by cellular O2 tension. Proc Natl Acad Sci U S A *92*, 5510-5514.

Wang, P., Yu, J., and Zhang, L. (2007). The nuclear function of p53 is required for PUMA-mediated apoptosis induced by DNA damage. Proc Natl Acad Sci U S A *104*, 4054-4059.

Wang, Q., Mora-Jensen, H., Weniger, M.A., Perez-Galan, P., Wolford, C., Hai, T., Ron, D., Chen, W., Trenkle, W., Wiestner, A.*, et al.* (2009). ERAD inhibitors integrate ER stress with an epigenetic mechanism to activate BH3-only protein NOXA in cancer cells. Proc Natl Acad Sci U S A *106*, 2200-2205.

Wang, X.Z., Kuroda, M., Sok, J., Batchvarova, N., Kimmel, R., Chung, P., Zinszner, H., and Ron, D. (1998). Identification of novel stress-induced genes downstream of chop. EMBO J *17*, 3619-3630.

Wei, Y., Pattingre, S., Sinha, S., Bassik, M., and Levine, B. (2008a). JNK1-mediated phosphorylation of Bcl-2 regulates starvation-induced autophagy. Mol Cell *30*, 678-688.

Wei, Y., Sinha, S., and Levine, B. (2008b). Dual role of JNK1-mediated phosphorylation of Bcl-2 in autophagy and apoptosis regulation. Autophagy *4*, 949-951.

Wek, R.C., Jiang, H.Y., and Anthony, T.G. (2006). Coping with stress: eIF2 kinases and translational control. Biochem Soc Trans *34*, 7-11.

White, E. (1993). Regulation of apoptosis by the transforming genes of the DNA tumor virus adenovirus. Proc Soc Exp Biol Med *204*, 30-39.

White, E., Karp, C., Strohecker, A.M., Guo, Y., and Mathew, R. (2010). Role of autophagy in suppression of inflammation and cancer. Curr Opin Cell Biol *22*, 212-217.

Willis, S.N., Fletcher, J.I., Kaufmann, T., van Delft, M.F., Chen, L., Czabotar, P.E., Ierino, H., Lee, E.F., Fairlie, W.D., Bouillet, P.*, et al.* (2007). Apoptosis initiated when BH3 ligands engage multiple Bcl-2 homologs, not Bax or Bak. Science *315*, 856-859.

Wilson, R.E., Keng, P.C., and Sutherland, R.M. (1989). Drug resistance in Chinese hamster ovary cells during recovery from severe hypoxia. J Natl Cancer Inst *81*, 1235-1240.

Winter, S.C., Buffa, F.M., Silva, P., Miller, C., Valentine, H.R., Turley, H., Shah, K.A., Cox, G.J., Corbridge, R.J., Homer, J.J.*, et al.* (2007). Relation of a hypoxia metagene derived from head and neck cancer to prognosis of multiple cancers. Cancer Res *67*, 3441-3449.

Wirapati, P., Sotiriou, C., Kunkel, S., Farmer, P., Pradervand, S., Haibe-Kains, B., Desmedt, C., Ignatiadis, M., Sengstag, T., Schutz, F.*, et al.* (2008). Meta-analysis of gene expression profiles in breast cancer: toward a unified understanding of breast cancer subtyping and prognosis signatures. Breast Cancer Res *10*, R65.

Wouters, B.G., and Brown, J.M. (1997). Cells at intermediate oxygen levels can be more important than the "hypoxic fraction" in determining tumor response to fractionated radiotherapy. Radiat Res *147*, 541-550.

Wouters, B.G., and Koritzinsky, M. (2008). Hypoxia signalling through mTOR and the unfolded protein response in cancer. Nat Rev Cancer *8*, 851-864.

Wouters, B.G., van den Beucken, T., Magagnin, M.G., Koritzinsky, M., Fels, D., and Koumenis, C. (2005). Control of the hypoxic response through regulation of mRNA translation. Semin Cell Dev Biol *16*, 487-501.

Wouters, B.G., van den Beucken, T., Magagnin, M.G., Lambin, P., and Koumenis, C. (2004). Targeting hypoxia tolerance in cancer. Drug Resist Updat *7*, 25-40.

Wullschleger, S., Loewith, R., and Hall, M.N. (2006). TOR signaling in growth and metabolism. Cell *124*, 471-484.

Xie, Z., and Klionsky, D.J. (2007). Autophagosome formation: core machinery and adaptations. Nat Cell Biol *9*, 1102-1109.

Yan, J., Kuroyanagi, H., Kuroiwa, A., Matsuda, Y., Tokumitsu, H., Tomoda, T., Shirasawa, T., and Muramatsu, M. (1998). Identification of mouse ULK1, a novel protein kinase structurally related to C. elegans UNC-51. Biochem Biophys Res Commun *246*, 222-227.

Yang, S., Wang, X., Contino, G., Liesa, M., Sahin, E., Ying, H., Bause, A., Li, Y., Stommel, J.M., Dell'antonio, G.*, et al.* (2011). Pancreatic cancers require autophagy for tumor growth. Genes Dev. *25(7),* 717-29.

Ye, J., Kumanova, M., Hart, L.S., Sloane, K., Zhang, H., De Panis, D.N., Bobrovnikova-Marjon, E., Diehl, J.A., Ron, D., and Koumenis, C. (2010). The GCN2-ATF4 pathway is critical for tumour cell survival and proliferation in response to nutrient deprivation. EMBO J *29*, 2082-2096.

Yee, K.S., Wilkinson, S., James, J., Ryan, K.M., and Vousden, K.H. (2009). PUMA- and Bax-induced autophagy contributes to apoptosis. Cell Death Differ *16*, 1135-1145.

Yeh, Y.Y., Wrasman, K., and Herman, P.K. (2010). Autophosphorylation within the Atg1 activation loop is required for both kinase activity and the induction of autophagy in Saccharomyces cerevisiae. Genetics *185*, 871-882.

Yin, K.J., Kim, G.M., Lee, J.M., He, Y.Y., Xu, J., and Hsu, C.Y. (2005). JNK activation contributes to DP5 induction and apoptosis following traumatic spinal cord injury. Neurobiol Dis *20*, 881-889.

Yoshizawa, T., Hinoi, E., Jung, D.Y., Kajimura, D., Ferron, M., Seo, J., Graff, J.M., Kim, J.K., and Karsenty, G. (2009). The transcription factor ATF4 regulates glucose metabolism in mice through its expression in osteoblasts. J Clin Invest *119*, 2807-2817.

Youle, R.J., and Narendra, D.P. (2011). Mechanisms of mitophagy. Nat Rev Mol Cell Biol *12*, 9-14.

Young, A.R., Chan, E.Y., Hu, X.W., Kochl, R., Crawshaw, S.G., High, S., Hailey, D.W., Lippincott-Schwartz, J., and Tooze, S.A. (2006). Starvation and ULK1-dependent cycling of mammalian Atg9 between the TGN and endosomes. J Cell Sci *119*, 3888-3900.

Young, J.E., Garden, G.A., Martinez, R.A., Tanaka, F., Sandoval, C.M., Smith, A.C., Sopher, B.L., Lin, A., Fischbeck, K.H., Ellerby, L.M*., et al.* (2009). Polyglutamine-expanded androgen receptor truncation fragments activate a Bax-dependent apoptotic cascade mediated by DP5/Hrk. J Neurosci *29*, 1987-1997.

Yu, J., Wang, Z., Kinzler, K.W., Vogelstein, B., and Zhang, L. (2003). PUMA mediates the apoptotic response to p53 in colorectal cancer cells. Proc Natl Acad Sci U S A *100*, 1931-1936.

Yu, J., Yue, W., Wu, B., and Zhang, L. (2006a). PUMA sensitizes lung cancer cells to chemotherapeutic agents and irradiation. Clin Cancer Res *12*, 2928-2936.

Yu, J., Zhang, L., Hwang, P.M., Kinzler, K.W., and Vogelstein, B. (2001). PUMA induces the rapid apoptosis of colorectal cancer cells. Mol Cell *7*, 673-682.

Yu, L., Alva, A., Su, H., Dutt, P., Freundt, E., Welsh, S., Baehrecke, E.H., and Lenardo, M.J. (2004). Regulation of an ATG7-beclin 1 program of autophagic cell death by caspase-8. Science *304*, 1500-1502.

Yu, L., Wan, F., Dutta, S., Welsh, S., Liu, Z., Freundt, E., Baehrecke, E.H., and Lenardo, M. (2006b). Autophagic programmed cell death by selective catalase degradation. Proc Natl Acad Sci U S A *103*, 4952-4957.

Yu, Z., Luo, H., Fu, W., and Mattson, M.P. (1999). The endoplasmic reticulum stress-responsive protein GRP78 protects neurons against excitotoxicity and apoptosis:

suppression of oxidative stress and stabilization of calcium homeostasis. Exp Neurol *155*, 302-314.

Yue, Z., Jin, S., Yang, C., Levine, A.J., and Heintz, N. (2003). Beclin 1, an autophagy gene essential for early embryonic development, is a haploinsufficient tumor suppressor. Proc Natl Acad Sci U S A *100*, 15077-15082.

Zeng, X., Overmeyer, J.H., and Maltese, W.A. (2006). Functional specificity of the mammalian Beclin-Vps34 PI 3-kinase complex in macroautophagy versus endocytosis and lysosomal enzyme trafficking. J Cell Sci *119*, 259-270.

Zhang, H., Bosch-Marce, M., Shimoda, L.A., Tan, Y.S., Baek, J.H., Wesley, J.B., Gonzalez, F.J., and Semenza, G.L. (2008). Mitochondrial autophagy is an HIF-1-dependent adaptive metabolic response to hypoxia. J Biol Chem *283*, 10892-10903.

Zhang, J., and Ney, P.A. (2008). NIX induces mitochondrial autophagy in reticulocytes. Autophagy *4*, 354-356.

Zhang, P., McGrath, B.C., Reinert, J., Olsen, D.S., Lei, L., Gill, S., Wek, S.A., Vattem, K.M., Wek, R.C., Kimball, S.R*., et al.* (2002). The GCN2 eIF2alpha kinase is required for adaptation to amino acid deprivation in mice. Mol Cell Biol *22*, 6681-6688.

Zhao, M., and Klionsky, D.J. (2011). AMPK-Dependent Phosphorylation of ULK1 Induces Autophagy. Cell Metab *13*, 119-120.

Zhu, S., Sobolev, A.Y., and Wek, R.C. (1996). Histidyl-tRNA synthetase-related sequences in GCN2 protein kinase regulate in vitro phosphorylation of eIF-2. J Biol Chem *271*, 24989-24994.

Zinszner, H., Kuroda, M., Wang, X., Batchvarova, N., Lightfoot, R.T., Remotti, H., Stevens, J.L., and Ron, D. (1998). CHOP is implicated in programmed cell death in response to impaired function of the endoplasmic reticulum. Genes Dev *12*, 982-995.